© 2020 by Ryne Beeson. All rights reserved.

NONLINEAR FILTERING OF HIGH DIMENSIONAL, CHAOTIC, MULTIPLE TIMESCALE CORRELATED SYSTEMS

BY

RYNE BEESON

DISSERTATION

Submitted in partial fulfillment of the requirements
for the degree of Doctor of Philosophy in Aerospace Engineering
in the Graduate College of the
University of Illinois at Urbana-Champaign, 2020

Urbana, Illinois

Doctoral Committee:

Professor N. Sri Namachchivaya, Chair and Director of Research
Professor Bruce Conway
Professor Nicolas Perkowski, Freie Universität Berlin
Associate Professor Zoi Rapti
Professor Renming Song

Abstract

This dissertation addresses theoretical and numerical questions in nonlinear filtering theory for high dimensional, chaotic, multiple timescale correlated systems. The research is motivated by problems in the geosciences, in particular oceanic or atmospheric estimation and climate prediction. As the capability and need to further resolve the physics models on finer scales continues, greater spatial and temporal scales become present and the dimension of the models becomes increasingly large. In the atmospheric sciences, these models can be of the order $\mathcal{O}(10^9)$ degrees of freedom and require assimilation of the order $\mathcal{O}(10^7)$ observations during a single day. The models are chaotic and the observing sensors may be correlated with the physical processes themselves. The goal of the dissertation is to develop theoretical results that can provide the mathematical justification for new filtering algorithms on a lower dimensional problem, and to develop novel methods for dealing with issues that plague particle filtering when applied to high dimensional, chaotic, multiple timescale correlated systems.

The first half of the dissertation is theoretical and addresses the question of approximating the continuous time nonlinear filtering equation for a multiple timescale correlated system by an averaged filtering equation in the limit of large timescale separation. The first result in this direction is within the context of a slow-fast system with correlation between the slow process and the observation process, and when we are only interested in estimating functions of the slow process. The main result is that we can retrieve a rate of convergence and that there is a metric generating the topology of weak convergence, such that the marginal filter converges to the averaged filter at the given rate in the limit of large timescale separation. The proof uses a probabilistic representation (backward doubly stochastic differential equation) of the dual process to the unnormalized filter, and sharp estimates on the transition density and semigroup of the fast process.

The second theoretical result of the dissertation addresses the same question for a broader problem, where the slow signal dynamics include an intermediate timescale forcing. We prove that the marginal filter converges in probability to the average filter for a metric that generates the topology of weak convergence. The method of proof is by showing tightness of the measure-valued process, characterizing the weak limits, and proving the limit is unique. The perturbation test function (also known as method of corrector) is used to

deal with the intermediate timescale forcing term, where the corrector is the solution of a Poisson equation.

The second half of the dissertation develops filtering algorithms that leverage the theoretical results from the first half of the thesis to produce particle filtering methods for the averaged filtering equation. We also develop particle methods that address the issue of particle collapse for filtering on general high dimensional chaotic systems. Using the two timescale Lorenz 1996 atmospheric model, we show that the reduced order particle filtering methods are shown to be at least an order of magnitude faster than standard particle methods. We develop a method for particle filtering when the signal and observation processes are correlated. We also develop extensions to controlled optimal proposal particle filters that improve the diversity of the particle ensemble when tested on the Lorenz 1963 model.

In the last chapter of the dissertation, we adopt a dynamical systems viewpoint to address the issue of particle collapse. This time the goal is to exploit the chaotic properties of the system being filtered to perform assimilation in a lower dimensional subspace. A new approach is developed which enables data assimilation in the unstable subspace for particle filtering. We introduce the idea of future right-singular vectors to produce projection operators, enabling assimilation in a lower dimensional subspace. We show that particle filtering algorithms using dynamically generator projection operators, in particular the future right-singular vectors, outperforms standard particle methods in terms of root-mean-square-error, diversity of the particle ensemble, and robustness when applied to the single timescale Lorenz 1996 model.

To my mother and father.

Acknowledgments

Without the support, inspiration, enthusiasm, guidance and mentoring of many individuals, this dissertation would not be what it is. From my initial life as a Ph.D. candidate in astrodynamics, I thank Alex Ghosh, Jacob Englander, Donald Ellison, Bindu Jagannatha, Pat Haddox, Vishwa Shah, Joshua Aurich, and Devin Bunce. I learned a great deal from each, and all have been wonderful friends to have during graduate school. I am thankful that Professor Victoria Coverstone took me on as a Ph.D. student and for her encouragement. I greatly enjoyed working on varied projects with Kyle Cochran, Kaushik Ponnapalli, Professor Koki Ho, Mihir Patel, Onalli Gunasekara, and Kento Tomita. Thank you to David Carroll for the opportunities and steady support. I give much credit to Hoong Chieh Yeong for helping me learn nonlinear filtering theory. He was a delightful person to do research with, as well as chat and spend time together.

My committee have all played important roles during my time as a Ph.D. student. Besides having taken an astrodynamics course with Professor Bruce Conway, he and his former Ph.D. student, Chris Martin, worked on a problem that greatly inspired me early on. That problem led me to take courses in dynamical systems. The first such course in the mathematics department that I took was with Professor Zoi Rapti, who was an enthusiastic teacher. I then enrolled in Professor N. Sri Namachchivaya courses and subsequently switched advisors to work on nonlinear filtering theory under him. Not yet having studied probability theory, I took the courses from the mathematics department with Professor Renming Song, who taught a clear and rigorous course. At the same time I was very fortunate to be able to start working with Professor Nicolas Perkowski. He has been an excellent and patient, mentor and advisor for me. Besides playing a key role in advising the research for this dissertation, Professor Namachchivaya has also been a valuable friend and mentor in life. I have very much enjoyed working with him.

My family has provided a great amount of support over the years; I am very fortunate to have each of you in my life. To all my siblings: Colleen, Kathleen, Myles, Drew, Callan, Haley, Clair, Nolan, Charly and Wesley; thank you for your endless support. To Hilary, thank you for always being there with your uplifting words, excitement, and love during the last few critical years of this dissertation. To my parents, your example of dedication and perseverance has been a valuable one. Thank you for inspiring me and for always having me in your thoughts. I love you all.

The work in this dissertation was partially support by the Air Force Office of Scientific Research under grant number FA9550-17-1-0001, an Illinois Space Grant Consortium Graduate Fellowship, a Children of Veteran Tuition Waiver, and the Avery-Brundage Scholarship.

Table of Contents

List of Tables . . . . . **x**

List of Figures . . . . . **xi**

List of Abbreviations . . . . . **xiv**

Chapter 1 Introduction and Motivation **1**

Chapter 2 Nonlinear Filtering Theory **6**
2.1 Multiple Timescale Correlated Systems 7
2.1.1 Markov Transition Semigroups and Infinitesimal Generators 9
2.2 A Change of Probability Measure Transformation 11
2.2.1 Girsanov's Theorem 13
2.2.2 The Kallianpur-Striebel Formula 13
2.3 The Zakai Equation 14
2.4 The Kushner-Stratonovich Equation 17

Chapter 3 Quantitative Convergence of the Filter Solution for Multiple Timescale Nonlinear Systems with Coarse-Grain Correlated Noise **18**
3.1 Notation 21
3.2 Diffusion Approximation, the Averaged Filtering Equation, and Main Theorem 22
3.2.1 The Averaged Unnormalized Conditional Distribution 24
3.2.2 Representation of the Averaged Unnormalized Conditional Distribution 25
3.3 Dual Process to the Unnormalized Conditional Distribution 26
3.3.1 The Dual Process and Filter Convergence 27
3.3.2 Evolution Equations for the Dual Process 28
3.3.3 Expansion of the Dual Process 28
3.4 Probabilistic Representation of Stochastic PDEs 29
3.4.1 Backward Doubly Stochastic Differential Equations 31
3.5 Preliminary Estimates 34
3.5.1 Estimates on SDE Solutions 34
3.5.2 Estimates with the Fast Semigroup 36
3.5.3 Estimates for the Corrector Term 39
3.6 Main Analysis 42
3.6.1 Moment Estimates for Dual Processes 42
3.6.2 Estimates of Dual and Filter Error 52
3.7 Remarks on Intermediate Timescale 58

Chapter 4 Approximation of the Filter Equation for Multiple Timescale Nonlinear Systems with Correlated Noise . . . 60
4.1 Notation . . . 61
4.2 Homogenization of Stochastic Differential Equations . . . 62
4.3 The Averaged Filtering Equation and Main Theorem . . . 63
4.3.1 The Averaged Unnormalized Filtering Equations . . . 65
4.4 Preliminary Estimates . . . 66
4.4.1 Estimates with the Fast Semigroup . . . 68
4.4.2 Estimates on SDE Solutions . . . 70
4.4.3 Estimates using the Poisson Equation . . . 74
4.4.4 Estimates of the Unnormalized Conditional Distribution . . . 76
4.5 Existence, Characterization and Uniqueness of Weak Limits . . . 77
4.6 Remark on Conditions for the Fast Semigroup . . . 95
4.6.1 Counter Example . . . 96
4.6.2 List of Changes . . . 97

Chapter 5 Standard and Optimal Proposal Particle Methods for Multiple Timescale, Correlated Systems . . . 98
5.1 Bayesian Filtering . . . 99
5.1.1 Sequential Importance Sampling . . . 100
5.1.2 The Sequential Importance Sampling Particle Filter (PF) . . . 101
5.2 Multiple Timescales . . . 103
5.2.1 The Heterogenous Multiscale Method . . . 105
5.2.2 The Lorenz 1996 Model . . . 105
5.3 Homogenized Hybrid Particle Filter (HHPF) . . . 112
5.3.1 Exploiting Model Symmetry and Parameterizations . . . 112
5.3.2 Application to the Lorenz 1996 Model . . . 115
5.4 Correlated Noise . . . 119
5.4.1 Likelihood for Correlated Sparse Observation . . . 119
5.4.2 Application to the Lorenz 1996 Model . . . 122
5.5 Optimal Proposal Particle Filtering and Tempering . . . 128
5.5.1 The Nudged Particle Filter (nPF) . . . 129
5.5.2 Insight on the Nudged Particle Filter . . . 132
5.5.3 Relaxed Particle Filter (rPF) . . . 135
5.5.4 The Lorenz 1963 Model . . . 136
5.5.5 Tempering . . . 136

Chapter 6 Particle Filtering and High Dimensional Chaotic Systems . . . 142
6.1 Introduction . . . 142
6.2 Lyapunov Exponents, Vectors, and Variants . . . 143
6.2.1 Dimension of the Attractor and Entropy . . . 145
6.2.2 Finite-Time Lyapunov Exponents and Vectors . . . 145
6.2.3 Singular Vectors of the Fundamental Matrix . . . 146
6.3 The Single Timescale Lorenz 1996 Model . . . 147
6.3.1 Weakly Chaotic, Non-Gaussian Regime . . . 149
6.3.2 Strongly Chaotic, Near-Gaussian Regime . . . 151
6.3.3 Projected Particle Filtering . . . 153
6.4 Application to the Single Timescale Lorenz 1996 Model . . . 155
6.4.1 Results of the Weakly Chaotic, Non-Gaussian Regime . . . 156
6.4.2 Results of the Strongly Chaotic, Near-Gaussian Regime . . . 159
6.5 Remarks . . . 160

Chapter 7 Conclusions . . . 162

Appendix **166**
A.1 Inverses and Factorizations of Symmetric Positive Definite Matrices 166
A.2 Extension of Itô's Formula 167
A.3 An Inequality and Limits 170

References **173**

List of Tables

5.1 Filtering application of PF, HHPF, and eHHPF to the Lorenz '96 model. 116
5.2 Filtering application of eHHnPF to the Lorenz '96 model. 117
5.3 Filtering application of PF to the Lorenz '96 model with fast forcing neglected. 117
5.4 Filtering results for various filter algorithms applied to the Lorenz '96 model. RMSE integrated over time, and filter run-time (per simulation) averaged over 24 experiments. 125
5.5 Average RMSE at each integration step, averaged over 32 experiments. 140

6.1 Results for 96 simulations of filtering on the Lorenz '96 model with $F = 5$, using 8 particles and $\Delta t = 0.05$. The average rank of the right-singular value projection operators was 14.6, in comparison to the dimension Lorenz '96 at $N = 40$. The average RMSE for the observation error was 1.41. 158
6.2 Results for 96 simulations of filtering on the Lorenz '96 model with $F = 5$, using 8 particles and $\Delta t = 0.05$. The average RMSE for the observation error was 1.41. 158
6.3 Results for 96 simulations of filtering on the Lorenz '96 model with $F = 8$, using 16 particles and $\Delta t = 0.05$. For the projected filters, indicated by $\cdot^{\ddagger}$, the average rank of the projection operator was 15.6, in comparison with the dimension Lorenz '96 at $N = 40$. The average RMSE for the observation error was 1.41. An asterisk in the results identifies that the average (or total run-time) was only taken for those simulations that completed. 159
6.4 Results for 96 simulations of filtering on the Lorenz '96 model with $F = 8$, using 16 particles and $\Delta t = 0.05$. The average RMSE for the observation error was 1.41. An asterisk in the results identifies that the average (or total run-time) was only taken for those simulations that completed. 159

List of Figures

1.1 (CO2) concentrations at Mauna Loa, Hawaii, and column CO2 mixing ratios dispersed by weather systems within the large-scale flow in a 7-km global simulation with the Goddard Earth Observing System Model, Version 5 (GEOS-5)[Put20] 2

5.1 A recreation of a similar image by Wilks [Wil05], that provides a visualization of the two timescale Lorenz '96 model. 106
5.2 Direct numerical solution of the Lorenz '96 model: X_t^1 in orange, $Z_t^{1,1} \ldots, Z_t^{1,9}$ in gray, and the fast scale forcing $(h_x/J)\sum_{j=1}^J Z_t^{1,j}$ on X_t^1 in light blue. 108
5.3 An HMM solution of the Lorenz '96 model: $X_t^{0,1}$ in orange, $\mathcal{R} = 1$ realizations of $Z_t^{1,1} \ldots, Z_t^{1,9}$ with fixed X_t^0 in gray, and the averaged fast scale forcing on $X_t^{0,1}$ in light blue. 108
5.4 Direct numerical solution of the Lorenz '96 model: X_t^1 in orange, $Z_t^{1,1} \ldots, Z_t^{1,9}$ in gray, and the fast scale forcing $(h_x/J)\sum_{j=1}^J Z_t^{1,j}$ on X_t^1 in light blue. 109
5.5 An HMM solution for the Lorenz '96 model: $X_t^{0,1}$ in orange, $\mathcal{R} = 1$ realizations of $Z_t^{1,1} \ldots, Z_t^{1,9}$ with fixed X_t^0 in gray, and the averaged fast scale forcing on $X_t^{0,1}$ in light blue. 109
5.6 Simulation of Eq. 5.2.2. Shown in gray is the X_t^1 (i.e., first component) marginal density when $\epsilon =$ 1E-2 and similarly in light blue the X_t^1 marginal density when $\epsilon =$ 1E-3. 111
5.7 Transition densities of the first component of Z_t^ϵ: $\mu_{15\cdot\Delta_m}(z; X_0^\epsilon = x, Z_0^\epsilon)$, for randomly generated Z_0^ϵ; the first component of Z_0^ϵ is shown as Z_0^1 in the legend for four different simulations. $X_0^\epsilon = x$ is a fixed slow state. 111
5.8 Direct numerical simulation of the Lorenz '96 model: X_t^1 in orange, $Z_t^{1,1} \ldots, Z_t^{1,9}$ in gray, and the fast scale forcing η_t^1 on X_t^1 in light blue. 115
5.9 An HMM simulation of the Lorenz '96 model: X_t^1 in orange, $Z_t^{1,1} \ldots, Z_t^{1,9}$ in gray, and the fast scale forcing η_t^1 on X_t^1 in light blue. 115
5.10 A solution of the Lorenz '96 model using pre-computed $\psi_\eta(x)$: X_t^1 in orange and the sampled fast scale forcing ψ_{η^1} on X_t^1 in light blue. 116
5.11 PF showing the signal $X_t^{\epsilon,1}$ (first component) in black, the estimate $\mathbb{E}\, X_t^{\epsilon,1}$ in orange, observations in green, particles in light blue. 118
5.12 eHHPF showing the signal $X_t^{\epsilon,1}$ (first component) in black, the estimate $\mathbb{E}\, X_t^{\epsilon,1}$ in orange, observations in green, 16 particles in light blue. 118
5.13 A pictorial representation of Eq. 5.4.2 with arrows between v_j and e_k indicating sensor-signal correlation. 120
5.14 PF, $\alpha = \gamma = \sigma_x/\sqrt{2}, N = 16, N_{\text{eff}} = 8$. Top graph: the signal $X_t^{\epsilon,1}$ (first component) in black, the estimate $\mathbb{E}\, X_t^{\epsilon,1}$ in orange, observations in green. Bottom graph: RMSE in light blue. . . 123
5.15 HHPF, $\alpha = 0, \gamma = \sigma_x, N = 16, N_{\text{eff}} = 8$. Top graph: the signal $X_t^{\epsilon,1}$ (first component) in black, the estimate $\mathbb{E}\, X_t^{\epsilon,1}$ in orange, observations in green. Bottom graph: RMSE in light blue. . . 123
5.16 HHPF with $\alpha = \gamma = \sigma_x/\sqrt{2}, N = 16, N_{\text{eff}} = 8$. Top graph: the signal $X_t^{\epsilon,1}$ (first component) in black, the estimate $\mathbb{E}\, X_t^{\epsilon,1}$ in orange, observations in green. Bottom graph: RMSE in light blue. 124
5.17 HHnPF with $\alpha = \gamma = \sigma_x/\sqrt{2}, N = 16, N_{\text{eff}} = 8$. Top graph: the signal $X_t^{\epsilon,1}$ (first component) in black, the estimate $\mathbb{E}\, X_t^{\epsilon,1}$ in orange, observations in green. Bottom graph: RMSE in light blue. 124

5.18 HHnPF with $\alpha = \gamma = \sigma_x/\sqrt{2}, N = 8, N_{\text{eff}} = 4$. Top graph: the signal $X_t^{\epsilon,1}$ (first component) in black, the estimate $\mathbb{E}\, X_t^{\epsilon,1}$ in orange, observations in green. Bottom graph: RMSE in light blue. . . . 125
5.19 PF with $\alpha = \gamma = \sigma_x/\sqrt{2}, N = 16, N_{\text{eff}} = 8$. The signal $X_t^{\epsilon,1}$ (first component) in black, the estimate $\mathbb{E}\, X_t^{\epsilon,1}$ in orange, observations in green, particles in light blue. . . . 126
5.20 HHPF with $\alpha = 0, \gamma = \sigma_x, N = 16, N_{\text{eff}} = 8$. The signal $X_t^{\epsilon,1}$ (first component) in black, the estimate $\mathbb{E}\, X_t^{\epsilon,1}$ in orange, observations in green, particles in light blue. . . . 126
5.21 HHPF with $\alpha = \gamma = \sigma_x/\sqrt{2}, N = 16, N_{\text{eff}} = 8$. The signal $X_t^{\epsilon,1}$ (first component) in black, the estimate $\mathbb{E}\, X_t^{\epsilon,1}$ in orange, observations in green, particles in light blue. . . . 127
5.22 HHnPF with $\alpha = \gamma = \sigma_x/\sqrt{2}, N = 16, N_{\text{eff}} = 8$. The signal $X_t^{\epsilon,1}$ (first component) in black, the estimate $\mathbb{E}\, X_t^{\epsilon,1}$ in orange, observations in green, particles in light blue. . . . 127
5.23 HHnPF with $\alpha = \gamma = \sigma_x/\sqrt{2}, N = 8, N_{\text{eff}} = 4$. The signal $X_t^{\epsilon,1}$ (first component) in black, the estimate $\mathbb{E}\, X_t^{\epsilon,1}$ in orange, observations in green, particles in light blue. . . . 128
5.24 The effective number N_{eff} at observation times versus time. PF shown in black, HHnPF in orange, and HHPF in light blue. Values below 8 indicate re-sampling occurs. . . . 128
5.25 Time history of relative particle weights for a simulation of PF on the Lorenz '63 model (see Section 5.5.4). Observations are shown in green. Particles that are blue have essentially zero weight relative to the rest of the ensemble. A color of white indicates an average weight relative to the ensemble, and coloring of red indicates the particle is overweighted relative to the rest of the ensemble. . . . 133
5.26 Time history of relative particle weights for a simulation of nPF on the Lorenz '63 model (see Section 5.5.4). Observations are shown in green. Particles that are blue have essentially zero weight relative to the rest of the ensemble. A color of white indicates an average weight relative to the ensemble, and coloring of red indicates the particle is overweighted relative to the rest of the ensemble. . . . 134
5.27 Time history (at observation time) of effective sample size (number) for a simulation of PF and nPF on the Lorenz '63 model (see Section 5.5.4). . . . 135
5.28 Relaxation method applied to the Lorenz '63 model. True signal shown in black, particles in light blue, mean of the particles in orange, and observation in green. . . . 139
5.29 Optimal particle filter method without and with tempering of the likelihood applied to the Lorenz '63 model. True signal shown in black, particles in light blue, mean of the particles in orange, and observation in green. . . . 139
5.30 Time history of relative particle weights for a simulation of rPF on the Lorenz '63 model (see Section 5.5.4). Observations are shown in green. Particles that are blue have essentially zero weight relative to the rest of the ensemble. A color of white indicates an average weight relative to the ensemble, and coloring of red indicates the particle is overweighted relative to the rest of the ensemble. . . . 140
5.31 Time history (at observation time) of effective sample size (number) for a simulation of rPF and nPF on the Lorenz '63 model (see Section 5.5.4). . . . 141

6.1 Depiction of the dynamics of the Lorenz '96 model with $F = 5$ and $J = 40$. The top x-axis provides time in the natural units of the Lorenz '96 model, while the bottom x-axis provides the Lyapunov time $\lambda_1 t$. . . . 150
6.2 Depiction of a stochastic realization of the Lorenz '96 model with $F = 5, J = 40$ and $Q = I$. The top x-axis provides time in the natural units of the Lorenz '96 model, while the bottom x-axis provides the Lyapunov time $\lambda_1 t$, with λ_1 calculated from the deterministic model. . . . 150
6.3 Depiction of the dynamics of the Lorenz '96 model with $F = 8$ and $J = 40$. The top x-axis provides time in the natural units of the Lorenz '96 model, while the bottom x-axis provides the Lyapunov time $\lambda_1 t$. . . . 152
6.4 Depiction of a stochastic realization of the Lorenz '96 model with $F = 8, J = 40$ and $Q = I$. The top x-axis provides time in the natural units of the Lorenz '96 model, while the bottom x-axis provides the Lyapunov time $\lambda_1 t$, with λ_1 calculated from the deterministic model. . . . 152

6.5 The absolute error between the true state and the mean state for a single simulation of the Lorenz '96 model with $F = 5$ using the PF algorithm. The average RMSE for this simulation was 10.85. The top x-axis provides time in the natural units of the Lorenz '96 model, while the bottom x-axis provides the Lyapunov time $\lambda_1 t$. 157
6.6 The absolute error between the true state and the mean state for a single simulation of the Lorenz '96 model with $F = 5$ using the nPF algorithm. The average RMSE for this simulation was 4.31. The top x-axis provides time in the natural units of the Lorenz '96 model, while the bottom x-axis provides the Lyapunov time $\lambda_1 t$. 157

List of Abbreviations

SDE	Stochastic Differential Equation
BDSDE	Backward Doubly Stochastic Differential Equation
FBDSDE	Forward Backward Doubly Stochastic Differential Equation
PDE	Partial Differential Equation
SPDE	Stochastic Partial Differential Equation
BSPDE	Backward Stochastic Partial Differential Equation
SIS	Sequential Importance Sampling
PF	Particle Filter
nPF	Nudged Particle Filter
HMM	Heterogeneous Multiscale Method
HHPF	Homogenized Hybrid Particle Filter
eHHPF	Efficient Homogenized Hybrid Particle Filter
HHnPF	Nudge Variant of HHPF
eHHnPF	Nudged Variant of eHHPF
$PF^{\star}$	Project Particle Filter using Finite-Time Lyapunov Vectors
$PF^{\dagger}$	Project Particle Filter using Left-Singular Vectors
$PF^{\ddagger}$	Project Particle Filter using Future Right-Singular Vectors
$nPF^{\ddagger}$	Nudged Variant of $PF^{\ddagger}$
RMSE	Root Mean Square Error
AUS	Assimilation in the Unstable Subspace
SVD	Singular Value Decomposition
EKF	Extended Kalman Filter
IEnKS	Iterative Ensemble Kalman Smoother
SRB	Sinai-Ruelle-Bowen
RK4	Runge-Kutta 4

Chapter 1

Introduction and Motivation

The mathematical object of interest in filtering theory is a conditional probability distribution for an unobserved signal process given indirect observations, which we refer to as the filter. In different contexts, filtering is also known as data assimilation or estimation. The signal process may be taken as deterministic or stochastic, but one assumes that the observation process is noisy. Efficient and accurate assimilation is an important capability in many applications. It allows for informed decision making, synthesis of effective control, and accurate future prediction of the model being estimated.

In this dissertation, we are driven by current issues in filtering for the geosciences (e.g., oceanic, atmospheric, or climate problems), which is a slowly maturing field [Lee+19]. Models in this field have dynamics that are chaotic, which means that small errors in the filter estimate grow exponentially with time. If observations are sparse temporally and spatial (a commonality for problems in the geosciences) or excessively noisy, then it may be hard to quell the error growth due to the chaotic stretching. The models are also high dimensional, due to discretization of the governing partial differential equations into a system of ordinary differential equations; global circulation models in the atmospheric and weather sciences can be of the order $\mathcal{O}(10^9)$ degrees of freedom. The global circulation models can also receive on the order of $\mathcal{O}(10^7)$ observations during a 6-12 hr timespan for assimilation. The size of such problems means that even linear data assimilation cannot be solved adequately [Lee+19]. Additionally, these observations may be correlated with the environment (e.g., ocean buoys or unmanned aerial vehicles being actively disturbed by the ocean or atmosphere). Appropriately accounting for this correlation can improve the data assimilation accuracy.

An additional property of the geoscience models is that they may possess multiple spatial and temporal scales; a natural consequence due to the necessity of resolving the fundamental partial differential equations accurately. Resolving the models on finer scales, for example convective processes, is becoming necessary and hence more common [Yan+18]. The presence of multiple timescales leads to two issues for efficient filtering. The first is that when the faster timescales correspond to smaller spatial scales, then the dimension of the model increases more quickly for modeling the fast scale versus a slower scale. The second issue is that stable numerical integration requires an integration step size that is bounded above by some factor

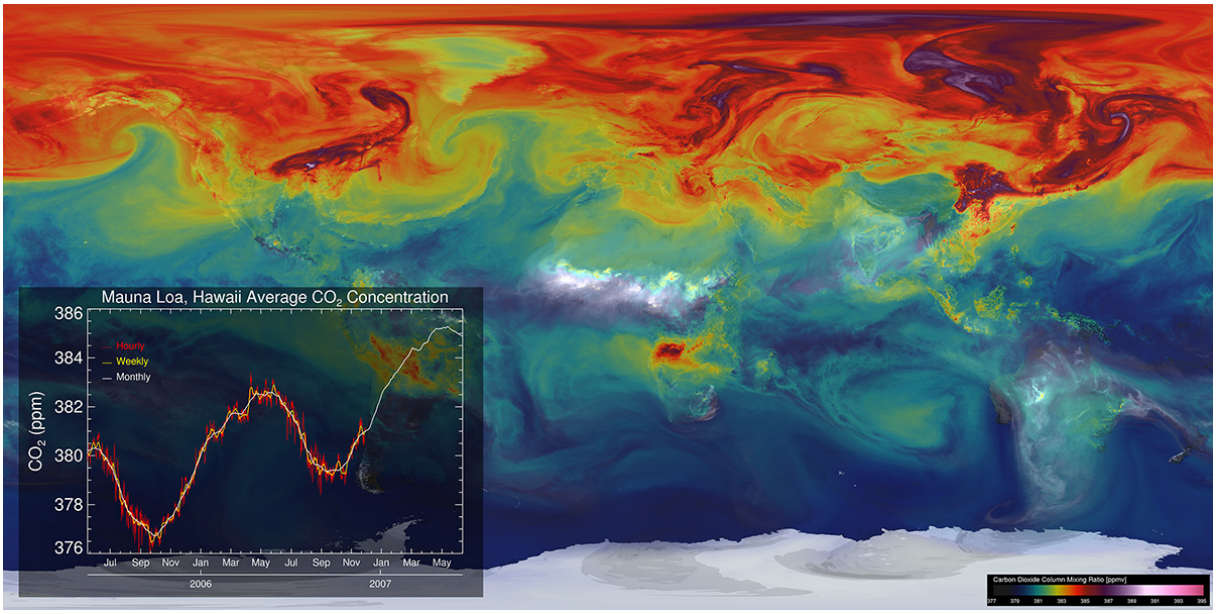

Figure 1.1: (CO2) concentrations at Mauna Loa, Hawaii, and column CO2 mixing ratios dispersed by weather systems within the large-scale flow in a 7-km global simulation with the Goddard Earth Observing System Model, Version 5 (GEOS-5)[Put20]

of the fastest scale process (i.e., the problem becomes numerically stiff). Therefore simulating the model becomes computationally burdensome over long time intervals, and the brute force solution is to provide larger computational processing power.

As an example to visually understand the high dimensionality of such problems, as well as the spatial and timescale variability and the associated computational requirements, we include an image by Willam Putnam of NASA Goddard Space Flight Center's Global Modeling and Assimilation Office [Put20] in Figure 1.1. The primary purpose of the model is for understanding the dynamics of CO2 concentrations. It uses a 7 km spatial scale with inclusion of modeling for aerosols (dust, sea salt, sulfate, and black and organic carbon), trace gas concentrations (ozone, carbon monoxide, and carbon dioxide) and emissions downscaled to 10 km using ancillary information such as power plant location, population density, and night-light information. Simulating such a model required the NASA Discover supercomputer (480 2.8-GHz, 16-core Xeon Sandy Bridge nodes). A simulation for May 2005 through June 2007 at 30 minute intervals required 75 days of computation (13 million processor hours), with 4 petabytes of data output.

In this dissertation, we do not attempt to solve such large problems directly, but instead use such problems as motivation to concentrate on proving fundamental theoretical results that can provide justification for more efficient numerical methods in filtering theory. We are also interested in developing novel algorithms to address the central issues with applying filtering in the geosciences.

Our initial efforts will focus on the question of how to use the multiple timescales present in such models to our advantage. We emphasize in Chapters 3 and 4, that if we have a multiple timescale system, and we are only interested in estimation of the slow timescale process, then we should try to find a reduced order filter that approximates the true filter, but with the fast timescales averaged out in an appropriate sense. The reduced order filter should then be defined on a state space with dimension equal to that of the slow process. Such a result does two things to improve the computational tractability of solving the filtering problem: 1. it reduces the dimension of the filtering problem, and 2. it removes the stiffness property of the differential equations by eliminating the timescale separation. In Chapters 3 and 4, we frame this problem in the context of asymptotic analysis, where we considered the limit of large timescale separation. The results we prove in these chapters provides the mathematical justification that enables practitioners to devise more efficient methods for estimation of the slow process with small loss of accuracy–as demonstrated in Chapter 5 as well as the work by Park et al. [PNY11], Kang and Harlim [KH12], Berry and Harlim [BH14], and Yeong et al. [Yeo+20].

To prove that the filter converges to a reduced order filter, we make use of the assumption that an averaging or homogenization result holds for our multiple timescale signal in the limit of large timescale separation. The filter convergence will not be a trivial consequence of this assumption. In Chapter 2 we provide the necessary background on the homogenization (and hence averaging) principles for the multiple timescale signal. In the context of a correlated filtering problem, we derive the nonlinear evolution equation driven by the observation process that describes the time evolution of the conditional probability distribution.

In Chapter 3 we consider the question of filter approximation in the limit of large timescale separation for the case of a slow-fast dynamical system with correlation between the slow signal and observation processes. We follow the approach taken by Imkeller et al. [Imk+13] to use a linear expansion of the dual process to the unnormalized filter, and a probabilistic representation with backward doubly stochastic differential equations (BDSDE) for terms in this linear expansion. The unnormalized filter is a measure-valued process and the dual process, due to Pardoux [Par80], satisfies a backward stochastic partial differential equation. Therefore the approach using BDSDEs gives a finite-dimensional representation upon which Grönwall's lemma is applicable. From this approach and the use of sharp estimates for the transition density and semigroup of the fast process by Pardoux and Veretennikov [PV03], we are able to prove a rate of convergence of the filter to an averaged version in the limit of large timescale separation. The convergence of the filter occurs almost surely in the topology of weak convergence.

With Chapter 4 we consider a similar problem as the one addressed in Chapter 3, but this time we allow for an intermediate timescale forcing to the slow signal process. The inclusion of the intermediate

timescale prevents us from using the same mathematical approach of Chapter 3. We instead pursue an idea that parallels the work of Kushner [Kus90, Chapter 6]. The main idea is to first show tightness of (signed) measure-valued processes parameterized by the timescale separation parameter, which proves the existence of weak limits. We then characterize those limits, showing they satisfy the averaged equation, and prove the limit to be unique. The main result is that the filter converges in probability for a metric that generates the topology of weak convergence.

The second half of the dissertation pivots to the development of numerical algorithms to realize the theoretical results of Chapters 3 and 4, and to produce methods based on control, transportation, and dynamical systems theory that further address the issues of filtering high dimensional chaotic systems. We focus on the development of particle filtering methods, also known as sequential Monte Carlo methods. Particle filtering is a general approach that can handle the nonlinear, non-Gaussian case. The central issue with applying particle filters is that they suffer from particle collapse; this also goes by the name of particle degeneracy or particle impoverishment. The issue is more pronounced in high dimensional systems; it is a curse of dimensionality. It is for this reason that application of particle filters in the geosciences is still in its infancy. Therefore the numerical algorithms that we develop in Chapters 5 and 6 are often aimed at rectifying this issue.

We begin Chapter 5 with an overview of Bayesian filtering and introduce the sequential importance sampling particle filter, which we will refer to as the standard particle filter. This filter is then modified using the heterogenous multiscale method by E and Engquist [EE03] to create a reduced order filter for the averaged filtering equation. We further enhance the reduced order filter by taking into account the symmetric graph structure of models in the geosciences and the effects of correlation between the signal and observation processes. Using a two timescale, stochastic version of the Lorenz '96 model [Lor95], we demonstrate that for a fixed accuracy, our reduced order methods perform an order of magnitude quicker than the standard particle filter. We then enhance optimal proposal particle filtering algorithms, that control particles to guide them to more representative locations at the observation time, with a tempering phase at the time of assimilation (a transportation particle filter approach). These methods are tested on a stochastic version of the Lorenz '63 model [Lor63], where the efficacy of the controlled particle and tempering approach is demonstrated.

In Chapter 6 we adopt a dynamical systems viewpoint to address the issue of particle collapse. We focus on chaotic systems, which have a splitting of the tangent space corresponding to stable, neutral, and unstable subspaces. The theme of the chapter is to perform data assimilation in the unstable subspace to reduce the observation dimension and therefore mitigate particle collapse. Assimilation in the unstable subspace

was made popular by Trevisan and colleagues [TDT10], but for the case of linear Gaussian estimation, and therefore had a different justification for using such approaches. We use a similar projection framework by Maclean and Van Vleck [MV19] to achieve this result, but generate our projection operators from both finite-time Lyapunov vectors and singular vectors. We demonstrate the efficacy of our methods on the single timescale Lorenz '96 model in both weakly chaotic, non-Gaussian and strongly chaotic, near-Gaussian regimes. Our projection particle filtering method using future right-singular vectors outperforms the standard particle filtering approach in root-mean-square error, diversity of the particle ensemble, and robustness.

We end the dissertation with Chapter 7, which provides a summary of the problems addressed, our approaches to solve them, and the main theoretical and numerical results. We also provide guidance for future research on the topics of this dissertation.

Chapter 2

Nonlinear Filtering Theory

In this chapter, we introduce the problem of continuous time nonlinear filtering theory, which is concerned with the computation of a conditional probability distribution π for an unobserved nonlinear signal process X given an indirect nonlinear observation process Y. The signal process may be taken as deterministic or stochastic, but one assumes that the observation process is noisy. For instance, consider (X, Y) as a solution to the following system of stochastic differential equations

$$\begin{aligned} dX_t &= b(X_t)dt + \sigma(X_t)dW_t, \\ dY_t &= h(X_t)dt + dU_t, \quad Y_0 = 0, \end{aligned} \tag{2.0.1}$$

driven by independent Brownian motions W and U. The filter, π, is then a process taking values in the space of probability measures. In particular, at time $t > 0$, π_t is the conditional distribution of X_t given the information $\mathcal{Y}_t = \sigma(\{Y_s \,|\, 0 \leq s \leq t\})$, the σ-algebra generated by Y up to time t. A useful characterization of π_t then comes from its action on integrable functions φ, $\pi_t(\varphi) = \mathbb{E}\left[\varphi(X_t) \,|\, \mathcal{Y}_t\right]$, as the conditional expectation. If the drift coefficient b, dispersion coefficient σ, or sensor function h in Eq. 2.0.1 are nonlinear, then the problem of computing π_t is said to be a nonlinear filtering problem.

In the sections to follow, we will develop the necessary tools to build towards a presentation of the continuous time nonlinear filtering equations in the context of a multiple timescale signal process with correlation between the observation process and the slow component of the signal process. The usage of the multiple timescale and correlated noise filtering equations will be used in Chapters 3 and 4. There is also great interest in filtering theory for discrete time signal or observation processes (i.e., sequences of random variables). In Chapters 5 and 6 we will introduce numerical approaches for solving the nonlinear filtering equations in the context of continuous time signal process and discrete time observation process. These numerical methods will then be applied to test problems in Chapters 5 and 6.

2.1 Multiple Timescale Correlated Systems

This section introduces the background and notation for the stochastic differential equations, their semigroups and generators, to be considered in the dissertation. We start by introducing the multiple timescale correlated system that will be consider in Chapter 4. A simpler version is considered in Chapter 3. Consider a filtered probability space $(\Omega, \mathcal{F}, (\mathcal{F}_t)_{t\geq 0}, \mathbb{Q})$ supporting a $(w+v+u)$ real-valued $\mathcal{F}_t$-adapted Brownian motion (W, V, U). The signal and observation processes consist of the following SDEs,

$$\begin{aligned} dX_t^\epsilon &= \left[b(X_t^\epsilon, Z_t^\epsilon) + \frac{1}{\epsilon} b_I(X_t^\epsilon, Z_t^\epsilon)\right] dt + \sigma(X_t^\epsilon, Z_t^\epsilon) dW_t, \\ dZ_t^\epsilon &= \frac{1}{\epsilon^2} f(X_t^\epsilon, Z_t^\epsilon) dt + \frac{1}{\epsilon} g(X_t^\epsilon, Z_t^\epsilon) dV_t, \\ dY_t^\epsilon &= h(X_t^\epsilon, Z_t^\epsilon) dt + \alpha dW_t + \beta dV_t + \gamma dU_t, \quad Y_0^\epsilon = 0 \in \mathbb{R}^d, \end{aligned} \tag{2.1.1}$$

where $b, b_{\mathrm{I}} : \mathbb{R}^m \times \mathbb{R}^n \to \mathbb{R}^m$, $\sigma : \mathbb{R}^m \times \mathbb{R}^n \to \mathbb{R}^m \times \mathbb{R}^w$, $f : \mathbb{R}^m \times \mathbb{R}^n \to \mathbb{R}^n$, $g : \mathbb{R}^m \times \mathbb{R}^n \to \mathbb{R}^n \times \mathbb{R}^v$ and $h : \mathbb{R}^m \times \mathbb{R}^n \to \mathbb{R}^d$ are Borel measurable functions. The initial distribution of the signal process $(X_0^\epsilon, Z_0^\epsilon)$ at $t = 0$ is denoted by $\mathbb{Q}_{(X_0^\epsilon, Z_0^\epsilon)}$ and is assumed independent of the (W, V, U) Brownian motion. $\mathbb{Q}_{(X_0^\epsilon, Z_0^\epsilon)}$ is also assumed to have finite moments for all orders.

In Eq. 2.1.1, $0 < \epsilon \ll 1$ is a timescale separation parameter. Therefore X^ϵ is a slow process and Z^ϵ is the fast process. The slow process also possesses an intermediate timescale due to the intermediate drift coefficient b_{I}. We will also refer to the slow process as the coarse-grain process, and the fast process as the fine-grain process. In Chapters 3 and 4, we consider the limit of the x-marginal of the nonlinear filter when the timescale separation parameter tends to zero.

The presence of αdW_t for $\alpha \neq 0$ in the observation process implies that the observation process and the slow process are correlated. Similarly, βdV_t for $\beta \neq 0$ implies correlation between the observation and fast process. We consider the case where $\alpha \in \mathbb{R}^{d\times w}, \beta \in \mathbb{R}^{d\times v}, \gamma \in \mathbb{R}^{d\times u}$, and assume the following to be true

$$K \equiv \alpha\alpha^* + \beta\beta^* + \gamma\gamma^* \succ 0, \qquad \gamma\gamma^* \succ 0, \tag{2.1.2}$$

where $\succ$ is the order relation implying that $K, \gamma\gamma^*$ are positive definite, and γ^* is the transpose of the matrix γ. Eq. 2.1.2 implies the existence of a unique $\mathbb{R}^{d\times d} \ni \kappa \succ 0$ of lower triangular form, such that $K = \kappa\kappa^*$ (see for instance Proposition A.1.2). Hence there exists a unique κ^{-1} (see for instance Proposition A.1.3), such

that we can define an auxiliary observation process

$$Y_t^{\epsilon,\kappa} = \int_0^t \kappa^{-1} dY_s^\epsilon = \int_0^t \kappa^{-1} h(X_s^\epsilon, Z_s^\epsilon) ds + B_t, \quad Y_0^{\epsilon,\kappa} = 0 \in \mathbb{R}^d,$$

where

$$B_t = \kappa^{-1} \left(\alpha W_t + \beta dV_t + \gamma dU_t \right),$$

is a standard Brownian motion under $\mathbb{Q}$.

The filter, π^ϵ, is a condition distribution of the signal given the observation filtration. In particular, for a fixed test function $\varphi \in C_b^2(\mathbb{R}^m \times \mathbb{R}^n; \mathbb{R})$ and time $t \in [0, T]$, the filter can be characterized as

$$\pi_t^\epsilon(\varphi) = \mathbb{E}_\mathbb{Q} \left[\varphi(X_t^\epsilon, Z_t^\epsilon) \,|\, \mathcal{Y}_t^\epsilon \right], \tag{2.1.3}$$

where $\mathcal{Y}_t^\epsilon \equiv \sigma(\{Y_s^\epsilon \mid s \in [0,t]\}) \vee \mathcal{N}$: the first part is the σ-algebra generated by the observation process over the interval $[0,t]$, $\mathcal{N}$ is the $\mathbb{Q}$ negligible sets, and $\vee$ is the joining of the two σ-algebras (i.e., the σ-algebra of the union). By the measurability of h, $(\mathcal{Y}_t^\epsilon)_{t\geq 0}$ is a subfiltration of $(\mathcal{F}_t)_{t\geq 0}$ and is complete with respect to $\mathbb{Q}$ due to the joining of $\mathcal{N}$ at each time t. Assuming h is a measurable function, $(\mathcal{Y}_t^\epsilon)_{t\geq 0}$ will also be a right-continuous filtration [BC09, Theorem 2.35, p.40],

$$\mathcal{Y}_t^\epsilon = \bigcap_{s>t} \mathcal{Y}_s^\epsilon, \quad \forall t \geq 0.$$

The filtrations generated by Y^ϵ and $Y^{\epsilon,\kappa}$ are equivalent (see for instance [Kal97, Lemma 1.13, p.7]), and therefore either can be used in the definition of π^ϵ. Therefore in Chapters 3 and 4, where we will consider the correlated noise case, we will work with a redefined observation process, which we define as follows: the sensor function is redefined as $h \leftarrow \kappa^{-1} h$, and $\alpha \leftarrow \kappa^{-1}\alpha$, $\beta \leftarrow \kappa^{-1}\beta$, $\gamma \leftarrow \kappa^{-1}\gamma$, so that the observation process can be redefined as

$$dY_t^\epsilon = h(X_t^\epsilon, Z_t^\epsilon) dt + dB_t, \quad Y_0^\epsilon = 0 \in \mathbb{R}^d, \tag{2.1.4}$$

where $B = \alpha W + \beta V + \gamma U$ is a standard Brownian motion under $\mathbb{Q}$ and still correlated with W and V.

2.1.1 Markov Transition Semigroups and Infinitesimal Generators

In the case where the coefficients of Eq. 2.1.1 are Lipschitz, the solutions to the SDEs satisfy strong existence and uniqueness conditions, and are Markov processes with Feller semigroups, whose infinitesimal generators are second order differential operators [Le 14, Chapter 8]. Because the signal process (X^ϵ, Z^ϵ) is a Markov process, it possesses a Markov transition semigroup $(T_t^\epsilon)_{t\geq 0}$ (a collection of Markov transition kernels), such that the following hold:

1. For every $(x,z) \in \mathbb{R}^m \times \mathbb{R}^n$, $T_0^\epsilon((x,z), dx \times dz) = \delta_{(x,z)}(dx \times dz)$,
2. For every $s,t \geq 0$ and measurable $A \subseteq \mathbb{R}^m \times \mathbb{R}^n$,

$$T_{t+s}^\epsilon((x,z),A) = \int_{\mathbb{R}^m \times \mathbb{R}^n} T_t^\epsilon((x,z), dx' \times dz') T_s^\epsilon((x',z'),A),$$

3. For every measurable $A \subseteq \mathbb{R}^m \times \mathbb{R}^n$, the function $(t,(x,z)) \mapsto T_t^\epsilon((x,z),A)$ is measurable with respect to the σ-field $\mathcal{B}(\mathbb{R}_+) \otimes \mathcal{B}(\mathbb{R}^m \times \mathbb{R}^n)$.

The second condition is the Chapman-Kolmogorov identity and in the third condition, $\mathcal{B}$ is the Borel σ-algebra. An important property of the Markov transition kernels $T_\cdot^\epsilon$ is that their action on bounded measurable functions $\varphi : \mathbb{R}^m \times \mathbb{R}^n \to \mathbb{R}$, is the following:

$$T_\cdot^\epsilon \varphi(x,z) = \int_{\mathbb{R}^m \times \mathbb{R}^n} \varphi(x',z') T_\cdot^\epsilon((x,z), dx' \times dz'),$$

where the subscript $\cdot$ indicates that the statement holds for any $t \geq 0$. That is, $T_\cdot^\epsilon$ maps the function φ to a new function: $T_\cdot^\epsilon \varphi : \mathbb{R}^m \times \mathbb{R}^n \to \mathbb{R}$. Because the semigroup $(T_t^\epsilon)_{t\geq 0}$ is associated to the Markov process (X^ϵ, Z^ϵ), we can similarly characterize this action as

$$T_t^\epsilon \varphi(x,z) = \mathbb{E}_{\mathbb{Q}} \left[\varphi \left(X_t^{\epsilon;(0,x)}, Z_t^{\epsilon;(0,z)} \right) \right],$$

or if the probability measures induced by (X^ϵ, Z^ϵ) possess a density with respect to Lebesgue measure μ_L, we can write

$$T_t^\epsilon \varphi(x,z) = \int_{\mathbb{R}^m \times \mathbb{R}^n} \varphi(x',z') p_t(x',z';x,z) \mu_L(dx \times dz).$$

Some clarification of the notation in the previous lines are that $(X_t^{\epsilon;(0,x)}, Z_t^{\epsilon;(0,z)})$ is the solution to the signal process of Eq. 2.1.1 at time $t > 0$ with deterministic initial conditions (x,z) at time 0. And $p_t(x',z';x,z)$ is

the transition density of the same process at time $t > 0$.

If the semigroup $(T_t^\epsilon)_{t\geq 0}$ is a Feller semigroup, we have that: 1. $T_\cdot^\epsilon(\varphi) \in C_0(\mathbb{R}^m \times \mathbb{R}^n; \mathbb{R})$ for all $\varphi \in C_0(\mathbb{R}^m \times \mathbb{R}^n; \mathbb{R})$, and 2. $\lim_{t\to 0} |T_t^\epsilon \varphi - \varphi| = 0$ for all $\varphi \in C_0(\mathbb{R}^m \times \mathbb{R}^n; \mathbb{R})$, where C_0 is the space of continuous functions that vanish at infinity and $|\cdot|$ is the supremum norm [Le 14, p.158]. We can therefore talk about the set of functions

$$D(\mathcal{G}^\epsilon) = \left\{ \varphi \in C_0(\mathbb{R}^m \times \mathbb{R}^n; \mathbb{R}) \;\middle|\; \lim_{t\to 0} \frac{T_t^\epsilon \varphi - \varphi}{t} \in C_0(\mathbb{R}^m \times \mathbb{R}^n; \mathbb{R}) \right\},$$

and for every $\varphi \in D(\mathcal{G}^\epsilon)$ we then define

$$\mathcal{G}^\epsilon \varphi = \lim_{t\to 0} \frac{T_t^\epsilon \varphi - \varphi}{t}.$$

$\mathcal{G}^\epsilon$ is called the generator of the Markov semigroup $(T_t^\epsilon)_{t\geq 0}$, or analogously of the Markov process (X^ϵ, Z^ϵ). Still considering $(T_t^\epsilon)_{t\geq 0}$ to be a Feller semigroup, we have that $C_c^2(\mathbb{R}^m \times \mathbb{R}^n; \mathbb{R}) \subset D(\mathcal{G}^\epsilon)$ and for every $\varphi \in C_c^2(\mathbb{R}^m \times \mathbb{R}^n; \mathbb{R})$, we can characterize $\mathcal{G}^\epsilon$ as a linear second order differential operator [Le 14, p.222],

$$\begin{aligned} \mathcal{G}^\epsilon(\varphi)(x,z) = &\sum_{i=1}^m \left(b_i + \frac{1}{\epsilon} b_{I,i} \right)(x,z) \frac{\partial}{\partial x_i} \varphi(x,z) + \frac{1}{2} \sum_{i,j=1}^m (\sigma\sigma^*)_{ij}(x,z) \frac{\partial^2}{\partial x_i \partial x_j} \varphi(x,z) \\ &+ \frac{1}{\epsilon^2} \sum_{i=1}^n f_i(x,z) \frac{\partial}{\partial z_i} \varphi(x,z) + \frac{1}{2\epsilon^2} \sum_{i,j=1}^n (gg^*)_{ij}(x,z) \frac{\partial^2}{\partial z_i \partial z_j} \varphi(x,z). \end{aligned} \tag{2.1.5}$$

For future convenience, we identify components of the linear operator in Eq. 2.1.5 as follows,

$$\begin{aligned} \mathcal{G}_S(x,z) &\equiv \sum_{i=1}^m b_i(x,z) \frac{\partial}{\partial x_i} + \frac{1}{2} \sum_{i,j=1}^m (\sigma\sigma^*)_{ij}(x,z) \frac{\partial^2}{\partial x_i \partial x_j}, \\ \mathcal{G}_I(x,z) &\equiv \sum_{i=1}^m b_{I,i}(x,z) \frac{\partial}{\partial x_i}, \\ \mathcal{G}_F(x,z) &\equiv \sum_{i=1}^n f_i(x,z) \frac{\partial}{\partial z_i} + \frac{1}{2} \sum_{i,j=1}^n (gg^*)_{ij}(x,z) \frac{\partial^2}{\partial z_i \partial z_j}, \\ \mathcal{G}_S^\epsilon &\equiv \frac{1}{\epsilon} \mathcal{G}_I + \mathcal{G}_S, \\ \mathcal{G}^\epsilon &= \frac{1}{\epsilon^2} \mathcal{G}_F + \frac{1}{\epsilon} \mathcal{G}_I + \mathcal{G}_S. \end{aligned}$$

The operators can be can be thought of as generators in their own right. For instance, $\mathcal{G}_F$ is the generator of

the process

$$dZ_t^x = f(x, Z_t^x)dt + g(x, Z_t^x)dV_t, \tag{2.1.6}$$

where $x \in \mathbb{R}^m$ is a fixed value. This process will be useful in the work of Chapters 3 and 4. The semigroup of $\mathcal{G}_F$ will be denoted $(T_t^{F,x})_{t\geq 0}$.

2.2 A Change of Probability Measure Transformation

The derivation of the evolutionary equation for π^ϵ typically proceeds in one of two ways. The first approach uses a change of probability measure transformation so that the observation process becomes a Brownian motion under the new probability measure (Girsanov's theorem). From here, measure-valued process ρ^ϵ can be related to the probability measure-valued process π^ϵ by the Kallianpur-Striebel formula. An evolutionary equation is then derived for ρ^ϵ and by Itô's formula, one retrieves the evolutionary equation for π^ϵ. The evolutionary equation for ρ^ϵ is known as the Zakai equation (or sometimes referred to as the Duncan-Mortensen-Zakai equation in the literature) and will be derived in Section 2.3. The evolutionary equation for π^ϵ is known as the Kushner-Stratonovich equation (or sometimes referred to as the Fujisaki-Kallianpur-Kunita equation in the literature) and will be given in Section 2.4. This first approach is the tact we will take in deriving the Kushner-Stratonovich equation. The second approach makes use of the realization that under appropriate conditions, the process

$$I_t^\epsilon = Y_t^\epsilon - \int_0^t \pi_s^\epsilon(h)ds,$$

is a $\mathcal{Y}_t^\epsilon$-adapted Brownian motion under $\mathbb{Q}$. The innovation process is then identified as the Brownian motion driving the stochastic evolution equation for π^ϵ, and then identification of the terms in the Doob-Meyer decomposition of π^ϵ yields the Kushner-Stratonovich equation (see for instance [BC09, Chapter 3.7, p.70]).

We now present the usual construction for the change of probability measure that will be necessary to define the Zakai equation. Before doing so, let us provide the following notation: the usage of brackets such as $\langle h(X_s^\epsilon, Z_s^\epsilon), dB_s\rangle$ will indicate the operation of the inner product, whereas the operation on two continuous local martingales $\langle M^\epsilon, M^\epsilon\rangle$ indicates the operation of the quadratic variation; and lastly, we use $|\cdot|$ for absolute value on scalar-valued arguments, euclidean norm for vector-valued arguments, and for the Frobenius norm (i.e., $|A| = \sqrt{\mathrm{Tr}(AA^*)}$) when matrix-valued arguments are given.

To define a new probability measure $\mathbb{P}^\epsilon \ll \mathbb{Q}$, absolutely continuous with respect to $\mathbb{Q}$, for a fixed ϵ, we

start be defining the process,

$$D_t^\epsilon = \exp\left(-\int_0^t \langle h(X_s^\epsilon, Z_s^\epsilon), dB_s\rangle - \frac{1}{2}\int_0^t |h(X_s^\epsilon, Z_s^\epsilon)|^2\, ds\right),$$

and assume that $\mathbb{E}_{\mathbb{Q}}\left[\int_0^\infty |h(X_s^\epsilon, Z_s^\epsilon)|^2 ds\right] < \infty$. The continuous local martingale

$$M_t^\epsilon = -\int_0^t \langle h(X_s^\epsilon, Z_s^\epsilon), dB_s\rangle,$$

then has the properties that $\mathbb{Q}$-a.s. $M_0^\epsilon = 0$ and $\langle M^\epsilon, M^\epsilon\rangle_\infty < \infty$.

If $\mathbb{E}_{\mathbb{Q}}\left[D_\infty^\epsilon\right] = 1$, then D^ϵ will be a nonnegative uniformly integrable martingale and we can define D_∞^ϵ to be the density of the probability measure $\mathbb{P}^\epsilon$ with respect to $\mathbb{Q}$. The classical condition that implies $\mathbb{E}_{\mathbb{Q}}\left[D_\infty^\epsilon\right] = 1$ is Novikov's condition (see for instance [Le 14, Theorem 5.23, p.137]),

$$\mathbb{E}_{\mathbb{Q}}\left[\exp\left(\frac{1}{2}\langle M^\epsilon, M^\epsilon\rangle_\infty\right)\right] < \infty. \tag{2.2.1}$$

It turns out that $\mathbb{P}^\epsilon$ is in fact mutually absolutely continuous with respect to $\mathbb{Q}$, and our process D^ϵ is the Radon-Nikodym derivative of $\mathbb{P}^\epsilon$ with respect to $\mathbb{Q}$ restricted to the filtration $\mathcal{F}_t$ (see for instance [Le 14, Proposition 5.20, p.132]),

$$D_t^\epsilon = \left.\frac{d\mathbb{P}^\epsilon}{d\mathbb{Q}}\right|_{\mathcal{F}_t} = \exp\left(-\int_0^t \langle h(X_s^\epsilon, Z_s^\epsilon), dB_s\rangle - \frac{1}{2}\int_0^t |h(X_s^\epsilon, Z_s^\epsilon)|^2\, ds\right).$$

Because $\mathbb{Q} \ll \mathbb{P}^\epsilon$, we also have

$$\widetilde{D}_t^\epsilon \equiv (D_t^\epsilon)^{-1} = \left.\frac{d\mathbb{Q}}{d\mathbb{P}^\epsilon}\right|_{\mathcal{F}_t} = \exp\left(\int_0^t \langle h(X_s^\epsilon, Z_s^\epsilon), dY_s^\epsilon\rangle - \frac{1}{2}\int_0^t |h(X_s^\epsilon, Z_s^\epsilon)|^2\, ds\right).$$

Identifying $\Lambda_t = -\int_0^t \langle h(X_s^\epsilon, Z_s^\epsilon), dB_s\rangle - \frac{1}{2}\int_0^t |h(X_s^\epsilon, Z_s^\epsilon)|^2\, ds$ as a semimartingale, we get from Itô's formula for $\exp(\Lambda_t)$ the evolution equation for D_t^ϵ and $\widetilde{D}_t^\epsilon$,

$$D_t^\epsilon = 1 - \int_0^t \langle D_s^\epsilon h(X_s^\epsilon, Z_s^\epsilon), dB_s\rangle,$$
$$\widetilde{D}_t^\epsilon = 1 + \int_0^t \langle \widetilde{D}_s^\epsilon h(X_s^\epsilon, Z_s^\epsilon), dY_s^\epsilon\rangle.$$

Novikov's condition given in Eq. 2.2.1, is quite restrictive, requiring the consideration of the term $\langle M^\epsilon, M^\epsilon\rangle_\infty$. In practice we are only concerned with the case of finite time $t > 0$. Therefore it is useful in

filtering to instead consider the condition for D^ϵ to be a martingale for all $t > 0$, which is given by

$$\mathbb{E}_{\mathbb{Q}}\left[\exp\left(\frac{1}{2}\langle M^\epsilon, M^\epsilon\rangle_t\right)\right] < \infty, \quad \forall t > 0.$$

Sufficient conditions for the this to be true are (see for example [BC09, Proposition 3.12, p.54])

$$\mathbb{E}_{\mathbb{Q}}\left[\int_0^t |h(X_s^\epsilon)|^2 ds\right] < \infty, \quad \mathbb{E}_{\mathbb{Q}}\left[\int_0^t \widetilde{D}_s^\epsilon |h(X_s^\epsilon)|^2 ds\right] < \infty, \quad \forall t > 0.$$

2.2.1 Girsanov's Theorem

An application of Girsanov's theorem [Le 14, Theorem 5.22, p.134], now states that

$$B_t - \langle B, M\rangle_t = B_t + \int_0^t h(X_s^\epsilon, Z_s^\epsilon) ds = Y_t^\epsilon$$

is a Brownian motion under $\mathbb{P}^\epsilon$. This fact will be useful in deriving the Zakai equation of Section 2.3. We also note that in the case of correlation between the observation process and the signal process, the following are Brownian motions under $\mathbb{P}^\epsilon$,

$$\widetilde{W}_t = W_t - \langle W, M\rangle_t = W_t + \int_0^t \alpha^* h(X_s^\epsilon, Z_s^\epsilon) ds,$$
$$\widetilde{V}_t = V_t - \langle V, M\rangle_t = V_t + \int_0^t \beta^* h(X_s^\epsilon, Z_s^\epsilon) ds,$$

and therefore

$$dX_t^\epsilon = \left[b(X_t^\epsilon, Z_t^\epsilon) + \frac{1}{\epsilon} b_I(X_t^\epsilon, Z_t^\epsilon) - \sigma(X_t^\epsilon, Z_t^\epsilon)\alpha^* h(X_s^\epsilon, Z_s^\epsilon)\right] dt + \sigma(X_t^\epsilon, Z_t^\epsilon) d\widetilde{W}_t,$$
$$dZ_t^\epsilon = \frac{1}{\epsilon^2} f(X_t^\epsilon, Z_t^\epsilon) dt - \frac{1}{\epsilon} g(X_t^\epsilon, Z_t^\epsilon)\beta^* h(X_s^\epsilon, Z_s^\epsilon) dt + \frac{1}{\epsilon} g(X_t^\epsilon, Z_t^\epsilon) d\widetilde{V}_t,$$

are stochastic differential equations driven by the Brownian motion $(\widetilde{W}, \widetilde{V})$ under $\mathbb{P}^\epsilon$.

2.2.2 The Kallianpur-Striebel Formula

Having defined the Radon-Nikodym derivatives D_t^ϵ and $\widetilde{D}_t^\epsilon$, we now explain how the normalized conditional distribution π_t^ϵ can be related to an unnormalized conditional distribution. Let us define ρ^ϵ, an unnormalized conditional distribution, with action on integrable functions φ as $\rho^\epsilon(\varphi) = \mathbb{E}_{\mathbb{P}^\epsilon}\left[\varphi(X_t^\epsilon, Z_t^\epsilon)\widetilde{D}_t^\epsilon \mid \mathcal{Y}_t^\epsilon\right]$. This finite positive measure-valued process is related to the normalized conditional distribution through the

Kallianpur-Striebel formula,

$$\pi_t^\epsilon(\varphi) = \frac{\mathbb{E}_{\mathbb{P}^\epsilon}\left[\varphi(X_t^\epsilon, Z_t^\epsilon)\widetilde{D}_t^\epsilon \mid \mathcal{Y}_t^\epsilon\right]}{\mathbb{E}_{\mathbb{P}^\epsilon}\left[\widetilde{D}_t^\epsilon \mid \mathcal{Y}_t^\epsilon\right]} = \frac{\rho_t^\epsilon(\varphi)}{\rho_t^\epsilon(1)}, \qquad \forall t \in [0,\infty), \qquad \mathbb{Q}, \mathbb{P}^\epsilon\text{-a.s.}$$

For a derivation of the Kallianpur-Striebel formula, which can by thought of as an equivalent of Bayes' theorem in our context (see for instance [BC09, Proposition 3.16, p.57]).

2.3 The Zakai Equation

The Zakai equation is the evolutionary equation for the unnormalized conditional distribution ρ^ϵ. Derivations of the equation can be found in the works of Bain and Crisan [BC09, Chapter 3.5, p.61] or Bensoussan [Ben04], with an extension for the correlated case given in Bain and Crisan's text [BC09, Chapter 3.8, p.73] using the innovation process approach. In this section, we provide a non-standard proof with stronger assumptions on the process $\widetilde{D}^\epsilon$ and the coefficients of the signal and observation processes (cf. [Han07, p.180]). We do this to provide a more intuitive reference for the averaged Zakai equations that will arise in Chapters 3 and 4.

The derivation starts by considering the characterization of $\rho_t^\epsilon(\varphi)$ for a fixed test function $\varphi \in C_b^2(\mathbb{R}^m \times \mathbb{R}^n; \mathbb{R})$ and times $0 < t \leq T < \infty$,

$$\rho_t^\epsilon(\varphi) = \mathbb{E}_{\mathbb{P}^\epsilon}\left[\varphi(X_t^\epsilon, Z_t^\epsilon)\widetilde{D}_t^\epsilon \mid \mathcal{Y}_t^\epsilon\right].$$

Applying Itô's formula to the product $\varphi(X_t^\epsilon, Z_t^\epsilon)\widetilde{D}_t^\epsilon$ yields,

$$\begin{aligned}\varphi(X_t^\epsilon, Z_t^\epsilon)\widetilde{D}_t^\epsilon = \varphi(X_0^\epsilon, Z_0^\epsilon)\widetilde{D}_0^\epsilon &+ \int_0^t \langle \widetilde{D}_r^\epsilon \varphi h(X_r^\epsilon, Z_r^\epsilon), dY_r^\epsilon\rangle + \int_0^t \widetilde{D}_r^\epsilon \mathcal{G}^\epsilon \varphi(X_r^\epsilon, Z_r^\epsilon) dr \\ &+ \int_0^t \langle \widetilde{D}_r^\epsilon \nabla_x \varphi(X_r^\epsilon, Z_r^\epsilon), \sigma(X_r^\epsilon, Z_r^\epsilon) d\widetilde{W}_r\rangle + \int_0^t \langle \widetilde{D}_r^\epsilon \frac{1}{\epsilon}\nabla_z \varphi(X_r^\epsilon, Z_r^\epsilon), g(X_r^\epsilon, Z_r^\epsilon) d\widetilde{V}_r\rangle.\end{aligned}$$

Now taking the conditional expectation of each side of the equation gives,

$$\begin{aligned}\rho_t^\epsilon(\varphi) = \rho_0^\epsilon(\varphi) &+ \mathbb{E}_{\mathbb{P}^\epsilon}\left[\int_0^t \langle \widetilde{D}_r^\epsilon \varphi h(X_r^\epsilon, Z_r^\epsilon), dY_r^\epsilon\rangle \,\middle|\, \mathcal{Y}_t^\epsilon\right] + \mathbb{E}_{\mathbb{P}^\epsilon}\left[\int_0^t \widetilde{D}_r^\epsilon \mathcal{G}^\epsilon \varphi(X_r^\epsilon, Z_r^\epsilon) dr \,\middle|\, \mathcal{Y}_t^\epsilon\right] \\ &+ \mathbb{E}_{\mathbb{P}^\epsilon}\left[\int_0^t \langle \widetilde{D}_r^\epsilon \nabla_x \varphi(X_r^\epsilon, Z_r^\epsilon), \sigma(X_r^\epsilon, Z_r^\epsilon) d\widetilde{W}_r\rangle \,\middle|\, \mathcal{Y}_t^\epsilon\right] + \mathbb{E}_{\mathbb{P}^\epsilon}\left[\int_0^t \langle \widetilde{D}_r^\epsilon \frac{1}{\epsilon}\nabla_z \varphi(X_r^\epsilon, Z_r^\epsilon), g(X_r^\epsilon, Z_r^\epsilon) d\widetilde{V}_r\rangle \,\middle|\, \mathcal{Y}_t^\epsilon\right],\end{aligned} \tag{2.3.1}$$

where $\rho_0^\epsilon(\varphi) = \mathbb{E}_{\mathbb{Q}}\left[\varphi(X_0^\epsilon, Z_0^\epsilon)\right]$ since there is no observation information at the initial time and $\widetilde{D}_0^\epsilon = 1$ almost surely. The main task is to show that the conditional expectation can be interchanged with the stochastic

and finite variation integrals to yield an evolution equation for $\rho^\epsilon(\varphi)$ driven by the Brownian motion Y^ϵ (under $\mathbb{P}^\epsilon$). Assume for the time being that each of the integrands are elements of $L^2_{\mu_L([0,t])\times\mathbb{P}^\epsilon}$, where μ_L is Lebesgue measure on $\mathbb{R}_+$. We address the first stochastic integral of Eq. 2.3.1 by letting $A \in \mathcal{Y}_t^\epsilon$ and then by Itô's representation theorem, there exists a function $F \in L^2_{\mu_L([0,t])\times\mathbb{P}^\epsilon}$ that is $\mathcal{Y}_t^\epsilon$-adapted such that

$$1_A = \mathbb{P}^\epsilon(A) + \int_0^t \langle F_r, dY_r^\epsilon \rangle.$$

Then we have

$$\begin{aligned}\mathbb{E}_{\mathbb{P}^\epsilon}\left[1_A \int_0^t \langle \widetilde{D}_r^\epsilon \varphi h(X_r^\epsilon, Z_r^\epsilon), dY_r^\epsilon\rangle\right] &= \mathbb{P}^\epsilon(A)\mathbb{E}_{\mathbb{P}^\epsilon}\left[\int_0^t \langle \widetilde{D}_r^\epsilon \varphi h(X_r^\epsilon, Z_r^\epsilon), dY_r^\epsilon\rangle\right] \\ &\quad + \mathbb{E}_{\mathbb{P}^\epsilon}\left[\int_0^t \langle F_r, dY_r^\epsilon\rangle \int_0^t \langle \widetilde{D}_r^\epsilon \varphi h(X_r^\epsilon, Z_r^\epsilon), dY_r^\epsilon\rangle\right],\end{aligned} \tag{2.3.2}$$

but the first term vanishes because the stochastic integral is a martingale. Then by Itô's isometry, Fubini's theorem, the tower property of conditional expectation and again Fubini's theorem,

$$\begin{aligned}\mathbb{E}_{\mathbb{P}^\epsilon}\left[\int_0^t \langle F_r, dY_r^\epsilon\rangle \int_0^t \langle \widetilde{D}_r^\epsilon \varphi h(X_r^\epsilon, Z_r^\epsilon), dY_r^\epsilon\rangle\right] &= \mathbb{E}_{\mathbb{P}^\epsilon}\left[\int_0^t \langle F_r, \widetilde{D}_r^\epsilon \varphi h(X_r^\epsilon, Z_r^\epsilon)\rangle dr\right] \\ &= \mathbb{E}_{\mathbb{P}^\epsilon}\left[\int_0^t \langle F_r, \mathbb{E}_{\mathbb{P}^\epsilon}\left[\widetilde{D}_r^\epsilon \varphi h(X_r^\epsilon, Z_r^\epsilon)\,\middle|\,\mathcal{Y}_r^\epsilon\right]\rangle dr\right]\end{aligned}$$

Repeating the same process from Eq. 2.3.2 by changing the integrand of the stochastic integral from $\widetilde{D}_r^\epsilon \varphi h(X_r^\epsilon, Z_r^\epsilon)$ to $\mathbb{E}_{\mathbb{P}^\epsilon}\left[\widetilde{D}_r^\epsilon \varphi h(X_r^\epsilon, Z_r^\epsilon)\,\middle|\,\mathcal{Y}_r^\epsilon\right]$, we get the same result

$$\mathbb{E}_{\mathbb{P}^\epsilon}\left[1_A \int_0^t \langle \mathbb{E}_{\mathbb{P}^\epsilon}\left[\widetilde{D}_r^\epsilon \varphi h(X_r^\epsilon, Z_r^\epsilon)\,\middle|\,\mathcal{Y}_r^\epsilon\right], dY_r^\epsilon\rangle\right] = \mathbb{E}_{\mathbb{P}^\epsilon}\left[\int_0^t \langle F_r, \mathbb{E}_{\mathbb{P}^\epsilon}\left[\widetilde{D}_r^\epsilon \varphi h(X_r^\epsilon, Z_r^\epsilon)\,\middle|\,\mathcal{Y}_r^\epsilon\right]\rangle dr\right].$$

Because the statement holds for all $A \in \mathcal{Y}_t^\epsilon$, by Kolmogorov's characterization of conditional expectation, we have that

$$\mathbb{E}_{\mathbb{P}^\epsilon}\left[\int_0^t \langle \widetilde{D}_r^\epsilon \varphi h(X_r^\epsilon, Z_r^\epsilon), dY_r^\epsilon\rangle\,\middle|\,\mathcal{Y}_t^\epsilon\right] = \int_0^t \langle \mathbb{E}_{\mathbb{P}^\epsilon}\left[\widetilde{D}_r^\epsilon \varphi h(X_r^\epsilon, Z_r^\epsilon)\,\middle|\,\mathcal{Y}_r^\epsilon\right], dY_r^\epsilon\rangle = \int_0^t \langle \rho_r^\epsilon(\varphi h), dY_r^\epsilon\rangle.$$

The same arguments apply for the time integral; an application of Fubini's theorem and the tower property of conditional expectation to the time integral of Eq. 2.3.1 gives

$$\mathbb{E}_{\mathbb{P}^\epsilon}\left[\int_0^t \widetilde{D}_r^\epsilon \mathcal{G}^\epsilon \varphi(X_r^\epsilon, Z_r^\epsilon) dr\,\middle|\,\mathcal{Y}_t^\epsilon\right] = \int_0^t \mathbb{E}_{\mathbb{P}^\epsilon}\left[\widetilde{D}_r^\epsilon \mathcal{G}^\epsilon \varphi(X_r^\epsilon, Z_r^\epsilon)\,\middle|\,\mathcal{Y}_r^\epsilon\right] dr = \int_0^t \rho_r^\epsilon(\mathcal{G}^\epsilon \varphi) dr.$$

Let us now consider the terms

$$\mathbb{E}_{\mathbb{P}^\epsilon}\left[\int_0^t \langle \widetilde{D}_r^\epsilon \nabla_x \varphi(X_r^\epsilon, Z_r^\epsilon), \sigma(X_r^\epsilon, Z_r^\epsilon) d\widetilde{W}_r\rangle \,\middle|\, \mathcal{Y}_t^\epsilon\right] \quad \text{and} \quad \mathbb{E}_{\mathbb{P}^\epsilon}\left[\int_0^t \langle \widetilde{D}_r^\epsilon \frac{1}{\epsilon}\nabla_z \varphi(X_r^\epsilon, Z_r^\epsilon), g(X_r^\epsilon, Z_r^\epsilon) d\widetilde{V}_r\rangle \,\middle|\, \mathcal{Y}_t^\epsilon\right]$$

in Eq. 2.3.1, which are due to the signal and observation correlation. These terms are handled in a similar manner as $\mathbb{E}_{\mathbb{P}^\epsilon}\left[\int_0^t \langle \widetilde{D}_r^\epsilon \varphi h(X_r^\epsilon, Z_r^\epsilon), dY_r^\epsilon\rangle \,\middle|\, \mathcal{Y}_t^\epsilon\right]$, but we would like for the resulting stochastic integrals to be driven by Y^ϵ as opposed to $\widetilde{W}$ or $\widetilde{V}$. Therefore consider the term $\mathbb{E}_{\mathbb{P}^\epsilon}\left[\int_0^t \langle \widetilde{D}_r^\epsilon \nabla_x \varphi(X_r^\epsilon, Z_r^\epsilon), \sigma(X_r^\epsilon, Z_r^\epsilon) d\widetilde{W}_r\rangle \,\middle|\, \mathcal{Y}_t^\epsilon\right]$ (the other correlation term follows the exact same logic), after applying the usual procedure starting from Eq. 2.3.2, we have

$$\mathbb{E}_{\mathbb{P}^\epsilon}\left[\int_0^t \langle \widetilde{D}_r^\epsilon \nabla_x \varphi(X_r^\epsilon, Z_r^\epsilon), \sigma(X_r^\epsilon, Z_r^\epsilon) d\widetilde{W}_r\rangle \,\middle|\, \mathcal{Y}_t^\epsilon\right] = \int_0^t \langle \mathbb{E}_{\mathbb{P}^\epsilon}\left[\widetilde{D}_r^\epsilon \sigma^* \nabla_x \varphi(X_r^\epsilon, Z_r^\epsilon) \,\middle|\, \mathcal{Y}_r^\epsilon\right], d\widetilde{W}_r\rangle$$

By the martingale representation theorem, there is a $C \in \mathbb{R}$ and $H \in L^2_{\mu_L([0,t])\times\mathbb{P}^\epsilon}$ such that the left side of this equation is

$$\mathbb{E}_{\mathbb{P}^\epsilon}\left[\int_0^t \langle \widetilde{D}_r^\epsilon \nabla_x \varphi(X_r^\epsilon, Z_r^\epsilon), \sigma(X_r^\epsilon, Z_r^\epsilon) d\widetilde{W}_r\rangle \,\middle|\, \mathcal{Y}_t^\epsilon\right] = C + \int_0^t \langle H_r, dY_r^\epsilon\rangle,$$

but C is just the expectation at the initial time, which is zero almost surely. Therefore the quadratic variation with $\int_0^t dY_r^\epsilon$ is

$$\langle \int_0^t \langle H_r, dY_r^\epsilon\rangle, \int_0^t dY_r^\epsilon\rangle = \int_0^t H_r dr.$$

Similarly, we have

$$\langle \int_0^t \langle \mathbb{E}_{\mathbb{P}^\epsilon}\left[\widetilde{D}_r^\epsilon \sigma^* \nabla_x \varphi(X_r^\epsilon, Z_r^\epsilon) \,\middle|\, \mathcal{Y}_r^\epsilon\right], d\widetilde{W}_r\rangle, \int_0^t dY_r^\epsilon\rangle = \int_0^t \mathbb{E}_{\mathbb{P}^\epsilon}\left[\widetilde{D}_r^\epsilon \alpha\sigma^* \nabla_x \varphi(X_r^\epsilon, Z_r^\epsilon) \,\middle|\, \mathcal{Y}_r^\epsilon\right] dr,$$

which implies that $H_r = \mathbb{E}_{\mathbb{P}^\epsilon}\left[\widetilde{D}_r^\epsilon \alpha\sigma^* \nabla_x \varphi(X_r^\epsilon, Z_r^\epsilon) \,\middle|\, \mathcal{Y}_r^\epsilon\right]$ with equivalence up to indistinguishability. Hence,

$$\mathbb{E}_{\mathbb{P}^\epsilon}\left[\int_0^t \langle \widetilde{D}_r^\epsilon \nabla_x \varphi(X_r^\epsilon, Z_r^\epsilon), \sigma(X_r^\epsilon, Z_r^\epsilon) d\widetilde{W}_r\rangle \,\middle|\, \mathcal{Y}_t^\epsilon\right] = \int_0^t \langle \rho_r^\epsilon(\alpha\sigma^* \nabla_x \varphi), dY_r^\epsilon\rangle.$$

Therefore we arrive at the Zakai evolution equation,

$$\begin{aligned} \rho_t^\epsilon(\varphi) &= \rho_0^\epsilon(\varphi) + \int_0^t \rho_s^\epsilon\left(\mathcal{G}^\epsilon \varphi\right) ds + \int_0^t \langle \rho_s^\epsilon(\varphi h + \alpha\sigma^* \nabla_x \varphi + \frac{1}{\epsilon}\beta g^* \nabla_z \varphi), dY_s^\epsilon\rangle, \\ \rho_0^\epsilon(\varphi) &= \mathbb{E}_{\mathbb{Q}}\left[\varphi(X_0^\epsilon, Z_0^\epsilon)\right]. \end{aligned} \tag{2.3.3}$$

The assumption on the integrands being in $L^2_{\mu_L([0,t])\times\mathbb{P}^\epsilon}$ and boundedness of $\widetilde{D}^\epsilon$ can be weakened. For instance, by replacing $\widetilde{D}^\epsilon_t$ with

$$\widetilde{D}^{\epsilon,\delta}_t = \frac{\widetilde{D}^\epsilon_t}{1+\delta\widetilde{D}^\epsilon_t},$$

the same result can be proven and then the limit $\delta \to 0$ can be taken (see for instance [BC09, Chapter 3.3, p.52] or [Ben04]).

2.4 The Kushner-Stratonovich Equation

In contrast to the Zakai equation, which is a linear evolution equation, the Kushner-Stratonovich equation is nonlinear. Having derived the Zakai equation, we can simply apply Itô's formula to the product relation given by the Kallianpur-Striebel formula to yield the Kushner-Stratonovich equation. This yields the following for the time evolution of the filter π^ϵ, acting on a test function $\varphi \in C^2_b(\mathbb{R}^m \times \mathbb{R}^n; \mathbb{R})$,

$$\begin{aligned}
\pi^\epsilon_t(\varphi) &= \pi^\epsilon_0(\varphi) + \int_0^t \pi^\epsilon_s(\mathcal{G}^\epsilon\varphi)ds + \int_0^t \langle \pi^\epsilon_s(\varphi h + \alpha\sigma^*\nabla_x\varphi + \frac{1}{\epsilon}\beta g^*\nabla_z\varphi) - \pi^\epsilon_s(\varphi)\pi^\epsilon_s(h), dY^\epsilon_s - \pi^\epsilon_s(h)ds\rangle, \\
\pi^\epsilon_0(\varphi) &= \mathbb{E}_{\mathbb{Q}}\left[\varphi(X^\epsilon_0, Z^\epsilon_0)\right].
\end{aligned} \tag{2.4.1}$$

In Chapters 3 and 4, we will make use of the Zakai equation's linear form to show convergence results of the filter to a lower dimensional version when filtering multiple timescale systems, and taking the timescale separation parameter in the limit. Although we will work with the Zakai equation, the real objective is to show the result for the solution of the Kushner-Stratonovich equation.

Chapter 3

Quantitative Convergence of the Filter Solution for Multiple Timescale Nonlinear Systems with Coarse-Grain Correlated Noise

In this chapter, we consider a problem of filter convergence to a reduced order filter when the signal and observation processes take the following form,

$$\begin{aligned} dX_t^\epsilon &= b(X_t^\epsilon, Z_t^\epsilon)dt + \sigma(X_t^\epsilon, Z_t^\epsilon)dW_t, \\ dZ_t^\epsilon &= \frac{1}{\epsilon^2} f(X_t^\epsilon, Z_t^\epsilon)dt + \frac{1}{\epsilon} g(X_t^\epsilon, Z_t^\epsilon)dV_t, \\ dY_t^\epsilon &= h(X_t^\epsilon, Z_t^\epsilon)dt + \alpha dW_t + \gamma dU_t, \quad Y_0^\epsilon = 0 \in \mathbb{R}^d. \end{aligned} \tag{3.0.1}$$

As in the previous chapter, we assume that $b : \mathbb{R}^m \times \mathbb{R}^n \to \mathbb{R}^m$, $\sigma : \mathbb{R}^m \times \mathbb{R}^n \to \mathbb{R}^m \times \mathbb{R}^w$, $f : \mathbb{R}^m \times \mathbb{R}^n \to \mathbb{R}^n$, $g : \mathbb{R}^m \times \mathbb{R}^n \to \mathbb{R}^n \times \mathbb{R}^v$ and $h : \mathbb{R}^m \times \mathbb{R}^n \to \mathbb{R}^d$ are Borel measurable functions and the presence of $\mathbb{R}^{d\times w} \ni \alpha \neq 0$ indicates correlation between the observation and slow (coarse-grain) process. We additionally assume that the initial distribution of the signal process $(X_0^\epsilon, Z_0^\epsilon)$ at $t = 0$ is denoted by $\mathbb{Q}_{(X_0^\epsilon, Z_0^\epsilon)}$, is independent of the (W, V, U) Brownian motion, and has finite moments for all orders. Besides the simplification of Eq. 3.0.1 from Eq. 2.1.1, we otherwise consider the same setup as in Section 2.1, including the redefinition of Y^ϵ as

$$dY_t^\epsilon = h(X_t^\epsilon, Z_t^\epsilon)dt + dB_t, \quad Y_0^\epsilon = 0 \in \mathbb{R}^d, \tag{2.1.4}$$

where B is a Brownian motion under $\mathbb{Q}$.

Recall that π_t^ϵ for $t \geq 0$ acts on test functions $\varphi \in C_b^2(\mathbb{R}^m \times \mathbb{R}^n; \mathbb{R})$ by integration $\pi_t^\epsilon(\varphi) = \int \varphi(x, z)\pi_t^\epsilon(dx, dz)$. When we are interested in estimating test functions of X^ϵ only, i.e., $\varphi \in C_b^2(\mathbb{R}^m; \mathbb{R})$, we consider the x-marginal of π^ϵ,

$$\pi_t^{\epsilon,x}(\varphi) = \int \varphi(x)\pi_t^\epsilon(dx, dz). \tag{3.0.2}$$

The motivating question of this chapter then comes from the known result that if for every fixed x, the solution Z^x of

$$dZ_t^x = f(x, Z_t^x)dt + g(x, Z_t^x)dV_t, \tag{2.1.6}$$

is ergodic with stationary distribution $\mu_\infty(x)$, then under appropriate assumptions, the process X^ϵ converges in distribution to a Markov process X^0 with infinitesimal generator $\overline{\mathcal{G}_S}$ in the limit as $\epsilon \to 0$ [PSV76; PV03; KY05; PS08]. Therefore, if we are only interested in statistics of X^ϵ (i.e., estimation of test functions $\varphi : \mathbb{R}^m \to \mathbb{R}$), then it would be computationally advantageous to know if $\pi^{\epsilon,x} \to \pi^0$ converges in an appropriate sense to a lower dimensional filtering equation (π_t^0 being a random probability measure for each time t on $\mathbb{R}^m$). In this chapter, we show that this is indeed possible and in fact, one can retrieve a rate of convergence.

Filtering theory has widespread application in many fields including various disciplines of engineering for decision and control systems, the geosciences, weather and climate prediction. In many of these fields, it is not uncommon to have physics based models with multiple timescales as seen in Eq. 3.0.1, and also have the case where estimation of the slow process is solely of interest; for example the estimation of the ocean temperature, which is necessary for climate prediction, but the ocean model may also be coupled to a fast atmospheric model. Knowing that mathematically $\pi^{\epsilon,x} \to \pi^0$ in the limit as $\epsilon \to 0$, enables practitioners to devise more efficient methods for estimation of the coarse-grain process without great loss of accuracy (see Chapter 5 as well as [PNY11; KH12; BH14; Yeo+20]).

There are several papers providing results for $\pi^{\epsilon,x} \to \pi^0$ (or the associated unnormalized conditional measure or density versions) on variations of the multiple timescale filtering problem. In the work by Park et al. [PSN10], (X^ϵ, Z^ϵ) is a two dimensional process with no drift in the fast component, no intermediate scale, and no correlation. The authors made use of a representation of the slow component by a time-changed Brownian motion under a suitable measure to yield weak convergence of the filter. Homogenization of the nonlinear filter was studied by Bensoussan and Blankenship [BB86] and Ichihara [Ich04] by way of asymptotic analysis on a dual representation of the nonlinear filtering equation. In these papers, the coefficients of the signal processes are assumed to be periodic. The approach by Ichihara [Ich04] is novel as the first application of backward stochastic differential equations for homogenization of Zakai-type stochastic partial differential equations (SPDEs).

Convergence of the filter for a random ordinary differential equation with intermediate timescale and perturbed by a fast Markov process was investigated by Lucic and Heunis [LH03]. Qiao [Qia19] investigated

a two timescale problem with correlation between the slow process and observation process, but where the slow dispersion coefficient does not depend on the fast process. The main result is that the filter converges in L^1 sense to the lower dimensional filter. An energy method approach was used by Zhang and Ren [ZR19] to show the probability density of the reduced nonlinear filtering problem approximates the original problem when the signal process has constant diffusion coefficients, periodic drift coefficients and the observation process is only dependent on the slow process.

Convergence of the nonlinear filter is shown in a very general setting by Kleptsina et al. [KLS97], based on convergence in total variation distance of the law of (X^ϵ, Y^ϵ). In the examples of Kleptsina et al. [KLS97], the diffusion coefficient is not allowed to depend on the fast component.

In contrast to other papers on the convergence of the nonlinear filter for the multiple timescale problem, Imkeller et al. [Imk+13] are able to provide a quantitative rate of convergence of ϵ for the two-timescale non-correlated system. This is accomplished using a suitable asymptotic expansion of the dual of the Zakai equation and then harnessing a probabilistic representation of the SPDEs in terms of backward doubly stochastic differential equations. The approach by Imkeller et al. [Imk+13] is extended in this chapter to cover the case of correlation between the observation process and the coarse-grain process. The analysis is therefore similar, with the exception of additional methods to handle the components of the dual of the Zakai equation due to the correlation and the final argument of the main proof.

Theorem (Main Result)
Under the assumptions stated in Theorem 3.2.1, for every $p \geq 1$, $T \geq 0$, there exists a $C > 0$ such that for every $\varphi \in C_b^4(\mathbb{R}^m; \mathbb{R})$,

$$\mathbb{E}_{\mathbb{Q}} \left[\left| \pi_T^{\epsilon,x}(\varphi) - \pi_T^0(\varphi) \right|^p \right] \leq \epsilon^p C |\varphi|_{4,\infty}^p.$$

In particular, there exists a metric d on the space of probability measures on $\mathbb{R}^m$, such that d generates the topology of weak convergence, and such that for every $T \geq 0$, there exists $C > 0$ so that

$$\mathbb{E}_{\mathbb{Q}} \left[d(\pi_T^{\epsilon,x}, \pi_T^0) \right] \leq \epsilon C.$$

This chapter proceeds by first introducing some useful notation and definitions that will be used throughout. We then state the averaged SDE, Kushner-Stratonovich and Zakai equations and provide the main theorem result with full assumptions. We then introduce an idea by Pardoux [Par80] that lets us transform the question of convergence for conditional distributions to one of solutions to backward stochastic partial differential equations (BSPDE). These BSPDEs are linear second order parabolic PDEs and therefore, under

the correct assumptions, have solutions given by BDSDEs. Having provided the necessary mathematical machinery for the analysis, we then give preliminary estimates in Section 3.5 and the main analysis in Section 3.6. We conclude with some additional remarks. The results of this chapter have been made available in the work by Beeson et al. [BNP20b].

3.1 Notation

In this section, we set a few definitions and assumptions that will be used throughout the chapter. We will use $\mathbb{N}_0$ to denote $\{0, 1, 2, \ldots\}$ and $\mathbb{N}$ for $\{1, 2, \ldots\}$. Let H_f denote the assumption that there exists a constant $C > 0$, exponent $\alpha > 0$ and an $R > 0$ such that for all $|z| > R$,

$$\sup_{x \in \mathbb{R}^m} \langle f(x, z), z \rangle \leq -C|z|^\alpha. \tag{H_f}$$

H_f is a recurrence condition, which provides the existence of a stationary distribution, $\mu_\infty(x)$, for the process Z^x. Let H_g denote the assumption that there are $0 < \lambda \leq \Lambda < \infty$, such that for any $(x, z) \in \mathbb{R}^m \times \mathbb{R}^n$,

$$\lambda I \preceq gg^*(x, z) \preceq \Lambda I, \tag{H_g}$$

where $\preceq$ is the order relation in the sense of positive semidefinite matrices. H_g is a uniform ellipticity condition, which provides the uniqueness of the stationary distribution. We will say that a function $\theta : \mathbb{R}^m \times \mathbb{R}^n \to \mathbb{R}$ is centered with respect to $\mu_\infty(x)$, if for each x

$$\int \theta(x, z)\mu_\infty(dz; x) = 0, \quad \forall x \in \mathbb{R}^m.$$

If $\varphi(x, z) \in C_b^{k,l}(\mathbb{R}^m \times \mathbb{R}^n; \mathbb{R}^n)$, then φ is k-times continuously differentiable in the x-component, l-times continuously differentiable in the z-component, and all partial derivatives $\partial_z^{l'} \partial_x^{k'} \varphi$ for $0 \leq k' \leq k$, $0 \leq l' \leq l$ are bounded. Let $HF^{k,l}$ for $k, l \in \mathbb{N}_0$ denote the following assumption:

$$f \in C_b^{k,l}(\mathbb{R}^m \times \mathbb{R}^n; \mathbb{R}^n) \qquad \text{and} \qquad g \in C_b^{k,l}(\mathbb{R}^m \times \mathbb{R}^n; \mathbb{R}^{n \times k}). \tag{$HF^{k,l}$}$$

Similarly, let $HS^{k,l}$ for $k, l \in \mathbb{N}_0$ denote the assumption:

$$b \in C_b^{k,l}(\mathbb{R}^m \times \mathbb{R}^n; \mathbb{R}^m) \qquad \text{and} \qquad \sigma \in C_b^{k,l}(\mathbb{R}^m \times \mathbb{R}^n; \mathbb{R}^{m \times k}), \tag{$HS^{k,l}$}$$

and $HO^{k,l}$ for $k, l \in \mathbb{N}_0$ denote the assumption:

$$h \in C_b^{k,l}(\mathbb{R}^m \times \mathbb{R}^n; \mathbb{R}^d). \tag{$HO^{k,l}$}$$

We use the notation $k = (k_1, \ldots, k_m) \in \mathbb{N}_0^m$ for a multiindex with order $|k| = k_1 + \ldots + k_m$ and define the differential operator

$$D_x^k = \frac{\partial^{|k|}}{\partial {x_1}^{k_1} \ldots \partial x_m^{k_m}}.$$

Lastly, the relation $a \lesssim b$ will indicate that $a \leq Cb$ for a constant $C > 0$ that is independent of a and b, but that may depend on parameters that are not critical for the bound being computed.

3.2 Diffusion Approximation, the Averaged Filtering Equation, and Main Theorem

The theory of homogenization of stochastic differential equations shows that if the process $Z^{\epsilon,x}$,

$$dZ_t^{\epsilon,x} = \frac{1}{\epsilon^2} f(x, Z_t^{\epsilon,x})dt + \frac{1}{\epsilon} g(x, Z_t^{\epsilon,x})dV_t, \tag{3.2.1}$$

is ergodic with stationary distribution $\mu_\infty(x)$, then under appropriate conditions, in the limit $\epsilon \to 0$ the process X^ϵ converges in distribution to a Markov process X^0 with infinitesimal generator

$$\overline{\mathcal{G}_S}(x) \equiv \sum_{i=1}^m \bar{b}_i(x) \frac{\partial}{\partial x_i} + \frac{1}{2} \sum_{i,j=1}^m \bar{a}_{ij}(x) \frac{\partial^2}{\partial x_i \partial x_j}, \tag{3.2.2}$$

where the averaged drift and diffusion coefficients are

$$\bar{b}(x) \equiv \int_{\mathbb{R}^n} b(x,z)\mu_\infty(dz;x), \qquad \text{and} \qquad \bar{a}(x) \equiv \int_{\mathbb{R}^n} a(x,z)\mu_\infty(dz;x).$$

Here we denote the diffusion coefficient $a = \sigma\sigma^*$. We then define the averaged filter π^0, which will $\mathbb{Q}$-a.s. be a probability measure-valued process satisfying the following evolution equation,

$$\begin{aligned} \pi_t^0(\varphi) &= \pi_0^0(\varphi) + \int_0^t \pi_s^0(\overline{\mathcal{G}_S}\varphi)ds + \int_0^t \langle \pi_s^0(\varphi\bar{h} + \alpha\bar{\sigma}^*\nabla_x\varphi) - \pi_s^0(\varphi)\pi_s^0(\bar{h}), dY_s^\epsilon - \pi_s^0(\bar{h})ds \rangle, \\ \pi_0^0(\varphi) &= \mathbb{E}_{\mathbb{Q}}\left[\varphi(X_0^0)\right]. \end{aligned} \tag{3.2.3}$$

The definitions of $\bar{h}, \bar{\sigma}$ are

$$\bar{h}(x) \equiv \int_{\mathbb{R}^n} h(x,z)\mu_\infty(dz;x), \qquad \text{and} \qquad \bar{\sigma}(x) \equiv \int_{\mathbb{R}^n} \sigma(x,z)\mu_\infty(dz;x).$$

Note that π_t^0 is not exactly the conditional distribution for the averaged system X^0. To contrast, the equation for the filter of the averaged system is

$$\begin{aligned} \bar{\pi}_t(\varphi) &= \bar{\pi}_0(\varphi) + \int_0^t \bar{\pi}_s(\overline{\mathcal{G}_S}\varphi)ds + \int_0^t \langle \bar{\pi}_s(\varphi\bar{h} + \alpha\sqrt{\bar{a}}^*\nabla_x\varphi) - \bar{\pi}_s(\varphi)\bar{\pi}_s(\bar{h}), dY_s^0 - \bar{\pi}_s(\bar{h})ds\rangle, \\ \bar{\pi}_0(\varphi) &= \mathbb{E}_{\mathbb{Q}}\left[\varphi(X_0^0)\right]. \end{aligned} \tag{3.2.4}$$

Here Y^0 satisfies the equation,

$$Y_t^0 = \int_0^t \bar{h}(X_s^0)ds + \int_0^t dB_s.$$

To be explicit, the difference in Eq. 3.2.3 and Eq. 3.2.4 is that $\bar{\sigma}$ is used instead of $\sqrt{\bar{a}}$ and we drive the system with Y^ϵ instead of Y^0.

Having introduced the necessary definitions and equations, we can now state the main result fully.

Theorem 3.2.1

Assume H_f, H_g, $HF^{8,4}$, $b \in C_b^{7,4}$, $\sigma \in C_b^{8,4}$, and $HO^{8,4}$. Additionally, assume that the initial distribution $\mathbb{Q}_{(X_0^\epsilon, Z_0^\epsilon)}$ has finite moments of every order. Then for any $p \geq 1, T \geq 0$ we have that for every $\varphi \in C_b^4(\mathbb{R}^m;\mathbb{R})$,

$$\mathbb{E}_{\mathbb{Q}}\left[\left|\pi_T^{\epsilon,x}(\varphi) - \pi_T^0(\varphi)\right|^p\right] \lesssim \epsilon^p |\varphi|_{4,\infty}^p.$$

Further, there exists a metric d on the space of probability measures on $\mathbb{R}^m$ that generates the topology of weak convergence, such that

$$\mathbb{E}_{\mathbb{Q}}\left[d(\pi_T^{\epsilon,x}, \pi_T^0)\right] \lesssim \epsilon.$$

Proof. The proof of the first result is given by Corollary 3.6.1. The proof of the second result is from Lemma 3.6.9. □

Before moving beyond this theorem statement, we provide some quick remarks.

Remark. From $\lim_{\epsilon\to 0}\mathbb{E}_{\mathbb{Q}}\left[d(\pi_T^{\epsilon,x}, \pi_T^0)\right] = 0$, we can retrieve convergence in probability,

$$\lim_{\epsilon\to 0}\mathbb{Q}\left(d(\pi_T^{\epsilon,x}, \pi_T^0) \geq \delta\right) \leq \frac{1}{\delta}\lim_{\epsilon\to 0}\mathbb{E}_{\mathbb{Q}}\left[d(\pi_T^{\epsilon,x}, \pi_T^0)\right] = 0, \qquad \text{for each } \delta > 0.$$

By the Borel-Cantelli lemma, we can choose (ϵ_n) so that $\pi_n^{\epsilon,x}$ will a.s. converge weakly to π^0. For instance, take $\delta_n = 1/n$ and $\epsilon_n = 1/(n2^n)$, which gives a summable series,

$$\sum_{n=1}^{\infty} \mathbb{Q}\left(d(\pi_T^{\epsilon_n,x}, \pi_T^0) \geq \delta_n\right) \lesssim \sum_{n=1}^{\infty} \frac{1}{2^n} = 1.$$

Remark. Some quick comparisons to the main result by Imkeller et al. [Imk+13]. There the scaling for the fast process was of order one, whereas in this chapter we use order two. Therefore, the rate of convergence is the same in the two works. We simply use order two, since in Chapter 4, we will have an intermediate forcing term of order one, and therefore we have the fast process of order two. The only difference in the conditions of our Theorem 3.2.1 and the equivalent one by Imkeller et al. [Imk+13], is that we require $\sigma \in C_b^{8,4}$ instead of $C_b^{7,4}$. This extra regularity in the slow component of the function is due to the correlation between the slow process and observation process, which then appears in our backward stochastic differential equations of Section 3.6.

3.2.1 The Averaged Unnormalized Conditional Distribution

Motivated by the fact that π^ϵ can be related to the unnormalized conditional distribution ρ^ϵ, and that ρ^ϵ satisfies a linear evolution equation (see Eq. 2.3.3), instead of the nonlinear equation for π^ϵ, we would like to show the analogous result of Theorem 3.2.1 but with unnormalized conditional distributions (see definitions below):

$$\mathbb{E}_{\mathbb{Q}}\left[\left|\rho_T^{\epsilon,x}(\varphi) - \rho_T^0(\varphi)\right|^p\right] \lesssim \epsilon^p |\varphi|_{4,\infty}^p.$$

This will indeed work out, and will be stated and proven in Lemma 3.6.8. Therefore let us consider equivalent definitions for the x-marginal $\pi^{\epsilon,x}$ and the averaged filter π^0.

As we have considered the x-marginal of π^ϵ, we also consider the x-marginal of the unnormalized conditional distribution when we are interested in $\varphi \in C_b^2(\mathbb{R}^m; \mathbb{R})$,

$$\rho_t^{\epsilon,x}(\varphi) = \int \varphi(x) \rho_t^\epsilon(dx, dz).$$

$\rho^{\epsilon,x}$ is related to $\pi^{\epsilon,x}$ through the Kallianpur-Striebel relation (see for instance Section 2.2.2),

$$\pi_t^{\epsilon,x}(\varphi) = \frac{\rho_t^{\epsilon,x}(\varphi)}{\rho_t^{\epsilon,x}(1)}, \qquad \forall t \in [0,\infty), \qquad \mathbb{Q}, \mathbb{P}^\epsilon\text{-a.s.}$$

It is easy to see that $\rho^\epsilon(1) = \rho^{\epsilon,x}(1)$.

To relate the averaged (normalized) filter π^0 to an unnormalized variant, we define the averaged unnormalized filter as the solution to the evolution equation

$$\rho_t^0(\varphi) = \rho_0^0(\varphi) + \int_0^t \rho_s^0(\overline{\mathcal{G}_S}\varphi)ds + \int_0^t \langle \rho_s^0(\varphi\bar{h} + \alpha\bar{\sigma}^*\nabla_x\varphi), dY_s^\epsilon\rangle,$$
$$\rho_0^0(\varphi) = \mathbb{E}_{\mathbb{Q}}\left[\varphi(X_0^0)\right],$$

where $\varphi \in C_b^2(\mathbb{R}^m;\mathbb{R})$ are test functions. Again, note that this is not the Zakai equation for the averaged system because we use $\bar{\sigma}$ instead of $\sqrt{\bar{a}}$ and drive the system with Y^ϵ instead of Y^0.

We can relate π^0 to ρ^0 from the Kallianpur-Striebel formula,

$$\pi_t^0(\varphi) = \frac{\rho_t^0(\varphi)}{\rho_t^0(1)}, \qquad \forall t \in [0,\infty), \qquad \mathbb{Q},\mathbb{P}^\epsilon\text{-a.s.}$$

The uniqueness of ρ^0 follows from a result by Rozovskii [Roz91, Theorem 3.1, p.454]. We will use this result in Lemma 4.5.4 of Chapter 4. For the purpose here, it will suffice for the coefficients of $\overline{\mathcal{G}_S}$ and $\bar{h},\bar{\sigma}$ to be C_b^3 (see Lemma 4.5.4).

3.2.2 Representation of the Averaged Unnormalized Conditional Distribution

As explained with Eq. 3.2.4, π^0 is not the filter for the averaged system, but instead an averaged filter. For the same reason ρ^0 is not the unnormalized conditional distribution for the averaged system, and therefore a representation of this measure acting on $\varphi \in C_b^2$ test functions as conditional expectation requires a bit more work. Such a representation will be necessary for the computation of some bounds.

First we introduce a signal process, that given appropriate conditions on the coefficients, give a representation of ρ^0 as we did in Section 2.3 for ρ^ϵ. We require X^0 to be a diffusion process with infinitesimal generator $\overline{\mathcal{G}_S}$. Therefore, consider the following SDE,

$$dX_t^0 = \bar{b}(X_t^0)dt + (\bar{a}(X_t^0) - \bar{\sigma}\bar{\sigma}^*(X_t^0))^{1/2}d\widehat{W}_t + \bar{\sigma}(X_t^0)dW_t, \tag{3.2.5}$$
$$X_0^0 \sim \mathbb{Q}_{X_0^\epsilon}.$$

Here $\widehat{W}$ is a new m-dimensional Brownian motion, independent of V,W,U under $\mathbb{Q}$ as well as independent of the initial condition $\mathbb{Q}_{X_0^\epsilon}$. We note that the Cholesky factor $(\bar{a}(X_t^0) - \bar{\sigma}\bar{\sigma}^*(X_t^0))^{1/2}$ exists, since from an application of Jensen's inequality, one can show that $\bar{a}(x) - \bar{\sigma}\bar{\sigma}^*(x)$ is positive semidefinite for each $x \in \mathbb{R}^m$. For this dispersion coefficient to be Lipschitz continuous, we require $(\bar{a} - \bar{\sigma}\bar{\sigma}^*) \in C_b^2$ (see for example [Str08,

Lemma 2.3.3]). This condition will be made stronger for the uniqueness of the solution ρ^0 (as we will shortly see).

We now define the process

$$\widetilde{D}_t^0 = \exp\left(\int_0^t \langle \bar{h}(X_s^0), dY_s^\epsilon \rangle - \frac{1}{2}\int_0^t \left|\bar{h}(X_s^0)\right|^2 ds\right),$$

and observe that based on the derivation in Section 2.3, we have a representation of ρ^0 on C_b^2 test functions as follows,

$$\rho_t^0(\varphi) = \mathbb{E}_{\mathbb{P}^\epsilon}\left[\varphi(X_t^0)\widetilde{D}_t^0 \mid \mathcal{Y}_t^\epsilon\right].$$

Remark. An interesting observation regarding Eq. 3.2.5, is that we may have $\bar{\sigma} = 0$, and this implies that the SDE for the averaged filter may have no or less correlation than the original system.

3.3 Dual Process to the Unnormalized Conditional Distribution

We now introduce an idea by Pardoux [Par80] that is an important transition to the method of proof used in this chapter. The idea is to define a function-valued process (i.e., solution of a stochastic partial differential equation) for any fixed $\varphi \in C_b^2(\mathbb{R}^m;\mathbb{R})$. The function-valued process will be the dual of ρ^ϵ in an appropriate sense.

First we observe that $\widetilde{D}_T^\epsilon$ can be written as

$$\begin{aligned}
\widetilde{D}_T^\epsilon &= \exp\left(\int_0^T \langle h(X_s^\epsilon, Z_s^\epsilon), dY_s^\epsilon\rangle - \frac{1}{2}\int_0^T |h(X_s^\epsilon, Z_s^\epsilon)|^2 ds\right) \\
&= \exp\left(\int_t^T \langle h(X_s^\epsilon, Z_s^\epsilon), dY_s^\epsilon\rangle - \frac{1}{2}\int_t^T |h(X_s^\epsilon, Z_s^\epsilon)|^2 ds\right)\exp\left(\int_0^t \langle h(X_s^\epsilon, Z_s^\epsilon), dY_s^\epsilon\rangle - \frac{1}{2}\int_0^t |h(X_s^\epsilon, Z_s^\epsilon)|^2 ds\right) \\
&= \widetilde{D}_{t,T}^\epsilon \widetilde{D}_t^\epsilon.
\end{aligned}$$

For this reason, we see that $\mathbb{Q}$-a.s we have $\widetilde{D}_{t,T}^\epsilon = \widetilde{D}_T^\epsilon (\widetilde{D}_t^\epsilon)^{-1}$.

Fixing $\varphi \in C_b^2(\mathbb{R}^m;\mathbb{R})$, we then define the dual process at time $t \in [0,T]$ as

$$v_t^{\epsilon,T,\varphi}(x,z) \equiv \mathbb{E}_{\mathbb{P}_{t,x,z}^\epsilon}\left[\varphi(X_T^\epsilon)\widetilde{D}_{t,T}^\epsilon \,\middle|\, \mathcal{Y}_{t,T}^\epsilon\right],$$

where $\mathbb{P}_{t,x,z}^\epsilon$ is the probability measure constructed from the procedure in Section 2.2 when $(X_s^\epsilon, Z_s^\epsilon)$ take the

constant values (x, z) for $s \in [0, t]$ and then follows the dynamics given by Eq. 3.0.1 for $s > t$. $v_t^{\epsilon,T,\varphi}(x, z)$ is called the dual process, because for any $t \in [0, T]$ we have

$$\rho_T^{\epsilon,x}(\varphi) = \rho_t^{\epsilon}(v_t^{\epsilon,T,\varphi}), \qquad \mathbb{P}^{\epsilon}\text{-a.s.}$$

That is, the composition $\rho_t^{\epsilon}(v_t^{\epsilon,T,\varphi})$ is almost surely a constant value for any $t \in [0, T]$. This also means that $\rho_T^{\epsilon,x}(\varphi) = \rho_0^{\epsilon}(v_0^{\epsilon,T,\varphi})$ and therefore

$$\rho_T^{\epsilon,x}(\varphi) = \int_{\mathbb{R}^m \times \mathbb{R}^n} v_0^{\epsilon,T,\varphi}(x, z) \mathbb{Q}_{(X_0^{\epsilon}, Z_0^{\epsilon})}(dx, dz).$$

We can similarly define the dual process for ρ^0 as

$$v_t^{0,T,\varphi}(x) \equiv \mathbb{E}_{\mathbb{P}_{t,x}^{\epsilon}} \left[\varphi(X_T^0) \widetilde{D}_{t,T}^0 \mid \mathcal{Y}_{t,T}^{\epsilon} \right],$$

with the same property that $\rho_T^0(\varphi) = \rho_0^0(v_0^{0,T,\varphi})$. Again $\mathbb{P}_{t,x}^{\epsilon}$ is the probability measure constructed from the procedure in Section 2.2, but for the case where X_s^0 takes the constant value x for $s \in [0, t]$ and then follows the dynamics given by the generator in Eq. 3.2.2. The definition of $\widetilde{D}_{t,T}^0$ in $v_t^{0,T,\varphi}$ is

$$\widetilde{D}_{t,T}^0 = \exp\left(\int_t^T \langle \bar{h}(X_s^0), dY_s^{\epsilon} \rangle - \frac{1}{2} \int_t^T \left| \bar{h}(X_s^0) \right|^2 ds \right),$$

which is $\mathbb{Q}$-a.s. equal to $\widetilde{D}_{t,T}^0 = \widetilde{D}_T^0 (\widetilde{D}_t^0)^{-1}$.

3.3.1 The Dual Process and Filter Convergence

We now show the usefulness of the dual process in showing the convergence of $\rho^{\epsilon,x} \to \rho^0$. We again fix $\varphi \in C_b^2(\mathbb{R}^m; \mathbb{R})$ and $p \geq 1$. Then from Jensen's inequality and Fubini's theorem we have the following relation,

$$\begin{aligned}
\mathbb{E}_{\mathbb{P}^{\epsilon}} \left[\left| \rho_T^{\epsilon,x}(\varphi) - \rho_T^0(\varphi) \right|^p \right] &= \mathbb{E}_{\mathbb{P}^{\epsilon}} \left[\left| \int v_0^{\epsilon,T,\varphi}(x, z) - v_0^{0,T,\varphi}(x) \mathbb{Q}_{(X_0^{\epsilon}, Z_0^{\epsilon})}(dx, dz) \right|^p \right] \\
&\leq \mathbb{E}_{\mathbb{P}^{\epsilon}} \left[\int \left| v_0^{\epsilon,T,\varphi}(x, z) - v_0^{0,T,\varphi}(x) \right|^p \mathbb{Q}_{(X_0^{\epsilon}, Z_0^{\epsilon})}(dx, dz) \right] \\
&= \int \mathbb{E}_{\mathbb{P}^{\epsilon}} \left[\left| v_0^{\epsilon,T,\varphi}(x, z) - v_0^{0,T,\varphi}(x) \right|^p \right] \mathbb{Q}_{(X_0^{\epsilon}, Z_0^{\epsilon})}(dx, dz).
\end{aligned}$$

This implies that if $\mathbb{Q}_{(X_0^{\epsilon}, Z_0^{\epsilon})}(dx, dz)$ is well behaved (e.g., finite moments of every order) then convergence of the p-th moment of $v_0^{\epsilon,T,\varphi}(x, z) - v_0^{0,T,\varphi}(x)$ to zero will imply convergence of the p-th moment of $\rho_T^{\epsilon,x}(\varphi) - \rho_T^0(\varphi)$ to zero. We also make the reminder that integrating out the z component of $\mathbb{Q}_{(X_0^{\epsilon}, Z_0^{\epsilon})}$ yields $\mathbb{Q}_{(X_0^0)}$ (i.e., X^{ϵ}

and X^0 have the same initial distribution).

3.3.2 Evolution Equations for the Dual Process

To introduce the next step in the techniques to prove convergence of the marginalized filter to the reduced order filter, we need to state the evolution equations for the dual processes $v^{\epsilon,T,\varphi}$ and $v^{0,T,\varphi}$. Both processes satisfy backward stochastic partial differential equations. To facilitate the reading, we use v^ϵ and v^0 instead of the more verbose $v^{\epsilon,T,\varphi}$ and $v^{0,T,\varphi}$ in most of what follows. When clarity is needed, we will use the explicit notation.

The evolution equation for v^ϵ is given by

$$-dv_t^\epsilon = \mathcal{G}^\epsilon v_t^\epsilon dt + \langle v_t^\epsilon h + \alpha\sigma^* \nabla_x v_t^\epsilon, d\overleftarrow{B}_t \rangle, \qquad v_T^\epsilon = \varphi, \tag{3.3.1}$$

where $\int d\overleftarrow{B}_t$ will denote the backward Itô integral. And the process v^0 is given by

$$-dv_t^0 = \overline{\mathcal{G}_S} v_t^0 dt + \langle v_t^0 \bar{h} + \alpha\bar{\sigma}^* \nabla_x v_t^0, d\overleftarrow{B}_t \rangle, \qquad v_T^0 = \varphi. \tag{3.3.2}$$

The standard way of showing that these are indeed the evolution equations, is to show that the BSPDEs have unique solutions in appropriate Sobolev spaces, and then apply Itô's (or Itô-Wentzell's) formula to verify that indeed the process is dual to the unnormalized conditional distribution [Ver16, p.2]. The dual process has also been addressed by Krylov and Rozovskii [KR82] and Rozovskii [Roz90], and plays a role in showing convergence of particle approximations (summation of weighted Dirac distributions) to the normalized conditional distribution [BC09, p.180]. Unlike the aforementioned efforts that assume the form of the dual process from the beginning, Veretennikov [Ver16] uses a direct approach to derive the evolution equation for the dual process.

3.3.3 Expansion of the Dual Process

Because v^ϵ satisfies a linear BSPDE, we can consider by superposition, an expansion of v^ϵ using v^0 and a corrector ψ and remainder R term. Using the following expansion

$$v_t^\epsilon(x,z) = v_t^0(x) + \psi_t(x,z) + R_t(x,z),$$

in Eq. 3.3.1 and introducing terms for Eq. 3.3.2, we define ψ and R to satisfy the following linear BSPDEs

$$\begin{aligned} -d\psi_t &= \left[\frac{1}{\epsilon^2}\mathcal{G}_F\psi_t + (\mathcal{G}_S - \overline{\mathcal{G}_S})v_t^0\right]dt + \langle v_t^0(h-\bar{h}), d\overleftarrow{B}_t\rangle + \langle \alpha(\sigma-\bar{\sigma})^*\nabla_x v_t^0, d\overleftarrow{B}_t\rangle, && \psi_T = 0, \\ -dR_t &= (\mathcal{G}^\epsilon R_t + \mathcal{G}_S\psi_t)dt + \langle(\psi_t + R_t)h, d\overleftarrow{B}_t\rangle + \langle \alpha\sigma^*\nabla_x(\psi_t + R_t), d\overleftarrow{B}_t\rangle, && R_T = 0. \end{aligned} \tag{3.3.3}$$

Therefore to show convergence of the difference $v^\epsilon - v^0$, we can equivalently show convergence of ψ and R to zero as $\epsilon \to 0$:

$$\mathbb{E}_{\mathbb{P}^\epsilon}\left[\left|v_t^{\epsilon,T,\varphi}(x,z) - v_t^{0,T,\varphi}(x)\right|^p\right] = \mathbb{E}_{\mathbb{P}^\epsilon}\left[|\psi_t(x,z) + R_t(x,z)|^p\right] \lesssim \mathbb{E}_{\mathbb{P}^\epsilon}\left[|\psi_t(x,z)|^p\right] + \mathbb{E}_{\mathbb{P}^\epsilon}\left[|R_t(x,z)|^p\right].$$

This will be our strategy in Section 3.6.

3.4 Probabilistic Representation of Stochastic PDEs

We will now show that we can find a probabilistic representation of the dual processes. This representation will be given by backward doubly stochastic differential equations (BDSDEs), which are a generalization of the Feynman-Kac solution, but for semilinear second order parabolic SPDEs. First let us state a result for the classical solution of the dual processes, which are linear second order parabolic SPDEs of the general form:

$$\begin{aligned} -d\psi(\omega,t,x) = \mathcal{L}\psi(\omega,t,x)dt + f(\omega,t,x)dt + \langle g(\omega,t,x) + G(\omega,t,x)\psi(\omega,t,x), d\overleftarrow{B}_t\rangle \\ + \langle F(\omega,t,x)\nabla_x\psi(\omega,t,x), d\overleftarrow{B}_t\rangle, \\ \psi(T,x) = \varphi(\omega,x), \end{aligned} \tag{3.4.1}$$

where $\psi : \Omega \times [0,T] \times \mathbb{R}^m \to \mathbb{R}$, $f : \Omega \times [0,T] \times \mathbb{R}^m \to \mathbb{R}$, $g : \Omega \times [0,T] \times \mathbb{R}^m \to \mathbb{R}^d$, $G : \Omega \times [0,T] \times \mathbb{R}^m \to \mathbb{R}^d$, $F : \Omega \times [0,T] \times \mathbb{R}^m \to \mathbb{R}^{d\times m}$ and $\varphi : \Omega \times \mathbb{R}^m \to \mathbb{R}$ are all jointly measurable, and $\overleftarrow{B}_t$ is a d-dimensional standard backward Brownian motion. The generator given in Eq. 3.4.1 has the form

$$\mathcal{L}(x) = \sum_{i=1}^m b_i(x)\frac{\partial}{\partial x_i} + \frac{1}{2}\sum_{i,j=1}^m a_{ij}(x)\frac{\partial^2}{\partial x_i \partial x_j},$$

where $b : \mathbb{R}^m \to \mathbb{R}$ and $a : \mathbb{R}^m \to \mathbb{S}^{m\times m}$ are measurable ($\mathbb{S}^{m\times m}$ denotes the space of symmetric positive semidefinite matrices).

Once we have stated the results on BSPDEs, we will then give the BDSDE representation in Section 3.4.1.

We will need some definitions for the necessary conditions on the classical solution of the SPDEs. Let us state those now, starting with the definition for the filtration $\mathcal{F}_{t,s}^{0,B}$: let $0 \leq t \leq s \leq T$,

$$\mathcal{F}_{t,s}^{0,B} = \sigma(\{B_u - B_t \,|\, t \leq u \leq s\}),$$

and let $\mathcal{F}_{t,s}^{B}$ be the completion of $\mathcal{F}_{t,s}^{0,B}$ under $\mathbb{P}^\epsilon$. The space of adapted random fields of polynomial growth will be denoted by $\mathcal{P}_T(\mathbb{R}^m;\mathbb{R}^n)$:

Definition 3.4.1. $\mathcal{P}_T(\mathbb{R}^m;\mathbb{R}^n)$ is the space of random fields of polynomial growth

$$H : \Omega \times [0,T] \times \mathbb{R}^m \to \mathbb{R}^n$$

that are jointly measurable in (ω, t, x) and for fixed (t, x), $\omega \mapsto H(\omega, t, x)$ is $\mathcal{F}_{t,T}^{B}$-measurable. Further, for fixed ω outside a null set, H has to be jointly continuous in (t, x), and it has to satisfy the following inequality: For every $p \geq 1$ there is $C_p, q > 0$, such that for all $x \in \mathbb{R}^m$,

$$\mathbb{E}\left[\sup_{0\leq t\leq T} |H(t,x)|^p\right] \leq C_p(1 + |x|^q).$$

We denote with D^k a definition concerning conditions on the coefficients of the generator $\mathcal{L}$ of the BSPDE:

Definition 3.4.2. We define the condition D^k to indicate that $b \in C_b^k(\mathbb{R}^m;\mathbb{R}^n)$, $a \in C_b^k(\mathbb{R}^m;\mathbb{S}^{m\times m})$, and a is degenerate elliptic: For every $\xi \in \mathbb{R}^m$ and every $x \in \mathbb{R}^m$,

$$\langle a(x)\xi, \xi\rangle = \sum_{i,j=1}^{m} a_{ij}(x)\xi_i\xi_j \geq 0,$$

or succintly $a \succeq 0$.

We denote with S^k a definition concerning conditions on the coefficients (not including the generator) of the BSPDE:

Definition 3.4.3. The condition S^k indicates that f and g are k-times continuously differentiable and the partial derivatives up to order k are all in $\mathcal{P}_T$. G and F are $(k+1)$-times continuously differentiable and the partial derivatives up to order $(k+1)$ are all uniformly bounded in (ω, t, x). φ is k-times continuously differentiable, and all partial derivatives of order 0 to k grow at most polynomially.

Lemma 3.4.1

Assume D^k and S^k for some $3 \leq k \in \mathbb{N}$. Additionally, assume the parabolic condition $2a - F^*F \succeq 0$ holds. Then Eq. 3.4.1 has a unique classical solution ψ in the sense that for every fixed ω outside a null set, $\psi(\omega, \cdot, \cdot) \in C^{0,k-1}([0,T] \times \mathbb{R}^d; \mathbb{R})$, ψ and its partial derivatives are in $\mathcal{P}_T(\mathbb{R}^m; \mathbb{R})$, and ψ solves the integral equation. If $\widetilde{\psi}$ is any other solution of the integral equation, then ψ and $\widetilde{\psi}$ are indistinguishable. If further f, g and φ as well as their derivatives up to order k are uniformly bounded in (ω, t, x), then for any $p > 0$ there exist $q > 0$ and $C > 0$ (only depending on p, the dimensions involved, the bounds on a, b, G and F, and on T), such that for all $|\beta| \leq k-1$ and $x \in \mathbb{R}^m$,

$$\mathbb{E}\left[\sup_{t\leq T} |D^\beta \psi(t,x)|^p\right] \leq C(1+|x|^q)\mathbb{E}\left[|\varphi|^p_{k,\infty} + \sup_{t\leq T}|f(t,\cdot)|^p_{k,\infty} + \sup_{t\leq T}|g(t,\cdot)|^p_{k,\infty}\right].$$

Proof. This is a combination of Theorem 4.3.2 and Corollary 4.3.2 by Rozovskii [Roz90, p.170] (The claimed bound is only given for the equation in unweighted Sobolev spaces, in Corollary 4.2.2. From there, we can deduce the result for the weighted Sobolev case). The only thing we need to verify is that our polynomial growth assumption on the coefficients is compatible with the Sobolev norm condition there. But if $\theta \in \mathcal{P}_T(\mathbb{R}^m; \mathbb{R}^n)$, then for any $p \geq 1$ there certainly is an $r < 0$ such that θ takes its values in the weighted L^p-space with weight $(1+|x|^2)^{r/2}$,

$$\begin{aligned}
\mathbb{E}\left[\sup_{0\leq t\leq T}\int |\theta(t,x)|^p(1+|x|^2)^{r/2}dx\right] &\leq \mathbb{E}\left[\int \sup_{0\leq t\leq T}|\theta(t,x)|^p(1+|x|^2)^{r/2}dx\right] \\
&= \int \mathbb{E}\left[\sup_{0\leq t\leq T}|\theta(t,x)|^p\right](1+|x|^2)^{r/2}ds \\
&\leq \int C(1+|x|^q)(1+|x|^2)^{r/2}dx < \infty,
\end{aligned}$$

for small enough r. □

3.4.1 Backward Doubly Stochastic Differential Equations

The theory of backward doubly stochastic differential equations has its origin in the paper by Pardoux and Peng [PP94]. Although it is possible to get a different representation of the solutions of Eq. 3.4.1 by the method of stochastic characteristics [Roz90], one benefit of the BDSDE representation is that for fixed $(x, z) \in \mathbb{R}^m \times \mathbb{R}^n$, we will have a finite dimensional representation of $\psi(x, z)$ and therefore will be able to apply Grönwall's lemma in the final step of Lemma 3.6.3, as part of the main analysis.

A BDSDE is an integral equation of the form,

$$Y_t = \xi + \int_t^T f(s, \cdot, Y_s, Z_s)ds + \int_t^T \langle g(s, \cdot, Y_s, Z_s), d\overleftarrow{B}_s \rangle - \int_t^T \langle Z_s, dW_s \rangle, \tag{3.4.2}$$

where $f : [0,T] \times \Omega \times \mathbb{R} \times \mathbb{R}^n \to \mathbb{R}$, $g : [0,T] \times \Omega \times \mathbb{R} \times \mathbb{R}^n \to \mathbb{R}^d$, and for fixed $y \in \mathbb{R}$, $z \in \mathbb{R}^n$, the processes $(\omega, t) \mapsto f(t, \omega, x, z)$ and $(\omega, t) \mapsto g(t, \omega, x, z)$ are $(\mathcal{F}^B_{0,T} \vee \mathcal{F}^W_T) \otimes \mathcal{B}(\mathbb{R})$-measurable, and for every t, $f(t, \cdot, x, z)$ and $g(t, \cdot, x, z)$ are $\mathcal{F}_t$-measurable.

Let us clarify what we mean here by $\mathcal{F}_t$. W is an n-dimensional standard Brownian motion that is independent of B. We define the completed filtration generated by W for $t \in [0, s]$ as $\mathcal{F}^W_{t,s}$. Then we define $\mathcal{F}_t$ as

$$\mathcal{F}_t = \mathcal{F}^B_{t,T} \vee \mathcal{F}^W_t.$$

Because of this definition, $\mathcal{F}_t$ is not a filtration; it is neither strictly increasing nor decreasing in t.

Let us now introduce some additional notation that will make it easier to explain the main results of BDSDEs.

Definition 3.4.4. Let $H^2_T(\mathbb{R}^m)$ be the space of measurable $\mathbb{R}^m$-valued processes Y, such that Y_t is $\mathcal{F}_t$-measurable for almost any $t \in [0,T]$ and

$$\mathbb{E}\left[\int_0^T |Y_t|^2 dt\right] < \infty.$$

Definition 3.4.5. Let $S^2_T(\mathbb{R}^m)$ be the space of continuous adapted $\mathbb{R}^m$-valued processes Y, such that Y_t is $\mathcal{F}_t$-measurable for every $t \in [0,T]$ and

$$\mathbb{E}\left[\sup_{0 \le t \le T} |Y_t|^2 dt\right] < \infty.$$

The pair (Y, Z) will be called a solution of Eq. 3.4.2 if $(Y, Z) \in S^2_T(\mathbb{R}) \times H^2_T(\mathbb{R}^n)$, and if the pair solves the integral equation. We will also write BDSDEs in differential form at times, for example Eq. 3.4.2 in differential form would be,

$$-dY_t = f(t, \cdot, Y_t, Z_t)dt + \langle g(t, \cdot, Y_t, Z_t), d\overleftarrow{B}_t \rangle - \langle Z_t, dW_t \rangle.$$

Observe that with suitable adaptations, all of the following results also hold in the multidimensional case (i.e., $Y \in \mathbb{R}^m$). We restrict to one-dimensional Y for simplicity and because ultimately we are only interested in that case.

Pardoux and Peng [PP94] show that under the following conditions, Eq. 3.4.2 has a unique solution:

- $\xi \in L^2(\Omega, \mathcal{F}_T, \mathbb{P}^\epsilon; \mathbb{R})$,
- for any $(y, z) \in \mathbb{R} \times \mathbb{R}^n$, we have $f(\cdot, \cdot, y, z) \in H_T^2(\mathbb{R})$ and $g(\cdot, \cdot, y, z) \in H_T^2(\mathbb{R}^d)$
- f and g satisfy Lipschitz conditions and g is a contraction in z: there exists constants $L > 0$ and $0 < \beta < 1$ such that for any (ω, t) and y_1, y_2, z_1, z_2,

$$|f(t, \omega, y_1, z_1) - f(t, \omega, y_2, z_2)|^2 \leq L(|y_1 - y_2|^2 + |z_1 - z_2|^2),$$
$$|g(t, \omega, y_1, z_1) - g(t, \omega, y_2, z_2)|^2 \leq L|y_1 - y_2|^2 + \beta|z_1 - z_2|^2.$$

Now we associate a diffusion X to the differential operator $\mathcal{L}$ given in Eq. 3.4.1. To do so, assume D_k is satisfied for some $k \geq 2$. Then $\sigma \equiv a^{1/2}$ is Lipschitz continuous [Str08, Lemma 2.3.3]. Hence for every $(t, x) \in [0, T] \times \mathbb{R}^m$, there exists a strong solution of the SDE

$$X_s^{t,x} = x + \int_t^s b(X_s^{t,x})ds + \int_t^s \sigma(X_s^{t,x})dW_s, \qquad \text{for } s \geq t,$$
$$X_s^{t,x} = x \qquad \text{for } s \leq t.$$

For the theory of BDSDEs, we must assume that F has the form $F = \alpha\sigma^*$, and here we consider $\alpha \in \mathbb{R}^{d \times m}$ a constant matrix. We then associate the following BDSDE to Eq. 3.4.1,

$$-dY_s^{t,x} = f(s, X_s^{t,x})ds + \langle g(s, X_s^{t,x}) + G(s, X_s^{t,x})Y_s^{t,x} + \alpha Z_s^{t,x}, d\overleftarrow{B}_t\rangle - \langle Z_s^{t,x}, dW_s\rangle.$$
$$Y_T^{t,x} = \varphi(X_T^{t,x}).$$

Under the assumptions S_k and D_k for $k \geq 2$, this equation has a unique solution. The tuple $(X^{t,x}, Y^{t,x}, Z^{t,x})$ constitutes a forward backward doubly stochastic differential equation (FBDSDE).

Lemma 3.4.2

Assume S_k and D_k for $k \geq 3$ and $2a - F^*F \succeq 0$. Then the unique classical solution ψ of the BSPDE in Eq. 3.4.1 is given by $\psi(t, x) = Y_t^{t,x}$, where $(Y^{t,x}, Z^{t,x})$ is the unique solution of the BDSDE in Eq. 3.4.2.

Proof. See [PP94, Theorem 3.1, p.225]. □

A final remark before we turn to preliminary estimates and the main analysis where we will use BDSDEs, we will not be able to get an existence result for classical solutions of the SPDEs in Section 3.6 from the theory of BDSDEs. This is due to the fact that for this we would need smoothness properties of a square root of a. But even when a is smooth, in the degenerate elliptic case it does not need to have a smooth square root (see for example [Str08, Lemma 2.3.3]). We will instead use the existence result by Rozovskii [Roz90] stated in Lemma 3.4.1, and use the uniqueness result from Pardoux and Peng's work [PP94] in our setting. This works under Lipschitz continuity of $a^{1/2}$, which we used previously.

3.5 Preliminary Estimates

In this section, we prove several preliminary estimates to be used in Section 3.6. We start with results for the moments of the SDE solutions.

3.5.1 Estimates on SDE Solutions

Lemma 3.5.1

Assume that the drift coefficient b, and dispersion coefficient σ, of the slow motion X^ϵ are bounded. Then for any $p \geq 1$, and every $T > 0$, there exists $C_p > 0$ such that

$$\sup_{(t,\epsilon)\in[0,T]\times(0,1]} \mathbb{E}\left[|X_t^\epsilon|^p \,|\, (X_0^\epsilon, Z_0^\epsilon) = (x,z)\right] \leq C_p(1+|x|^p).$$

Proof. The result is trivial since we assume the coefficients to be bounded and consider finite T. □

Lemma 3.5.2

Assume f is bounded and that f and gg^* are Hölder continuous in z uniformly in x for some uniform constant. Assume that the conditions H_f and H_g hold. Then for any $p > 0$ there exists $C_p > 0$ such that

$$\sup_{(t,\epsilon,x)\in[0,\infty)\times(0,1]\times\mathbb{R}^m} \mathbb{E}\left[|Z_t^\epsilon|^p \,|\, (X_0^\epsilon, Z_0^\epsilon) = (x,z)\right] \leq C_p(1+|z|^p).$$

Proof. First consider a reparametrization of time $t = \epsilon^2\tau$, and define $\overline{Z}_\tau^\epsilon \equiv Z_{\epsilon^2\tau}^\epsilon$ to yield the SDE,

$$d\overline{Z}_\tau^\epsilon = f(X_{\epsilon^2\tau}^\epsilon, \overline{Z}_\tau^\epsilon)d\tau + g(X_{\epsilon^2\tau}^\epsilon, \overline{Z}_\tau^\epsilon)d\overline{V}_\tau^\epsilon,$$

where the process $\overline{V}_\tau^\epsilon = \epsilon^{-1}V_{\epsilon^2\tau}$ is a standard Brownian motion. $\overline{Z}^\epsilon$ is asymptotically identical in law to Z^x.

We perform a second reparametrization of time (see either [Ver97, p.125] or [PV01, p.1063]) by defining,

$$\kappa(x,z) \equiv |\langle g(x,z),z\rangle|/|z|, \qquad \gamma^\epsilon(\tau) \equiv \int_0^\tau \kappa^2(X^\epsilon_{\epsilon^2 s}, \overline{Z}^\epsilon_s)ds,$$
$$\bar{\tau}^\epsilon(\tau) \equiv (\gamma^\epsilon)^{-1}(\tau),$$

where $(\gamma^\epsilon)^{-1}$ is the inverse of γ^ϵ. Then defining $(\widetilde{X}^\epsilon_s, \widetilde{Z}^\epsilon_s) \equiv (X^\epsilon_{\epsilon^2\bar{\tau}^\epsilon(s)}, \overline{Z}^\epsilon_{\bar{\tau}^\epsilon(s)})$, we get an SDE with unit diffusion,

$$\widetilde{Z}^\epsilon_s = \kappa^{-2}(\widetilde{X}^\epsilon_s, \widetilde{Z}^\epsilon_s)f(\widetilde{X}^\epsilon_s, \widetilde{Z}^\epsilon_s)ds + \kappa^{-1}(\widetilde{X}^\epsilon_s, \widetilde{Z}^\epsilon_s)g(\widetilde{X}^\epsilon_s, \widetilde{Z}^\epsilon_s)d\widetilde{V}^\epsilon_s,$$

where $\widetilde{V}^\epsilon$ is a standard Brownian motion. Veretennikov [Ver97] shows that the solution of this unit diffusion SDE still has the property of positive recurrence and therefore the estimate now follows from [Ver97, Lemma 1, p.117]. □

Lemma 3.5.3

Assume h is bounded, then for $p \geq 1$ and $t \in [0,T]$,

$$\sup_{\epsilon\in(0,1]} \sup_{t\leq T} \mathbb{E}_{\mathbb{P}^\epsilon} \left|\widetilde{D}^\epsilon_t\right|^p < \infty.$$

Proof. Let $p \geq 2$ and $N \in \mathbb{N}$, and define the stopping time,

$$\tau_N \equiv \inf\{t \mid |\widetilde{D}^\epsilon_t| \geq N\},$$

with $\tau_N(\omega) = \infty$ if the set is empty. The stopped process $\widetilde{D}^\epsilon_{t\wedge\tau_N}$ satisfies the following evolution equation,

$$\widetilde{D}^\epsilon_{t\wedge\tau_N} = 1 + \int_0^{t\wedge\tau_N} \widetilde{D}^\epsilon_s \langle h(X^\epsilon_s, Z^\epsilon_s), dY^\epsilon_s\rangle = 1 + \int_0^t \widetilde{D}^\epsilon_{s\wedge\tau_N} \langle h(X^\epsilon_{s\wedge\tau_N}, Z^\epsilon_{s\wedge\tau_N}), dY^\epsilon_s\rangle$$

and therefore by the Burkholder-Davis-Gundy inequality,

$$\begin{aligned}\mathbb{E}_{\mathbb{P}^\epsilon}\left|\widetilde{D}^\epsilon_{t\wedge\tau_N}\right|^p &\leq 2^{p-1} + 2^{p-1}\mathbb{E}_{\mathbb{P}^\epsilon}\left(\sup_{u\leq t}\left|\int_0^u \widetilde{D}^\epsilon_{s\wedge\tau_N}\langle h(X^\epsilon_{s\wedge\tau_N}, Z^\epsilon_{s\wedge\tau_N}), dY^\epsilon_s\rangle\right|\right)^p \\ &\leq 2^{p-1} + 2^{p-1}C_p\mathbb{E}_{\mathbb{P}^\epsilon}\left(\int_0^t |\widetilde{D}^\epsilon_{s\wedge\tau_N}|^2 |h(X^\epsilon_{s\wedge\tau_N}, Z^\epsilon_{s\wedge\tau_N})|^2 ds\right)^{p/2}.\end{aligned}$$

By boundedness of h, Hölder's inequality, and Fubini's theorem,

$$\mathbb{E}_{\mathbb{P}^\epsilon}\left|\widetilde{D}^\epsilon_{t\wedge\tau_N}\right|^p \leq 2^{p-1} + 2^{p-1}C_p|h|^p_\infty T^{p/2-1}\int_0^t \mathbb{E}_{\mathbb{P}^\epsilon}|\widetilde{D}^\epsilon_{s\wedge\tau_N}|^p ds.$$

Grönwall's lemma now gives,

$$\mathbb{E}_{\mathbb{P}^\epsilon}\left|\widetilde{D}^\epsilon_{t\wedge\tau_N}\right|^p \leq 2^{p-1}\exp\left(2^{p-1}C_p|h|^p_\infty T^{p/2}\right) < \infty.$$

Because the right hand side does not depend on N nor ϵ, bounded convergence gives us the estimate in the limit $N \to \infty$. The case $1 \leq p < 2$ follows from $L^p(\mathbb{P}^\epsilon) \subset L^2(\mathbb{P}^\epsilon)$. □

Lemma 3.5.4

Assume h is bounded, then for $p \geq 1$ and $t \in [0,T]$,

$$\sup_{t\leq T}\mathbb{E}_{\mathbb{P}^\epsilon}\left|\widetilde{D}^0_t\right|^p < \infty.$$

Proof. The argument follows the same line of reasoning as Lemma 3.5.3. □

3.5.2 Estimates with the Fast Semigroup

In this section we provide estimates relating to the semigroup of the fast process.

Lemma 3.5.5

Assume $HF^{k,l}$, with $k \in \mathbb{N}_0, l \in \mathbb{N}$, and let $\theta \in C^{k,j}(\mathbb{R}^m \times \mathbb{R}^n; \mathbb{R})$ for $j \leq l$ satisfy for some $C, p > 0$

$$\sum_{|\alpha|\leq k}\sum_{|\beta|\leq j}|D^\alpha_x D^\beta_z \theta(x,z)| \leq C(1 + |x|^p + |z|^p).$$

Then

$$(t,x,z) \mapsto T^{F,x}_t\left(\theta(x,\cdot)\right)(z) \in C^{0,k,j}(\mathbb{R}^+ \times \mathbb{R}^m \times \mathbb{R}^n; \mathbb{R})$$

and there exist $C_1, p_1 > 0$, such that for all $(t,x,z) \in [0,\infty) \times \mathbb{R}^m \times \mathbb{R}^n$

$$\sum_{|\alpha|\leq k}\sum_{|\beta|\leq j}|D^\alpha_x D^\beta_z T^{F,x}_t\left(\theta(x,\cdot)\right)(z)| \leq C_1 e^{C_1 t}(1 + |x|^{p_1} + |z|^{p_1}).$$

If the bound on the derivatives of θ can be chosen uniformly in x, that is,

$$\sum_{|\alpha|\leq k}\sum_{|\beta|\leq j}\sup_x |D_x^\alpha D_z^\beta \theta(x,z)| \leq C(1+|z|^p),$$

then the bound on the derivatives of $T_t^{F,x}(\theta(x,\cdot))(z)$ is also uniform in x,

$$\sum_{|\alpha|\leq k}\sum_{|\beta|\leq j}\sup_x |D_x^\alpha D_z^\beta T_t^{F,x}(\theta(x,\cdot))(z)| \leq C_1 e^{C_1 t}(1+|z|^{p_1}).$$

Proof. Note that

$$T_t^{F,x}(\theta(x,\cdot))(z) = \mathbb{E}\left[\theta(x, Z_t^x) \,|\, Z_0^x = z\right] = \mathbb{E}\left[\theta(X_t, Z_t) \,|\, (X_0, Z_0) = (x,z)\right]$$

is the solution of Kolmogorov's backward equation associated to (X, Z), where

$$\begin{aligned} X_t &= X_0, \\ Z_t &= Z_0 + \int_0^t f(X_s, Z_s)ds + \int_0^t g(X_s, Z_s)dV_s. \end{aligned}$$

In this formulation, the first result is standard (see for instance [Str08, Corollary 2.2.8]) and the second statement can be proven in the same way. □

Lemma 3.5.6

Assume H_f, H_g and $HF^{k,3}$ for $k \in \mathbb{N}_0$. Let $\theta \in C^{k,0}(\mathbb{R}^m \times \mathbb{R}^n; \mathbb{R})$ satisfy for some $C, p > 0$,

$$\sum_{|\gamma|\leq k}\sup_x |D_x^\gamma \theta(x,z)| \leq C(1+|z|^p).$$

Then

$$x \mapsto \mu_\infty(\theta; x)(x') = \int_{\mathbb{R}^n} \theta(x', z)\mu_\infty(dz; x) = \int_{\mathbb{R}^n} \theta(x', z)p_\infty(z; x)dz \in C_b^k(\mathbb{R}^m; \mathbb{R}).$$

Proof. From [PV03, Theorem 1, p.1170], we have that for any $q > 0$ there exists $C_q > 0$, such that,

$$\sum_{|\gamma|\leq k}\sup_x |D_x^\gamma p_\infty(z; x)| \leq \frac{C_q}{1+|z|^q}.$$

Therefore if q is chosen large enough, and we differentiate $p_\infty(z; x)$ under the integral sign, and using the growth constraint on θ and its derivatives, we obtain the result. □

Lemma 3.5.7

Assume H_f, H_g and $HF^{k,3}$ with $k \in \mathbb{N}_0$. Let $\theta \in C^{k,1}(\mathbb{R}^m \times \mathbb{R}^n; \mathbb{R})$ satisfy the growth condition,

$$\sum_{|\alpha|\leq k} \sum_{|\beta|\leq 1} \sup_x |D_x^\alpha D_z^\beta \theta(x,z)| \leq C(1+|z|^p),$$

for some $C, p > 0$. Assume additionally that θ satisfies the centering condition,

$$\int_{\mathbb{R}^n} \theta(x,z)\mu_\infty(dz;x) = 0, \quad \forall x \in \mathbb{R}^m.$$

Then

$$(x,z) \mapsto \int_0^\infty T_t^{F,x}(\theta(x,\cdot))(z)dt \in C^{k,1}(\mathbb{R}^m \times \mathbb{R}^n; \mathbb{R}),$$

and for every $q > 0$ there exists $C', q' > 0$, such that,

$$\sum_{|\alpha|\leq k} \sum_{|\beta|\leq 1} \int_0^\infty \sup_x |D_x^\alpha D_z^\beta T_t^{F,x}(\theta(x,\cdot))(z)|^q dt \leq C'(1+|z|^{q'}).$$

Proof. For the proof, we use the representation

$$\int_0^\infty T_t^{F,x}(\theta(x,\cdot))(z)dt = \int_0^1 \int_{\mathbb{R}^n} \theta(x,z')p_t(z';x,z)dz'dt + \int_1^\infty T_t^{F,x}(\theta(x,\cdot))(z)dt.$$

Then the statement,

$$\int_0^\infty T_t^{F,x}(\theta(x,\cdot))(z)dt \in C^{k,1}(\mathbb{R}^m \times \mathbb{R}^n; \mathbb{R}),$$

follows from the existence of the derivatives on $t \in [0,1)$ from Lemma 3.5.5 and $t \in [1,\infty)$ from [PV03, Theorem 2, p.1171]. Similarly, the bound on the growth of the derivatives of $T_t^{F,x}(\theta(x,\cdot))(z)$ given in [PV03, Theorem 2, p.1171], formula (15) states: For any $p_1 > 0$ there exist $C_1, p_1' > 0$, such that for any $(t,x,z) \in [1,\infty) \times \mathbb{R}^m \times \mathbb{R}^n$,

$$\sum_{|\alpha|\leq k} \sum_{|\beta|\leq 1} \left| D_x^\alpha D_z^\beta T_t^{F,x}(\theta(x,\cdot))(z) \right| \leq C_1 \frac{1+|z|^{p_1'}}{(1+t)^{p_1}}.$$

We combine this estimate with Lemma 3.5.5, from where we obtain for $(t,x,z) \in [0,\infty) \times \mathbb{R}^m \times \mathbb{R}^n$

$$\sum_{|\alpha|\leq k} \sum_{|\beta|\leq 1} \sup_x \left| D_x^\alpha D_z^\beta T_t^{F,x}(\theta(x,\cdot))(z) \right| \leq C_2 e^{C_2 t}(1+|z|^{p_2}).$$

We choose p_1 such that $qp_1 > 1$ and use the first estimate on $[1, \infty)$ and the second estimate on $[0, 1)$. The result follows. □

Lemma 3.5.8

Assume H_f, H_g and $HF^{k,3}$ with $k \in \mathbb{N}_0$. If $HS^{k,1}$ holds, then $\bar{b}, \bar{\sigma}, \bar{a} \in C_b^k$. Similarly, if $HO^{k,1}$ holds, then $\bar{h} \in C_b^k$.

Proof. The result follows from Lemma 3.5.7. □

3.5.3 Estimates for the Corrector Term

We now introduce a few lemmas that will help to streamline the main ideas in the analysis of the corrector term given in Lemma 3.6.2.

Lemma 3.5.9

Assume that $u \in C([0,T] \times \mathbb{R}^m; \mathbb{R})$ and is an element of $\mathcal{P}_T(\mathbb{R}^m; \mathbb{R})$. Assume H_f, H_g and $HF^{0,3}$. Let $\psi \in C_b^{0,1}(\mathbb{R}^m \times \mathbb{R}^n; \mathbb{R})$. Assume additionally that ψ satisfies the centering condition,

$$\int_{\mathbb{R}^n} \psi(x,z)\mu_\infty(dz;x) = 0, \quad \forall x \in \mathbb{R}^m.$$

Then given $(x,z) \in \mathbb{R}^m \times \mathbb{R}^n$ and $t \in [0,T]$, there exists $q > 0$ such that

$$\mathbb{E}\left[\left|\mathbb{E}\left[\int_t^T \psi(x, Z_s^{\epsilon,x;(t,z)})u_s(x)ds \,\middle|\, \mathcal{F}_{t,T}^B\right]\right|^p\right] \lesssim \epsilon^{2p}(1+|z|^q)\mathbb{E}\left[\sup_{t\le s\le T}|u_s(x)|^p\right].$$

Here $Z^{\epsilon,x}$ is the diffusion process with generator $\frac{1}{\epsilon^2}\mathcal{G}_F$ (in particular, the Brownian motion driving $Z^{\epsilon,x}$ is independent of the Brownian motion $\overleftarrow{B}_t$ that generates the backward filtration $\mathcal{F}_{t,T}^B$).

Proof. Because u_s is measurable with respect to $\mathcal{F}_{s,T}^B$ and $Z^{\epsilon,x;(t,z)}$ is independent of B, we get from the conditional expectation with respect to $\mathcal{F}_{t,T}^B$ and definition of the semigroup $T^{F,x}$ the following identity

$$\mathbb{E}\left[\int_t^T \psi(x, Z_s^{\epsilon,x;(t,z)})u_s(x)ds \,\middle|\, \mathcal{F}_{t,T}^B\right] = \int_t^T \mathbb{E}\left[\psi(x, Z_s^{\epsilon,x;(t,z)})\right]u_s(x)ds = \int_t^T T^{F,x}_{(s-t)/\epsilon^2}(\psi(x,\cdot))(z)u_s(x)ds.$$

Now taking the absolute value, using Hölder's inequality, and removing $|u_s(x)|$ from the integral by taking the supremum over $[t,T]$ gives

$$\left|\int_t^T T^{F,x}_{(s-t)/\epsilon^2}(\psi(x,\cdot))(z)u_s(x)ds\right| \lesssim \sup_{t\le s\le T}|u_s(x)| \int_t^T \left|T^{F,x}_{(s-t)/\epsilon^2}(\psi(x,\cdot))(z)\right| ds. \tag{3.5.1}$$

Performing a time reparametrization and then using Lemma 3.5.7, we have for some $q' > 0$,

$$\begin{aligned}\sup_{t\le s\le T}|u_s(x)|\int_t^T \left|T^{F,x}_{(s-t)/\epsilon^2}(\psi(x,\cdot))(z)\right| ds &\lesssim \epsilon^2 \sup_{t\le s\le T}|u_s(x)|\int_0^{(T-t)/\epsilon^2}\left|T^{F,x}_r(\psi(x,\cdot))(z)\right| dr\\ &\lesssim \epsilon^2 \sup_{t\le s\le T}|u_s(x)|\int_0^{\infty}\left|T^{F,x}_r(\psi(x,\cdot))(z)\right| dr\\ &\lesssim \epsilon^2(1+|z|^{q'})\sup_{t\le s\le T}|u_s(x)|.\end{aligned}$$

Lastly, taking the p-th power and applying the expectation gives the desired result. □

Lemma 3.5.10

Assume that $u \in C([0,T]\times\mathbb{R}^m;\mathbb{R}^k)$ and is an element of $\mathcal{P}_T(\mathbb{R}^m;\mathbb{R}^k)$ for $k \ge 1$. Assume H_f, H_g and $HF^{0,3}$. Let $\psi \in C_b^{0,1}(\mathbb{R}^m\times\mathbb{R}^n;\mathbb{R}^{d\times k})$. Assume additionally that ψ satisfies the centering condition,

$$\int_{\mathbb{R}^n}\psi(x,z)\mu_\infty(dz;x) = 0, \quad \forall x\in\mathbb{R}^m.$$

Then given $(x,z)\in\mathbb{R}^m\times\mathbb{R}^n$ and $t\in[0,T]$, there exists $q>0$ such that

$$\mathbb{E}\left[\left|\mathbb{E}\left[\int_t^T \langle\psi(x,Z_s^{\epsilon,x;(t,z)})u_s(x), d\overleftarrow{B}_s\rangle \,\middle|\, \mathcal{F}^B_{t,T}\right]\right|^p\right] \lesssim \epsilon^p(1+|z|^q)\mathbb{E}\left[\sup_{t\le s\le T}|u_s(x)|^p\right].$$

Here $Z^{\epsilon,x}$ is the diffusion process with generator $\frac{1}{\epsilon^2}\mathcal{G}_F$ (in particular, the Brownian motion driving $Z^{\epsilon,x}$ is independent of the Brownian motion $\overleftarrow{B}_t$ that generates the backward filtration $\mathcal{F}^B_{t,T}$).

Proof. Because u_s is measurable with respect to $\mathcal{F}^B_{s,T}$ and $Z^{\epsilon,x;(t,z)}$ is independent of B, we get from the conditional expectation with respect to $\mathcal{F}^B_{t,T}$ and definition of the semigroup $T^{F,x}$ the following identity

$$\begin{aligned}\mathbb{E}\left[\int_t^T \langle\psi(x,Z_s^{\epsilon,x;(t,z)})u_s(x), d\overleftarrow{B}_s\rangle \,\middle|\, \mathcal{F}^B_{t,T}\right] &= \int_t^T \langle\mathbb{E}\left[\psi(x,Z_s^{\epsilon,x;(t,z)})\right]u_s(x), d\overleftarrow{B}_s\rangle\\ &= \int_t^T \langle T^{F,x}_{(s-t)/\epsilon^2}(\psi(x,\cdot))(z)u_s(x), d\overleftarrow{B}_s\rangle.\end{aligned}$$

Now by application of the Burkholder-Davis-Gundy inequality we get

$$\begin{aligned}\mathbb{E}\left[\left|\int_t^T \langle T^{F,x}_{(s-t)/\epsilon^2}(\psi(x,\cdot))(z)u_s(x), d\overleftarrow{B}_s\rangle\right|^p\right] &\le \mathbb{E}\left[\left(\sup_{t\le r\le T}\left|\int_r^T \langle T^{F,x}_{(s-t)/\epsilon^2}(\psi(x,\cdot))(z)u_s(x), d\overleftarrow{B}_s\rangle\right|\right)^p\right]\\ &\lesssim \mathbb{E}\left[\left\langle\int_t^T \langle T^{F,x}_{(s-t)/\epsilon^2}(\psi(x,\cdot))(z)u_s(x), d\overleftarrow{B}_s\rangle\right\rangle^{p/2}\right].\end{aligned}$$

Computing the quadratic variation gives

$$\left\langle \int_t^T \langle T^{F,x}_{(s-t)/\epsilon^2}(\psi(x,\cdot))(z)u_s(x), d\overleftarrow{B}_s \rangle \right\rangle = \int_t^T |T^{F,x}_{(s-t)/\epsilon^2}(\psi(x,\cdot))(z)u_s(x)|^2 ds. \tag{3.5.2}$$

In the case that u is real-valued, the integrand is bounded by

$$|T^{F,x}_{(s-t)/\epsilon^2}(\psi(x,\cdot))(z)u_s(x)|^2 = \langle T^{F,x}_{(s-t)/\epsilon^2}(\psi(x,\cdot))(z)u_s(x) \rangle \leq |u_s(x)|^2 |T^{F,x}_{(s-t)/\epsilon^2}(\psi(x,\cdot))(z)|^2, \tag{3.5.3}$$

where $\langle \beta \rangle$ is a short-hand notation for the inner product $\langle \beta, \beta \rangle$. Similarly, in the case where u is a vector with values in $\mathbb{R}^k$ for some $k > 1$, then $T^{F,x}_{(s-t)/\epsilon^2}(\psi(x,\cdot))(z)$ takes values in $\mathbb{R}^{d\times k}$. For temporary brevity, let $A_s \equiv T^{F,x}_{(s-t)/\epsilon^2}(\psi(x,\cdot))(z)$. Then by Lemma A.3.1 we have the same inequality for the integrand, but this time $|A_s|^2$ corresponds to the trace of the matrix $A_s^* A_s$ and the inequality is multiplied by some constant C that depends on the dimension of the problem.

Therefore using Eq. 3.5.3 in the quadratic variation of Eq. 3.5.2 and then taking the function $|u_s(x)|$ outside the integral by using its supremum value over $[t, T]$, we get

$$\begin{aligned}\left\langle \int_t^T \langle T^{F,x}_{(s-t)/\epsilon^2}(\psi(x,\cdot))(z)u_s(x), d\overleftarrow{B}_s \rangle \right\rangle &\leq \int_t^T |T^{F,x}_{(s-t)/\epsilon^2}(\psi(x,\cdot))(z)|^2 |u_s(x)|^2 ds \\ &= \sup_{t\leq s\leq T} |u_s(x)|^2 \int_t^T |T^{F,x}_{(s-t)/\epsilon^2}(\psi(x,\cdot))(z)|^2 ds.\end{aligned}$$

We now perform a time reparametrization and use Lemma 3.5.7, so that for some $q' > 0$ we get

$$\begin{aligned}\sup_{t\leq s\leq T} |u_s(x)|^2 \int_t^T |T^{F,x}_{(s-t)/\epsilon^2}(\psi(x,\cdot))(z)|^2 ds &= \epsilon^2 \sup_{t\leq s\leq T} |u_s(x)|^2 \int_0^{(T-t)/\epsilon^2} |T^{F,x}_r(\psi(x,\cdot))(z)|^2 dr \\ &= \epsilon^2 \sup_{t\leq s\leq T} |u_s(x)|^2 \int_0^{\infty} |T^{F,x}_r(\psi(x,\cdot))(z)|^2 dr \\ &\lesssim \epsilon^2 (1 + |z|^{q'}) \sup_{t\leq s\leq T} |u_s(x)|^2. \end{aligned} \tag{3.5.4}$$

To see that the last step still holds in the case that ψ is matrix-valued, consider the following relations

$$\begin{aligned}|T^{F,x}_r(\psi(x,\cdot))(z)|^2 &= \sum_{i=1}^d \left(T^{F,x}_r(\psi(x,\cdot))(z) T^{F,x}_r(\psi(x,\cdot))(z)^* \right)_{ii} \\ &= \sum_{i,j=1}^d \left(T^{F,x}_r(\psi(x,\cdot))(z) \right)^2_{ij} = \sum_{i,j=1}^d |T^{F,x}_r(\psi(x,\cdot)_{ij})(z)|,\end{aligned}$$

which shows that the same analysis holds, but now for a summation over the centered entries of ψ. Finally,

taking the $p/2$ power and applying the expectation to Eq. 3.5.4 gives the desired result. □

3.6 Main Analysis

3.6.1 Moment Estimates for Dual Processes

In this section, we compute the main estimates for v^0, ψ and R associated with an arbitrary fixed test function $\varphi \in C_b^2$. The estimates for ψ and R are then used in Section 3.6.2 to prove Theorem 3.2.1.

Lemma 3.6.1

Let $3 \leq k \in \mathbb{N}$ and assume $\bar{b}, \bar{a}, \varphi \in C_b^k$ and $\bar{h}, \bar{\sigma} \in C_b^{k+1}$. Then $v^0 \in C^{0,k-1}([0,T] \times \mathbb{R}^m; \mathbb{R})$, and for any $p \geq 1$ there exist $q > 0$, such that for all $x \in \mathbb{R}^m$,

$$\sum_{|j| \leq k-1} \mathbb{E}\left[\sup_{0 \leq t \leq T} |D_x^j v_t^0(x)|^p\right] \lesssim (1 + |x|^q)|\varphi|_{k,\infty}^p.$$

In particular, v^0 and all its partial derivatives up to order $(0, k-1)$ are in $\mathcal{P}_T(\mathbb{R}^m; \mathbb{R})$.

Proof. The result follows from Lemma 3.4.1. The only condition from Lemma 3.4.1 that is not immediately obvious is the parabolic condition, $2\bar{a} - \bar{\sigma}\alpha^*\alpha\bar{\sigma}^* \succeq 0$. This condition indeed holds for the same reason as given in the paragraph below Eq. 3.2.5 and the fact that $I - \alpha^*\alpha \succeq 0$, where I is the identity matrix (recall that α was redefined in Section 2.1 as $\alpha \leftarrow \kappa^{-1}\alpha$, and note that $(\kappa^{-1})^* = (\kappa^*)^{-1}$). □

Lemma 3.6.2

Let $3 \leq k, l \in \mathbb{N}$ and assume H_f, H_g, $HF^{k,l}$, $HS^{k,l}$, $HO^{k,l}$, and that $\bar{\sigma}, \bar{a}, \bar{b}, \bar{h} \in C_b^k$. Let $v^0 \in C^{0,k}([0,T] \times \mathbb{R}^m; \mathbb{R})$, and assume that all its partial derivatives in x up to order k are in $\mathcal{P}_T(\mathbb{R}^m; \mathbb{R})$.

Then $\psi \in C^{0,k-1,l-1}([0,T] \times \mathbb{R}^m \times \mathbb{R}^n; \mathbb{R})$, and ψ as well as its partial derivatives up to order $(0, k-1, l-1)$ are in $\mathcal{P}_T(\mathbb{R}^m \times \mathbb{R}^n; \mathbb{R})$. For any $p \geq 1$ there exists $q > 0$, such that for any $(x, z) \in \mathbb{R}^m \times \mathbb{R}^n$ and any $\epsilon \in (0,1)$

$$\sum_{|\beta| \leq k-2} \sup_{0 \leq t \leq T} \mathbb{E}\left[|D_x^\beta \psi_t(x,z)|^p\right] \lesssim \epsilon^p (1 + |z|^q) \sum_{|\beta| \leq k} \mathbb{E}\left[\sup_{0 \leq t \leq T} |D_x^\beta v_t^0(x)|^p\right].$$

Proof. $\psi_t(x,z)$ solves the following BSPDE

$$-d\psi_t(x,z) = \left[\frac{1}{\epsilon^2}\mathcal{G}_F \psi_t(x,z) + (\mathcal{G}_S - \overline{\mathcal{G}_S}) v_t^0(x,z)\right] dt + \langle v_t^0(h - \bar{h})(x,z), d\overleftarrow{B}_t \rangle + \langle \alpha(\sigma - \bar{\sigma})^* \nabla_x v_t^0(x,z), d\overleftarrow{B}_t \rangle,$$

$$\psi_T(x,z) = 0.$$

Existence of the solution ψ and its derivatives as well as the polynomial growth follow from Lemma 3.4.1. From Lemma 3.4.2, the solution, $\psi_t(x,z)$, has a representation in terms of a FBDSDE, $\psi_t(x,z) = \theta_t^{t,x,z}$. Where θ is a component of the pair of processes $(\theta, \gamma^\epsilon)$ satisfying the BDSDE

$$\begin{aligned} -d\theta_s^{t,x,z} &= \left[\mathcal{G}_S(x, Z_s^{\epsilon,x;(t,z)}) - \overline{\mathcal{G}_S}(x)\right] v_s^0(x) ds \\ &\quad + \langle v_s^0(x)(h(x, Z_s^{\epsilon,x;(t,z)}) - \bar{h}(x)), d\overleftarrow{B}_s\rangle + \langle \alpha(\sigma(x, Z_s^{\epsilon,x;(t,z)}) - \bar{\sigma}(x))^* \nabla_x v_s^0(x), d\overleftarrow{B}_s\rangle \\ &\quad - \langle \gamma_s^{\epsilon;(t,x,z)}, dV_s\rangle, \\ \theta_T^{t,x,z} &= 0, \end{aligned} \tag{3.6.1}$$

and $(x, Z_s^{\epsilon,x;(t,z)})$ is a joint diffusion process with $X_s^{\epsilon;(t,x)}$ having the zero generator,

$$X_s^{\epsilon;(t,x)} = x, \qquad \forall\, s \in [t,T],$$

and $Z_s^{\epsilon,x;(t,z)}$ satisfying the stochastic differential equation

$$\begin{aligned} dZ_s^{\epsilon,x;(t,z)} &= \frac{1}{\epsilon^2} f(x, Z_s^{\epsilon,x;(t,z)}) ds + \frac{1}{\epsilon} g(x, Z_s^{\epsilon,x;(t,z)}) dV_s, \qquad s \geq t, \\ Z_s^{\epsilon,x;(t,z)} &= z, \qquad s \leq t. \end{aligned}$$

The second component of the pair $(\theta_t^{t,x,z}, \gamma_t^{\epsilon;(t,x,z)})$, has a representation as

$$\gamma_t^{\epsilon;(t,x,z)} = \frac{1}{\epsilon} g^* \nabla_z \psi_t(x,z).$$

For brevity, let us temporarily drop from the notation, superscripts and part of superscripts that indicate initial conditions (for example, (t,x,z) and (t,z)).

Since ψ_t is $\mathcal{F}_{t,T}^B$-measurable, so is θ_t, and therefore conditioning θ_t on $\mathcal{F}_{t,T}^B$ gives $\theta_t = \mathbb{E}\left[\theta_t \,\middle|\, \mathcal{F}_{t,T}^B\right]$. We also observe that V and B are independent. Therefore, V is a Brownian motion in the larger filtration $(\mathcal{F}_s^V \vee \mathcal{F}_{t,T}^B)_{s\in[0,T]}$. Hence, if we condition the integral version of Eq. 3.6.1, the stochastic integral will vanish. Specifically, consider an application of the tower property of conditional expectation,

$$\mathbb{E}\left[\int_t^T \langle \gamma_s^\epsilon, dV_s\rangle \,\middle|\, \mathcal{F}_{t,T}^B\right] = \mathbb{E}\left[\mathbb{E}\left[\int_t^T \langle \gamma_s^\epsilon, dV_s\rangle \,\middle|\, \mathcal{F}_t^V \vee \mathcal{F}_{t,T}^B\right] \,\middle|\, \mathcal{F}_{t,T}^B\right] = 0.$$

Therefore, we condition the integral form of Eq. 3.6.1 on $\mathcal{F}^B_{t,T}$ to get

$$\begin{aligned}\theta_t = &\mathbb{E}\left[\int_t^T \left[\mathcal{G}_S(x, Z_s^{\epsilon,x}) - \overline{\mathcal{G}_S}(x)\right] v_s^0(x) ds \,\middle|\, \mathcal{F}^B_{t,T}\right] \\ &+ \mathbb{E}\left[\int_t^T \langle v_s^0(x)(h(x, Z_s^{\epsilon,x}) - \bar{h}(x)), d\overleftarrow{B}_s\rangle \,\middle|\, \mathcal{F}^B_{t,T}\right] \\ &+ \mathbb{E}\left[\int_t^T \langle \alpha(\sigma(x, Z_s^{\epsilon,x}) - \bar{\sigma}(x))^* \nabla_x v_s^0(x), d\overleftarrow{B}_s\rangle \,\middle|\, \mathcal{F}^B_{t,T}\right].\end{aligned} \tag{3.6.2}$$

Then we take the p-th moment, and separate terms on the right side of the equation by Hölder's inequality to get

$$\mathbb{E}\left[|\theta_t|^p\right] \lesssim \mathbb{E}\left[\left|\mathbb{E}\left[\int_t^T \left[\mathcal{G}_S(x, Z_s^{\epsilon,x}) - \overline{\mathcal{G}_S}(x)\right] v_s^0(x) ds \,\middle|\, \mathcal{F}^B_{t,T}\right]\right|^p\right] \tag{3.6.3}$$

$$+ \mathbb{E}\left[\left|\mathbb{E}\left[\int_t^T \langle v_s^0(x)(h(x, Z_s^{\epsilon,x}) - \bar{h}(x)), d\overleftarrow{B}_s\rangle \,\middle|\, \mathcal{F}^B_{t,T}\right]\right|^p\right] \tag{3.6.4}$$

$$+ \mathbb{E}\left[\left|\mathbb{E}\left[\int_t^T \langle \alpha(\sigma(x, Z_s^{\epsilon,x}) - \bar{\sigma}(x))^* \nabla_x v_s^0(x), d\overleftarrow{B}_s\rangle \,\middle|\, \mathcal{F}^B_{t,T}\right]\right|^p\right]. \tag{3.6.5}$$

The first term, Eq. 3.6.3, has an integrand that can be written as

$$\left[\mathcal{G}_S(x, Z_s^{\epsilon,x}) - \overline{\mathcal{G}_S}(x)\right] v_s^0(x) = \sum_{i=1}^m (b - \bar{b})_i \frac{\partial}{\partial x_i} v_s^0(x, Z_s^{\epsilon,x}) + \frac{1}{2}\sum_{i,j=1}^m (a - \bar{a})_{ij} \frac{\partial^2}{\partial x_i \partial x_j} v_s^0(x, Z_s^{\epsilon,x}),$$

which shows that this term is a summation of terms that fit the conditions of Lemma 3.5.9 (i.e., a centered function driven by $Z^{\epsilon,x}$ and multiplied with a term that has the correct bounds and measurability properties) and therefore we get for some $q_0 > 0$ the following estimate for this term

$$\mathbb{E}\left[\left|\mathbb{E}\left[\int_t^T \left[\mathcal{G}_S(x, Z_s^{\epsilon,x}) - \overline{\mathcal{G}_S}(x)\right] v_s^0(x) ds \,\middle|\, \mathcal{F}^B_{t,T}\right]\right|^p\right] \lesssim \epsilon^{2p}(1 + |z|^{q_0}) \sum_{1 \le |\beta| \le 2} \mathbb{E}\left[\sup_{t \le s \le T} \left|D_x^\beta v_s^0(x)\right|^p\right]. \tag{3.6.6}$$

The second term, Eq. 3.6.4, fits the assumptions of Lemma 3.5.10, and therefore we get for some $q_1 > 0$ the following estimate for this term

$$\mathbb{E}\left[\left|\mathbb{E}\left[\int_t^T \langle v_s^0(x)(h(x, Z_s^{\epsilon,x}) - \bar{h}(x)), d\overleftarrow{B}_s\rangle \,\middle|\, \mathcal{F}^B_{t,T}\right]\right|^p\right] \lesssim \epsilon^p(1 + |z|^{q_1}) \mathbb{E}\left[\sup_{t \le s \le T} \left|v_s^0(x)\right|^p\right]. \tag{3.6.7}$$

Unlike the time integral term, we only get ϵ^p for this estimate because of the application of the Burkholder-Davis-Gundy inequality in the proof of Lemma 3.5.10.

Lemma 3.5.10 also covers the case where the integrand of the stochastic integral is a matrix-vector product,

as occurs in Eq. 3.6.5. Because each entry in Eq. 3.6.5 is centered and v^0 meets the required conditions of Lemma 3.5.10, we get for some $q_2 > 0$ the following estimate

$$\mathbb{E}\left[\left|\mathbb{E}\left[\int_t^T \langle \alpha(\sigma(x, Z_s^{\epsilon,x}) - \bar{\sigma}(x))^* \nabla_x v_s^0(x), d\overleftarrow{B}_s \rangle \,\middle|\, \mathcal{F}_{t,T}^B\right]\right|^p\right] \lesssim \epsilon^p (1 + |z|^{q_2}) \sum_{|\beta|=1} \mathbb{E}\left[\sup_{t \le s \le T} \left|D_x^\beta v_s^0(x)\right|^p\right]. \quad (3.6.8)$$

Collecting the estimates from Eqs. 3.6.6, 3.6.7, and 3.6.8, we get for some $q_3 > 0$ the following estimate for the BDSDE solution,

$$\mathbb{E}\left[|\theta_t|^p\right] \lesssim \epsilon^p (1 + |z|^{q_3}) \sum_{|\beta| \le 2} \mathbb{E}\left[\sup_{t \le s \le T} \left|D_x^\beta v_s^0(x)\right|^p\right]. \quad (3.6.9)$$

We will also need estimates of the first and second order derivatives of ψ in x for estimating the remainder term R in Lemma 3.6.3 (see for instance Eq. 3.3.3). Therefore consider taking a first order derivative of Eq. 3.6.2, and then taking the p-th moment, and separating terms on the right side of the equation by Hölder's inequality,

$$\mathbb{E}\left[\left|\frac{\partial}{\partial x_k}\theta_t\right|^p\right] \lesssim \mathbb{E}\left[\left|\frac{\partial}{\partial x_k}\mathbb{E}\left[\int_t^T \left[\mathcal{G}_S(x, Z_s^{\epsilon,x}) - \overline{\mathcal{G}_S}(x)\right] v_s^0(x) ds \,\middle|\, \mathcal{F}_{t,T}^B\right]\right|^p\right] \quad (3.6.10)$$

$$+ \mathbb{E}\left[\left|\frac{\partial}{\partial x_k}\mathbb{E}\left[\int_t^T \langle v_s^0(x)(h(x, Z_s^{\epsilon,x}) - \bar{h}(x)), d\overleftarrow{B}_s \rangle \,\middle|\, \mathcal{F}_{t,T}^B\right]\right|^p\right] \quad (3.6.11)$$

$$+ \mathbb{E}\left[\left|\frac{\partial}{\partial x_k}\mathbb{E}\left[\int_t^T \langle \alpha(\sigma(x, Z_s^{\epsilon,x}) - \bar{\sigma}(x))^* \nabla_x v_s^0(x), d\overleftarrow{B}_s \rangle \,\middle|\, \mathcal{F}_{t,T}^B\right]\right|^p\right]. \quad (3.6.12)$$

Just as we dealt with Eq. 3.6.3 by first expanding the difference of the generators we can do the same for Eq. 3.6.10 to get

$$\mathbb{E}\left[\left|\frac{\partial}{\partial x_k}\mathbb{E}\left[\int_t^T \left[\mathcal{G}_S(x, Z_s^{\epsilon,x}) - \overline{\mathcal{G}_S}(x)\right] v_s^0(x) ds \,\middle|\, \mathcal{F}_{t,T}^B\right]\right|^p\right] \lesssim \sum_{1 \le |\beta| \le 2} \mathbb{E}\left[\left|\frac{\partial}{\partial x_k}\mathbb{E}\left[\int_t^T \psi^\beta(x, Z_s^{\epsilon,x}) D_x^\beta v_s^0(x) ds \,\middle|\, \mathcal{F}_{t,T}^B\right]\right|^p\right],$$

where ψ^β is either an entry of $b - \bar{b}$ or $\frac{1}{2}(a - \bar{a})$, and hence centered. Now following the same arguments as in

the proof of Lemma 3.5.9, we are able to get for any multiindex $1 \leq |\beta| \leq 2$,

$$\mathbb{E}\left[\left|\frac{\partial}{\partial x_k}\mathbb{E}\left[\int_t^T \psi^\beta(x, Z_s^{\epsilon,x}) D_x^\beta v_s^0(x) ds \,\middle|\, \mathcal{F}_{t,T}^B\right]\right|^p\right] = \mathbb{E}\left[\left|\frac{\partial}{\partial x_k}\int_t^T \mathbb{E}\left[\psi^\beta(x, Z_s^{\epsilon,x})\right] D_x^\beta v_s^0(x) ds\right|^p\right]$$
$$= \mathbb{E}\left[\left|\frac{\partial}{\partial x_k}\int_t^T T^{F,x}_{(s-t)/\epsilon^2}(\psi^\beta(x,\cdot))(z) D_x^\beta v_s^0(x) ds\right|^p\right].$$

Distributing the derivative inside the time integral now gives (ignoring the p-th power and expectation for clarity in the next argument)

$$\left|\frac{\partial}{\partial x_k}\int_t^T T^{F,x}_{(s-t)/\epsilon^2}(\psi^\beta(x,\cdot))(z) D_x^\beta v_s^0(x) ds\right| \leq \left|\int_t^T \frac{\partial}{\partial x_k} T^{F,x}_{(s-t)/\epsilon^2}(\psi^\beta(x,\cdot))(z) D_x^\beta v_s^0(x) ds\right|$$
$$+ \left|\int_t^T T^{F,x}_{(s-t)/\epsilon^2}(\psi^\beta(x,\cdot))(z) \frac{\partial}{\partial x_k} D_x^\beta v_s^0(x) ds\right|.$$

Estimates for both terms are now achieved by applying the procedure in the proof of Lemma 3.5.9 starting from Eq. 3.5.1 onwards (and using the fact that Lemma 3.5.7 gives bounds for the derivative of the semigroup) to get for some $q_4 > 0$

$$\mathbb{E}\left[\left|\frac{\partial}{\partial x_k}\mathbb{E}\left[\int_t^T \left[\mathcal{G}_S(x, Z_s^{\epsilon,x}) - \overline{\mathcal{G}_S}(x)\right] v_s^0(x) ds \,\middle|\, \mathcal{F}_{t,T}^B\right]\right|^p\right]$$
$$\lesssim \epsilon^{2p}(1+|z|^{q_4}) \sum_{1\leq|\beta|\leq 3} \mathbb{E}\left[\sup_{t\leq s\leq T} \left|D_x^\beta v_s^0(x)\right|^p\right]. \quad (3.6.13)$$

Turning our attention now to Eq. 3.6.11, we follow the procedure of Lemma 3.5.10 to interchange the conditional expectation and stochastic integration, and then because of $HO^{k+1,l+1}$, we can interchange ordinary differentiation and stochastic integration [Kar83], and distribute the derivative to get

$$\mathbb{E}\left[\left|\frac{\partial}{\partial x_k}\mathbb{E}\left[\int_t^T \langle v_s^0(x)(h(x, Z_s^{\epsilon,x}) - \bar{h}(x)), d\overleftarrow{B}_s\rangle \,\middle|\, \mathcal{F}_{t,T}^B\right]\right|^p\right]$$
$$\lesssim \mathbb{E}\left[\left|\int_t^T \langle \frac{\partial}{\partial x_k} v_s^0(x) T^{F,x}_{(s-t)/\epsilon^2}((h-\bar{h})(x,\cdot))(z), d\overleftarrow{B}_s\rangle\right|^p\right]$$
$$+ \mathbb{E}\left[\left|\int_t^T \langle v_s^0(x) \frac{\partial}{\partial x_k} T^{F,x}_{(s-t)/\epsilon^2}((h-\bar{h})(x,\cdot))(z), d\overleftarrow{B}_s\rangle\right|^p\right].$$

Estimates for both terms on the right side of the equation now follow from the same arguments in the proof of Lemma 3.5.10, starting from the application of the Burkholder-Davis-Gundy inequality (and again using

the fact that Lemma 3.5.7 gives bounds for the derivative of the semigroup), to yield for some $q_5 > 0$

$$\mathbb{E}\left[\left|\frac{\partial}{\partial x_k}\mathbb{E}\left[\int_t^T \langle v_s^0(x)(h(x, Z_s^{\epsilon,x}) - \bar{h}(x)), d\overleftarrow{B}_s\rangle \,\middle|\, \mathcal{F}_{t,T}^B\right]\right|^p\right] \lesssim \epsilon^p(1+|z|^{q_5}) \sum_{|\beta|\leq 1} \mathbb{E}\left[\sup_{t\leq s\leq T}\left|D_x^\beta v_s^0(x)\right|^p\right]. \quad (3.6.14)$$

The last term to address is Eq. 3.6.12. Just as we did when handling Eq. 3.6.11, we follow the procedure of Lemma 3.5.10 to interchange the conditional expectation and stochastic integration, and then because of $HO^{k+1,l+1}$ interchange ordinary differentiation and stochastic integration [Kar83], and distribute the derivative to get

$$\begin{aligned}\mathbb{E}\left[\left|\frac{\partial}{\partial x_k}\mathbb{E}\left[\int_t^T \langle \alpha(\sigma(x, Z_s^{\epsilon,x}) - \bar{\sigma}(x))^* \nabla_x v_s^0(x), d\overleftarrow{B}_s\rangle \,\middle|\, \mathcal{F}_{t,T}^B\right]\right|^p\right] \\ \lesssim \mathbb{E}\left[\left|\int_t^T \langle \frac{\partial}{\partial x_k} T^{F,x}_{(s-t)/\epsilon^2}(\alpha(\sigma-\bar{\sigma})^*(x,\cdot))(z)\nabla_x v_s^0(x), d\overleftarrow{B}_s\rangle\right|^p\right] \\ + \mathbb{E}\left[\left|\int_t^T \langle T^{F,x}_{(s-t)/\epsilon^2}(\alpha(\sigma-\bar{\sigma})^*(x,\cdot))(z)\frac{\partial}{\partial x_k}\nabla_x v_s^0(x), d\overleftarrow{B}_s\rangle\right|^p\right].\end{aligned}$$

Estimates for both terms on the right side of the equation now follow from the same arguments in the proof of Lemma 3.5.10, starting from the application of the Burkholder-Davis-Gundy inequality (and again using the fact that Lemma 3.5.7 gives bounds for the derivative of the semigroup), to yield for some $q_6 > 0$

$$\mathbb{E}\left[\left|\frac{\partial}{\partial x_k}\mathbb{E}\left[\int_t^T \langle \alpha(\sigma(x, Z_s^{\epsilon,x}) - \bar{\sigma}(x))^* \nabla_x v_s^0(x), d\overleftarrow{B}_s\rangle \,\middle|\, \mathcal{F}_{t,T}^B\right]\right|^p\right] \lesssim \epsilon^p(1+|z|^{q_6}) \sum_{1\leq|\beta|\leq 2} \mathbb{E}\left[\sup_{t\leq s\leq T}\left|D_x^\beta v_s^0(x)\right|^p\right]. \quad (3.6.15)$$

Collecting the estimates from Eqs. 3.6.13, 3.6.14, and 3.6.15 then yields for some $q_7 > 0$

$$\mathbb{E}\left[\left|\frac{\partial}{\partial x_k}\theta_t\right|^p\right] \lesssim \epsilon^p(1+|z|^{q_7}) \sum_{|\beta|\leq 3} \mathbb{E}\left[\sup_{t\leq s\leq T}\left|D_x^\beta v_s^0(x)\right|^p\right].$$

The procedure to take higher-order derivatives is the same as that for the first order derivatives (simply involving more terms), and therefore taking the supremum of the estimates of these derivatives over $[0, T]$

and summing the terms, we get for some $q > 0$

$$\sum_{|\beta|\leq k-1} \sup_{0\leq t\leq T} \mathbb{E}\left[\left|D_x^\beta \theta_t\right|^p\right] \lesssim \epsilon^p(1+|z|^q) \sum_{|\beta|\leq k+1} \mathbb{E}\left[\sup_{0\leq t\leq T}\left|D_x^\beta v_t^0(x)\right|^p\right].$$

□

Lemma 3.6.3

Let $3 \leq k, l \in \mathbb{N}$ and assume $HF^{k,l}$, $HS^{k,l}$, $\sigma \in C_b^{k+1,l+1}$, and $HO^{k+1,l+1}$. Let $\psi \in C^{0,k+2,l}([0,T]\times\mathbb{R}^m\times\mathbb{R}^n;\mathbb{R})$ and assume that all its partial derivatives up to order $(0,k+2,l)$ are in $\mathcal{P}_T(\mathbb{R}^m\times\mathbb{R}^n;\mathbb{R})$. Then for any $p > 2$, we have that for any $(x,z)\in\mathbb{R}^m\times\mathbb{R}^n$, $\epsilon\in(0,1)$, and $t\in[0,T]$,

$$\mathbb{E}\left[|R_t(x,z)|^p\right] \lesssim \sum_{|j|\leq 2} \int_t^T \mathbb{E}\left[\mathbb{E}\left[|D_x^j\psi_s(x',z')|^p\right]_{(x',z')=(X_s^{\epsilon;(t,x)},Z_s^{\epsilon;(t,z)})}\right] ds.$$

Proof. $R_t(x,z)$ solves the following BSPDE

$$-dR_t = (\mathcal{G}^\epsilon R_t + \mathcal{G}_S\psi_t)dt + \langle(\psi_t+R_t)h, d\overleftarrow{B}_t\rangle + \langle\alpha\sigma^*\nabla_x(\psi_t+R_t), d\overleftarrow{B}_t\rangle, \qquad R_T = 0. \tag{3.6.16}$$

Existence of the solution R and its derivatives as well as the polynomial growth all follow from Lemma 3.4.1. The parabolic condition of Lemma 3.4.1 holds because $I - \alpha^*\alpha \succeq 0$, where I is the identity matrix. From Lemma 3.4.2, the solution, $R_t(x,z)$, has a representation in terms of a FBDSDE, $R_t(x,z) = \theta_t^{t,x,z}$. Where θ_t is the first component of the tuple of processes $(\theta_s, \gamma_s^\epsilon, \eta_s)$ satisfying the BDSDE

$$\begin{aligned}
-d\theta_s^{t,x,z} &= \mathcal{G}_S\psi_s(X_s^{\epsilon;(t,x)}, Z_s^{\epsilon;(t,z)})ds \\
&\quad + \langle\psi_s h(X_s^{\epsilon;(t,x)}, Z_s^{\epsilon;(t,z)}), d\overleftarrow{B}_s\rangle + \langle\theta_s^{t,x,z}h(X_s^{\epsilon;(t,x)}, Z_s^{\epsilon;(t,z)}), d\overleftarrow{B}_s\rangle \\
&\quad + \langle\alpha\sigma^*\nabla_x\psi_s(X_s^{\epsilon;(t,x)}, Z_s^{\epsilon;(t,z)}), d\overleftarrow{B}_s\rangle + \langle\alpha\eta_s^{t,x,z}, d\overleftarrow{B}_s\rangle \\
&\quad - \langle\eta_s^{t,x,z}, dW_s\rangle - \langle\gamma_s^{\epsilon;t,x,z}, dV_s\rangle, \\
\theta_T^{t,x,z} &= 0,
\end{aligned} \tag{3.6.17}$$

and $(X_s^{\epsilon;(t,x)}, Z_s^{\epsilon;(t,z)})$ is a joint diffusion process satisfying the SDEs

$$\begin{aligned}
dX_s^{\epsilon;(t,x)} &= b(X_s^{\epsilon;(t,x)}, Z_s^{\epsilon;(t,z)})ds + \sigma(X_s^{\epsilon;(t,x)}, Z_s^{\epsilon;(t,z)})dW_s, \qquad s \geq t, \\
X_s^{\epsilon;(t,x)} &= x, \qquad s \leq t, \\
dZ_s^{\epsilon;(t,z)} &= \frac{1}{\epsilon} f(X_s^{\epsilon;(t,x)}, Z_s^{\epsilon;(t,z)})ds + \frac{1}{\sqrt{\epsilon}} g(X_s^{\epsilon;(t,x)}, Z_s^{\epsilon;(t,z)})dV_s, \qquad s \geq t, \\
Z_s^{\epsilon;(t,z)} &= z, \qquad s \leq t,
\end{aligned}$$

where we choose (W, V) and B to be independent standard Brownian motions. This is necessary when working with a stochastic representation of Eq. 3.6.16. The second and third components of the tuple $(\theta_t^{t,x,z}, \gamma_t^{\epsilon;(t,x,z)}, \eta_t^{t,x,z})$, have representations as

$$\gamma_t^{\epsilon;(t,x,z)} = \frac{1}{\epsilon} g^* \nabla_z R_t(x,z) \qquad \text{and} \qquad \eta_t^{t,x,z} = \sigma^* \nabla_x R_t(x,z).$$

Let $\mathcal{A}$ be the integrand for the backward stochastic integral in Eq. 3.6.17; it takes the following definition

$$\mathcal{A} = \psi_s h(X_s^{\epsilon;(t,x)}, Z_s^{\epsilon;(t,z)}) + \theta_s^{t,x,z} h(X_s^{\epsilon;(t,x)}, Z_s^{\epsilon;(t,z)}) + \alpha\sigma^* \nabla_x \psi_s(X_s^{\epsilon;(t,x)}, Z_s^{\epsilon;(t,z)}) + \alpha\eta_s^{t,x,z},$$

or stripping function arguments and superscripts,

$$\mathcal{A} = \psi_s h + \theta_s h + \alpha\sigma^* \nabla_x \psi_s + \alpha\eta_s.$$

We now consider the p-th moment of θ_t, which is (see for instance Corollary A.2.1, the multidimensional case is given in Lemma A.2.1),

$$\begin{aligned}
\mathbb{E}\left[|\theta_t|^p\right] = &\int_t^T \mathbb{E}\left[p|\theta_s|^{p-2}\theta_s \mathcal{G}_S \psi_s\right] ds + \frac{p(p-1)}{2} \int_t^T \mathbb{E}\left[|\theta_s|^{p-2}|\mathcal{A}|^2\right] ds \\
&- \frac{p(p-1)}{2} \int_t^T \mathbb{E}\left[|\theta_s|^{p-2}|\eta_s|^2\right] ds - \frac{p(p-1)}{2} \int_t^T \mathbb{E}\left[|\theta_s|^{p-2}|\gamma_s|^2\right] ds.
\end{aligned} \tag{3.6.18}$$

Using the fact that θ, ψ are real-valued functions, and $b, \sigma \in C_b^{k,l}$, applying Young's inequality to the first term on the right side of Eq. 3.6.18 yields,

$$\int_t^T \mathbb{E}\left[p|\theta_s|^{p-2}\theta_s \mathcal{G}_S \psi_s\right] ds \leq \frac{p}{2} \int_t^T \mathbb{E}\left[|\theta_s|^p\right] ds + \frac{p}{2} \int_t^T \mathbb{E}\left[|\theta_s|^{p-2}|\mathcal{G}_S \psi_s|^2\right] ds.$$

Now applying Hölder's inequality, with $p' = p/(p-2) > 1$ and $q' = p/2 > 1$ (as we have assumed $p > 2$), and

then applying Young's inequality (again with p' and q'), the last term becomes,

$$\begin{aligned}\frac{p}{2}\int_t^T \mathbb{E}\left[|\theta_s|^{p-2}|\mathcal{G}_S\psi_s|^2\right] ds &\leq \frac{p}{2}\left(\int_t^T \mathbb{E}\left[|\theta_s|^p\right] ds\right)^{1/p'} \left(\int_t^T \mathbb{E}\left[|\mathcal{G}_S\psi_s|^{2q'}\right] ds\right)^{1/q'} \\ &\leq \frac{p}{2p'}\int_t^T \mathbb{E}\left[|\theta_s|^p\right] ds + \frac{p}{2q'}\int_t^T \mathbb{E}\left[|\mathcal{G}_S\psi_s|^{2q'}\right] ds \\ &= \frac{p-2}{2}\int_t^T \mathbb{E}\left[|\theta_s|^p\right] ds + \int_t^T \mathbb{E}\left[|\mathcal{G}_S\psi_s|^p\right] ds.\end{aligned} \tag{3.6.19}$$

Application of Hölder's inequality and the use of the boundedness of b and a, then the tower property of conditional expectation, and lastly the Markov property of (X^ϵ, Z^ϵ) gives the following bound for the last term on the right side of Eq. 3.6.19,

$$\begin{aligned}\int_t^T \mathbb{E}\left[|\mathcal{G}_S\psi_s|^p\right] ds &\lesssim \int_t^T \sum_{|j|\leq 2} \mathbb{E}\left[\left|D_x^j\psi(X_s^{\epsilon;(t,x)}, Z_s^{\epsilon;(t,z)})\right|^p\right] ds \\ &= \int_t^T \sum_{|j|\leq 2} \mathbb{E}\left[\mathbb{E}\left[\left|D_x^j\psi(X_s^{\epsilon;(t,x)}, Z_s^{\epsilon;(t,z)})\right|^p \,\middle|\, \mathcal{F}_s^W \vee \mathcal{F}_s^V\right]\right] ds \\ &= \int_t^T \sum_{|j|\leq 2} \mathbb{E}\left[\mathbb{E}\left[\left|D_x^j\psi(x',z')\right|^p\right]_{(x',z')=(X_s^{\epsilon;(t,x)}, Z_s^{\epsilon;(t,z)})}\right] ds.\end{aligned}$$

Therefore the first term on the right side of Eq. 3.6.18 is bounded by,

$$\begin{aligned}\int_t^T \mathbb{E}\left[p|\theta_s|^{p-2}\theta_s\mathcal{G}_S\psi_s\right] ds &\lesssim (p-1)\int_t^T \mathbb{E}\left[|\theta_s|^p\right] ds \\ &\quad + \int_t^T \sum_{|j|\leq 2} \mathbb{E}\left[\mathbb{E}\left[\left|D_x^j\psi(x',z')\right|^p\right]_{(x',z')=(X_s^{\epsilon;(t,x)}, Z_s^{\epsilon;(t,z)})}\right] ds.\end{aligned} \tag{3.6.20}$$

Now addressing the second term on the right side of Eq. 3.6.18, expanding the inner product $|\mathcal{A}|^2 = \langle \mathcal{A}, \mathcal{A}\rangle$ and separating terms using Young's inequality with values $\lambda_1, \ldots, \lambda_6 > 0$ to be chosen later, we get

$$\begin{aligned}\langle \mathcal{A}, \mathcal{A}\rangle &\leq \left(1 + \frac{1}{\lambda_1} + \frac{1}{\lambda_2} + \frac{1}{\lambda_3}\right)|\psi_s h|^2 + \left(1 + \lambda_1 + \frac{1}{\lambda_4} + \frac{1}{\lambda_5}\right)|\theta_s h|^2 \\ &\quad + \left(1 + \lambda_2 + \lambda_4 + \frac{1}{\lambda_6}\right)|\alpha\sigma^*\nabla_x\psi_s|^2 + (1 + \lambda_3 + \lambda_5 + \lambda_6)\,|\alpha\eta_s|^2,\end{aligned}$$

Therefore the second term on the right side of Eq. 3.6.18 is bounded by

$$\frac{p(p-1)}{2}\int_t^T \mathbb{E}\left[|\theta_s|^{p-2}|\mathcal{A}|^2\right] ds \leq \left(1+\frac{1}{\lambda_1}+\frac{1}{\lambda_2}+\frac{1}{\lambda_3}\right)\frac{p(p-1)}{2}\int_t^T \mathbb{E}\left[|\theta_s|^{p-2}|\psi_s h|^2\right] ds \tag{3.6.21}$$

$$+\left(1+\lambda_1+\frac{1}{\lambda_4}+\frac{1}{\lambda_5}\right)\frac{p(p-1)}{2}\int_t^T \mathbb{E}\left[|\theta_s|^{p-2}|\theta_s h|^2\right] ds \tag{3.6.22}$$

$$+\left(1+\lambda_2+\lambda_4+\frac{1}{\lambda_6}\right)\frac{p(p-1)}{2}\int_t^T \mathbb{E}\left[|\theta_s|^{p-2}|\alpha\sigma^*\nabla_x\psi_s|^2\right] ds \tag{3.6.23}$$

$$+\left(1+\lambda_3+\lambda_5+\lambda_6\right)\frac{p(p-1)}{2}\int_t^T \mathbb{E}\left[|\theta_s|^{p-2}|\alpha\eta_s|^2\right] ds. \tag{3.6.24}$$

We now consider pairing the term given by Eq. 3.6.24 and the third term on the right side of Eq. 3.6.18,

$$\begin{aligned}\underbrace{\left(1+\lambda_3+\lambda_5+\lambda_6\right)}_{\equiv\Lambda}\frac{p(p-1)}{2}\int_t^T \mathbb{E}\left[|\theta_s|^{p-2}|\alpha\eta_s|^2\right] ds - \frac{p(p-1)}{2}\int_t^T \mathbb{E}\left[|\theta_s|^{p-2}|\eta_s|^2\right] ds \\ = \frac{p(p-1)}{2}\int_t^T \mathbb{E}\left[|\theta_s|^{p-2}\left(\Lambda\eta_s^*\alpha^*\alpha\eta_s - \eta_s^*\,\mathrm{Id}\,\eta_s\right)\right] ds \\ = \frac{p(p-1)}{2}\int_t^T \mathbb{E}\left[|\theta_s|^{p-2}\left(\eta_s^*\left(\Lambda\alpha^*\alpha - \mathrm{Id}\right)\eta_s\right)\right] ds.\end{aligned} \tag{3.6.25}$$

The matrix $\alpha^*\alpha - \mathrm{Id} \prec 0$ is constant and we can choose $\lambda_3, \lambda_5, \lambda_6 > 0$, small enough such that $\Lambda\alpha^*\alpha - \mathrm{Id} \prec 0$.

Turning our attention to the three terms of Eq. 3.6.21, 3.6.22, and 3.6.23, we use the same technique as in Eq. 3.6.19 with $|h|_\infty < \infty$ on the first term (Eq. 3.6.21) to get

$$\begin{aligned}\left(1+\frac{1}{\lambda_1}+\frac{1}{\lambda_2}+\frac{1}{\lambda_3}\right)\frac{p(p-1)}{2}\int_t^T \mathbb{E}\left[|\theta_s|^{p-2}|\psi_s h|^2\right] ds &\lesssim \int_t^T \mathbb{E}\left[|\theta_s|^{p-2}|\psi_s h|^2\right] ds \\ &\lesssim \int_t^T \mathbb{E}\left[|\theta_s|^p\right] ds + \int_t^T \sum_{|j|\leq 0} \mathbb{E}\left[\mathbb{E}\left[\left|D_x^j\psi(x',z')\right|^p\right]_{(x',z')=(X_s^{\epsilon;(t,x)},Z_s^{\epsilon;(t,z)})}\right] ds.\end{aligned} \tag{3.6.26}$$

Similarly, again using $|h|_\infty < \infty$, Eq. 3.6.22 is bounded by

$$\left(1+\lambda_1+\frac{1}{\lambda_4}+\frac{1}{\lambda_5}\right)\frac{p(p-1)}{2}\int_t^T \mathbb{E}\left[|\theta_s|^{p-2}|\theta_s h|^2\right] ds \lesssim \int_t^T \mathbb{E}\left[|\theta_s|^p\right] ds. \tag{3.6.27}$$

And now Eq. 3.6.23 using $|\sigma|_\infty < \infty$,

$$\begin{aligned}\left(1+\lambda_2+\lambda_4+\frac{1}{\lambda_6}\right)\frac{p(p-1)}{2}\int_t^T \mathbb{E}\left[|\theta_s|^{p-2}|\alpha\sigma^*\nabla_x\psi_s|^2\right] ds \\ \lesssim \int_t^T \mathbb{E}\left[|\theta_s|^p\right] ds + \int_t^T \sum_{|j|\leq 1} \mathbb{E}\left[\mathbb{E}\left[\left|D_x^j\psi(x',z')\right|^p\right]_{(x',z')=(X_s^{\epsilon;(t,x)},Z_s^{\epsilon;(t,z)})}\right] ds.\end{aligned} \tag{3.6.28}$$

Collecting the bounds of Eqs. 3.6.20, 3.6.25, 3.6.26, 3.6.27, and 3.6.28 we get for Eq. 3.6.18,

$$\begin{aligned}\mathbb{E}\left[|\theta_t|^p\right] \lesssim \int_t^T \mathbb{E}\left[|\theta_s|^p\right] ds + \int_t^T \sum_{|j|\leq 2} \mathbb{E}\left[\mathbb{E}\left[\left|D_x^j \psi(x',z')\right|^p\right]_{(x',z')=(X_s^{\epsilon;(t,x)},Z_s^{\epsilon;(t,z)})}\right] ds \\ + \frac{p(p-1)}{2}\int_t^T \mathbb{E}\left[|\theta_s|^{p-2}\left(\eta_s^*\left(\Lambda\alpha^*\alpha - \mathrm{Id}\right)\eta_s\right)\right] ds \\ - \frac{p(p-1)}{2}\int_t^T \mathbb{E}\left[|\theta_s|^{p-2}|\gamma_s|^2\right] ds.\end{aligned}$$

Rearranging this equation gives

$$\begin{aligned}\mathbb{E}\left[|\theta_t|^p\right] - \frac{p(p-1)}{2}\int_t^T \mathbb{E}\left[|\theta_s|^{p-2}\left(\eta_s^*\left(\Lambda\alpha^*\alpha - \mathrm{Id}\right)\eta_s\right)\right] ds + \frac{p(p-1)}{2}\int_t^T \mathbb{E}\left[|\theta_s|^{p-2}|\gamma_s|^2\right] ds \\ \lesssim \int_t^T \mathbb{E}\left[|\theta_s|^p\right] ds + \int_t^T \sum_{|j|\leq 2} \mathbb{E}\left[\mathbb{E}\left[\left|D_x^j \psi(x',z')\right|^p\right]_{(x',z')=(X_s^{\epsilon;(t,x)},Z_s^{\epsilon;(t,z)})}\right] ds.\end{aligned}$$

From the fact that $\Lambda\alpha^*\alpha - \mathrm{Id} \prec 0$, the subtraction of the second term on the left side of the equation is a non-negative value. The third term on the left side of the equation is also non-negative, and therefore we can drop them from the inequality to get

$$\mathbb{E}\left[|\theta_t|^p\right] \lesssim \int_t^T \mathbb{E}\left[|\theta_s|^p\right] ds + \int_t^T \sum_{|j|\leq 2} \mathbb{E}\left[\mathbb{E}\left[\left|D_x^j \psi(x',z')\right|^p\right]_{(x',z')=(X_s^{\epsilon;(t,x)},Z_s^{\epsilon;(t,z)})}\right] ds,$$

Now applying Grönwall's lemma yields,

$$\mathbb{E}\left[|\theta_t|^p\right] \lesssim \int_t^T \sum_{|j|\leq 2} \mathbb{E}\left[\mathbb{E}\left[\left|D_x^j \psi(x',z')\right|^p\right]_{(x',z')=(X_s^{\epsilon;(t,x)},Z_s^{\epsilon;(t,z)})}\right] ds.$$

Using the fact that the solution to the BDSDE provides the classical solution to the BSPDE, $R_t(x,z) = \theta_t^{t,x,z}$, we get the desired result. □

3.6.2 Estimates of Dual and Filter Error

We now complete the final estimates that lead to the proof of Theorem 3.2.1.

Lemma 3.6.4

Assume H_f, H_g, $HF^{8,4}$, $b \in C_b^{7,4}$, $\sigma \in C_b^{8,4}$, $HO^{8,4}$, and $\varphi \in C_b^7(\mathbb{R}^m;\mathbb{R})$. Then for every $p \geq 1$ there exists $q > 0$, such that

$$\sup_{0\leq t\leq T} \mathbb{E}_{\mathbb{P}^\epsilon}\left[\left|v_t^{\epsilon,T,\varphi}(x,z) - v_t^{0,T,\varphi}(x)\right|^p\right] \lesssim \epsilon^p(1+|x|^q+|z|^q)|\varphi|_{4,\infty}^p.$$

Proof. First we collect the conditions in reverse order of our main estimates.

(i) For the solution of R in Lemma 3.6.3, we require $HF^{3,3}$, $HS^{3,3}$, $\sigma \in C_b^{4,4}$, $HO^{4,4}$, and $\psi \in C^{0,5,3}$. The polynomial growth will be satisfied.

(ii) For the solution of $\psi \in C^{0,5,3}$ in Lemma 3.6.2, we require $HF^{6,4}$, $HS^{6,4}$, $HO^{6,4}$, and $v^0 \in C^{0,6}$. The conditions on $\bar{\sigma}, \bar{a}, \bar{b}$, and $\bar{h}$ will already be covered by the stronger conditions just stated. The polynomial growth will also be satisfied. And we require H_f and H_g.

(iii) For the solution of $v^0 \in C^{0,6}$ in Lemma 3.6.1, we require $\bar{b}, \bar{a} \in C_b^7$, that $\bar{h}, \bar{\sigma} \in C_b^8$, and $\varphi \in C_b^7$.

(iv) Using Lemma 3.5.8, for $\bar{h}, \bar{\sigma} \in C_b^8$ requires $HF^{8,3}$, $HO^{8,1}$, and $\sigma \in C_b^{8,1}$. And this also implies $\bar{a} \in C_b^7$. For $\bar{b} \in C_b^7$, we need $b \in C_b^{7,1}$. We also require H_f and H_g.

(v) Therefore the sufficient conditions are H_f, H_g, $HF^{8,4}$, $b \in C_b^{7,4}$, $\sigma \in C_b^{8,4}$, $HO^{8,4}$, and $\varphi \in C_b^7$.

Now we show the inequality result. Let $p > 2$. Because $v^\epsilon = v^0 + \psi + R$, we have

$$\begin{aligned}\sup_{0\le t\le T} \mathbb{E}_{\mathbb{P}^\epsilon}\left[\left|v_t^{\epsilon,T,\varphi}(x,z) - v_t^{0,T,\varphi}(x)\right|^p\right] &= \sup_{0\le t\le T} \mathbb{E}_{\mathbb{P}^\epsilon}\left[|\psi_t(x,z) + R_t(x,z)|^p\right] \\ &\lesssim \sup_{0\le t\le T} \mathbb{E}_{\mathbb{P}^\epsilon}\left[|\psi_t(x,z)|^p\right] + \sup_{0\le t\le T} \mathbb{E}_{\mathbb{P}^\epsilon}\left[|R_t(x,z)|^p\right]. \end{aligned} \tag{3.6.29}$$

Using Lemma 3.6.1 with Lemma 3.6.2 we have that the first term is bounded for $q_1, q_2 > 0$ by

$$\begin{aligned}\sup_{0\le t\le T} \mathbb{E}_{\mathbb{P}^\epsilon}\left[|\psi_t(x,z)|^p\right] &\lesssim \epsilon^p(1+|z|^{q_1}) \sum_{|\beta|\le 2} \mathbb{E}_{\mathbb{P}^\epsilon}\left[\sup_{0\le t\le T} |D_x^\beta v_t^0(x)|^p\right] \\ &\lesssim \epsilon^p(1+|z|^{q_1})(1+|x|^{q_2})|\varphi|_{2,\infty}^p. \end{aligned} \tag{3.6.30}$$

First making use of Lemma 3.6.2 in Lemma 3.6.3 we have that

$$\begin{aligned}\mathbb{E}_{\mathbb{P}^\epsilon}\left[|R_t(x,z)|^p\right] &\lesssim \sum_{|j|\le 2} \int_t^T \mathbb{E}_{\mathbb{P}^\epsilon}\left[\mathbb{E}_{\mathbb{P}^\epsilon}\left[|D_x^j \psi_s(x',z')|^p\right]_{(x',z')=(X_s^{\epsilon;(t,x)}, Z_s^{\epsilon;(t,z)})}\right] ds \\ &\lesssim \mathbb{E}_{\mathbb{P}^\epsilon}\left[\sum_{|j|\le 2} \sup_{t\le s\le T} \mathbb{E}_{\mathbb{P}^\epsilon}\left[|D_x^j \psi_s(x',z')|^p\right]_{(x',z')=(X_s^{\epsilon;(t,x)}, Z_s^{\epsilon;(t,z)})}\right] \\ &\lesssim \mathbb{E}_{\mathbb{P}^\epsilon}\left[\sum_{|j|\le 2} \sup_{0\le s\le T} \mathbb{E}_{\mathbb{P}^\epsilon}\left[|D_x^j \psi_s(x',z')|^p\right]_{(x',z')=(X_s^{\epsilon;(0,x)}, Z_s^{\epsilon;(0,z)})}\right]. \end{aligned}$$

Now using the estimate of Lemma 3.6.1, we have for some $q_3, q_4, q_5, q_6 > 0$,

$$\begin{aligned}
\mathbb{E}_{\mathbb{P}^\epsilon}\left[|R_t(x,z)|^p\right] &\lesssim \epsilon^p \sup_{0\le t\le T} \mathbb{E}_{\mathbb{P}^\epsilon}\left[(1+|Z_t^\epsilon|^{q_3}) \sum_{|\beta|\le 4} \mathbb{E}_{\mathbb{P}^\epsilon}\left[\sup_{0\le s\le T} |D_x^\beta v_s^0(X_t^\epsilon)|^p\right] \middle| (X_0^\epsilon, Z_0^\epsilon) = (x,z)\right] \\
&\lesssim \epsilon^p \sup_{0\le t\le T} \mathbb{E}_{\mathbb{P}^\epsilon}\left[(1+|Z_t^\epsilon|^{q_3})(1+|X_t^\epsilon|^{q_4}) \,|\, (X_0^\epsilon, Z_0^\epsilon) = (x,z)\right] |\varphi|_{4,\infty}^p \\
&\lesssim \epsilon^p \sup_{0\le t\le T} \left(1+\mathbb{E}_{\mathbb{P}^\epsilon}\left[|X_t^\epsilon|^{q_5} + |Z_t^\epsilon|^{q_6} \,|\, (X_0^\epsilon, Z_0^\epsilon) = (x,z)\right]\right) |\varphi|_{4,\infty}^p.
\end{aligned}$$

The moment bounds for the processes (X^ϵ, Z^ϵ), given in Lemmas 3.5.1 and 3.5.2, now gives

$$\sup_{0\le t\le T} \mathbb{E}_{\mathbb{P}^\epsilon}\left[|R_t(x,z)|^p\right] \lesssim \epsilon^p (1+|x|^{q_7}+|z|^{q_7})|\varphi|_{4,\infty}^p, \tag{3.6.31}$$

for some $q_7 > 0$. And therefore putting together the estimates of Eq. 3.6.30 and Eq. 3.6.31, and choosing a different $q > 0$, yields the desired result for the case $p > 2$. For the case $p \in [1,2]$, we use Hölder's inequality with $r > 2$ to get the desired result,

$$\begin{aligned}
\mathbb{E}_{\mathbb{P}^\epsilon}\left[\left|v_t^{\epsilon,T,\varphi}(x,z) - v_t^{0,T,\varphi}(x)\right|^p\right] \le \mathbb{E}_{\mathbb{P}^\epsilon}\left[\left|v_t^{\epsilon,T,\varphi}(x,z) - v_t^{0,T,\varphi}(x)\right|^{rp}\right]^{1/r} &\lesssim \epsilon^p (1+|x|^q+|z|^q)^{1/r} |\varphi|_{4,\infty}^p \\
&\lesssim \epsilon^p (1+|x|^q+|z|^q) |\varphi|_{4,\infty}^p,
\end{aligned}$$

since $(1+|x|^q+|z|^q) \ge 1$ and therefore $(1+|x|^q+|z|^q)^{1/r} \le (1+|x|^q+|z|^q)$. □

We now show that the moment estimate of the difference of v^ϵ and v^0 continues to hold under the original measure $\mathbb{Q}$.

Lemma 3.6.5

Assume H_f, H_g, $HF^{8,4}$, $b \in C_b^{7,4}$, $\sigma \in C_b^{8,4}$, $HO^{8,4}$, and $\varphi \in C_b^7(\mathbb{R}^m;\mathbb{R})$. Then for every $p \ge 1$ there exists $q > 0$, such that

$$\sup_{0\le t\le T} \mathbb{E}_{\mathbb{Q}}\left[\left|v_t^{\epsilon,T,\varphi}(x,z) - v_t^{0,T,\varphi}(x)\right|^p\right] \lesssim \epsilon^p (1+|x|^q+|z|^q)|\varphi|_{4,\infty}^p.$$

Proof. Performing a change of measure from $\mathbb{Q}$ to $\mathbb{P}^\epsilon$, then an application of the Cauchy-Schwarz inequality, and usage of Lemma 3.5.3 for the finiteness of the moments of the Radon-Nikodym derivative $\widetilde{D}_t^\epsilon$ yields the

desired result,

$$\begin{aligned}\mathbb{E}_{\mathbb{Q}}\left[\left|v_t^{\epsilon,T,\varphi}(x,z)-v_t^{0,T,\varphi}(x)\right|^p\right] &= \mathbb{E}_{\mathbb{P}^\epsilon}\left[\left|v_t^{\epsilon,T,\varphi}(x,z)-v_t^{0,T,\varphi}(x)\right|^p \widetilde{D}_t^\epsilon\right] \\ &\leq \mathbb{E}_{\mathbb{P}^\epsilon}\left[\left|v_t^{\epsilon,T,\varphi}(x,z)-v_t^{0,T,\varphi}(x)\right|^{2p}\right]^{1/2}\mathbb{E}_{\mathbb{P}^\epsilon}\left[\left(\widetilde{D}_t^\epsilon\right)^2\right]^{1/2} \\ &\lesssim \mathbb{E}_{\mathbb{P}^\epsilon}\left[\left|v_t^{\epsilon,T,\varphi}(x,z)-v_t^{0,T,\varphi}(x)\right|^{2p}\right]^{1/2}.\end{aligned}$$

□

Lemma 3.6.6

Assume H_f, H_g, $HF^{8,4}$, $b \in C_b^{7,4}$, $\sigma \in C_b^{8,4}$, $HO^{8,4}$, and $\varphi \in C_b^7(\mathbb{R}^m;\mathbb{R})$. Additionally, assume that the initial distribution $\mathbb{Q}_{(X_0^\epsilon,Z_0^\epsilon)}$ has finite moments of every order. Then for every $p \geq 1$ there exists $q > 0$, such that

$$\mathbb{E}_{\mathbb{Q}}\left[\left|\rho_T^{\epsilon,x}(\varphi)-\rho_T^0(\varphi)\right|^p\right] \lesssim \epsilon^p|\varphi|_{4,\infty}^p.$$

Proof. The proof follows the same inequality relations as given in Section 3.3.1, but now with expectations under $\mathbb{Q}$. Specifically, we have

$$\begin{aligned}\mathbb{E}_{\mathbb{Q}}\left[\left|\rho_T^{\epsilon,x}(\varphi)-\rho_T^0(\varphi)\right|^p\right] &= \mathbb{E}_{\mathbb{Q}}\left[\left|\int v_0^{\epsilon,T,\varphi}(x,z)-v_0^{0,T,\varphi}(x)\mathbb{Q}_{(X_0^\epsilon,Z_0^\epsilon)}(dx,dz)\right|^p\right] \\ &\leq \mathbb{E}_{\mathbb{Q}}\left[\int\left|v_0^{\epsilon,T,\varphi}(x,z)-v_0^{0,T,\varphi}(x)\right|^p\mathbb{Q}_{(X_0^\epsilon,Z_0^\epsilon)}(dx,dz)\right] \\ &= \int\mathbb{E}_{\mathbb{Q}}\left[\left|v_0^{\epsilon,T,\varphi}(x,z)-v_0^{0,T,\varphi}(x)\right|^p\right]\mathbb{Q}_{(X_0^\epsilon,Z_0^\epsilon)}(dx,dz).\end{aligned}$$

And now by Lemma 3.6.5 and finite moments of every order for the initial distribution, we get the desired result

$$\mathbb{E}_{\mathbb{Q}}\left[\left|\rho_T^{\epsilon,x}(\varphi)-\rho_T^0(\varphi)\right|^p\right] \leq \epsilon^p|\varphi|_{4,\infty}^p\int(1+|x|^q+|z|^q)\mathbb{Q}_{(X_0^\epsilon,Z_0^\epsilon)}(dx,dz) \lesssim \epsilon^p|\varphi|_{4,\infty}^p.$$

□

Lemma 3.6.7

Let $p \geq 1$ and assume h is bounded. Then

$$\sup_{\epsilon\in(0,1]}\sup_{0\leq t\leq T}\left(\mathbb{E}_{\mathbb{Q}}\left[|\rho_t^{\epsilon,x}(1)|^{-p}\right]+\mathbb{E}_{\mathbb{Q}}\left[|\rho_t^0(1)|^{-p}\right]\right)<\infty.$$

Proof. We first show the statement to be true for the term $\mathbb{E}_{\mathbb{Q}}\left[|\rho_t^{\epsilon,x}(1)|^{-p}\right]$. Using our change of probability

measure, application of the Cauchy-Schwarz inequality, and Lemma 3.5.3 gives

$$\begin{aligned}\mathbb{E}_{\mathbb{Q}}\left[|\rho_t^{\epsilon,x}(1)|^{-p}\right] &= \mathbb{E}_{\mathbb{P}^\epsilon}\left[|\rho_t^{\epsilon,x}(1)|^{-p}\widetilde{D}_t^\epsilon\right] \\ &\leq \mathbb{E}_{\mathbb{P}^\epsilon}\left[|\rho_t^{\epsilon,x}(1)|^{-2p}\right]^{1/2}\mathbb{E}_{\mathbb{P}^\epsilon}\left[|\widetilde{D}_t^\epsilon|^2\right]^{1/2} \lesssim \mathbb{E}_{\mathbb{P}^\epsilon}\left[|\rho_t^{\epsilon,x}(1)|^{-2p}\right]^{1/2}.\end{aligned}$$

Now from the definition of $\rho_t^{\epsilon,x}(1)$ and applications of Jensen's inequality ($x \mapsto x^{-2p}$ is convex on $\mathbb{R}_+$), then the tower property of conditional expectation yields

$$\mathbb{E}_{\mathbb{P}^\epsilon}\left[|\rho_t^{\epsilon,x}(1)|^{-2p}\right] = \mathbb{E}_{\mathbb{P}^\epsilon}\left[\left|\mathbb{E}_{\mathbb{P}^\epsilon}\left[\widetilde{D}_t^\epsilon \,\middle|\, \mathcal{Y}_t^\epsilon\right]\right|^{-2p}\right] \leq \mathbb{E}_{\mathbb{P}^\epsilon}\left[\left|\widetilde{D}_t^\epsilon\right|^{-2p}\right].$$

Recalling that $D_t^\epsilon = \left(\widetilde{D}_t^\epsilon\right)^{-1}$, again using a change of measure, and lastly the finiteness of the moments of D_t^ϵ under $\mathbb{Q}$ (which follows from the same arguments as given in Lemma 3.5.3), gives the desired result

$$\mathbb{E}_{\mathbb{P}^\epsilon}\left[\left|\widetilde{D}_t^\epsilon\right|^{-2p}\right] = \mathbb{E}_{\mathbb{P}^\epsilon}\left[|D_t^\epsilon|^{2p}\right] = \mathbb{E}_{\mathbb{Q}}\left[|D_t^\epsilon|^{2p+1}\right] \leq \infty. \tag{3.6.32}$$

The proof of $\sup_{\epsilon\in(0,1]}\sup_{0\leq t\leq T}\mathbb{E}_{\mathbb{Q}}\left[|\rho_t^0(1)|^{-p}\right] < \infty$ is identical, but now making use of Lemma 3.5.4.

□

Lemma 3.6.8

Assume H_f, H_g, $HF^{8,4}$, $b \in C_b^{7,4}$, $\sigma \in C_b^{8,4}$, $HO^{8,4}$, and $\varphi \in C_b^7(\mathbb{R}^m;\mathbb{R})$. Additionally, assume that the initial distribution $\mathbb{Q}_{(X_0^\epsilon,Z_0^\epsilon)}$ has finite moments of every order. Then for every $p \geq 1$ there exists $q > 0$, such that

$$\mathbb{E}_{\mathbb{Q}}\left[\left|\pi_T^{\epsilon,x}(\varphi) - \pi_T^0(\varphi)\right|^p\right] \lesssim \epsilon^p|\varphi|_{4,\infty}^p.$$

Proof. We start by showing the following simple relation

$$\begin{aligned}\pi_T^{\epsilon,x}(\varphi) - \pi_T^0(\varphi) = \pi_T^{\epsilon,x}(\varphi) - \frac{\rho_T^0(\varphi)}{\rho_T^0(1)} &= \pi_T^{\epsilon,x}(\varphi)\frac{\rho_T^0(1)}{\rho_T^0(1)} - \frac{\rho_T^0(\varphi)}{\rho_T^0(1)} + \frac{\rho_T^{\epsilon,x}(\varphi)}{\rho_T^0(1)} - \frac{\rho_T^{\epsilon,x}(\varphi)}{\rho_T^0(1)}\frac{\rho_T^{\epsilon,x}(1)}{\rho_T^{\epsilon,x}(1)} \\ &= \pi_T^{\epsilon,x}(\varphi)\frac{\rho_T^0(1)}{\rho_T^0(1)} - \frac{\rho_T^0(\varphi)}{\rho_T^0(1)} + \frac{\rho_T^{\epsilon,x}(\varphi)}{\rho_T^0(1)} - \pi_T^{\epsilon,x}(\varphi)\frac{\rho_T^{\epsilon,x}(1)}{\rho_T^0(1)} \\ &= \frac{\rho_T^{\epsilon,x}(\varphi) - \rho_T^0(\varphi)}{\rho_T^0(1)} - \pi_T^{\epsilon,x}(\varphi)\frac{\rho_T^{\epsilon,x}(1) - \rho_T^0(1)}{\rho_T^0(1)}.\end{aligned}$$

Therefore, using this manipulation, the fact that $\pi^{\epsilon,x}$ is $\mathbb{Q}$-a.s. a probability measure, and an application of

the Cauchy-Schwarz inequality, we have

$$\begin{aligned}\mathbb{E}_{\mathbb{Q}}\left[\left|\pi_T^{\epsilon,x}(\varphi)-\pi_T^0(\varphi)\right|^p\right] &= \mathbb{E}_{\mathbb{Q}}\left[\left|\frac{\rho_T^{\epsilon,x}(\varphi)-\rho_T^0(\varphi)}{\rho_T^0(1)}-\pi_T^{\epsilon,x}(\varphi)\frac{\rho_T^{\epsilon,x}(1)-\rho_T^0(1)}{\rho_T^0(1)}\right|^p\right]\\ &\lesssim \mathbb{E}_{\mathbb{Q}}\left[\left|\frac{\rho_T^{\epsilon,x}(\varphi)-\rho_T^0(\varphi)}{\rho_T^0(1)}\right|^p\right]+|\varphi|_\infty^p\mathbb{E}_{\mathbb{Q}}\left[\left|\frac{\rho_T^{\epsilon,x}(1)-\rho_T^0(1)}{\rho_T^0(1)}\right|^p\right]\\ &\leq \mathbb{E}_{\mathbb{Q}}\left[\left|\rho_T^0(1)\right|^{-2p}\right]^{1/2}\left(\mathbb{E}_{\mathbb{Q}}\left[\left|\rho_T^{\epsilon,x}(\varphi)-\rho_T^0(\varphi)\right|^{2p}\right]^{1/2}+|\varphi|_\infty^p\mathbb{E}_{\mathbb{Q}}\left[\left|\rho_T^{\epsilon,x}(1)-\rho_T^0(1)\right|^{2p}\right]^{1/2}\right).\end{aligned}$$

Now using Lemma 3.6.7 for the bound on $\mathbb{E}_{\mathbb{Q}}\left[\left|\rho_T^0(1)\right|^{-2p}\right]$ and Lemma 3.6.6 for the other terms, gives the desired result. □

Observing that the bound in the result of Lemma 3.6.8 only depends on $|\varphi|_{4,\infty}^p$, even though the assumption requires $\varphi \in C_b^7$, encourages us to instead approximate a fixed test function $\varphi \in C_b^4$ by a sequence $(\varphi^n \in C_b^7)$ in the $|\cdot|_{4,\infty}$-norm, and take advantage of the fact that $\pi_T^{\epsilon,x}$ and π_T^0 are $\mathbb{Q}$-a.s. equal to probability measures. Therefore we can relax this condition in Lemma 3.6.8 slightly with the following corollary.

Corollary 3.6.1

Assume H_f, H_g, $HF^{8,4}$, $b \in C_b^{7,4}$, $\sigma \in C_b^{8,4}$, and $HO^{8,4}$. Additionally, assume that the initial distribution $\mathbb{Q}_{(X_0^\epsilon,Z_0^\epsilon)}$ has finite moments of every order. Then for any $p \geq 1$ we have that for every $\varphi \in C_b^4(\mathbb{R}^m;\mathbb{R})$,

$$\mathbb{E}_{\mathbb{Q}}\left[\left|\pi_T^{\epsilon,x}(\varphi)-\pi_T^0(\varphi)\right|^p\right] \lesssim \epsilon^p|\varphi|_{4,\infty}^p.$$

The next lemma shows that indeed we have weak convergence of $\pi^{\epsilon,x}$ to π^0. First recall that a sequence of functions $(\varphi_i)_{i\in\mathbb{N}}$ is called convergence determining for the topology of weak convergence of probability measures on $\mathbb{R}^m$, if for a sequence (μ_n) of probability measures, and μ another probability measure, we have

$$\lim_{n\to\infty}\mu_n(\varphi_i)=\mu(\varphi_i),$$

for every $i \in \mathbb{N}$, then μ_n converges weakly to μ.

Lemma 3.6.9

Assume H_f, H_g, $HF^{8,4}$, $b \in C_b^{7,4}$, $\sigma \in C_b^{8,4}$, and $HO^{8,4}$. Additionally, assume that the initial distribution $\mathbb{Q}_{(X_0^\epsilon,Z_0^\epsilon)}$ has finite moments of every order. Then there exists a metric d on the space of probability measures

on $\mathbb{R}^m$ that generates the topology of weak convergence, such that

$$\mathbb{E}_{\mathbb{Q}}\left[d(\pi_T^{\epsilon,x}, \pi_T^0)\right] \lesssim \epsilon.$$

Proof. By [EK08, Theorem 3.4.5], given a sequence of convergence determining functions $(\varphi_i)_{i\in\mathbb{N}}$ for the topology of weak convergence of probability measures on $\mathbb{R}^m$, one can define the following metric d on the space of probability measures,

$$d(\nu,\mu) = d_{(\varphi_i)}(\nu,\mu) = \sum_{i=1}^{\infty} \frac{|\nu(\varphi_i) - \mu(\varphi_i)|}{2^i},$$

that generates the topology of weak convergence. All that remains is to identify a sequence of convergence determining functions. This will be satisfied for a countable algebra of functions $(\varphi_i)_{i\in\mathbb{N}}$ that strongly separates points in $\mathbb{R}^m$. That is, for every $x \in \mathbb{R}^m$ and $\delta > 0$, there exists $i \in \mathbb{N}$, such that

$$\inf_{\{y \,:\, |x-y|>\delta\}} |\varphi_i(x) - \varphi_i(y)| > 0.$$

We require these functions to be C_b^4. The following collection of functions satisfies all these conditions and therefore completes the proof,

$$\left\{ \exp\left(-\sum_{i=1}^{n} q_i(x - x_i)^2\right) \middle| n \in \mathbb{N}, q_i \in \mathbb{Q}_+, x_j \in \mathbb{Q}^m \right\}.$$

□

3.7 Remarks on Intermediate Timescale

In this section, we provide a brief overview of the difficulties encountered in the approach of this chapter when applied to the broader multiple timescale correlated system that will be dealt with in Chapter 4. A different approach will be needed in the next chapter, and we will not be able to get a rate of convergence. But we can still show that the x-marginal filter converges in probability to the averaged filter.

Specifically, the averaged SDE in Chapter 4 is more complicated due to the intermediate scale forcing term b_{I}. Without jumping too far ahead in notation, the generator of X^0 will become $\mathcal{G}^\dagger = \overline{\mathcal{G}_S} + \widetilde{\mathcal{G}}$. Let us consider the non-correlated case for simplicity and recall the notation $\mathcal{G}^\epsilon$ and $\mathcal{G}_I$ from Chapter 2.

The dual equation for v^ϵ is then given by,

$$-dv_t^\epsilon = \left(\frac{1}{\epsilon^2}\mathcal{G}_F + \frac{1}{\epsilon}\mathcal{G}_I + \mathcal{G}_S\right) v_t^\epsilon dt + \langle v_t^\epsilon h, d\overleftarrow{B}_t\rangle, \qquad v_T^\epsilon = \varphi,$$

and the process v^0 will be given by,

$$-dv_t^0 = (\overline{\mathcal{G}_S} + \widetilde{\mathcal{G}})v_t^0 dt + \langle v_t^0 \bar{h}, d\overleftarrow{B}_t\rangle, \qquad v_T^0 = \varphi.$$

Because of the intermediate timescale, we need to consider a larger expansion of v^ϵ,

$$v_t^\epsilon(x,z) = v_t^0(x) + u^1(x,z) + \psi_t(x,z) + R_t(x,z).$$

A sensible splitting of terms (having considered some ideas on perturbation expansions from the text of Pavliotis and Stuart [PS08], this was deemed the best out of a few arrangements) is then,

$$\begin{aligned}
-dv_t^0 &= (\overline{\mathcal{G}_S} + \widetilde{\mathcal{G}})v_t^0 dt + \langle v_t^0 \bar{h}, d\overleftarrow{B}_t\rangle, && v_T^0 = \varphi,\\
-du_t^1 &= \frac{1}{\epsilon^2}\mathcal{G}_F u_t^1 dt + \frac{1}{\epsilon}\mathcal{G}_I v_t^0 dt, && \psi_T = 0,\\
-d\psi_t &= \frac{1}{\epsilon^2}\mathcal{G}_F \psi_t dt + (\mathcal{G}_S - \overline{\mathcal{G}_S})v_t^0 dt + \left(\frac{1}{\epsilon}\mathcal{G}_I u_t^1 - \widetilde{\mathcal{G}} v_t^0\right) dt, && \psi_T = 0,\\
-dR_t &= \mathcal{G}^\epsilon R_t + \left(\frac{1}{\epsilon}\mathcal{G}_I + \mathcal{G}_S\right)\psi_t dt + \mathcal{G}_S u_t^1 dt + \langle v_t^0(h-\bar{h}), d\overleftarrow{B}_t\rangle + \langle (u_t^1 + \psi_t + R_t)h, d\overleftarrow{B}_t\rangle, && R_T = 0.
\end{aligned}$$

From the first equation, we get the standard bound from Lemma 3.4.1. One is then able to get the term $\mathbb{E}|u^1|^p$ bounded by ϵ^p (not getting ϵ^{2p} due to the $\epsilon^{-1}\mathcal{G}_I u_t^0$ forcing). Difficulty then arises with the term ψ, since looking forward to the R term, where application of Grönwall's lemma would again be desired, would require having ψ bounded by $\epsilon^{(1+\delta)}$ for some $\delta > 0$. This is an issue with the second forcing term in ψ. Additionally, the centered term $(h - \bar{h})$ on the right side of the R equation will require a technique that must be used in Chapter 4 and yields at best a logarithmic rate of convergence.

Chapter 4

Approximation of the Filter Equation for Multiple Timescale Nonlinear Systems with Correlated Noise

In this chapter, we consider a problem of filter convergence to a reduced order filter when the signal and observation processes take the following form,

$$\begin{aligned} dX_t^\epsilon &= \left[b(X_t^\epsilon, Z_t^\epsilon) + \frac{1}{\epsilon} b_I(X_t^\epsilon, Z_t^\epsilon)\right] dt + \sigma(X_t^\epsilon, Z_t^\epsilon) dW_t, \\ dZ_t^\epsilon &= \frac{1}{\epsilon^2} f(X_t^\epsilon, Z_t^\epsilon) dt + \frac{1}{\epsilon} g(X_t^\epsilon, Z_t^\epsilon) dV_t, \\ dY_t^\epsilon &= h(X_t^\epsilon, Z_t^\epsilon) dt + \alpha dW_t + \gamma dU_t, \quad Y_0^\epsilon = 0 \in \mathbb{R}^d, \end{aligned} \tag{4.0.1}$$

where $b, b_{\mathrm{I}} : \mathbb{R}^m \times \mathbb{R}^n \to \mathbb{R}^m$, $\sigma : \mathbb{R}^m \times \mathbb{R}^n \to \mathbb{R}^m \times \mathbb{R}^w$, $f : \mathbb{R}^m \times \mathbb{R}^n \to \mathbb{R}^n$, $g : \mathbb{R}^m \times \mathbb{R}^n \to \mathbb{R}^n \times \mathbb{R}^v$ and $h : \mathbb{R}^m \times \mathbb{R}^n \to \mathbb{R}^d$ are Borel measurable functions. As before, the presence of $\mathbb{R}^{d\times w} \ni \alpha \neq 0$ indicates correlation between the observation and slow (coarse-grain) process. And we again assume that the initial distribution of the signal process $(X_0^\epsilon, Z_0^\epsilon)$ at $t = 0$ is denoted by $\mathbb{Q}_{(X_0^\epsilon, Z_0^\epsilon)}$, is independent of the (W, V, U) Brownian motion, and to have finite moments of every order.

Besides the literature provided at the start of Chapter 3, we need to mention the work of nonlinear filter approximation by Kushner [Kus90, Chapter 6]. The approach, or main steps, of showing weak convergence of the marginalized filter to an averaged filter is similar to that work. Although Kushner [Kus90, Chapter 6] only considers a two timescale jump-diffusion process. The signal process does not include an intermediate forcing, as we do here. There is also no consideration of correlation between signal and observation processes in his work [Kus90, Chapter 6]. In the work by Kushner [Kus90, Chapter 6], the difference of the actual unnormalized conditional measure and the reduced conditional measure converges to zero in distribution. Standard results then yield convergence in probability of the fixed time marginals. The method of proof is by averaging the coefficients of the SDEs for the unnormalized filters and showing that the limits of both filters satisfy the same SDE, which possess a unique solution.

In our attempt at approaching the broader multiple timescale correlated filtering problem for nonlinear systems, we have to modify the approach by Kushner [Kus90, Chapter 6]. At this time, it does not appear

that anyone else has successfully dealt with the broader problem, as addressed in this chapter. For this we make use of the perturbed test function approach where the correctors are solutions of Poisson equations. We make use of the sharp results on existence, regularity and growth of the transition densities and semigroups associated with the process Z^x and Poisson equations for the corrector terms from the work by Pardoux and Veretennikov [PV03]. To show tightness of the measure-valued filtering solutions, we make use the work by Jakubowski [Jak86] which gives conditions for tightness of probability measures on path spaces with ranges being completely regular topological spaces. A lemma providing a sufficient condition to one of the requirements by Jakubowski [Jak86] is also given. The main result of the chapter is the following:

Theorem (Main Result of Chapter)
Recall that $\pi^{\epsilon,x}$ is the x-marginal of the conditional distribution π^ϵ and π^0 is the conditional distribution for the averaged filter equation (see for instance Eqs. 2.1.3, 3.0.2, and 4.3.1). Then under the assumptions stated in Theorem 4.3.1, $\pi^{\epsilon,x} \to \pi^0$ in probability.

We now provide an outline of this chapter. In the next section, Section 4.1, we quickly re-state some notation from Chapter 3 for convenience and provide a new definition that will be useful for stating results. Then in Section 4.2, we provide the form of the generator $\mathcal{G}^\dagger$ for the averaged diffusion process and this is used in Section 4.3, which states the averaged filtering equations and the main theorem result with full assumptions detailed. After this, we move to Section 4.4, which provides preliminary estimates which are needed for the main estimates. The next section, Section 4.5, provides the existence of weak limits of the probability measure induced by the signed measured-valued process $\rho^{\epsilon,x} - \rho^0$, as well as the characterization of this process and the uniqueness of its limit. At the end of Section 4.5, the main result for convergence of $\rho^{\epsilon,x} - \rho^0$ is stated alongside a lemma that proves the convergence of $\pi^{\epsilon,x} - \pi^0$. We close the chapter with Section 4.6, which points out a correction for [PV03, Theorem 2, p.1171], and hence why the assumptions needed for Theorem 4.3.1 are not as relaxed as what might first be expected when using the estimates by Pardoux and Veretennikov [PV03]. The results of this chapter have been made available in the work by Beeson et al. [BNP20a].

4.1 Notation

Let us recall some notation and definitions from Chapter 3. We use $\mathbb{N}_0$ to denote $\{0, 1, 2, \ldots\}$ and $\mathbb{N}$ for $\{1, 2, \ldots\}$. We use H_f to denote the assumption that there exists a constant $C > 0$, exponent $\alpha > 0$ and an

$R > 0$ such that for all $|z| > R$,

$$\sup_{x \in \mathbb{R}^m} \langle f(x,z), z \rangle \leq -C|z|^\alpha. \tag{H_f}$$

H_f is a recurrence condition, which provides the existence of a stationary distribution, $\mu_\infty(x)$, for the process Z^x. We use H_g to denote the assumption that there are $0 < \lambda \leq \Lambda < \infty$, such that for any $(x,z) \in \mathbb{R}^m \times \mathbb{R}^n$,

$$\lambda I \preceq gg^*(x,z) \preceq \Lambda I, \tag{H_g}$$

where $\preceq$ is the order relation in the sense of positive semidefinite matrices. H_g is a uniform ellipticity condition, which provides the uniqueness of the stationary distribution. We will say that a function $\theta : \mathbb{R}^m \times \mathbb{R}^n \to \mathbb{R}$ is centered with respect to $\mu_\infty(x)$, if for each x

$$\int \theta(x,z)\mu_\infty(dz;x) = 0, \quad \forall x \in \mathbb{R}^m.$$

Recall the use of the notation $k = (k_1, \ldots, k_m) \in \mathbb{N}_0^m$ for a multiindex with order $|k| = k_1 + \ldots + k_m$ and define the differential operator

$$D_x^k = \frac{\partial^{|k|}}{\partial {x_1}^{k_1} \ldots \partial x_m^{k_m}}.$$

We will use the notation $H^{i,j+\alpha}$ to specify the regularity and boundedness of f and gg^*,

$$f \in C_b^{i,j+\alpha}(\mathbb{R}^m \times \mathbb{R}^n; \mathbb{R}^n), \quad gg^* \in C_b^{i,j+\alpha}(\mathbb{R}^m \times \mathbb{R}^n; \mathbb{R}^{n \times n}), \quad i,j \in \mathbb{N}, \quad \alpha \in (0,1), \tag{$H^{i,j+\alpha}$}$$

where $\varphi(x,z) \in C_b^{i,j+\alpha}$ denotes that φ has i bounded derivatives in the x-component, j bounded derivatives in the z-component, and all derivatives $\partial_z^{j'} \partial_x^{i'} \varphi$ for $0 \leq i' \leq i$, $0 \leq j' \leq j$ are α-Hölder continuous in z uniformly in x.

4.2 Homogenization of Stochastic Differential Equations

In this section, we state the main result on the theory of homogenization of SDEs. The result is that if the process $Z^{\epsilon,x}$,

$$dZ_t^{\epsilon,x} = \frac{1}{\epsilon^2} f(x, Z_t^{\epsilon,x})dt + \frac{1}{\epsilon} g(x, Z_t^{\epsilon,x})dV_t, \tag{4.2.1}$$

is ergodic with stationary distribution $\mu_\infty(x)$, then under appropriate conditions, in the limit $\epsilon \to 0$ the process X^ϵ converges in distribution to a Markov process X^0 with infinitesimal generator,

$$\mathcal{G}^\dagger \equiv \overline{\mathcal{G}_S} + \widetilde{\mathcal{G}},$$

where

$$\begin{aligned}
\overline{\mathcal{G}_S}(x) &\equiv \sum_{i=1}^m \bar{b}_i(x)\frac{\partial}{\partial x_i} + \frac{1}{2}\sum_{i,j=1}^m \bar{a}_{ij}(x)\frac{\partial^2}{\partial x_i \partial x_j}, \\
\bar{b}(x) &\equiv \int_{\mathbb{R}^n} b(x,z)\mu_\infty(dz;x), \\
\bar{a}(x) &\equiv \int_{\mathbb{R}^n} a(x,z)\mu_\infty(dz;x),
\end{aligned}$$

$a = \sigma\sigma^*$, and

$$\begin{aligned}
\widetilde{\mathcal{G}}(x) &\equiv \sum_{i=1}^m \widetilde{b}_i(x)\frac{\partial}{\partial x_i} + \frac{1}{2}\sum_{i,j=1}^m \widetilde{a}_{ij}(x)\frac{\partial^2}{\partial x_i \partial x_j}, \\
\widetilde{b}(x) &\equiv \int_{\mathbb{R}^n} \left(\nabla_x \mathcal{G}_F^{-1}(-b_{\mathrm{I}})\right) b_{\mathrm{I}}(x,z)\mu_\infty(dz;x), \\
\widetilde{a}(x) &\equiv \int_{\mathbb{R}^n} \left(b_{\mathrm{I}} \otimes \mathcal{G}_F^{-1}(-b_{\mathrm{I}})\right)(x,z) + \left(\mathcal{G}_F^{-1}(-b_{\mathrm{I}}) \otimes b_{\mathrm{I}}\right)(x,z)\mu_\infty(dz;x),
\end{aligned}$$

where $\mathcal{G}_F^{-1}(-b_{\mathrm{I}})$ is the solution of a Poisson equation.

4.3 The Averaged Filtering Equation and Main Theorem

We can now define the averaged filter π^0, a probability measure-valued process satisfying the following evolution equation,

$$\begin{aligned}
\pi_t^0(\varphi) &= \pi_0^0(\varphi) + \int_0^t \pi_s^0(\mathcal{G}^\dagger\varphi)ds + \int_0^t \langle \pi_s^0(\varphi\bar{h} + \alpha\bar{\sigma}^*\nabla_x\varphi) - \pi_s^0(\varphi)\pi_s^0(\bar{h}), dY_s^\epsilon - \pi_s^0(\bar{h})ds\rangle, \\
\pi_0^0(\varphi) &= \mathbb{E}_{\mathbb{Q}}\left[\varphi(X_0^0)\right].
\end{aligned} \tag{4.3.1}$$

The definitions of $\bar{h}$ and $\bar{\sigma}$ are

$$\bar{h}(x) \equiv \int_{\mathbb{R}^n} h(x,z)\mu_\infty(dz;x), \quad \bar{\sigma}(x) \equiv \int_{\mathbb{R}^n} \sigma(x,z)\mu_\infty(dz;x).$$

We now give the main result of the chapter with full conditions.

Theorem 4.3.1

Assume that f and g satisfy H_f and H_g, that b_{I} is centered with respect to $\mu_\infty(x)$ for each x and that $\mathbb{Q}_{(X_0^\epsilon, Z_0^\epsilon)}$ has finite moments of every order. Additionally, assume either a. high regularity conditions or b. low regularity with uniform ellipticity:

a. *$H^{4,2+\alpha}$ holds for $\alpha \in (0,1)$; for each z, $b(\cdot,z), \sigma(\cdot,z) \in C^3$, and $b_{\mathrm{I}}(\cdot,z) \in C^4$; that b and b_{I} are Lipschitz in z, and σ is globally Lipschitz in z; that $b, b_{\mathrm{I}}, \sigma$ satisfy the growth conditions*

$$|b(x,z)| + |b_{\mathrm{I}}(x,z)| + |\sigma\sigma^*(x,z)| \le C(1+|z|)^\beta,$$
$$\sum_{|k|=1}^{2} \left|D_x^k b(x,z)\right| + \left|D_x^k \sigma\sigma^*(x,z)\right| \le C(1+|z|^q),$$
$$\sum_{|k|=1}^{3} \left|D_x^k b_{\mathrm{I}}(x,z)\right| \le C(1+|z|^q),$$

for some $\beta < -2$ and $q > 0$; that h is bounded in (x,z), $h(\cdot,z) \in C^3$ for each z, and h is globally Lipschitz in z.

b. *$\bar{a} + \widetilde{a} \succ 0$ uniformly in x; $H^{2,2+\alpha}$ holds for $\alpha \in (0,1)$; for each z, $b(\cdot,z), b_{\mathrm{I}}(\cdot,z), \sigma(\cdot,z) \in C^2$; that b and b_{I} are Lipschitz in z, and σ is globally Lipschitz in z; that $b, b_{\mathrm{I}}, \sigma$ satisfy the growth conditions*

$$|b(x,z)| + |b_{\mathrm{I}}(x,z)| + |\sigma\sigma^*(x,z)| \le C(1+|z|)^\beta,$$
$$\sum_{|k|=1}^{2} \left|D_x^k b(x,z)\right| + \left|D_x^k b_{\mathrm{I}}(x,z)\right| + \left|D_x^k \sigma\sigma^*(x,z)\right| \le C(1+|z|^q),$$

for some $\beta < -2$ and $q > 0$; h is bounded in (x,z), that h is globally Lipschitz in (x,z). If $a \succ 0$, which implies $\bar{a} + \widetilde{a} \succ 0$, then the Lipschitz condition in z for b, b_{I} can be relaxed to α-Hölder continuity.

Then there exists a metric d on $C([0,T]; P(\mathbb{R}^m))$, the space of continuous processes from $[0,T]$ to the space of probability measures on $\mathbb{R}^m$, that generates the topology of weak convergence, such that $\pi^{\epsilon,x} \to \pi^0$ in probability.

Proof. From Theorem 4.5.1 and Lemma 4.5.5 we get $\pi^{\epsilon,x} - \pi^0 \Rightarrow 0$ as $\epsilon \to 0$. $\pi^{\epsilon,x}$ and π^0 are random variables in the space $C([0,T]; P(\mathbb{R}^m))$. We define a continuous bounded metric d on this space that generates the topology of weak convergence as follows,

$$d(\mu,\nu) = 1 \wedge \left(\sup_{0 \le t \le T} \widetilde{d}(\mu_t, \nu_t)\right),$$

where $\widetilde{d}$ is the metric defined in the proof of Lemma 3.6.9 (see [Jak86] for a generalization of this idea for Skorohod topologies). The metric $\widetilde{d}$ is translation invariant and generates the topology of weak convergence on $P(\mathbb{R}^m)$. Therefore d inherits the translation invariant property from $\widetilde{d}$. From weak convergence of $\pi^{\epsilon,x} - \pi^0$ in the space of signed measures and translation invariance of d, we have

$$\lim_{\epsilon\to 0} \mathbb{E}_{\mathbb{Q}}\left[d(\pi^{\epsilon,x}, \pi^0)\right] = \lim_{\epsilon\to 0} \mathbb{E}_{\mathbb{Q}}\left[d(\pi^{\epsilon,x} - \pi^0, 0)\right] = 0.$$

And therefore we retrieve convergence in probability,

$$\lim_{\epsilon\to 0} \mathbb{Q}\left(d(\pi^{\epsilon,x}, \pi^0) \geq \delta\right) \leq \frac{1}{\delta} \lim_{\epsilon\to 0} \mathbb{E}_{\mathbb{Q}}\left[d(\pi^{\epsilon,x}, \pi^0)\right] = 0, \qquad \text{for each } \delta > 0.$$

□

4.3.1 The Averaged Unnormalized Filtering Equations

As we did in Chapter 3, we now provide the unnormalized filter definitions. When $\varphi \in C_b^2(\mathbb{R}^m;\mathbb{R})$, we consider the x-marginal,

$$\rho_t^{\epsilon,x}(\varphi) = \int \varphi(x)\rho_t^{\epsilon}(dx, dz).$$

$\rho^{\epsilon,x}$ is related to $\pi^{\epsilon,x}$ through the Kallianpur-Striebel relation,

$$\pi_t^{\epsilon,x}(\varphi) = \frac{\rho_t^{\epsilon,x}(\varphi)}{\rho_t^{\epsilon,x}(1)}, \qquad \forall t \in [0,\infty), \qquad \mathbb{Q}, \mathbb{P}^{\epsilon}\text{-a.s.}$$

which is easy to see since $\rho_t^{\epsilon}(1) = \rho_t^{\epsilon,x}(1)$.

As we did at the end of Section 3.2, we define the averaged unnormalized filter as the solution of the following SPDE

$$\begin{aligned} \rho_t^0(\varphi) &= \rho_0^0(\varphi) + \int_0^t \rho_s^0(\mathcal{G}^{\dagger}\varphi)ds + \int_0^t \langle \rho_s^0(\varphi\bar{h} + \alpha\bar{\sigma}^*\nabla_x\varphi), dY_s^{\epsilon}\rangle, \\ \rho_0^0(\varphi) &= \mathbb{E}_{\mathbb{Q}}\left[\varphi(X_0^0)\right], \end{aligned} \tag{4.3.2}$$

where $\varphi \in C_b^2(\mathbb{R}^m;\mathbb{R})$ are test functions. And then by the Kallianpur-Striebel formula we relate the averaged (normalized) filter π^0 to the unnormalized variant,

$$\pi_t^0(\varphi) = \frac{\rho_t^0(\varphi)}{\rho_t^0(1)}, \qquad \forall t \in [0,T], \qquad \mathbb{Q}, \mathbb{P}^{\epsilon}\text{-a.s.}$$

The uniqueness of ρ^0 follows from the same assumptions and proof to be given in Lemma 4.5.4.

We will later show in Lemma 4.5.5 that under appropriate assumptions, weak convergence of $\rho^{\epsilon,x} - \rho^0$ to zero will imply weak convergence of $\pi^{\epsilon,x} - \pi^0$ to zero, and therefore we can focus on showing convergence of the unnormalized difference for the main analysis.

Representation of the Averaged Unnormalized Conditional Distribution

We now give a representation of ρ^0 as a conditional expectation following the approach in Section 3.2.2. The only difference here is that our SDE must have generator $\mathcal{G}^\dagger$. Therefore the following will suffice to give the correct equation for ρ^0,

$$dX_t^0 = \left[\bar{b}(X_t^0) + \widetilde{b}(X_t^0)\right] dt + \widetilde{a}^{1/2}(X_t^0)d\widetilde{W}_t + (\bar{a}(X_t^0) - \bar{\sigma}\bar{\sigma}^*(X_t^0))^{1/2}d\widehat{W}_t + \bar{\sigma}(X_t^0)dW_t, \tag{4.3.3}$$

where $\widetilde{W}$ and $\widehat{W}$ are new m-dimensional independent Brownian motions, independent of V, W, U under $\mathbb{Q}$ as well as independent of the initial condition $\mathbb{Q}_{X_0^\epsilon}$. All the same considerations as required in Section 3.2.2 are again required here, only in this chapter we allow for more relaxed conditions on the coefficients. The details of which are provided in Lemma 4.5.4.

A similar remark as that given in Section 3.2.2 is warranted here. It is as follows:

Remark. An interesting observation regarding Eq. 4.3.3, is that we may have $\bar{\sigma} = 0$, and this implies that the SDE for the averaged filter may have less correlation than the original system, or even none at all.

Now as we did in Section 3.2.2, we define the process

$$\widetilde{D}_t^0 = \exp\left(\int_0^t \langle \bar{h}(X_s^0), dY_s^\epsilon \rangle - \frac{1}{2}\int_0^t \left|\bar{h}(X_s^0)\right|^2 ds\right),$$

and the conditional expectation

$$\rho_t^0(\varphi) = \mathbb{E}_{\mathbb{P}^\epsilon}\left[\varphi(X_t^0)\widetilde{D}_t^0 \mid \mathcal{Y}_t^\epsilon\right].$$

4.4 Preliminary Estimates

In this section we provide several preliminary estimates that will be needed for the main analysis. Some additional comments regarding notation are first introduced and then some assumptions are defined.

As done in Chapter 3, we will use the relation $a \lesssim b$ to indicate $a \leq Cb$ for a constant $C > 0$ that is independent of a and b, but that may depend on parameters that are not critical for the bound being

computed. We will use the notation $T^{F,x}$ for the semigroup of Z^x, and denote processes with $Z^{\epsilon,x;(s,z)}$ to represent the process $Z^{\epsilon,x}$ started at time s at $z \in \mathbb{R}^n$. We will say that a function $\theta(x,z)$ is centered with respect to μ_∞ (the family of invariant measures parameterized by $x \in \mathbb{R}^m$) if

$$\int_{\mathbb{R}^n} \theta(x,z)\mu(dz;x) = 0, \qquad \forall x \in \mathbb{R}^m.$$

Let H_L denote the assumption that for each $K > 0$, there exists a constant C_K such that for all $x, x' \in \mathbb{R}^m$, $|z| \leq K$:

$$|b(x,z) - b(x',z)| + |b_{\mathrm{I}}(x,z) - b_{\mathrm{I}}(x',z)| + |\sigma(x,z) - \sigma(x',z)| \leq C_K|x - x'|. \tag{H_L}$$

Let H_P denote the assumption that there exists $K, \alpha, p_1, p_2 > 0$ such that for all $(x,z) \in \mathbb{R}^m \times \mathbb{R}^n$:

$$\begin{aligned} &|b(x,z)| \leq K(1+|x|)(1+|z|^{p_1}), \\ &|\sigma(x,z)| = \sqrt{\mathrm{Tr}(\sigma\sigma^*(x,z))} \leq K(1+|x|^{1/2})(1+|z|^{p_2}). \end{aligned} \tag{H_P}$$

Note that from H_P we have $|\sigma(x,z)| \lesssim 1 + |x| + |z|^{2p_2}$ and hence implies a linear growth in x and polynomial growth in z. Also from H_P, $|\sigma\sigma^*(x,z)| \lesssim (1 + |x|^2 + |z|^{4p_2})$.

Let H_I denote the assumption that for some $K, p > 0$, b_{I} satisfies the following growth condition,

$$\sum_{|\alpha| \leq 2} \sup_{x \in \mathbb{R}^m} |D_x^\alpha b_{\mathrm{I}}(x,z)| \leq K(1+|z|^p). \tag{H_I}$$

The next result is from [PV03, p.1172] and provides the result that $X^\epsilon \Rightarrow X^0$ in the limit $\epsilon \to 0$.

Theorem 4.4.1

Let (X^ϵ, Z^ϵ) satisfy the stochastic differential equations of Eq. 4.0.1 with initial conditions $(X_0^\epsilon, Z_0^\epsilon) = (x,z) \in \mathbb{R}^m \times \mathbb{R}^n$ for each $\epsilon \in (0,1)$. Assume H_f, H_g, $H^{2,2+\alpha}$ for $\alpha \in (0,1)$, H_L, and H_P. Let $b_{\mathrm{I}} \in C^{2,\alpha}$ satisfy H_I and be centered with respect to μ_∞. Further, assume that b_{I} is centered with respect to μ_∞. Then for any $T > 0$, the process X^ϵ converges weakly in the limit $\epsilon \to 0$, to the Markov process X^0 with generator $\mathcal{G}^\dagger$.

Proof. See remarks in Section 4.6 and [PV03, p.1172]. □

4.4.1 Estimates with the Fast Semigroup

Lemma 4.4.1

Assume $H^{k,l}$, with $k \in \mathbb{N}_0, l \in \mathbb{N}$, and let $\theta \in C^{k,j}(\mathbb{R}^m \times \mathbb{R}^n; \mathbb{R})$ for $j \leq l$ satisfy for some $C, p > 0$

$$\sum_{|\alpha| \leq k} \sum_{|\beta| \leq j} |D_x^\alpha D_z^\beta \theta(x,z)| \leq C(1 + |x|^p + |z|^p).$$

Then

$$(t,x,z) \mapsto T_t^{F,x}\left(\theta(x,\cdot)\right)(z) \in C^{0,k,j}(\mathbb{R}^+ \times \mathbb{R}^m \times \mathbb{R}^n; \mathbb{R})$$

and there exist $C_1, p_1 > 0$, such that for all $(t,x,z) \in [0,\infty) \times \mathbb{R}^m \times \mathbb{R}^n$

$$\sum_{|\alpha| \leq k} \sum_{|\beta| \leq j} |D_x^\alpha D_z^\beta T_t^{F,x}\left(\theta(x,\cdot)\right)(z)| \leq C_1 e^{C_1 t}(1 + |x|^{p_1} + |z|^{p_1}).$$

If the bound on the derivatives of θ can be chosen uniformly in x, that is,

$$\sum_{|\alpha| \leq k} \sum_{|\beta| \leq j} \sup_x |D_x^\alpha D_z^\beta \theta(x,z)| \leq C(1 + |z|^p),$$

then the bound on the derivatives of $T_t^{F,x}\left(\theta(x,\cdot)\right)(z)$ is also uniform in x,

$$\sum_{|\alpha| \leq k} \sum_{|\beta| \leq j} \sup_x |D_x^\alpha D_z^\beta T_t^{F,x}\left(\theta(x,\cdot)\right)(z)| \leq C_1 e^{C_1 t}(1 + |z|^{p_1}).$$

Proof. The proof is given in Lemma 3.5.5. □

Lemma 4.4.2

Assume H_f, H_g and $H^{k,2+\alpha}$ for $\alpha \in (0,1)$, and $k \in \mathbb{N}_0$. Let $\theta \in C^{k,0}(\mathbb{R}^m \times \mathbb{R}^n; \mathbb{R})$ satisfy for some $C, p > 0$,

$$\sum_{|\gamma| \leq k} \sup_x |D_x^\gamma \theta(x,z)| \leq C(1 + |z|^p).$$

Then

$$x \mapsto \mu_\infty(\theta; x)(x') = \int_{\mathbb{R}^n} \theta(x', z)\mu_\infty(dz; x) = \int_{\mathbb{R}^n} \theta(x', z) p_\infty(z; x) dz \in C_b^k(\mathbb{R}^m; \mathbb{R}).$$

Proof. From [PV03, Theorem 1, p.1170], we have that for any $q > 0$ there exists $C_q > 0$, such that,

$$\sum_{|\gamma| \leq k} \sup_x |D_x^\gamma p_\infty(z; x)| \leq \frac{C_q}{1 + |z|^q}.$$

Therefore if q is chosen large enough, and we differentiate $p_\infty(z;x)$ under the integral sign, and using the growth constraint on θ and its derivatives, we obtain the result. □

Lemma 4.4.3

Assume H_f, H_g and $H^{k,2+\alpha}$ for $\alpha \in (0,1)$ and $k \in \mathbb{N}_0$. Let $j \in \{0,1\}$, and $\theta \in C^{k,j+\alpha(1-j)}(\mathbb{R}^m \times \mathbb{R}^n;\mathbb{R})$ satisfy the growth condition,

$$\sum_{|\alpha|\le k}\sum_{|\beta|\le j}\sup_x |D_x^\alpha D_z^\beta \theta(x,z)| \le C(1+|z|^p),$$

for some $C, p > 0$. Assume additionally that θ satisfies the centering condition,

$$\int_{\mathbb{R}^n} \theta(x,z)\mu_\infty(dz;x) = 0, \quad \forall x \in \mathbb{R}^m.$$

Then

$$(x,z) \mapsto \int_0^\infty T_t^{F,x}(\theta(x,\cdot))(z)dt \in C^{k,j}(\mathbb{R}^m \times \mathbb{R}^n;\mathbb{R}),$$

and for every $q > 0$ there exists $C', q' > 0$, such that,

$$\sum_{|\alpha|\le k}\sum_{|\beta|\le j}\int_0^\infty \sup_x |D_x^\alpha D_z^\beta T_t^{F,x}(\theta(x,\cdot))(z)|^q dt \le C'(1+|z|^{q'}).$$

Proof. For the proof, we use the representation

$$\int_0^\infty T_t^{F,x}(\theta(x,\cdot))(z)dt = \int_0^1 \int_{\mathbb{R}^n} \theta(x,z')p_t(z';x,z)dz'dt + \int_1^\infty T_t^{F,x}(\theta(x,\cdot))(z)dt.$$

Then the statement,

$$\int_0^\infty T_t^{F,x}(\theta(x,\cdot))(z)dt \in C^{k,j}(\mathbb{R}^m \times \mathbb{R}^n;\mathbb{R}),$$

follows from the existence of the derivatives on $t \in [0,1)$ from Lemma 4.4.1 and $t \in [1,\infty)$ from [PV03, Theorem 2, p.1171]. Similarly, the bound on the growth of the derivatives of $T_t^{F,x}(\theta(x,\cdot))(z)$ given in [PV03, Theorem 2, p.1171], formula (15) states: For any $p_1 > 0$ there exist $C_1, p_1' > 0$, such that for any $(t,x,z) \in [1,\infty) \times \mathbb{R}^m \times \mathbb{R}^n$,

$$\sum_{|\alpha|\le k}\sum_{|\beta|\le 1}\left|D_x^\alpha D_z^\beta T_t^{F,x}(\theta(x,\cdot))(z)\right| \le C_1 \frac{1+|z|^{p_1'}}{(1+t)^{p_1}}.$$

We combine this estimate with Lemma 4.4.1, from where we obtain for $(t,x,z) \in [0,\infty) \times \mathbb{R}^m \times \mathbb{R}^n$

$$\sum_{|\alpha| \le k} \sum_{|\beta| \le j} \sup_x \left| D_x^\alpha D_z^\beta T_t^{F,x}(\theta(x,\cdot))(z) \right| \le C_2 e^{C_2 t}(1+|z|^{p_2}).$$

We choose p_1 such that $qp_1 > 1$ and use the first estimate on $[1,\infty)$ and the second estimate on $[0,1)$. The result follows. □

4.4.2 Estimates on SDE Solutions

The following lemma is given in Chapter 3, but we include the statement for ease of reference.

Lemma 4.4.4

Assume f is bounded and that f and gg^* are Hölder continuous in z uniformly in x for some uniform constant. Assume that the conditions H_f and H_g hold. Then for any $p > 0$ we have

$$\sup_{(t,\epsilon,x) \in [0,\infty) \times (0,1] \times \mathbb{R}^m} \mathbb{E}\left[|Z_t^\epsilon|^p \,|\, (X_0^\epsilon, Z_0^\epsilon) = (x,z) \right] \lesssim 1 + |z|^p.$$

Proof. The proof is given in Lemma 3.5.2. □

Lemma 4.4.5

Assume the conditions H_f, H_g and $H^{2,2+\alpha}$ for some $\alpha \in (0,1)$; that b, σ are bounded for all (x,z); and that $b_{\mathrm{I}} \in C^{2,1}(\mathbb{R}^m \times \mathbb{R}^n; \mathbb{R}^m)$ that satisfies the centering condition,

$$\int_{\mathbb{R}^n} b_{\mathrm{I}}(x,z) \mu_\infty(dz;x) = 0,$$

where $\mu_\infty(x)$ is the unique stationary distribution for the process Z^x, and that for some $C, q_1 > 0$, it has the following growth condition,

$$\sum_{|\alpha| \le 2} \sum_{|\beta| \le 1} \sup_x |D_x^\alpha D_z^\beta b_{\mathrm{I}}(x,z)| \le C(1+|z|^{q_1}).$$

Then for every $p \ge 2$ there exists $q > 0$ such that for $0 \le r < t < \infty$

$$\mathbb{E}\left| \frac{1}{\epsilon} \int_r^t b_{\mathrm{I}}(X_s^\epsilon, Z_s^\epsilon) ds \right|^p \lesssim \epsilon^p (1+|z|^q) + (t-r)^{p-1}(1+\epsilon^p) \int_r^t 1 + \mathbb{E}|Z_s^\epsilon|^q ds + (t-r)^{(p/2)-1}(1+\epsilon^p) \int_r^t 1 + \mathbb{E}|Z_s^\epsilon|^q ds.$$

Proof. We start by considering the solution of the following backward partial differential equation,

$$-\partial_s \psi_s(x,z) = \frac{1}{\epsilon^2}\mathcal{G}_F \psi_s(x,z) + \frac{1}{\epsilon} b_{\mathrm{I}}(x,z), \quad \psi_t(x,z) = 0.$$

The solution of which is given by a Feynman-Kac representation,

$$\psi_s(x,z) = \mathbb{E}\int_s^t \frac{1}{\epsilon} b_{\mathrm{I}}(x, Z_r^{\epsilon,x;(s,z)})dr = \frac{1}{\epsilon}\int_s^t T^{F,x}_{(r-s)/\epsilon^2}\left(b_{\mathrm{I}}(x,\cdot)\right)(z)dr = \epsilon\int_0^{(t-s)/\epsilon^2} T^{F,x}_u\left(b_{\mathrm{I}}(x,\cdot)\right)(z)du,$$

where $T^{F,x}$ is the semigroup associated with the process Z^x and a change of time has been used in the last equality relation. Then since b_{I} satisfies the conditions of Lemma 4.4.3, we have

$$\sum_{|\alpha|\leq 2}\sum_{|\beta|\leq 1}\sup_{s\in[0,t]}|D_x^\alpha D_z^\beta \psi_s(x,z)|^p \lesssim \epsilon^p(1+|z|^{q_2}),$$

for some $q_2 > 0$. Applying Itô's formula to $\psi_t(x,z)$ gives,

$$\begin{aligned}
0 = \psi_r(x,z) &+ \frac{1}{\epsilon^2}\int_r^t \mathcal{G}_F\psi_s(X_s^\epsilon, Z_s^\epsilon)ds + \frac{1}{\epsilon}\int_r^t \nabla_z\psi_s(X_s^\epsilon, Z_s^\epsilon)g(X_s^\epsilon, Z_s^\epsilon)dV_s \\
&+ \int_r^t \mathcal{G}_S^\epsilon\psi_s(X_s^\epsilon, Z_s^\epsilon)ds + \int_r^t \nabla_x\psi_s(X_s^\epsilon, Z_s^\epsilon)\sigma(X_s^\epsilon, Z_s^\epsilon)dW_s \\
&- \frac{1}{\epsilon^2}\int_r^t \mathcal{G}_F\psi_s(X_s^\epsilon, Z_s^\epsilon)ds - \frac{1}{\epsilon}\int_r^t b_{\mathrm{I}}(X_s^\epsilon, Z_s^\epsilon)ds.
\end{aligned}$$

Eliminating terms and rearranging simplifies to

$$\begin{aligned}
\frac{1}{\epsilon}\int_r^t b_{\mathrm{I}}(X_s^\epsilon, Z_s^\epsilon)ds = \psi_r(x,z) &+ \int_r^t \mathcal{G}_S\psi_s(X_s^\epsilon, Z_s^\epsilon)ds + \frac{1}{\epsilon}\int_r^t \nabla_x\psi_s(X_s^\epsilon, Z_s^\epsilon)b_{\mathrm{I}}(X_s^\epsilon, Z_s^\epsilon)ds \\
&+ \frac{1}{\epsilon}\int_r^t \nabla_z\psi_s(X_s^\epsilon, Z_s^\epsilon)g(X_s^\epsilon, Z_s^\epsilon)dV_s + \int_r^t \nabla_x\psi_s(X_s^\epsilon, Z_s^\epsilon)\sigma(X_s^\epsilon, Z_s^\epsilon)dW_s.
\end{aligned}$$

The first term will contribute,

$$\mathbb{E}|\psi_r(x,z)|^p \leq \sup_{s\in[0,t]}|\psi_s(x,z)|^p \lesssim \epsilon^p(1+|z|^{q_2}).$$

From the boundedness of b and σ we have for the second term

$$\begin{aligned}
\mathbb{E}\left|\int_r^t \mathcal{G}_S\psi_s(X_s^\epsilon, Z_s^\epsilon)ds\right|^p &\leq (t-r)^{p-1}|b|_\infty^p\int_r^t \mathbb{E}\left|\nabla_x\psi_s(X_s^\epsilon, Z_s^\epsilon)\right|^p ds + (t-r)^{p-1}|\sigma|_\infty^p\int_r^t \mathbb{E}\left|\nabla_x^2\psi_s(X_s^\epsilon, Z_s^\epsilon)\right|^p ds \\
&\lesssim (t-r)^{p-1}(|b|_\infty^p + |\sigma|_\infty^p)\epsilon^p\int_r^t 1 + \mathbb{E}\left|Z_s^\epsilon\right|^{q_2} ds.
\end{aligned}$$

For the third term,

$$|\nabla_x \psi_s(X_s^\epsilon, Z_s^\epsilon) b_{\mathrm{I}}(X_s^\epsilon, Z_s^\epsilon)|^p \leq |\nabla_x \psi_s(X_s^\epsilon, Z_s^\epsilon)|^p |b_{\mathrm{I}}(X_s^\epsilon, Z_s^\epsilon)|^p \lesssim \epsilon^p \left(1 + |Z_s^\epsilon|^{q_2}\right) \left(1 + |Z_s^\epsilon|^{q_1}\right)^p$$

and therefore

$$\mathbb{E}\left|\frac{1}{\epsilon}\int_r^t \nabla_x \psi_s(X_s^\epsilon, Z_s^\epsilon) b_{\mathrm{I}}(X_s^\epsilon, Z_s^\epsilon) ds\right|^p \lesssim (t-r)^{p-1} \int_r^t 1 + \mathbb{E}\,|Z_s^\epsilon|^{q_3}\, ds.$$

The stochastic integrals follow in a similar manner after application of the Burkholder-Davis-Gundy inequality, and the boundedness of σ and g,

$$\begin{aligned}
\mathbb{E}\left|\int_r^t \nabla_x \psi_s(X_s^\epsilon, Z_s^\epsilon)\sigma(X_s^\epsilon, Z_s^\epsilon) dW_s\right|^p &= \mathbb{E}\left(\sup_{u\in[r,t]}\left|\int_r^u \nabla_x \psi_s(X_s^\epsilon, Z_s^\epsilon)\sigma(X_s^\epsilon, Z_s^\epsilon) dW_s\right|\right)^p \\
&\leq C_p \mathbb{E}\left(\int_r^t \left|\nabla_x \psi_s(X_s^\epsilon, Z_s^\epsilon)\sigma(X_s^\epsilon, Z_s^\epsilon)\right|^2 ds\right)^{p/2} \\
&\leq C_p (t-r)^{(p/2)-1} \epsilon^p |\sigma|_\infty^p \int_r^t 1 + \mathbb{E}|Z_s^\epsilon|^{q_2} ds.
\end{aligned}$$

The bound for the other stochastic integral follows in the same manner,

$$\mathbb{E}\left|\frac{1}{\epsilon}\int_r^t \nabla_z \psi_s(X_s^\epsilon, Z_s^\epsilon) g(X_s^\epsilon, Z_s^\epsilon) dV_s\right|^p \leq C_p (t-r)^{(p/2)-1} |g|_\infty^p \int_r^t 1 + \mathbb{E}|Z_s^\epsilon|^{q_2} ds.$$

Collecting all the terms, now yields the desired result. □

Lemma 4.4.6

Assume the same setup as Lemma 4.4.5, then for every $p \geq 2$ there exists $q > 0$ such that for $T > 0$

$$\sup_{(t,\epsilon)\in[0,T]\times(0,1]} \mathbb{E}\left[|X_t^\epsilon|^p \mid (X_0^\epsilon, Z_0^\epsilon) = (x, z)\right] \lesssim 1 + |x|^p + |z|^q.$$

Proof. Since b and σ are bounded, we get,

$$\mathbb{E}|X_t^\epsilon|^p \lesssim 1 + \mathbb{E}|X_0^\epsilon|^p + \mathbb{E}\left|\int_0^t \frac{1}{\epsilon} b_{\mathrm{I}}(X_s^\epsilon, Z_s^\epsilon) ds\right|^p.$$

Using the result of Lemma 4.4.5 for the moment of the intermediate scale forcing and then Lemma 4.4.4 for

the moment of the fast process, we get

$$\mathbb{E}|X_t^\epsilon|^p \lesssim \mathbb{E}|X_0^\epsilon|^p + \epsilon^p(1+\mathbb{E}|Z_0^\epsilon|^q) + (1+\epsilon^p)\int_0^t 1+\mathbb{E}|Z_s^\epsilon|^q ds \lesssim \mathbb{E}|X_0^\epsilon|^p + (1+\epsilon^p)(1+\mathbb{E}|Z_0^\epsilon|^q).$$

Repeating the proof, but conditioning on $(X_0^\epsilon, Z_0^\epsilon) = (x,z)$ gives the desired result. □

Lemma 4.4.7

Assume the same setup as Lemma 4.4.5, then for $|t-s| \le 1$ and $p \ge 2$, there exists a $q \ge 0$ such that

$$\mathbb{E}\left[|X_t^\epsilon - X_s^\epsilon|^p \,|\, (X_0^\epsilon, Z_0^\epsilon) = (x,z)\right] \lesssim \epsilon^p(1+|z|^q) + (t-s)^{p/2}(1+\epsilon^p)(1+|z|^q).$$

Proof. Without loss of generality, assume $s < t$.

$$\begin{aligned}\mathbb{E}\left[|X_t^\epsilon - X_s^\epsilon|^p\right] &\lesssim (t-s)^{p-1}\int_s^t \mathbb{E}\,|b(X_u^\epsilon, Z_u^\epsilon)|^p\,du + \mathbb{E}\left|\frac{1}{\epsilon}\int_s^t b_{\mathrm{I}}(X_u^\epsilon, Z_u^\epsilon)du\right|^p + \mathbb{E}\left|\int_s^t \sigma(X_u^\epsilon, Z_u^\epsilon)dW_u\right|^p \\ &\le (t-s)^p|b|_\infty^p + (t-s)^{p/2}|\sigma|_\infty^p + \mathbb{E}\left|\frac{1}{\epsilon}\int_s^t b_{\mathrm{I}}(X_u^\epsilon, Z_u^\epsilon)du\right|^p.\end{aligned}$$

Now using Lemmas 4.4.5 and 4.4.4, we have

$$\begin{aligned}\mathbb{E}\left[|X_t^\epsilon - X_s^\epsilon|^p\right] &\lesssim (t-s)^p + (t-s)^{p/2} + \epsilon^p(1+\mathbb{E}|Z_0^\epsilon|^q) + (t-s)^p(1+\epsilon^p)(1+\mathbb{E}|Z_0^\epsilon|^q) + (t-s)^{p/2}(1+\epsilon^p)(1+\mathbb{E}|Z_0^\epsilon|^q) \\ &\lesssim \epsilon^p(1+\mathbb{E}|Z_0^\epsilon|^q) + (t-s)^{p/2}(1+\epsilon^p)(1+\mathbb{E}|Z_0^\epsilon|^q).\end{aligned}$$

Repeating the proof, but conditioning on $(X_0^\epsilon, Z_0^\epsilon) = (x,z)$ gives the desired result. □

Lemma 4.4.8

Assume h is bounded, then for $p \ge 2$ and $T > 0$,

$$\sup_{\epsilon\in(0,1]}\sup_{t\le T}\mathbb{E}_{\mathbb{P}^\epsilon}\left|\widetilde{D}_t^\epsilon\right|^p < \infty \quad \text{and} \quad \sup_{t\le T}\mathbb{E}_{\mathbb{P}^\epsilon}\left|\widetilde{D}_t^0\right|^p < \infty.$$

Further, for $|t-s| < 1$, we have

$$\sup_{\epsilon\in(0,1]}\mathbb{E}_{\mathbb{P}^\epsilon}\left|\widetilde{D}_t^\epsilon - \widetilde{D}_s^\epsilon\right|^p \lesssim C_p(t-s)^{p/2}|h|_\infty^p < \infty.$$

Proof. We have that $\widetilde{D}_t^\epsilon$ satisfies

$$\widetilde{D}_t^\epsilon = 1 + \int_0^t \widetilde{D}_s^\epsilon \langle h(X_s^\epsilon, Z_s^\epsilon), dY_s^\epsilon \rangle.$$

Using the boundedness of h, the first result now follows from an application of the Burkholder-Davis-Gundy inequality and Grönwall's lemma. The same proof applies for the moment bound of $\widetilde{D}^0$. The bound for the increment now follows,

$$\begin{aligned}\mathbb{E}_{\mathbb{P}^\epsilon}\left|\widetilde{D}_t^\epsilon - \widetilde{D}_s^\epsilon\right|^p &= \mathbb{E}_{\mathbb{P}^\epsilon}\left|\int_s^t \widetilde{D}_u^\epsilon \langle h(X_u^\epsilon, Z_u^\epsilon), dY_u^\epsilon\rangle\right|^p \\ &\leq C_p(t-s)^{(p/2)-1}\int_s^t \mathbb{E}_{\mathbb{P}^\epsilon}\left[\left|\widetilde{D}_u^\epsilon\right|^p |h(X_u^\epsilon, Z_u^\epsilon)|^p\right] du \lesssim C_p(t-s)^{p/2}|h|_\infty^p < \infty.\end{aligned}$$

□

4.4.3 Estimates using the Poisson Equation

Theorem 4.4.2

Consider the Poisson equation,

$$\mathcal{G}u(x,z) = -\psi(x,z),$$

where $x \in \mathbb{R}^m$ is a parameter, $\mathcal{G}$ is the generator

$$\mathcal{G}(x,z) \equiv \sum_{i=1}^n f_i(x,z)\frac{\partial}{\partial z_i} + \frac{1}{2}\sum_{i,j=1}^n (gg^*)_{ij}(x,z)\frac{\partial^2}{\partial z_i \partial z_j},$$

and $\psi \in C^{k,\alpha}$ for $k \geq 1$ and $\alpha > 0$. Assume that f, g satisfy the assumptions of H_f, H_g and $H^{k,2+\alpha}$. Let $\mu_\infty(x)$ be the unique stationary distribution of Z^x for each fixed $x \in \mathbb{R}^m$, and assume that ψ is centered for each $x \in \mathbb{R}^m$,

$$\int_{\mathbb{R}^n} \psi(x,z)\mu_\infty(dz;x) = 0.$$

Further, assume the growth conditions

$$|\psi(x,z)| \le C_0(1+|z|)^\beta,$$
$$\sum_{|j|=1}^{k} \left|D_x^j \psi(x,z)\right| \le C_1(x)(1+|z|^q),$$

for some $\beta < -2$ and $q > 0$. Then the solution of the Poisson equation exists, belongs to the Sobolev space $\cap_{p\in(1,\infty)} W^2_{p,\mathrm{loc}}$, is unique up to an additive constant such that for any x the centering condition

$$\int_{\mathbb{R}^n} u(x,y)\mu_\infty(dz;x) = 0$$

holds, the solution satisfies $u(\cdot,z) \in C^k$ for any z, and the following holds true from some q', q'' and some constants $C_2, C_3(x)$,

$$|u(x,z)| \le C_2,$$
$$\sum_{|j|=1}^{k} |D_x^j u(x,z)| \le C_3(x)(1+|z|^{q'}),$$
$$|\nabla_x \nabla_z u(x,z)| \le C_3(x)(1+|z|^{q''}).$$

Proof. This is a combination of Proposition 1 and Theorem 3 by Pardoux and Veretennikov [PV03], but restricted for our needs. □

Lemma 4.4.9

Assume H_f, H_g and $H^{k,2+\alpha}$ for $\alpha \in (0,1)$ and $k \in \mathbb{N}_0$. Let $b, \sigma, h \in C^{k,0}$ and satisfy for some $C, p > 0$,

$$\sum_{|\gamma|\le k} \sup_x \left(|D_x^\gamma b(x,z)| + |D_x^\gamma \sigma(x,z)| + |D_x^\gamma h(x,z)|\right) \le C(1+|z|^p).$$

Then $\bar{b}, \bar{\sigma}, \bar{a}, \bar{h} \in C_b^k$.

Proof. The result follows from Lemma 4.4.2. □

Lemma 4.4.10

Assume H_f, H_g and $H^{j,2+\alpha}$ for $\alpha \in (0,1)$. Let $b_{\mathrm{I}} \in C^{j,\alpha}$ for $j \in \mathbb{N}$ is centered with respect to $\mu_\infty(x)$ for all

x, with the growth condition

$$|b_{\mathrm{I}}(x,z)| \le C_0(1+|z|)^{\beta},$$
$$\sum_{|i|=1}^{j} \left|D_x^i b_{\mathrm{I}}(x,z)\right| \le C(1+|z|^q),$$

for $\beta < -2$. Then $\widetilde{a} \in C_b^j$ and $\widetilde{b} \in C_b^{j-1}$.

Proof. The result for $\widetilde{a}$ follows from the fact that the assumptions on b_{I} give $\mathcal{G}_F^{-1}(-b_{\mathrm{I}})(\cdot,z) \in C_b^j$ for each z by Theorem 4.4.2 and the rest then follows from Lemma 4.4.2. For $\widetilde{b}$, again from Theorem 4.4.2, we have that $|\nabla_x \mathcal{G}_F^{-1}(-b_{\mathrm{I}})| \lesssim (1+|z|^q)$ and $\nabla_x \mathcal{G}_F^{-1}(-b_{\mathrm{I}})(\cdot,z) \in C^{j-1}$ for each z, and therefore can use Lemma 4.4.2 to get the desired result. □

4.4.4 Estimates of the Unnormalized Conditional Distribution

Lemma 4.4.11

Assume ρ^0 satisfies Eq. 4.3.2, that $\bar{h}$ is bounded, and $\varphi \in C_b^2(\mathbb{R}^m;\mathbb{R})$. Then for $p \ge 2$,

$$\mathbb{E}_{\mathbb{Q}} \sup_{t\le T} |\rho_t^0(\varphi)|^p < \infty.$$

Proof. Since φ is bounded, we have $\rho_t^0(\varphi) \le |\varphi|_\infty \rho_t^0(1)$ and therefore we aim to show $\mathbb{E}_{\mathbb{Q}} \sup_{t\le T} |\rho_t^0(1)|^p < \infty$. Applying $\mathbb{E}_{\mathbb{Q}} \sup_{t\le T} |\cdot|^p$ to the evolution equation for $\rho_t^0(1)$ gives

$$\mathbb{E}_{\mathbb{Q}} \sup_{t\le T} |\rho_t^0(1)|^p \lesssim \mathbb{E}_{\mathbb{Q}} \left|\rho_0^0(1)\right|^p + \mathbb{E}_{\mathbb{Q}} \sup_{t\le T} \left| \int_0^t \langle \rho_s^0(\varphi\bar{h}), dY_s^\epsilon \rangle \right|^p.$$

The first term is simply,

$$\mathbb{E}_{\mathbb{Q}} \left|\rho_0^0(1)\right|^p = 1.$$

For the stochastic integral, application with the Burkholder-Davis-Gundy inequality, Hölder's inequality, and Fubini's theorem gives

$$\mathbb{E}_{\mathbb{Q}} \sup_{t\le T} \left| \int_0^t \langle \rho_s^0(\varphi\bar{h}), dY_s^\epsilon \rangle \right|^p \lesssim T^{(p/2)-1} \int_0^T \mathbb{E}_{\mathbb{Q}} |\rho_s^0(\varphi\bar{h})|^p ds.$$

Using the boundedness of $\varphi\bar{h}$ and Lemma 4.4.8, the integrand is bounded by,

$$\begin{aligned}\mathbb{E}_{\mathbb{Q}}|\rho_s^0(\varphi\bar{h})|^p &\leq \mathbb{E}_{\mathbb{Q}}\left[\mathbb{E}_{\mathbb{P}^\epsilon}\left[|\varphi\bar{h}(X_s^0)\widetilde{D}_s^0|^p \,\middle|\, \mathcal{Y}_s^\epsilon\right]\right] \\ &= \mathbb{E}_{\mathbb{P}^\epsilon}\left[\widetilde{D}_s^0\mathbb{E}_{\mathbb{P}^\epsilon}\left[|\varphi\bar{h}(X_s^0)\widetilde{D}_s^0|^p \,\middle|\, \mathcal{Y}_s^\epsilon\right]\right] \leq \frac{1}{2}\mathbb{E}_{\mathbb{P}^\epsilon}\left(\widetilde{D}_s^0\right)^2 + \frac{1}{2}|\varphi\bar{h}|_\infty^{2p}\mathbb{E}_{\mathbb{P}^\epsilon}\left(\widetilde{D}_s^0\right)^{2p} < \infty.\end{aligned}$$

□

Lemma 4.4.12

Assume ρ^ϵ satisfies Eq. 2.3.3 and that h is bounded. Then for $p \geq 2$,

$$\sup_{\epsilon\in(0,1]}\mathbb{E}_{\mathbb{Q}}\sup_{t\leq T}|\rho_t^\epsilon(1)|^p < \infty.$$

Proof. From Eq. 2.3.3 we get,

$$\sup_{\epsilon\in(0,1]}\mathbb{E}_{\mathbb{Q}}\sup_{t\leq T}|\rho_t^\epsilon(1)|^p \lesssim \sup_{\epsilon\in(0,1]}\mathbb{E}_{\mathbb{Q}}\,|\rho_0^\epsilon(1)|^p + \sup_{\epsilon\in(0,1]}\mathbb{E}_{\mathbb{Q}}\sup_{t\leq T}\left|\int_0^t\langle\rho_s^\epsilon(h), dY_s^\epsilon\rangle\right|^p.$$

The analysis now follows the same arguments as Lemma 4.4.11, but using boundedness of h and Lemma 4.4.8. □

4.5 Existence, Characterization and Uniqueness of Weak Limits

Let $S(\mathbb{R}^m)$ be the space of finite signed Borel measures on $\mathbb{R}^m$ with the weak topology induced by $C_b(\mathbb{R}^m;\mathbb{R})$, and $C([0,T];S(\mathbb{R}^m))$ the space of continuous paths with values in $S(\mathbb{R}^m)$ endowed with the topology of uniform convergence. For each ϵ, we denote the $C([0,T];S(\mathbb{R}^m))$-valued random variable $\zeta^\epsilon \equiv \rho^{\epsilon,x} - \rho^0$, the difference of the x-marginal and averaged filter. With this notation, now define the ϵ-parameterized family of Borel probability measures (P^ϵ) on $C([0,T];S(\mathbb{R}^m))$, to be those induced by (ζ^ϵ),

$$P^\epsilon(\cdot) = \mathbb{Q}\left((\zeta^\epsilon)^{-1}(\cdot)\right).$$

We will need to prove a uniform concentration condition[1] of the collection (P^ϵ) for the proof of the existence of weak limits of (ζ^ϵ). In the context of our problem, the uniform concentration condition is the following:

[1] This is sometimes referred to as compact confinement condition in the literature.

Definition 4.5.1 (Uniform Concentration Condition)**.** (P^ϵ) is said to satisfy the uniform concentration condition if for each $\delta > 0$, there exists a compact set $K_\delta \subset S(\mathbb{R}^m)$ such that

$$P^\epsilon(C([0,T]; K_\delta)) \geq 1 - \delta, \quad \forall \epsilon. \tag{4.5.1}$$

We now prove a lemma that provides a sufficient condition for the uniform concentration condition.

Lemma 4.5.1

The uniform concentration condition holds if for some $p > 0$ and continuous $M : \mathbb{R}^m \to (0, \infty)$ with $\lim_{|x|\to\infty} M(x) = \infty$, we have

$$\sup_\epsilon \mathbb{E}_\mathbb{Q} \sup_{t\leq T} \left(|\zeta_t^\epsilon|\,(M)\right)^p < \infty. \tag{4.5.2}$$

Here $|\zeta_t^\epsilon|$ is the total variation measure of ζ_t^ϵ.

Proof. We first show that for $C > 0$, the set

$$K = \{\mu \in S(\mathbb{R}^m) \mid |\mu|(M) \leq C\}$$

is tight. Given $\delta > 0$, choose $R > 0$ large enough such that $\inf_{|x|\geq R} M(x) \geq C/\delta$. Then denoting $A_\delta = B(0, R) \subset \mathbb{R}^m$, the closed ball centered at the origin with radius R, we have that for any $\mu \in K$

$$|\mu|(A_\delta^c) = |\mu|(1_{|\cdot|>R}) \leq |\mu|\left(\left(\frac{\delta}{C}M\right)1_{|\cdot|>R}\right) \leq \frac{\delta}{C}|\mu|(M) \leq \frac{\delta}{C}C = \delta.$$

This shows that K is tight. Moreover, since M is bounded from below by some $m > 0$, we have

$$\sup_{\mu\in K} |\mu|(1) \leq \frac{1}{m} \sup_{\mu\in K} |\mu|(M) \leq \frac{C}{m},$$

and therefore K is bounded in total variation norm. Since $S(\mathbb{R}^m)$ with the weak topology induced by $C_b(\mathbb{R}^m; \mathbb{R})$ is Polish, we have by Prokhorov's theorem that K is relatively compact. Further, by Fatou's lemma for weak convergence, K is also closed and therefore compact.

Given $\delta > 0$, choose $C > 0$ large enough so that

$$\frac{\sup_{\epsilon\in(0,1]} \mathbb{E}_\mathbb{Q} \sup_{t\leq T} \left(|\zeta_t^\epsilon|\,(M)\right)^p}{C^p} < \delta.$$

Defining our compact set $K_\delta = \{\mu \in S(\mathbb{R}^m) \,|\, |\mu|(M) \leq C\}$, we have

$$\mathbb{Q}\left(\zeta^\epsilon \notin C([0,T];K_\delta)\right) \leq \mathbb{Q}\left(\sup_{t\leq T} |\zeta_t^\epsilon|(M) > C\right) \leq \frac{\sup_{\epsilon\in(0,1]} \mathbb{E}_{\mathbb{Q}} \sup_{t\leq T} \left(|\zeta_t^\epsilon|\,(M)\right)^p}{C^p} \leq \delta.$$

□

The next result uses Lemma 4.5.1 to prove that (P^ϵ) is tight.

Lemma 4.5.2

Assume that f and g satisfy the assumptions of H_f, H_g and $H^{2,2+\alpha}$ for $\alpha \in (0,1)$, and that b, σ, h are bounded. Let $b_{\mathrm{I}} \in C^{2,\alpha}$ be centered with respect to $\mu_\infty(x)$ for each x, and satisfy the growth conditions

$$|b_{\mathrm{I}}(x,z)| \leq C(1+|z|)^\beta,$$
$$\sum_{|i|=1}^{2} \left|D_x^i b_{\mathrm{I}}(x,z)\right| \leq C(1+|z|^q),$$

for some $\beta < -2$ and $q > 0$. Assume that $\mathbb{Q}_{(X_0^\epsilon, Z_0^\epsilon)}$ has finite moments of every order. Then the ϵ-parameterized family of Borel probability measures (P^ϵ) is tight.

Proof. To prove the statement, we follow criteria provided in [Jak86, Theorem 3.1, p.276], which gives conditions for a family of Borel probability measures on $D([0,T];E)$, càdlàg path space with E a completely regular topological space with metrizable compacts, to be tight. $C([0,T];S(\mathbb{R}^m))$ is viewed as a subset of $D([0,T];S(\mathbb{R}^m))$, and $S(\mathbb{R}^m)$ with the weak topology induced by $C_b^2(\mathbb{R}^m;\mathbb{R})$ is Polish and therefore a completely regular topological space with metrizable compacts.

Specifically, let $\mathbb{F}$ be the natural injection of $C_b^2(\mathbb{R}^m;\mathbb{R})$ into its double dual. This collection satisfies criteria for [Jak86, Theorem 3.1, p.276], i.e., it is a collection of continuous functions that separate points in $S(\mathbb{R}^m)$, and is closed under addition (i.e., $f, g \in \mathbb{F}$, then $f+g \in \mathbb{F}$). Then to each $f \in \mathbb{F}$ associate a map $\widetilde{f} \in \widetilde{\mathbb{F}}$, characterized as follows,

$$\widetilde{f} : C([0,T];S(\mathbb{R}^m)) \longrightarrow C([0,T];\mathbb{R})$$
$$\mu \longmapsto f \circ \mu.$$

The conditions for tightness by Jakubowski [Jak86, Theorem 3.1, p.276] then states that (P^ϵ) is tight if and only if the following two conditions are satisfied:

(i) For each $\delta > 0$ there is a compact set $K_\delta \subset S(\mathbb{R}^m)$ such that

$$P^\epsilon(C([0,T];K_\delta)) > 1-\delta, \quad \forall \epsilon$$

(ii) The family (P^ϵ) is $\mathbb{F}$-weakly tight, i.e., for each $f \in \mathbb{F}$ the family $(P^\epsilon \circ (\widetilde{f}^{-1}))$ of probability measures on $C([0,T];\mathbb{R})$ is tight.

The proof of (i) will follow from Lemma 4.5.1, which provides a sufficient condition for the uniform concentration condition. To prove the lemma, we define $M(x) = (1+|x|^2)^{1/2}$, let $p \geq 2$ and check that the following condition holds,

$$\sup_{\epsilon\in(0,1]} \mathbb{E}_{\mathbb{Q}} \sup_{t\leq T} \left(|\zeta_t^\epsilon|\,(M)\right)^p < \infty. \tag{4.5.2}$$

Note that $M(x)$ satisfies the conditions for Lemma 4.5.1 and has bounded first and second order derivatives,

$$\begin{aligned}\left|\frac{\partial}{\partial x_i}M(x)\right| &= \left|\frac{x_i}{M(x)}\right| \lesssim 1,\\ \left|\frac{\partial^2}{\partial x_i \partial x_j}M(x)\right| &= \left|-\frac{x_i x_j}{M(x)^3} + \frac{\delta_{ij}}{M(x)}\right| \lesssim \frac{1}{M(x)} \lesssim 1.\end{aligned}$$

Directly estimating, we have

$$\sup_{\epsilon\in(0,1]} \mathbb{E}_{\mathbb{Q}} \sup_{t\leq T} \left(|\zeta_t^\epsilon|(M)\right)^p = \sup_{\epsilon\in(0,1]} \mathbb{E}_{\mathbb{Q}} \sup_{t\leq T} \left(\rho_t^{\epsilon,x}(M) + \rho_t^0(M)\right)^p \lesssim \sup_{\epsilon\in(0,1]} \mathbb{E}_{\mathbb{Q}} \sup_{t\leq T} |\rho_t^{\epsilon,x}(M)|^p + \mathbb{E}_{\mathbb{Q}} \sup_{t\leq T} \left|\rho_t^0(M)\right|^p.$$

Dealing with each term separately, we first address $\sup_{\epsilon\in(0,1]} \mathbb{E}_{\mathbb{Q}} \sup_{t\leq T} \left(\rho_t^{\epsilon,x}(M)\right)^p$. To handle the singular term (the intermediate drift) in the slow process, we perturb M by a corrector term. Define the perturbed test function,

$$M^\epsilon(x,z) = M(x) + \epsilon\chi(x,z),$$

with $\chi(x,z)$ the solution of the Poisson equation,

$$\mathcal{G}_F \chi = -\mathcal{G}_I M.$$

The Poisson equation is well-posed with the right hand side satisfying the conditions of Theorem 4.4.2 (recall that b_{I} has the correct decay in the z variable), and therefore the regularity and bounds of χ come from

Theorem 4.4.2. Specifically,

$$|\chi(x,z)| \lesssim 1,$$
$$\sum_{|i|=1}^{2} |D_x^i \chi(x,z)| \lesssim (1+|z|^{q'}),$$

for some $q' > 0$. Using the identity $\rho_t^\epsilon(M^\epsilon) = \rho_t^{\epsilon,x}(M) + \epsilon\rho_t^\epsilon(\chi)$, we have the representation

$$\begin{aligned}\rho_t^{\epsilon,x}(M) = -\epsilon\rho_t^\epsilon(\chi) + \rho_0^\epsilon(M^\epsilon) + \int_0^t \rho_s^\epsilon(\mathcal{G}_S M)ds + \int_0^t \rho_s^\epsilon(\mathcal{G}_{\mathrm{I}}\chi)ds + \epsilon\int_0^t \rho_s^\epsilon(\mathcal{G}_S\chi)ds \\ + \int_0^t \langle \rho_s^\epsilon(Mh + \alpha\sigma^*\nabla_x M), dY_s^\epsilon\rangle + \epsilon\int_0^t \langle \rho_s^\epsilon(\chi h + \alpha\sigma^*\nabla_x\chi), dY_s^\epsilon\rangle.\end{aligned}$$

And therefore,

$$\begin{aligned}\mathbb{E}_{\mathbb{Q}} \sup_{t\le T} |\rho_t^{\epsilon,x}(M)|^p \lesssim \epsilon^p \mathbb{E}_{\mathbb{Q}} \sup_{t\le T} |\rho_t^\epsilon(\chi)|^p + \mathbb{E}_{\mathbb{Q}} |\rho_0^\epsilon(M^\epsilon)|^p \\ + \mathbb{E}_{\mathbb{Q}} \int_0^T |\rho_s^\epsilon(\mathcal{G}_S M)|^p ds + \mathbb{E}_{\mathbb{Q}} \int_0^T |\rho_s^\epsilon(\mathcal{G}_{\mathrm{I}}\chi)|^p ds + \epsilon^p \mathbb{E}_{\mathbb{Q}} \int_0^T |\rho_s^\epsilon(\mathcal{G}_S\chi)|^p ds \\ + \mathbb{E}_{\mathbb{Q}} \sup_{t\le T} \left| \int_0^t \langle \rho_s^\epsilon(Mh), dY_s^\epsilon\rangle \right|^p + \mathbb{E}_{\mathbb{Q}} \sup_{t\le T} \left| \int_0^t \langle \rho_s^\epsilon(\alpha\sigma^*\nabla_x M), dY_s^\epsilon\rangle \right|^p \\ + \epsilon^p \mathbb{E}_{\mathbb{Q}} \sup_{t\le T} \left| \int_0^t \langle \rho_s^\epsilon(\chi h), dY_s^\epsilon\rangle \right|^p + \epsilon^p \mathbb{E}_{\mathbb{Q}} \sup_{t\le T} \left| \int_0^t \langle \rho_s^\epsilon(\alpha\sigma^*\nabla_x\chi), dY_s^\epsilon\rangle \right|^p.\end{aligned} \tag{4.5.3}$$

By the boundedness of χ and application of Lemma 4.4.11, the first term of Eq. 4.5.3 is

$$\sup_{\epsilon\in(0,1]} \mathbb{E}_{\mathbb{Q}} \sup_{t\le T} |\rho_t^\epsilon(\chi)|^p \lesssim \sup_{\epsilon\in(0,1]} \mathbb{E}_{\mathbb{Q}} \sup_{t\le T} \rho_t^\epsilon(|\chi|)^p \lesssim \sup_{\epsilon\in(0,1]} \mathbb{E}_{\mathbb{Q}} \sup_{t\le T} \rho_t^\epsilon(1)^p < \infty.$$

For the second term of Eq. 4.5.3, we have

$$\begin{aligned}\mathbb{E}_{\mathbb{Q}} |\rho_0^\epsilon(M^\epsilon)|^p = \mathbb{E}_{\mathbb{Q}} \left| \mathbb{E}_{\mathbb{P}^\epsilon} \left[M^\epsilon(X_0^\epsilon, Z_0^\epsilon)\widetilde{D}_0^\epsilon \,\middle|\, \mathcal{Y}_0^\epsilon \right] \right|^p = \mathbb{E}_{\mathbb{Q}} \left| \mathbb{E}_{\mathbb{Q}} \left[M^\epsilon(X_0^\epsilon, Z_0^\epsilon) \right] \right|^p \\ \le \int |M^\epsilon(x,z)|^p \mathbb{Q}_{(X_0^\epsilon, Z_0^\epsilon)}(dx,dz) \lesssim \int M(x)^p + \epsilon^p |\chi(x,z)|^p \mathbb{Q}_{(X_0^\epsilon, Z_0^\epsilon)}(dx,dz),\end{aligned}$$

and therefore

$$\sup_{\epsilon\in(0,1]} \mathbb{E}_{\mathbb{Q}} |\rho_0^\epsilon(M^\epsilon)|^p < \infty.$$

Where we used the boundedness of χ and the fact that we have finite moments of every order for $\mathbb{Q}_{(X_0^\epsilon, Z_0^\epsilon)}$. From the boundedness of $b, \sigma, D_x^\gamma M$, for $|\gamma| \in \{1,2\}$, Lemmas 4.4.8 and 4.4.11, we have for the third term of

Eq. 4.5.3

$$\sup_{\epsilon\in(0,1]}\mathbb{E}_{\mathbb{Q}}\int_0^T|\rho_s^\epsilon(\mathcal{G}_S M)|^p\,ds\le|\mathcal{G}_S M|_\infty^p\sup_{\epsilon\in(0,1]}\mathbb{E}_{\mathbb{Q}}\sup_{t\le T}\rho_s^\epsilon(1)^p ds<\infty.$$

For the fourth term of Eq. 4.5.3

$$\begin{aligned}\mathbb{E}_{\mathbb{Q}}\int_0^T|\rho_s^\epsilon(\mathcal{G}_{\mathrm{I}}\chi)|^p\,ds&\lesssim\int_0^T\mathbb{E}_{\mathbb{P}^\epsilon}\left[(\widetilde{D}_s^\epsilon)^2\right]^{1/2}\mathbb{E}_{\mathbb{P}^\epsilon}\left[\left|\mathcal{G}_{\mathrm{I}}\chi(X_s^\epsilon,Z_s^\epsilon)\widetilde{D}_s^\epsilon\right|^{2p}\right]^{1/2}ds\\&\le\int_0^T\mathbb{E}_{\mathbb{P}^\epsilon}\left[(\widetilde{D}_s^\epsilon)^2\right]^{1/2}\mathbb{E}_{\mathbb{P}^\epsilon}\left[\left(\widetilde{D}_s^\epsilon\right)^{4p}\right]^{1/4}\mathbb{E}_{\mathbb{P}^\epsilon}\left[|\mathcal{G}_{\mathrm{I}}\chi(X_s^\epsilon,Z_s^\epsilon)|^{4p}\right]^{1/4}ds.\end{aligned}$$

And we have

$$\sup_{\epsilon\in(0,1]}\mathbb{E}_{\mathbb{P}^\epsilon}\left[|\mathcal{G}_{\mathrm{I}}\chi(X_s^\epsilon,Z_s^\epsilon)|^{4p}\right]\lesssim\sup_{\epsilon\in(0,1]}\mathbb{E}_{\mathbb{P}^\epsilon}\left[1+|Z_s^\epsilon|^q\right]\lesssim 1+\sup_{\epsilon\in(0,1]}\mathbb{E}_{\mathbb{Q}}\left[|Z_0^\epsilon|^q\right]<\infty,\tag{4.5.4}$$

for some $q>0$, and therefore

$$\sup_{\epsilon\in(0,1]}\mathbb{E}_{\mathbb{Q}}\int_0^T|\rho_s^\epsilon(\mathcal{G}_{\mathrm{I}}\chi)|^p\,ds\lesssim\sup_{\epsilon\in(0,1]}\int_0^T\mathbb{E}_{\mathbb{P}^\epsilon}\left[|\mathcal{G}_{\mathrm{I}}\chi(X_s^\epsilon,Z_s^\epsilon)|^{4p}\right]^{1/4}ds<\infty.$$

By the same arguments as for the fourth term, we have that the fifth term of Eq. 4.5.3 is bounded uniformly in ϵ,

$$\sup_{\epsilon\in(0,1]}\mathbb{E}_{\mathbb{Q}}\int_0^T|\rho_s^\epsilon(\mathcal{G}_S\chi)|^p\,ds<\infty.$$

The first stochastic integral, sixth term of Eq. 4.5.3, is handled with application of the Burkholder-Davis-Gundy inequality, Hölder's inequality, and Fubini's theorem on the first line and then a change of measure, the Cauchy-Schwarz inequality, and Hölder's inequality to give

$$\begin{aligned}\sup_{\epsilon\in(0,1]}\mathbb{E}_{\mathbb{Q}}\sup_{t\le T}\left|\int_0^t\langle\rho_s^\epsilon(Mh),dY_s^\epsilon\rangle\right|^p&\lesssim\sup_{\epsilon\in(0,1]}\int_0^T\mathbb{E}_{\mathbb{Q}}\left|\rho_s^\epsilon(Mh)\right|^p ds\\&\lesssim\sup_{\epsilon\in(0,1]}\int_0^T\mathbb{E}_{\mathbb{P}^\epsilon}\left[(\widetilde{D}_s^\epsilon)^2\right]^{1/2}\mathbb{E}_{\mathbb{P}^\epsilon}\left[|\rho_s^\epsilon(Mh)|^{2p}\right]^{1/2}ds.\end{aligned}$$

And by further application of the Cauchy-Schwarz inequality, Hölder's inequality, boundedness of h, Lemma

4.4.6 for some $q > 0$, and finite moments of all orders for $\mathbb{Q}_{(X_0^\epsilon, Z_0^\epsilon)}$, we get

$$\begin{aligned}\sup_{\epsilon\in(0,1]} \mathbb{E}_{\mathbb{P}^\epsilon}\left[|\rho_s^\epsilon(Mh)|^{2p}\right]^{1/2} &\le \sup_{\epsilon\in(0,1]} \mathbb{E}_{\mathbb{P}^\epsilon}\left[(\widetilde{D}_s^\epsilon)^{4p}\right]^{1/4} |h|_\infty^p \mathbb{E}_{\mathbb{P}^\epsilon}\left[|M(X_s^\epsilon)|^{4p}\right]^{1/4} \\ &\lesssim \sup_{\epsilon\in(0,1]} \mathbb{E}_{\mathbb{P}^\epsilon}\left[(1+|X_s^\epsilon|^2)^{2p}\right]^{1/4} \lesssim \sup_{\epsilon\in(0,1]} \left(1+\mathbb{E}_{\mathbb{P}^\epsilon}\left[|X_s^\epsilon|^{4p}\right]\right)^{1/4} \\ &\lesssim \sup_{\epsilon\in(0,1]} \left(1+\mathbb{E}_{\mathbb{Q}}\left[|X_0^\epsilon|^{4p} + (1+\epsilon^{4p})(1+|Z_0^\epsilon|^q)\right]\right)^{1/4} < \infty.\end{aligned}$$

Because $\alpha\sigma^*\nabla_x M$ is bounded and by Lemma 4.4.11, the seventh term of Eq. 4.5.3 is bounded uniformly in ϵ,

$$\sup_{\epsilon\in(0,1]} \mathbb{E}_{\mathbb{Q}} \sup_{t\le T}\left|\int_0^t \langle \rho_s^\epsilon(\alpha\sigma^*\nabla_x M), dY_s^\epsilon\rangle\right|^p \lesssim \int_0^T \sup_{\epsilon\in(0,1]} \mathbb{E}_{\mathbb{Q}} \left|\rho_s^\epsilon(\alpha\sigma^*\nabla_x M)\right|^p ds < \infty.$$

Similarly using the boundedness of χh, the eighth term of Eq. 4.5.3 is bounded uniformly in ϵ,

$$\sup_{\epsilon\in(0,1]} \mathbb{E}_{\mathbb{Q}} \sup_{t\le T}\left|\int_0^t \langle \rho_s^\epsilon(\chi h), dY_s^\epsilon\rangle\right|^p < \infty.$$

Making use of the boundedness of σ, the polynomial growth of $\nabla_x\chi$ in z, and the finite moments of all orders for $\mathbb{Q}_{(X_0^\epsilon, Z_0^\epsilon)}$, the last term of Eq. 4.5.3 is

$$\begin{aligned}\sup_{\epsilon\in(0,1]} \mathbb{E}_{\mathbb{Q}} \sup_{t\le T}\left|\int_0^t \langle \rho_s^\epsilon(\alpha\sigma^*\nabla_x\chi), dY_s^\epsilon\rangle\right|^p &\lesssim \int_0^T \sup_{\epsilon\in(0,1]} \mathbb{E}_{\mathbb{Q}} \left|\rho_s^\epsilon(\alpha\sigma^*\nabla_x\chi)\right|^p ds \\ &\lesssim \int_0^T \sup_{\epsilon\in(0,1]} \mathbb{E}_{\mathbb{P}^\epsilon}\left[|\alpha\sigma^*\nabla_x\chi(X_s^\epsilon, Z_s^\epsilon)|^{4p}\right]^{1/4} ds \lesssim \int_0^T \sup_{\epsilon\in(0,1]} \mathbb{E}_{\mathbb{P}^\epsilon}\left[|\nabla_x\chi(X_s^\epsilon, Z_s^\epsilon)|^{4p}\right]^{1/4} ds \\ &\lesssim \int_0^T \sup_{\epsilon\in(0,1]} \left(1+\mathbb{E}_{\mathbb{P}^\epsilon}\left[|Z_s^\epsilon|^q\right]\right)^{1/4} ds \lesssim \int_0^T \sup_{\epsilon\in(0,1]} \left(1+\mathbb{E}_{\mathbb{Q}}\left[|Z_0^\epsilon|^q\right]\right)^{1/4} ds < \infty.\end{aligned}$$

This completes the calculation that $\sup_\epsilon \mathbb{E}_{\mathbb{Q}} \sup_{t\le T} |\rho_t^{\epsilon,x}(M)|^p < \infty$. We now show that $\mathbb{E}_{\mathbb{Q}} \sup_{t\le T} \left|\rho_t^0(M)\right|^p < \infty$. We have,

$$\begin{aligned}\mathbb{E}_{\mathbb{Q}} \sup_{t\le T} \left|\rho_t^0(M)\right|^p \lesssim \mathbb{E}_{\mathbb{Q}} \left|\rho_0^0(M)\right|^p &+ \int_0^T \mathbb{E}_{\mathbb{Q}} \left|\rho_s^0(\mathcal{G}^\dagger M)\right|^p ds \\ &+ \mathbb{E}_{\mathbb{Q}} \sup_{t\le T}\left|\int_0^t \langle \rho_s^0(M\bar{h}), dY_s^\epsilon\rangle\right|^p + \mathbb{E}_{\mathbb{Q}} \sup_{t\le T}\left|\int_0^t \langle \rho_s^0(\alpha\bar{\sigma}^*\nabla_x M), dY_s^\epsilon\rangle\right|^p.\end{aligned} \tag{4.5.5}$$

By Lemmas 4.4.9 and 4.4.10, we have that $\bar{b}, \bar{\sigma}, \bar{h}, \widetilde{a}$ and $\widetilde{b}$ are all bounded functions. Therefore, similar arguments as for ρ^ϵ show that the right side of Eq. 4.5.5 is finite.

We now prove (ii), the $\mathbb{F}$-weak tightness condition. Let $\varphi \in C_b^2(\mathbb{R}^m; \mathbb{R})$. There are two conditions that

must be checked for each fixed $\varphi \in \mathbb{F}$. The first one is a boundedness condition,

$$\lim_{N\to\infty} \sup_{\epsilon} \mathbb{Q}(|\zeta_0^\epsilon(\varphi)| \geq N) = 0,$$

which is trivially satisfied since $\zeta_0^\epsilon(\varphi) = \mathbb{E}_{\mathbb{Q}}\left[\varphi(X_0^\epsilon)\right] - \mathbb{E}_{\mathbb{Q}}\left[\varphi(X_0^0)\right] = 0$. The second one is an equicontinuity condition–for each $\delta > 0$ and $\eta > 0$ there are $\Delta > 0$ and $j < \infty$ such that

$$\mathbb{Q}\left(\sup_{|t-s|\leq\Delta} |\zeta_t^{\epsilon_i}(\varphi) - \zeta_s^{\epsilon_i}(\varphi)| \geq \delta\right) \leq \eta, \quad \forall i \geq j. \tag{4.5.6}$$

A sufficient condition for Eq. 4.5.6 is the following–there are $\mu, \beta, \gamma > 0$ and $K < \infty$ such that

$$\mathbb{E}_{\mathbb{Q}}|\zeta_t^{\epsilon_i}(\varphi) - \zeta_s^{\epsilon_i}(\varphi)|^\mu \leq K|t-s|^{1+\beta} + \epsilon_i^\gamma, \quad \forall i. \tag{4.5.7}$$

We now show that Eq. 4.5.7 is true. Let $\mu = 4$, $\epsilon > 0$ and $\varphi^\epsilon = \varphi + \epsilon\chi$, where χ solves the Poisson equation,

$$\mathcal{G}_F\chi = -\mathcal{G}_{\mathrm{I}}\varphi.$$

From $\zeta_t^\epsilon(\varphi) = \rho_t^{\epsilon,x}(\varphi) - \rho_t^0(\varphi)$ and $\rho_t^\epsilon(\varphi^\epsilon) = \rho_t^{\epsilon,x}(\varphi) + \rho_t^\epsilon(\epsilon\chi)$ we have

$$|\zeta_t^\epsilon(\varphi) - \zeta_s^\epsilon(\varphi)|^4 \lesssim |\rho_t^\epsilon(\varphi^\epsilon) - \rho_s^\epsilon(\varphi^\epsilon)|^4 + |\rho_t^0(\varphi) - \rho_s^0(\varphi)|^4 + |\rho_t^\epsilon(\epsilon\chi) - \rho_s^\epsilon(\epsilon\chi)|^4. \tag{4.5.8}$$

Working on the first term in this inequality,

$$\begin{aligned}\mathbb{E}_{\mathbb{Q}}|\rho_t^\epsilon(\varphi^\epsilon) - \rho_s^\epsilon(\varphi^\epsilon)|^4 &\lesssim \mathbb{E}_{\mathbb{Q}}\left|\int_s^t \rho_u^\epsilon(\mathcal{G}_S\varphi + \mathcal{G}_{\mathrm{I}}\chi + \epsilon\mathcal{G}_S\chi)du\right|^4 + \mathbb{E}_{\mathbb{Q}}\left|\int_s^t \langle\rho_u^\epsilon(\varphi^\epsilon h + \alpha\sigma^*\nabla_x\varphi^\epsilon), dY_u^\epsilon\rangle\right|^4 \\ &\lesssim (t-s)^3\int_s^t \mathbb{E}_{\mathbb{Q}}\left|\rho_u^\epsilon(\mathcal{G}_S\varphi + \mathcal{G}_{\mathrm{I}}\chi + \epsilon\mathcal{G}_S\chi)\right|^4 du + (t-s)\int_s^t \mathbb{E}_{\mathbb{Q}}\left|\rho_u^\epsilon(\varphi^\epsilon h + \alpha\sigma^*\nabla_x\varphi^\epsilon)\right|^4 du. \end{aligned} \tag{4.5.9}$$

First term of Eq. 4.5.9,

$$\int_s^t \mathbb{E}_{\mathbb{Q}}\left|\rho_u^\epsilon(\mathcal{G}_S\varphi + \mathcal{G}_{\mathrm{I}}\chi + \epsilon\mathcal{G}_S\chi)\right|^4 du \lesssim \int_s^t \mathbb{E}_{\mathbb{Q}}\left|\rho_u^\epsilon(\mathcal{G}_S\varphi)\right|^4 + \mathbb{E}_{\mathbb{Q}}\left|\rho_u^\epsilon(\mathcal{G}_{\mathrm{I}}\chi)\right|^4 + \mathbb{E}_{\mathbb{Q}}\left|\rho_u^\epsilon(\epsilon\mathcal{G}_S\chi)\right|^4 du.$$

By the boundedness of $b, \sigma, D_x^k\varphi$ for $|k| \leq 2$ and Lemma 4.4.8, we have the first term bounded by

$$\int_s^t \mathbb{E}_{\mathbb{Q}}\left|\rho_u^\epsilon(\mathcal{G}_S\varphi)\right|^4 du \lesssim (t-s).$$

By the boundedness of b, σ, the polynomial growth of $b_{\mathrm{I}}, D_x^k \chi$ in z, for $|k| \leq 2$ and Lemma 4.4.8, we have by the same arguments as Eq. 4.5.4

$$\int_s^t \mathbb{E}_{\mathbb{Q}} \left|\rho_u^\epsilon(\mathcal{G}_{\mathrm{I}}\chi)\right|^4 du + \int_s^t \mathbb{E}_{\mathbb{Q}} \left|\rho_u^\epsilon(\epsilon\mathcal{G}_S\chi)\right|^4 du \lesssim (t-s) + \epsilon^4(t-s) = (1+\epsilon^4)(t-s).$$

And therefore we have,

$$\int_s^t \mathbb{E}_{\mathbb{Q}} \left|\rho_u^\epsilon(\mathcal{G}_S\varphi + \mathcal{G}_{\mathrm{I}}\chi + \epsilon\mathcal{G}_S\chi)\right|^4 du \lesssim (1+\epsilon^4)(t-s).$$

The second term of Eq. 4.5.9 is bounded as follows,

$$\begin{aligned}\int_s^t \mathbb{E}_{\mathbb{Q}} \left|\rho_u^\epsilon(\varphi^\epsilon h + \alpha\sigma^*\nabla_x\varphi^\epsilon)\right|^4 du &\lesssim \int_s^t \mathbb{E}_{\mathbb{Q}} \left|\rho_u^\epsilon(\varphi h)\right|^4 + \mathbb{E}_{\mathbb{Q}} \left|\rho_u^\epsilon(\epsilon\chi h)\right|^4 du \\ &\quad + \int_s^t \mathbb{E}_{\mathbb{Q}} \left|\rho_u^\epsilon(\alpha\sigma^*\nabla_x\varphi)\right|^4 + \mathbb{E}_{\mathbb{Q}} \left|\rho_u^\epsilon(\epsilon\alpha\sigma^*\nabla_x\chi)\right|^4 du \\ &\lesssim (1+\epsilon^4)(t-s) + \mathbb{E}_{\mathbb{Q}} \left|\rho_u^\epsilon(\epsilon\alpha\sigma^*\nabla_x\chi)\right|^4 du,\end{aligned}$$

by boundedness of $h, \sigma, \chi, D_x^k\varphi$ for $|k| \leq 2$, and Lemma 4.4.8. The last term is bounded by $\lesssim \epsilon^4(t-s)$ due to boundedness of σ and polynomial growth of $\nabla_x\chi$ in z and finite moments of all orders for $\mathbb{Q}_{(X_0^\epsilon, Z_0^\epsilon)}$, and therefore

$$\int_s^t \mathbb{E}_{\mathbb{Q}} \left|\rho_u^\epsilon(\varphi^\epsilon h + \alpha\sigma^*\nabla_x\varphi^\epsilon)\right|^4 du \lesssim (1+\epsilon^4)(t-s).$$

The expectation of the second term in Eq. 4.5.8 is,

$$\begin{aligned}\mathbb{E}_{\mathbb{Q}}|\rho_t^0(\varphi) - \rho_s^0(\varphi)|^4 &\lesssim \mathbb{E}_{\mathbb{Q}} \left|\int_s^t \rho_u^0(\mathcal{G}^\dagger\varphi)du\right|^4 + \mathbb{E}_{\mathbb{Q}} \left|\int_s^t \langle \rho_u^0(\varphi\bar{h} + \alpha\bar{\sigma}^*\nabla_x\varphi), dY_u^\epsilon\rangle\right|^4 \\ &\lesssim (t-s)^3 \int_s^t \mathbb{E}_{\mathbb{Q}} \left|\rho_u^0(\mathcal{G}^\dagger\varphi)\right|^4 du + (t-s)\int_s^t \mathbb{E}_{\mathbb{Q}} \left|\rho_u^0(\varphi\bar{h} + \alpha\bar{\sigma}^*\nabla_x\varphi)\right|^4 du \\ &\lesssim (t-s)^4 + (t-s)^2,\end{aligned}$$

where we use the boundedness of $\bar{h}, \bar{\sigma}$ and the coefficients of $\mathcal{G}^\dagger$, which is a result of Lemmas 4.4.9 and 4.4.10, and the boundedness of $D_x^k\varphi$ for $k \leq 2$.

Using the fact that χ is bounded and Lemma 4.4.11, the last term of Eq. 4.5.8 is bounded by

$$\mathbb{E}_{\mathbb{Q}}|\rho_t^\epsilon(\epsilon\chi) - \rho_s^\epsilon(\epsilon\chi)|^4 \lesssim \epsilon^4\mathbb{E}_{\mathbb{Q}}\left[\rho_t^\epsilon(1)^4 + \rho_s^\epsilon(1)^4\right] \lesssim \epsilon^4.$$

Lastly, since we are interested in the case $(t-s)<1$, we satisfy Eq. 4.5.7 with $\mu=4$, $\beta=1$ and $\gamma=4$.

□

Now that (P^ϵ) has been shown to be tight, we need to show that this collection is weakly relatively compact and therefore any subsequence of (ϵ) will converge to a weak limit. The fact that (P^ϵ) is weakly relatively compact is given by the following corollary.

Corollary 4.5.1

Every subsequence of the ϵ-parameterized family of probability measures (P^ϵ) induced on path space $C([0,T];S(\mathbb{R}^m))$ by ζ^ϵ, has a weak limit.

Proof. From Lemma 4.5.2, (P^ϵ) is tight. Because $C([0,T];S(\mathbb{R}^m))$ is Hausdorff, since it is metrizable by [Jak86, Proposition 1.6iii, p.267] because $S(\mathbb{R}^m)$ is Polish, this implies that (P^ϵ) is relatively compact (see for instance [KX95, Theorem 2.2.1, p.56]). Therefore each sequence of (P^ϵ) has a convergent subsequence. □

Given a subsequence of (ϵ), we now let ζ be the limit point and characterize this limit point in the next lemma.

Lemma 4.5.3

Assume that f,g satisfy the assumptions of H_f, H_g and $H^{2,2+\alpha}$. Let $b,b_{\mathrm{I}},a\in C^{2,\alpha}$ and satisfy the growth conditions

$$|b(x,z)|+|b_{\mathrm{I}}(x,z)|+|a(x,z)|\le C(1+|z|)^\beta,$$
$$\sum_{|k|=1}^{2}\left|D_x^k b(x,z)\right|+\left|D_x^k b_{\mathrm{I}}(x,z)\right|+\left|D_x^k a(x,z)\right|\le C(1+|z|^q),$$

for some $\beta<-2$ and $q>0$. Let b_{I} be centered with respect to $\mu_\infty(x)$ for each x. Assume h is bounded and globally Lipschitz in (x,z). Let σ be globally Lipschitz in z. And assume that $\mathbb{Q}_{(X_0^\epsilon,Z_0^\epsilon)}$ has finite momentsz of every order. Then any limit point ζ of (ζ^ϵ) satisfies the equation,

$$\zeta_t(\varphi)=\int_0^t\zeta_s(\mathcal{G}^\dagger\varphi)ds+\int_0^t\langle\zeta_s(\varphi\bar{h}+\alpha\bar{\sigma}^*\nabla_x\varphi),dY_s\rangle,\qquad\zeta_0(\varphi)=0,\qquad\mathbb{Q}\text{-a.s. uniformly in } t\in[0,T].$$

Proof. With an abuse of notation, let ϵ be an element of the subsequence (ϵ), assume $\varphi\in C_b^2(\mathbb{R}^m;\mathbb{R})$, and consider the perturbed test function,

$$\varphi^\epsilon(x,z)=\varphi(x)+\epsilon\chi(x,z)+\epsilon^2\widetilde{\chi}(x,z),$$

where χ and $\widetilde{\chi}$ solve the Poisson equations,

$$\begin{aligned}\mathcal{G}_F\chi &= -\mathcal{G}_{\mathrm{I}}\varphi,\\ \mathcal{G}_F\widetilde{\chi} &= -\left(\mathcal{G}_S - \overline{\mathcal{G}_S}\right)\varphi - \left(\mathcal{G}_{\mathrm{I}}\chi - \overline{\mathcal{G}_{\mathrm{I}}\chi}\right).\end{aligned}$$

From Theorem 4.4.2, we have

$$\begin{aligned}|\chi(x,z)| + |\widetilde{\chi}(x,z)| &\lesssim 1,\\ \sum_{|i|=1}^{2} |D_x^i\chi(x,z)| + |D_x^i\widetilde{\chi}(x,z)| &\lesssim (1+|z|^{q'}),\end{aligned}$$

for some $q' > 0$. Because $\rho_t^{\epsilon,x}(\varphi) = \rho_t^\epsilon(\varphi^\epsilon) - \rho_t^\epsilon(\epsilon\chi) - \rho_t^\epsilon(\epsilon^2\widetilde{\chi})$, we have

$$\begin{aligned}\zeta_t^\epsilon(\varphi) = -\rho_t^\epsilon(\epsilon\chi) - \rho_t^\epsilon(\epsilon^2\widetilde{\chi}) + \rho_0^\epsilon(\varphi^\epsilon) - \rho_0^0(\varphi) + \int_0^t \rho_s^\epsilon(\mathcal{G}^\epsilon\varphi^\epsilon)ds - \int_0^t \rho_s^0(\mathcal{G}^\dagger\varphi)ds\\ + \int_0^t \langle \rho_s^\epsilon(\varphi^\epsilon h + \alpha\sigma^*\nabla_x\varphi^\epsilon), dY_s^\epsilon\rangle - \int_0^t \langle \rho_s^0(\varphi\bar{h} + \alpha\bar{\sigma}^*\nabla_x\varphi), dY_s^\epsilon\rangle. \qquad (4.5.10)\end{aligned}$$

When expanded, the Lebesgue integral for $\rho_s^\epsilon(\mathcal{G}^\epsilon\varphi^\epsilon)$ becomes,

$$\begin{aligned}\int_0^t \rho_s^\epsilon(\mathcal{G}^\epsilon\varphi^\epsilon)ds = \int_0^t \rho_s^{\epsilon,x}(\overline{\mathcal{G}_S}\varphi)ds + \int_0^t \rho_s^{\epsilon,x}(\overline{\mathcal{G}_{\mathrm{I}}\chi})ds\\ + \epsilon\int_0^t \rho_s^\epsilon(\mathcal{G}_S\chi)ds + \epsilon\int_0^t \rho_s^\epsilon(\mathcal{G}_{\mathrm{I}}\widetilde{\chi})ds + \epsilon^2\int_0^t \rho_s^\epsilon(\mathcal{G}_S\widetilde{\chi})ds.\end{aligned}$$

The term $\rho_0^\epsilon(\varphi^\epsilon) - \rho_0^0(\varphi)$ is,

$$\begin{aligned}\rho_0^\epsilon(\varphi^\epsilon) - \rho_0^0(\varphi) &= \rho_0^{\epsilon,x}(\varphi) + \rho_0^\epsilon(\epsilon\chi) + \rho_0^\epsilon(\epsilon^2\widetilde{\chi}) - \rho_0^0(\varphi)\\ &= \rho_0^\epsilon(\epsilon\chi) + \rho_0^\epsilon(\epsilon^2\widetilde{\chi}).\end{aligned}$$

And we group all terms of first order in ϵ involving χ into $\mathcal{O}_\chi(\epsilon)$,

$$\mathcal{O}_\chi(\epsilon) = -\rho_t^\epsilon(\epsilon\chi) + \rho_0^\epsilon(\epsilon\chi) + \epsilon\int_0^t \rho_s^\epsilon(\mathcal{G}_S\chi)ds + \epsilon\int_0^t \langle \rho_s^\epsilon(\chi h + \alpha\sigma^*\nabla_x\chi), dY_s^\epsilon\rangle.$$

Similarly, let the terms of first and second order in ϵ involving $\widetilde{\chi}$ be grouped into $\mathcal{O}_{\widetilde{\chi}}(\epsilon)$,

$$\mathcal{O}_{\widetilde{\chi}}(\epsilon) = -\rho_t^\epsilon(\epsilon^2\widetilde{\chi}) + \rho_0^\epsilon(\epsilon^2\widetilde{\chi}) + \epsilon\int_0^t \rho_s^\epsilon(\mathcal{G}_{\mathrm{I}}\widetilde{\chi})ds + \epsilon^2\int_0^t \rho_s^\epsilon(\mathcal{G}_S\widetilde{\chi})ds + \epsilon^2\int_0^t \langle \rho_s^\epsilon(\widetilde{\chi}h + \alpha\sigma^*\nabla_x\widetilde{\chi}), dY_s^\epsilon\rangle.$$

Eq. 4.5.10 now becomes,

$$\zeta_t^\epsilon(\varphi) = \int_0^t \zeta_s^\epsilon(\overline{\mathcal{G}_S}\varphi)ds + \int_0^t \rho_s^{\epsilon,x}(\overline{\mathcal{G}_{\mathrm{I}}\chi})ds + \mathcal{O}_\chi(\epsilon) + \mathcal{O}_{\widetilde{\chi}}(\epsilon) \\ + \int_0^t \langle \rho_s^\epsilon(\varphi h + \alpha\sigma^*\nabla_x\varphi), dY_s^\epsilon\rangle - \int_0^t \langle \rho_s^0(\varphi\bar{h} + \alpha\bar{\sigma}^*\nabla_x\varphi), dY_s^\epsilon\rangle. \tag{4.5.11}$$

Next, consider the equivalence of the following terms

$$\int_0^t \rho_s^{\epsilon,x}(\overline{\mathcal{G}_{\mathrm{I}}\chi})ds = \int_0^t \rho_s^{\epsilon,x}(\widetilde{\mathcal{G}}\varphi)ds.$$

This follows since $\nabla_x^{\otimes 2}\varphi = \nabla_x\nabla_x\varphi$ is symmetric, and therefore,

$$\begin{aligned}\langle \nabla_x^{\otimes 2}\varphi \mathcal{G}_F^{-1}(-b_{\mathrm{I}}), b_{\mathrm{I}}\rangle &= \sum_{i,j=1}^m \frac{\partial^2\varphi}{\partial x_i \partial x_j}\mathcal{G}_F^{-1}(-b_{\mathrm{I}})_i b_{\mathrm{I},j} \\ &= \sum_{i,j=1}^m \frac{\partial^2\varphi}{\partial x_i\partial x_j}\left(\frac{1}{2}(\mathcal{G}_F^{-1}(-b_{\mathrm{I}})\otimes b_{\mathrm{I}})_{ij} + \frac{1}{2}(b_{\mathrm{I}}\otimes \mathcal{G}_F^{-1}(-b_{\mathrm{I}}))_{ij}\right),\end{aligned}$$

which leads to the following,

$$\begin{aligned}\overline{\mathcal{G}_{\mathrm{I}}\chi}(x) &= \int_{\mathbb{R}^n}\langle \nabla_x\chi, b_{\mathrm{I}}\rangle(x,z)\mu_\infty(dz;x) = \int_{\mathbb{R}^n}\langle \nabla_x^{\otimes 2}\varphi\mathcal{G}_F^{-1}(-b_{\mathrm{I}}) + \left(\nabla_x\mathcal{G}_F^{-1}(-b_{\mathrm{I}})\right)^*\nabla_x\varphi, b_{\mathrm{I}}\rangle(x,z)\mu_\infty(dz;x) \\ &= \langle \nabla_x\varphi(x), \int_{\mathbb{R}^n}\left(\nabla_x\mathcal{G}_F^{-1}(-b_{\mathrm{I}})\right)b_{\mathrm{I}}(x,z)\mu_\infty(dz;x)\rangle + \int_{\mathbb{R}^n}\langle\nabla_x^{\otimes 2}\varphi\mathcal{G}_F^{-1}(-b_{\mathrm{I}}), b_{\mathrm{I}}\rangle(x,z)\mu_\infty(dz;x) \\ &= \widetilde{\mathcal{G}}\varphi(x).\end{aligned}$$

Using this equivalence, adding and subtracting the term, $\int_0^t\langle\rho_s^{\epsilon,x}(\varphi\bar{h} + \alpha\bar{\sigma}^*\nabla_x\varphi), dY_s^\epsilon\rangle$, then Eq. 4.5.11 becomes,

$$\zeta_t^\epsilon(\varphi) = \int_0^t \zeta_s^\epsilon(\mathcal{G}^\dagger\varphi)ds + \int_0^t\langle\zeta_s^\epsilon(\varphi\bar{h} + \alpha\bar{\sigma}^*\nabla_x\varphi), dY_s^\epsilon\rangle + \mathcal{O}_\chi(\epsilon) + \mathcal{O}_{\widetilde{\chi}}(\epsilon) \\ + \int_0^t\langle\rho_s^\epsilon(\varphi h + \alpha\sigma^*\nabla_x\varphi), dY_s^\epsilon\rangle - \int_0^t\langle\rho_s^{\epsilon,x}(\varphi\bar{h} + \alpha\bar{\sigma}^*\nabla_x\varphi), dY_s^\epsilon\rangle.$$

Therefore

$$\mathbb{E}_{\mathbb{Q}}\sup_{t\le T}\left|\zeta_t^\epsilon(\varphi) - \int_0^t\zeta_s^\epsilon(\mathcal{G}^\dagger\varphi)ds - \int_0^t\langle\zeta_s^\epsilon(\varphi\bar{h} + \alpha\bar{\sigma}^*\nabla_x\varphi), dY_s^\epsilon\rangle\right|^2 \lesssim \mathbb{E}_{\mathbb{Q}}\sup_{t\le T}|\mathcal{O}_\chi(\epsilon)|^2 + \mathbb{E}_{\mathbb{Q}}\sup_{t\le T}|\mathcal{O}_{\widetilde{\chi}}(\epsilon)|^2 \\ + \mathbb{E}_{\mathbb{Q}}\sup_{t\le T}\left|\int_0^t\langle\rho_s^\epsilon(\varphi(h-\bar{h})), dY_s^\epsilon\rangle\right|^2 + \mathbb{E}_{\mathbb{Q}}\sup_{t\le T}\left|\int_0^t\langle\rho_s^\epsilon(\alpha(\sigma-\bar{\sigma})^*\nabla_x\varphi), dY_s^\epsilon\rangle\right|^2. \tag{4.5.12}$$

From the boundedness of b, σ, a, h, the growth conditions on $D_x^k \chi$ for $|k| \leq 2$, and the finite moments of all orders for $\mathbb{Q}_{(X_0^\epsilon, Z_0^\epsilon)}$, we have that

$$\lim_{\epsilon \to 0} \mathbb{E}_{\mathbb{Q}} \sup_{t \leq T} |\mathcal{O}_\chi(\epsilon)|^2 = 0.$$

Similarly, from the boundedness of b, σ, a, h, the growth conditions on $D_x^k \widetilde{\chi}$ for $|k| \leq 2$ and b_{I}, and the finite moments of all orders for $\mathbb{Q}_{(X_0^\epsilon, Z_0^\epsilon)}$, we have that

$$\lim_{\epsilon \to 0} \mathbb{E}_{\mathbb{Q}} \sup_{t \leq T} |\mathcal{O}_{\widetilde{\chi}}(\epsilon)|^2 = 0.$$

Our focus now shifts to showing that

$$\lim_{\epsilon \to 0} \mathbb{E}_{\mathbb{Q}} \sup_{t \leq T} \left| \int_0^t \langle \rho_s^\epsilon(\varphi(h - \bar{h})), dY_s^\epsilon \rangle \right|^2 = 0, \quad \text{and} \quad \lim_{\epsilon \to 0} \mathbb{E}_{\mathbb{Q}} \sup_{t \leq T} \left| \int_0^t \langle \rho_s^\epsilon(\alpha(\sigma - \bar{\sigma})^* \nabla_x \varphi), dY_s^\epsilon \rangle \right|^2 = 0. \quad (4.5.13)$$

Let $\psi_h(x, z) \equiv \varphi(h - \bar{h})(x, z)$ and $\psi_\sigma(x, z) \equiv \alpha(\sigma - \bar{\sigma})^* \nabla_x \varphi(x, z)$. Because ψ_h and ψ_σ are both centered with respect to $\mu_\infty(x)$ for each x, globally Lipschitz in (x, z), and bounded in (x, z), we let ψ represent either ψ_h or ψ_σ and perform the same analysis for both.

Applying the Burkholder-Davis-Gundy inequality to either term in Eq. 4.5.13, we get

$$\mathbb{E}_{\mathbb{Q}} \sup_{t \leq T} \left| \int_0^t \langle \rho_s^\epsilon(\psi), dY_s^\epsilon \rangle \right|^2 \lesssim \mathbb{E}_{\mathbb{Q}} \int_0^T |\rho_s^\epsilon(\psi)|^2 \, ds = \mathbb{E}_{\mathbb{Q}} \int_0^T \left| \mathbb{E}_{\mathbb{P}^\epsilon} \left[\psi(X_s^\epsilon, Z_s^\epsilon) \widetilde{D}_s^\epsilon \,\middle|\, \mathcal{Y}_s^\epsilon \right] \right|^2 ds. \quad (4.5.14)$$

We now follow the argument by Kushner [Kus90, Chapter 6] to partition the domain of the time integral into intervals of length at most $0 < \delta \ll 1$, where $\delta = \delta(\epsilon)$ will later be chosen as a function of ϵ. Let $N = \lfloor \frac{T}{\delta} \rfloor \in \mathbb{N}_0$ such that $T = N\delta + \mathcal{O}(\delta)$. Then we have,

$$\begin{aligned} \mathbb{E}_{\mathbb{Q}} \int_0^T \left| \mathbb{E}_{\mathbb{P}^\epsilon} \left[\psi(X_s^\epsilon, Z_s^\epsilon) \widetilde{D}_s^\epsilon \,\middle|\, \mathcal{Y}_s^\epsilon \right] \right|^2 ds &= \mathbb{E}_{\mathbb{Q}} \sum_{i=0}^{N-1} \int_{t_i}^{t_{i+1}} \left| \mathbb{E}_{\mathbb{P}^\epsilon} \left[\psi(X_s^\epsilon, Z_s^\epsilon) \widetilde{D}_s^\epsilon \,\middle|\, \mathcal{Y}_s^\epsilon \right] \right|^2 ds \\ &\quad + \mathbb{E}_{\mathbb{Q}} \int_{N\delta}^T \left| \mathbb{E}_{\mathbb{P}^\epsilon} \left[\psi(X_s^\epsilon, Z_s^\epsilon) \widetilde{D}_s^\epsilon \,\middle|\, \mathcal{Y}_s^\epsilon \right] \right|^2 ds. \end{aligned}$$

with $t_{i+1} - t_i = \delta$, $\forall i$. We now consider a single time integral from $[t_i, t_{i+1}]$. For simplicity and clarity, let us use the notation $[t, t + \delta]$ instead. The analysis for the remainder term, over the interval $[N\delta, T]$, will follow from the same arguments.

We introduce terms to the conditional expectation with arguments X_t^ϵ and $\widetilde{D}_t^\epsilon$ fixed at the initial time of

the integral over $[t, t+\delta]$, to get,

$$\left|\mathbb{E}_{\mathbb{P}^\epsilon}\left[\psi(X_s^\epsilon, Z_s^\epsilon)\widetilde{D}_s^\epsilon \,\middle|\, \mathcal{Y}_s^\epsilon\right]\right|^2 \lesssim \left|\mathbb{E}_{\mathbb{P}^\epsilon}\left[(\psi(X_s^\epsilon, Z_s^\epsilon) - \psi(X_t^\epsilon, Z_s^\epsilon))\widetilde{D}_s^\epsilon \,\middle|\, \mathcal{Y}_s^\epsilon\right]\right|^2 + \left|\mathbb{E}_{\mathbb{P}^\epsilon}\left[\psi(X_t^\epsilon, Z_s^\epsilon)(\widetilde{D}_s^\epsilon - \widetilde{D}_t^\epsilon) \,\middle|\, \mathcal{Y}_s^\epsilon\right]\right|^2 + \left|\mathbb{E}_{\mathbb{P}^\epsilon}\left[\psi(X_t^\epsilon, Z_s^\epsilon)\widetilde{D}_t^\epsilon \,\middle|\, \mathcal{Y}_s^\epsilon\right]\right|^2. \tag{4.5.15}$$

The first term on the right side of Eq. 4.5.15, by way of Jensen's inequality and Fubini's theorem on the first line, a change of measure, the Cauchy-Schwarz inequality, Jensen's inequality, and the tower property of conditional expectation on the second line, contributes

$$\begin{aligned}\mathbb{E}_{\mathbb{Q}}\int_t^{t+\delta}\left|\mathbb{E}_{\mathbb{P}^\epsilon}\left[(\psi(X_s^\epsilon, Z_s^\epsilon) - \psi(X_t^\epsilon, Z_s^\epsilon))\widetilde{D}_s^\epsilon \,\middle|\, \mathcal{Y}_s^\epsilon\right]\right|^2 ds &\le \int_t^{t+\delta}\mathbb{E}_{\mathbb{Q}}\mathbb{E}_{\mathbb{P}^\epsilon}\left[\left|(\psi(X_s^\epsilon, Z_s^\epsilon) - \psi(X_t^\epsilon, Z_s^\epsilon))\,\widetilde{D}_s^\epsilon\right|^2 \,\middle|\, \mathcal{Y}_s^\epsilon\right] ds \\ &\le \int_t^{t+\delta}\mathbb{E}_{\mathbb{P}^\epsilon}\left[\left(\widetilde{D}_s^\epsilon\right)^2\right]^{1/2}\mathbb{E}_{\mathbb{P}^\epsilon}\left[\left|(\psi(X_s^\epsilon, Z_s^\epsilon) - \psi(X_t^\epsilon, Z_s^\epsilon))\,\widetilde{D}_s^\epsilon\right|^4\right]^{1/2} ds.\end{aligned}$$

By Lemma 4.4.8, $\mathbb{E}_{\mathbb{P}^\epsilon}\left[\left(\widetilde{D}_s^\epsilon\right)^2\right]^{1/2} < \infty$, and by application of the Cauchy-Schwarz inequality and then the Lipschitz property of ψ, we get

$$\begin{aligned}\mathbb{E}_{\mathbb{P}^\epsilon}\left[\left|(\psi(X_s^\epsilon, Z_s^\epsilon) - \psi(X_t^\epsilon, Z_s^\epsilon))\,\widetilde{D}_s^\epsilon\right|^4\right]^{1/2} &\le \mathbb{E}_{\mathbb{P}^\epsilon}\left[|\psi(X_s^\epsilon, Z_s^\epsilon) - \psi(X_t^\epsilon, Z_s^\epsilon)|^8\right]^{1/4}\mathbb{E}_{\mathbb{P}^\epsilon}\left[\left(\widetilde{D}_s^\epsilon\right)^8\right]^{1/4} \\ &\lesssim \mathbb{E}_{\mathbb{P}^\epsilon}\left[|X_s^\epsilon - X_t^\epsilon|^8\right]^{1/4}.\end{aligned}$$

ψ is globally Lipschitz in x, since each of the components of ψ are either globally Lipschitz in x or have a bounded derivative in x. Lemma 4.4.7 gives

$$\mathbb{E}_{\mathbb{P}^\epsilon}\left[|X_s^\epsilon - X_t^\epsilon|^8\right]^{1/4} \lesssim \left(\epsilon^8(1 + \mathbb{E}_{\mathbb{P}^\epsilon}|Z_0^\epsilon|^q) + \delta^4(1+\epsilon^8)(1 + \mathbb{E}\left[|Z_0^\epsilon|^q\right])\right)^{1/4},$$

for some $q \ge 0$, and therefore by the finite moments of $\mathbb{Q}_{(X_0^\epsilon, Z_0^\epsilon)}$, the first term of Eq. 4.5.15 is bounded by,

$$\mathbb{E}_{\mathbb{Q}}\int_t^{t+\delta}\left|\mathbb{E}_{\mathbb{P}^\epsilon}\left[(\psi(X_s^\epsilon, Z_s^\epsilon) - \psi(X_t^\epsilon, Z_s^\epsilon))\widetilde{D}_s^\epsilon \,\middle|\, \mathcal{Y}_s^\epsilon\right]\right|^2 ds \lesssim \delta(\epsilon^8 + \delta^4(1+\epsilon^8))^{1/4}. \tag{4.5.16}$$

The second term of Eq. 4.5.15 similarly contributes,

$$\begin{aligned}\mathbb{E}_{\mathbb{Q}}\int_t^{t+\delta}\left|\mathbb{E}_{\mathbb{P}^\epsilon}\left[\psi(X_t^\epsilon, Z_s^\epsilon)(\widetilde{D}_s^\epsilon - \widetilde{D}_t^\epsilon) \,\middle|\, \mathcal{Y}_s^\epsilon\right]\right|^2 ds &\le \int_t^{t+\delta}\mathbb{E}_{\mathbb{Q}}\mathbb{E}_{\mathbb{P}^\epsilon}\left[\left|\psi(X_t^\epsilon, Z_s^\epsilon)(\widetilde{D}_s^\epsilon - \widetilde{D}_t^\epsilon)\right|^2 \,\middle|\, \mathcal{Y}_s^\epsilon\right] ds \\ &\le \int_t^{t+\delta}\mathbb{E}_{\mathbb{P}^\epsilon}\left[\left(\widetilde{D}_s^\epsilon\right)^2\right]^{1/2}\mathbb{E}_{\mathbb{P}^\epsilon}\left[\left|\psi(X_t^\epsilon, Z_s^\epsilon)(\widetilde{D}_s^\epsilon - \widetilde{D}_t^\epsilon)\right|^4\right]^{1/2} ds.\end{aligned}$$

We now use the boundedness of ψ to get

$$\mathbb{E}_{\mathbb{P}^\epsilon}\left[\left|\psi(X_t^\epsilon, Z_s^\epsilon)(\widetilde{D}_s^\epsilon - \widetilde{D}_t^\epsilon)\right|^4\right]^{1/2} \leq |\psi|_\infty^2 \mathbb{E}_{\mathbb{P}^\epsilon}\left[\left|\widetilde{D}_s^\epsilon - \widetilde{D}_t^\epsilon\right|^4\right]^{1/2}.$$

Lemma 4.4.8 gives $\mathbb{E}_{\mathbb{P}^\epsilon}\left[\left|\widetilde{D}_s^\epsilon - \widetilde{D}_t^\epsilon\right|^4\right]^{1/2} \lesssim \delta$ and therefore

$$\mathbb{E}_{\mathbb{Q}} \int_t^{t+\delta} \left|\mathbb{E}_{\mathbb{P}^\epsilon}\left[\psi(X_t^\epsilon, Z_s^\epsilon)(\widetilde{D}_s^\epsilon - \widetilde{D}_t^\epsilon) \,\middle|\, \mathcal{Y}_s^\epsilon\right]\right|^2 ds \lesssim \delta^2. \tag{4.5.17}$$

Recall the last term in Eq. 4.5.15,

$$\mathbb{E}_{\mathbb{Q}} \int_t^{t+\delta} \left|\mathbb{E}_{\mathbb{P}^\epsilon}\left[\psi(X_t^\epsilon, Z_s^\epsilon)\widetilde{D}_t^\epsilon \,\middle|\, \mathcal{Y}_s^\epsilon\right]\right|^2 ds.$$

We first consider adding and subtracting the following term within the conditional expectation,

$$\psi(X_t^\epsilon, \widehat{Z}_s^{\epsilon, X_t^\epsilon})\widetilde{D}_t^\epsilon,$$

where $\widehat{Z}^{\epsilon, X_t^\epsilon}$ is the process satisfying Eq. 4.2.1, but with fixed random initial condition $x = X_t^\epsilon$. Then we have

$$\begin{aligned}\mathbb{E}_{\mathbb{Q}} \int_t^{t+\delta} \left|\mathbb{E}_{\mathbb{P}^\epsilon}\left[\psi(X_t^\epsilon, Z_s^\epsilon)\widetilde{D}_t^\epsilon \,\middle|\, \mathcal{Y}_s^\epsilon\right]\right|^2 ds \lesssim{}& \mathbb{E}_{\mathbb{Q}} \int_t^{t+\delta} \left|\mathbb{E}_{\mathbb{P}^\epsilon}\left[\psi(X_t^\epsilon, \widehat{Z}_s^{\epsilon, X_t^\epsilon})\widetilde{D}_t^\epsilon \,\middle|\, \mathcal{Y}_s^\epsilon\right]\right|^2 ds \\ &+ \mathbb{E}_{\mathbb{Q}} \int_t^{t+\delta} \left|\mathbb{E}_{\mathbb{P}^\epsilon}\left[\left(\psi(X_t^\epsilon, Z_s^\epsilon) - \psi(X_t^\epsilon, \widehat{Z}_s^{\epsilon, X_t^\epsilon})\right)\widetilde{D}_t^\epsilon \,\middle|\, \mathcal{Y}_s^\epsilon\right]\right|^2 ds. \end{aligned} \tag{4.5.18}$$

Concentrating on the second term of Eq. 4.5.18,

$$\begin{aligned}\mathbb{E}_{\mathbb{Q}} \int_t^{t+\delta} \left|\mathbb{E}_{\mathbb{P}^\epsilon}\left[\left(\psi(X_t^\epsilon, Z_s^\epsilon) - \psi(X_t^\epsilon, \widehat{Z}_s^{\epsilon, X_t^\epsilon})\right)\widetilde{D}_t^\epsilon \,\middle|\, \mathcal{Y}_s^\epsilon\right]\right|^2 ds &\lesssim \int_t^{t+\delta} \mathbb{E}_{\mathbb{P}^\epsilon}\left[\left|\psi(X_t^\epsilon, Z_s^\epsilon) - \psi(X_t^\epsilon, \widehat{Z}_s^{\epsilon, X_t^\epsilon})\right|^8\right]^{1/4} ds \\ &\lesssim \int_t^{t+\delta} \mathbb{E}_{\mathbb{P}^\epsilon}\left[\mathbb{E}_{\mathbb{P}^\epsilon}\left[\left|\psi(X_t^\epsilon, Z_s^\epsilon) - \psi(X_t^\epsilon, \widehat{Z}_s^{\epsilon, X_t^\epsilon})\right|^8 \,\middle|\, \mathcal{F}_t^{X^\epsilon} \vee \mathcal{F}_t^{Z^\epsilon}\right]\right]^{1/4} ds \\ &\lesssim \int_t^{t+\delta} \mathbb{E}_{\mathbb{P}^\epsilon}\left[\mathbb{E}_{\mathbb{P}^\epsilon}\left[\left|\psi(x, Z_s^{\epsilon;(t,x,z)}) - \psi(x, \widehat{Z}_s^{\epsilon,x;(t,z)})\right|^8 \,\middle|\, (x,z) = (X_t^\epsilon, Z_t^\epsilon)\right]\right]^{1/4} ds.\end{aligned}$$

From the global Lipschitz property of ψ in the z-component, we have the following estimate,

$$\mathbb{E}_{\mathbb{P}^\epsilon}\left[\left|\psi(x, Z_s^{\epsilon;(t,x,z)}) - \psi(x, \widehat{Z}_s^{\epsilon,x;(t,z)})\right|^8\right] \lesssim \mathbb{E}_{\mathbb{P}^\epsilon}\left[\left|Z_s^{\epsilon;(t,x,z)} - \widehat{Z}_s^{\epsilon,x;(t,z)}\right|^8\right].$$

In what follows, we use the notation $(X^{\epsilon;(t,x)}, Z^{\epsilon;(t,z)})$ for the pair process realized by $Z^{\epsilon;(t,x,z)}$. Similarly, we use $X^{\epsilon;(t,x,z)}$ when we must make clear that we are referring to the first entry of the pair $(X^{\epsilon;(t,x)}, Z^{\epsilon;(t,z)})$ which satisfies Eq. 4.0.1. The previous inequality is then bounded as follows,

$$\begin{aligned}
&\mathbb{E}_{\mathbb{P}^\epsilon}\left[\left|Z_s^{\epsilon;(t,x,z)} - \widehat{Z}_s^{\epsilon,x;(t,z)}\right|^8\right] \lesssim \\
&\frac{\delta^7}{\epsilon^{16}}\int_t^{t+\delta} \mathbb{E}_{\mathbb{P}^\epsilon}\left|f(X_s^{\epsilon;(t,x)}, Z_s^{\epsilon;(t,z)}) - f(x, \widehat{Z}_s^{\epsilon,x;(t,z)})\right|^8 ds + \frac{\delta^3}{\epsilon^8}\int_t^{t+\delta} \mathbb{E}_{\mathbb{P}^\epsilon}\left|g(X_s^{\epsilon;(t,x)}, Z_s^{\epsilon;(t,z)}) - g(x, \widehat{Z}_s^{\epsilon,x;(t,z)})\right|^8 ds \\
&\quad\lesssim \frac{\delta^7}{\epsilon^{16}}\int_t^{t+\delta} \mathbb{E}_{\mathbb{P}^\epsilon}\left|f(X_s^{\epsilon;(t,x)}, Z_s^{\epsilon;(t,z)}) - f(x, Z_s^{\epsilon;(t,z)})\right|^8 + \mathbb{E}_{\mathbb{P}^\epsilon}\left|f(x, Z_s^{\epsilon;(t,x,z)}) - f(x, \widehat{Z}_s^{\epsilon,x;(t,z)})\right|^8 ds \\
&\quad\quad + \frac{\delta^3}{\epsilon^8}\int_t^{t+\delta} \mathbb{E}_{\mathbb{P}^\epsilon}\left|g(X_s^{\epsilon;(t,x)}, Z_s^{\epsilon;(t,z)}) - g(x, Z_s^{\epsilon;(t,z)})\right|^8 + \mathbb{E}_{\mathbb{P}^\epsilon}\left|g(x, Z_s^{\epsilon;(t,x,z)}) - g(x, \widehat{Z}_s^{\epsilon,x;(t,z)})\right|^8 ds \\
&\quad\quad\quad\leq \frac{\delta^3}{\epsilon^8}\left(\frac{\delta^4}{\epsilon^8}|\nabla_x f|_\infty^8 + |\nabla_x g|_\infty^8\right)\int_t^{t+\delta} \mathbb{E}_{\mathbb{P}^\epsilon}\left|X_s^{\epsilon;(t,x,z)} - x\right|^8 ds \\
&\quad\quad\quad\quad + \frac{\delta^3}{\epsilon^8}\left(\frac{\delta^4}{\epsilon^8}|\nabla_z f|_\infty^8 + |\nabla_z g|_\infty^8\right)\int_t^{t+\delta} \mathbb{E}_{\mathbb{P}^\epsilon}\left|Z_s^{\epsilon;(t,x,z)} - \widehat{Z}_s^{\epsilon,x;(t,z)}\right|^8 ds.
\end{aligned}$$

From Lemma 4.4.7, for some $q \geq 0$, we get

$$\int_t^{t+\delta} \mathbb{E}_{\mathbb{P}^\epsilon}\left|X_s^{\epsilon;(t,x,z)} - x\right|^8 ds \lesssim \delta\epsilon^8(1+|z|^q) + \delta^5(1+\epsilon^8)(1+|z|^q).$$

Let

$$\eta(\epsilon,\delta) \equiv \left(\frac{\delta^8}{\epsilon^{16}} + \frac{\delta^4}{\epsilon^8}\right).$$

Therefore Grönwall's lemma gives us

$$\mathbb{E}_{\mathbb{P}^\epsilon}\left[\left|Z_s^{\epsilon;(t,x,z)} - \widehat{Z}_s^{\epsilon,x;(t,z)}\right|^8\right] \lesssim \eta(\epsilon,\delta)\left(\epsilon^8 + \delta^4(1+\epsilon^8)\right)\exp(\eta(\epsilon,\delta))(1+|z|^q).$$

For further brevity, let us define

$$\mathfrak{F}(\epsilon,\delta) \equiv \eta(\epsilon,\delta)\left(\epsilon^8 + \delta^4(1+\epsilon^8)\right)\exp(\eta(\epsilon,\delta)).$$

Therefore the second term in Eq. 4.5.18 is bounded by

$$\begin{aligned}
\mathbb{E}_{\mathbb{Q}}\int_t^{t+\delta}\left|\mathbb{E}_{\mathbb{P}^\epsilon}\left[\left(\psi(X_t^\epsilon, Z_s^\epsilon) - \psi(X_t^\epsilon, \widehat{Z}_s^{\epsilon,X_t^\epsilon})\right)\widetilde{D}_t^\epsilon \,\middle|\, \mathcal{Y}_s^\epsilon\right]\right|^2 ds &\lesssim \int_t^{t+\delta} \mathbb{E}_{\mathbb{P}^\epsilon}\left[\mathfrak{F}(\epsilon,\delta)(1+|Z_t^\epsilon|^q)\right]^{1/4} ds \\
&\lesssim \delta\mathfrak{F}(\epsilon,\delta)^{1/4}(1+\mathbb{E}_{\mathbb{P}^\epsilon}\left[|Z_0^\epsilon|^{q'}\right])^{1/4} \lesssim \delta\mathfrak{F}(\epsilon,\delta)^{1/4}. \qquad (4.5.19)
\end{aligned}$$

For the first term on the right hand side of Eq. 4.5.18, we condition the centering term on a larger filtration $\mathcal{H} = \mathcal{Y}_s^\epsilon \vee \mathcal{F}_t^{X^\epsilon} \vee \mathcal{F}_t^{Z^\epsilon}$, and then use the fact that $\sigma(\widehat{Z}_s^{\epsilon,X_t^\epsilon}) \vee \mathcal{Y}_t^\epsilon \vee \mathcal{F}_t^{X^\epsilon} \vee \mathcal{F}_t^{Z^\epsilon}$ is independent of $\sigma(Y_r^\epsilon - Y_t^\epsilon; r \in [t,s])$ under $\mathbb{P}^\epsilon$ and that $(X_t^\epsilon, \widehat{Z}_s^{\epsilon,X_t^\epsilon})$ is Markov in the larger filtration $\mathcal{Y}_s^\epsilon \vee \mathcal{F}_t^{X^\epsilon} \vee \mathcal{F}_s^{Z^\epsilon}$ to yield,

$$\begin{aligned}\mathbb{E}_{\mathbb{Q}} \int_t^{t+\delta} \left| \mathbb{E}_{\mathbb{P}^\epsilon} \left[\psi(X_t^\epsilon, \widehat{Z}_s^{\epsilon,X_t^\epsilon}) \widetilde{D}_t^\epsilon \,\middle|\, \mathcal{Y}_s^\epsilon \right] \right|^2 ds &= \mathbb{E}_{\mathbb{Q}} \int_t^{t+\delta} \left| \mathbb{E}_{\mathbb{P}^\epsilon} \left[\mathbb{E}_{\mathbb{P}^\epsilon} \left[\psi(X_t^\epsilon, \widehat{Z}_s^{\epsilon,X_t^\epsilon}) \,\middle|\, \mathcal{H} \right] \widetilde{D}_t^\epsilon \,\middle|\, \mathcal{Y}_s^\epsilon \right] \right|^2 ds \\ &= \mathbb{E}_{\mathbb{Q}} \int_t^{t+\delta} \left| \mathbb{E}_{\mathbb{P}^\epsilon} \left[\mathbb{E}_{\mathbb{P}^\epsilon} \left[\psi(x, \widehat{Z}_s^{\epsilon,x;(t,z)}) \,\middle|\, (x,z) = (X_t^\epsilon, Z_t^\epsilon) \right] \widetilde{D}_t^\epsilon \,\middle|\, \mathcal{Y}_s^\epsilon \right] \right|^2 ds.\end{aligned}$$

Applications of Jensen's inequality, the Cauchy-Schwarz inequality, the tower property of conditional expectation, Lemmas 4.4.8 and 4.4.3 then give the estimate,

$$\begin{aligned}&\mathbb{E}_{\mathbb{Q}} \int_t^{t+\delta} \left| \mathbb{E}_{\mathbb{P}^\epsilon} \left[\mathbb{E}_{\mathbb{P}^\epsilon} \left[\psi(x, \widehat{Z}_s^{\epsilon,x;(t,z)}) \,\middle|\, (x,z) = (X_t^\epsilon, Z_t^\epsilon) \right] \widetilde{D}_t^\epsilon \,\middle|\, \mathcal{Y}_s^\epsilon \right] \right|^2 ds \\ &\lesssim \int_t^{t+\delta} \mathbb{E}_{\mathbb{P}^\epsilon} \left[\left| \mathbb{E}_{\mathbb{P}^\epsilon} \left[\psi(x, \widehat{Z}_s^{\epsilon,x;(t,z)}) \,\middle|\, (x,z) = (X_t^\epsilon, Z_t^\epsilon) \right] \right|^8 \right]^{1/4} ds = \int_t^{t+\delta} \mathbb{E}_{\mathbb{P}^\epsilon} \left[\left| T^{F,x}_{(s-t)/\epsilon^2}(\psi(X_t^\epsilon, \cdot))(Z_t^\epsilon) \right|^8 \right]^{1/4} ds \\ &= \epsilon^2 \int_0^{\delta/\epsilon^2} \mathbb{E}_{\mathbb{P}^\epsilon} \left[\left| T^{F,x}_u(\psi(X_t^\epsilon, \cdot))(Z_t^\epsilon) \right|^8 \right]^{1/4} du \le \epsilon^2 \int_0^{\infty} \mathbb{E}_{\mathbb{P}^\epsilon} \left[\left| T^{F,x}_u(\psi(X_t^\epsilon, \cdot))(Z_t^\epsilon) \right|^8 \right]^{1/4} du \\ &\lesssim \epsilon^2 \left(1 + \mathbb{E}_{\mathbb{P}^\epsilon} \left[|Z_t^\epsilon|^q \right] \right)^{1/4} \lesssim \epsilon^2 \left(1 + \mathbb{E}_{\mathbb{Q}} \left[|Z_0^\epsilon|^{q'} \right] \right)^{1/4} \lesssim \epsilon^2. \quad (4.5.20)\end{aligned}$$

Collecting all our bounds for Eq. 4.5.14, that is Eqs. 4.5.16, 4.5.17, 4.5.19, and 4.5.20, and accounting for the discretization of the time integral into N segments, which results in T/δ times the estimates, we have

$$\mathbb{E}_{\mathbb{Q}} \sup_{t \le T} \left| \int_0^t \langle \rho_s^\epsilon(\psi), dY_s^\epsilon \rangle \right|^2 \lesssim (\epsilon^8 + \delta^4(1+\epsilon^8))^{1/4} + \delta + \mathfrak{F}(\epsilon, \delta)^{1/4} + \frac{\epsilon^2}{\delta}. \quad (4.5.21)$$

If we choose $\delta(\epsilon) = \epsilon^2(-\ln \epsilon)^p$ with $p \in (0, 1/8)$, then $\lim_{\epsilon \to 0^+} \delta(\epsilon) = 0$ (see Lemma A.3.2) , and $\mathfrak{F}(\epsilon, \delta) \to 0$ (see Lemma A.3.3), which completes the proof. □

Lemma 4.5.4

Under either of the assumptions:

a. the coefficients of $\mathcal{G}^\dagger$ and $\bar{h}, \bar{\sigma}$ are $C_b^{2+\alpha}$, for some $\alpha \in (0,1)$, or

b. $\bar{a} + \widetilde{a} \succ 0$ uniformly in x and the coefficients of $\mathcal{G}^\dagger$ and $\bar{h}, \bar{\sigma}$ are C_b^α, for some $\alpha \in (0,1)$,

the finite signed Borel measure-valued process ζ, has the unique solution $\zeta_t = 0$, $\mathbb{Q}$-a.s. $\forall t \in [0,T]$.

Proof. Our objective is simply to show that

$$\zeta_t(\varphi) = \int_0^t \zeta_s(\mathcal{G}^\dagger \varphi) ds + \int_0^t \langle \zeta_s(\varphi \bar{h} + \alpha \bar{\sigma}^* \nabla_x \varphi), dY_s \rangle, \quad \zeta_0(\varphi) = 0,$$

is a Zakai equation, since uniqueness then follows from [Roz91, Theorem 3.1, p.454].

Let X^0 be the diffusion process with infinitesimal generator $\mathcal{G}^\dagger$. In particular, consider the following system of equations,

$$\begin{aligned} dX_t^0 &= \left[\bar{b}(X_t^0) + \widetilde{b}(X_t^0)\right] dt + \widetilde{a}^{1/2}(X_t^0) d\widetilde{W}_t + (\bar{a}(X_t^0) - \bar{\sigma}\bar{\sigma}^*(X_t^0))^{1/2} d\widehat{W}_t + \bar{\sigma}(X_t^0) dW_t, \\ dY_t &= \bar{h}(X_t^0) dt + \alpha dW_t + \gamma dB_t, \end{aligned} \tag{4.3.3}$$

where $\alpha dW_t + \gamma dB_t$ is a standard Brownian motion, $\widetilde{W}, \widehat{W}, W, B$ are independent standard Brownian motions under $\mathbb{Q}$. This system of equations yield a Zakai equation of the desired form after the change of measure given by $D_t = \exp(-\int_0^t \langle \bar{h}(X_s^0), \alpha dW_s + \gamma dB_s \rangle - \frac{1}{2}\int_0^t |\bar{h}(X_s^0)|^2 ds)$ is performed. □

Theorem 4.5.1

Assume that f and g satisfy H_f and H_g, that b_{I} is centered with respect to $\mu_\infty(x)$ for each x and that $\mathbb{Q}_{(X_0^\epsilon, Z_0^\epsilon)}$ has finite moments of every order. Additionally, assume either:

a. $H^{4,2+\alpha}$ holds for $\alpha \in (0,1)$; for each z, $b(\cdot, z), \sigma(\cdot, z) \in C^3$, and $b_{\mathrm{I}}(\cdot, z) \in C^4$; that b and b_{I} are Lipschitz in z, and σ is globally Lipschitz in z; that $b, b_{\mathrm{I}}, \sigma$ satisfy the growth conditions

$$\begin{aligned} |b(x,z)| + |b_{\mathrm{I}}(x,z)| + |\sigma\sigma^*(x,z)| &\leq C(1+|z|)^\beta, \\ \sum_{|k|=1}^{2} \left|D_x^k b(x,z)\right| + \left|D_x^k \sigma\sigma^*(x,z)\right| &\leq C(1+|z|^q), \\ \sum_{|k|=1}^{3} \left|D_x^k b_{\mathrm{I}}(x,z)\right| &\leq C(1+|z|^q), \end{aligned}$$

for some $\beta < -2$ and $q > 0$; that h is bounded in (x,z), $h(\cdot, z) \in C^3$ for each z, and h is globally Lipschitz in z.

b. $\bar{a} + \widetilde{a} \succ 0$ uniformly in x; $H^{2,2+\alpha}$ holds for $\alpha \in (0,1)$; for each z, $b(\cdot, z), b_{\mathrm{I}}(\cdot, z), \sigma(\cdot, z) \in C^2$; that b and b_{I}

are Lipschitz in z, and σ is globally Lipschitz in z; that $b, b_{\mathrm{I}}, \sigma$ satisfy the growth conditions

$$|b(x,z)| + |b_{\mathrm{I}}(x,z)| + |\sigma\sigma^*(x,z)| \leq C(1+|z|)^{\beta},$$
$$\sum_{|k|=1}^{2} \left|D_x^k b(x,z)\right| + \left|D_x^k b_{\mathrm{I}}(x,z)\right| + \left|D_x^k \sigma\sigma^*(x,z)\right| \leq C(1+|z|^q),$$

for some $\beta < -2$ and $q > 0$; h is bounded in (x,z), that h is globally Lipschitz in (x,z). If $a \succ 0$, which implies $\bar{a} + \widetilde{a} \succ 0$, then the Lipschitz condition in z for b, b_{I} can be relaxed to α-Hölder continuity.

Then $\zeta^{\epsilon} = \rho^{\epsilon,x} - \rho^0 \Rightarrow 0$ as $\epsilon \to 0$.

Proof. This follows from Corollary 4.5.1–the existence of weak limits of the probability measures induced on path space by ζ^{ϵ}, Lemma 4.5.3–the characterization of the limit points, and Lemma 4.5.4 on the uniqueness of the limiting evolution equation. □

Lemma 4.5.5

Let ρ^{ϵ} be a solution of Eq. 2.3.3 and ρ^0 a solution of Eq. 4.3.2. Assume that $h, \bar{h}$ and the coefficients of $\mathcal{G}^{\dagger}$ are bounded. If $\rho^{\epsilon,x} - \rho^0 \Rightarrow 0$ as $\epsilon \to 0$, then $\pi^{\epsilon,x} - \pi^0 \Rightarrow 0$.

Proof. Let $\varphi \in C_b^2(\mathbb{R}^m; \mathbb{R})$ and $t \in [0,T]$, then

$$(\pi^{\epsilon,x} - \pi^0)_t(\varphi) = \frac{\rho_t^{\epsilon,x}(\varphi)}{\rho_t^{\epsilon,x}(1)} - \frac{\rho_t^0(\varphi)}{\rho_t^0(1)} = \frac{(\rho^{\epsilon,x} - \rho^0)_t(\varphi)}{\rho_t^{\epsilon,x}(1)} + \pi_t^0(\varphi)\frac{(\rho^0 - \rho^{\epsilon,x})_t(1)}{\rho_t^{\epsilon,x}(1)}.$$

The weak convergence of $(\pi^{\epsilon,x} - \pi^0)_t$ now follows from the estimate

$$\lim_{\delta \to 0} \inf_{\epsilon > 0} \mathbb{Q}\left(\inf_{t \leq T} \rho_t^{\epsilon,x}(1) > \delta\right) = 1,$$

and the fact that φ is bounded and π_t^0 is almost surely equal to a probability measure. □

4.6 Remark on Conditions for the Fast Semigroup

The purpose of this section is to clarify why necessary conditions in this chapter are sometimes at odds with Theorems 2 and 3 by Pardoux and Veretennikov [PV03, p.1171], which are used in this chapter for a number of propositions and theorems listed below. Specifically, in the work by Pardoux and Veretennikov [PV03], the condition in Theorems 2 and 3 are given as $H^{1,2+\alpha}$ (there are actually two scenarios to consider, but in this chapter we only consider one of them, which is the one just quoted). In particular, only one continuous

derivative in the x-component is ever needed in the coefficients f and g to be able to take $k \geq 1$ derivatives of the new function under the semigroup $T^{F,x}(\varphi)$, where $\varphi \in C^k$ for instance. Because the Poisson solution of [PV03, Theorem 3, p.1171] is proven based on Theorem 2, the same condition of $H^{1,2+\alpha}$ shows up there, even if $k \geq 1$ derivatives of the Poisson solution are desired. A counter example as to why this condition is insufficient is given next.

4.6.1 Counter Example

Let $g(x,z) = g(x)$ depend only on x and let $f(x,z) = -z$. Then the fast process is

$$dZ_t^x = -Z_t^x dt + g(x)dB_t,$$

and therefore Z^x is an Ornstein-Uhlenbeck process (in particular Gaussian), and hence satisfies the recurrence condition for [PV03, p.1171]. We can choose g to satisfy the uniform ellipticity condition as well, assume this to be true. If $Z_0^x = z$, then

$$Z_t^x = e^{-t}z + \int_0^t e^{-(t-s)}g(x)dB_s \sim \mathcal{N}\left(e^{-t}z, \frac{g(x)^2}{2}(1-e^{-2t})\right),$$

and thus the transition density at time t in z, having started from (x,z') at the initial time is

$$p_t(z,z';x) = r\left(\frac{g(x)^2}{2}(1-e^{-2t}), z' - e^{-t}z\right),$$

where $r(s,y)$ is the Gaussian density with variance s, evaluated in y. Consider now the test function $\psi(x,z) = \cos(z)$, which is infinitely smooth in x (and in z). Note that for $Y \sim \mathcal{N}(\mu, g^2)$ we have

$$\mathbb{E}[\cos(Y)] = \frac{1}{2}\mathbb{E}[e^{iY} + e^{-iY}] = \frac{1}{2}\left(e^{i\mu - \frac{1}{2}g^2} + e^{-i\mu - \frac{1}{2}g^2}\right) = e^{-\frac{1}{2}g^2}\cos(\mu),$$

and therefore the semigroup (notation from [PV03, p.1171]) is

$$p_t(z,\psi;x) = \mathbb{E}_z[\cos(Z_t^x)] = \exp\left(-\frac{1}{2}\frac{g(x)^2}{2}(1-e^{-2t})\right)\cos(e^{-t}z).$$

If $g^2 \notin C^2$, then this function is not C^2 in x.

4.6.2 List of Changes

The condition should be $H^{k,2+\alpha}$, and we use this condition in this chapter instead of the one given by Pardoux and Veretennikov [PV03]. The difference in the requirements of various propositions and theorems are subtle, but listed here for reference:

(i) Theorem 4.4.1, $H^{1,2+\alpha}$ has become $H^{2,2+\alpha}$.

(ii) Theorem 4.4.2, $H^{1,2+\alpha}$ has become $H^{k,2+\alpha}$.

(iii) Lemma 4.4.10, $H^{1,2+\alpha}$ has become $H^{j,2+\alpha}$.

(iv) Theorem 4.5.1, for a.) $H^{3,2+\alpha}$ has become $H^{4,2+\alpha}$. This was a result of needing the third derivative in x of $\widetilde{b}$, which required the fourth derivative in x of the Poisson solution $\mathcal{G}_F^{-1}(b_{\mathrm{I}})$.

A final remark, is that Lemma 4.4.3 is not affected by this, because there we are also using the density result of [PV03, Theorem 1, p.1170], which is correct and requires stronger conditions than [PV03, Theorem 2, p.1171]. This is also the reason why necessary conditions in Chapter 3 were not affected (also because that chapter did not require the solution of the Poisson equations and already had stronger conditions for the uniqueness of the Zakai equation).

Chapter 5

Standard and Optimal Proposal Particle Methods for Multiple Timescale, Correlated Systems

From this chapter onwards, we turn our attention to numerical methods for solution of the filtering equation. Unlike the theory of Chapters 2, 3, and 4, where a continuous time observation process was considered, in this chapter and the next, we are interested in the discrete time observation sequence scenario. We still consider the signal to be a continuous time process. This format of filtering problem is presented in Section 5.1. It is a natural choice for many problems, including those in the geosciences.

In this chapter and the next, we are driven by current issues in estimation for the geosciences, where models are chaotic and of very high dimension; at the very largest scales, they can be of the order $\mathcal{O}(10^9)$ degrees of freedom and require assimilation of $\mathcal{O}(10^7)$ observations during a single day. The models naturally have multiple timescales and spatial scales that can be considered, as well as symmetry in the modeling of the dynamics and possibility for correlation in the noise between the model and the observation process.

A trend in the geosciences is that the continual increase in the resolution of the models has begun to necessitate the need for modeling convective processes [Yan+18]. This has raised new issues on the assimilation side because most assimilation implementations in weather centers are based on Kalman updates or a smoothing method called 4D-var. Although these approaches may allow for nonlinear dynamics, they assume linear Gaussian updates for assimilating the observations. The new regime in which the geosciences is entering is one that is inherently nonlinear, non-Gaussian, and may require assimilation techniques more flexible for representing multimodal distributions [Car+18].

Particle filters, also known as sequential Monte Carlo methods, are general and theoretically could fill this need. Though it is known that particle filters suffer from degeneracy conditions, in particular in high dimensions [Sny+08; SBM15]. Because of the promising capabilities of particle filters, a great deal of research has been and is currently being performed on improvements to the approach [Lee+19]. This chapter and the next aim to provide several useful frameworks and algorithms that may be extended with further research to aid in this ever challenging problem of efficient and accurate estimation of key state variables in the geosciences. The methods discussed are general, and can be applied to areas outside of the geosciences–we

simply use this field of science as motivation. We focus solely on particle filters because of their generality and potential. Some positive results beyond that in research are already being attained, with particle filters starting to take a role in actual numerical weather prediction [Pot16; PWR19].

We start this chapter by providing a background on Bayesian filtering for the continuous time signal, discrete time observation case. This is done in Section 5.1 and finishes with a standard sequential importance sampling particle filter algorithm. We then turn to the consideration of filtering a multiple timescale system in Section 5.2. To do so, we first introduce the heterogenous multiscale method (HMM) for integrating multiple timescale processes. We then introduce a multiple timescale model that will be useful in demonstrating the methods. In the next section we introduce the homogenized hybrid particle filter (HHPF), which uses the HMM for filtering multiple timescale systems. We then provide remarks on alternative approaches for efficient filtering of multiple timescale systems. Results from Section 5.2 appeared in [BN19b], and Section 5.3.1 contains results from [BN19a]. Section 5.4 then discusses the handling of the correlated noise scenario; these results appear in [Bee+18]. We finish with Section 5.5, which presents particle methods that aim to addresses the issue of particle degeneracy in high dimensional problems by guiding the particles to more representative state values; the results of this section appear in [Yeo+20]. The ensemble of these methods are more likely to lose their diversity and therefore may not be representative of the actual posterior distribution. An attempt at mitigating this problem is then made by using a tempering scheme on the likelihood update procedure.

5.1 Bayesian Filtering

We consider the following formulation for the problem of data assimilation for a system with a continuous time stochastic signal process, a discrete time noisy observation process, and nonlinear coefficients,

$$dX_t = b(X_t)dt + \sigma(X_t)dW_t, \qquad X_0 = x \in \mathbb{R}^m, \tag{5.1.1}$$

$$Y_{t_k} = h(X_{t_k}) + \xi_{t_k}, \qquad Y_0 = 0 \in \mathbb{R}^d. \tag{5.1.2}$$

X is the unobserved signal process, W a standard Brownian motion taking values in $\mathbb{R}^m$, $(Y_{t_k})_{k\in\mathbb{N}}$ a sequence of observations that are available at increasing times (t_k), and $(\xi_{t_k})_{k\in\mathbb{N}}$ a sequence of independent Gaussian random variables with zero mean and covariance $R \in \mathbb{R}^{d\times d}$. It is assumed that W and ξ are independent. X takes values in $\mathbb{R}^m$ with deterministic initial condition x, b is referred to as the drift coefficient and σ the dispersion coefficient. Y takes values in $\mathbb{R}^d$ with deterministic initial condition zero and h is known as the sensor function. For conciseness, we will simply use the subscript k in lieu of t_k for the remainder of the

chapter (and also in Chapter 6).

Our goal in this chapter is to compute the posterior distribution, $\pi_{k|k}$, for each time t_k. Here $\pi_{k|k}$ is the condition distribution of X_k given $\mathcal{Y}_k$, the collection of all observations up to and including Y_k. To clarify notation, if we wrote $\pi_{j|k}$, this would correspond to the posterior distribution of X_j given $\mathcal{Y}_k$. Knowledge of the posterior distribution allows us to calculate any statistic of X_k,

$$\pi_{k|k}(\varphi) = \mathbb{E}\left[\varphi(X_k) \mid \mathcal{Y}_k\right], \tag{5.1.3}$$

where φ is a statistic of interest, with a common interest being simply the indicator function. When we want to emphasis the observation history that we are conditioning on, we will use the following notation for the posterior distribution,

$$\pi_{k|k}(\varphi) = \pi_k(\varphi|\mathcal{Y}_k).$$

Given the posterior distribution at t_k, one can define the prior distribution at t_{k+1} from the Chapman-Kolmogorov relation,

$$\pi_{k+1|k}(x|\mathcal{Y}) \equiv \int_{\mathbb{R}^m} \rho_{k+1|k}(x|x')\pi_{k|k}(dx'|\mathcal{Y}),$$

where ρ is the probability transition function from t_k to t_{k+1}.

The update of the posterior at time t_{k+1} can now be accomplished by Bayes' formula,

$$\pi_{k+1}(x|\mathcal{Y}_{k+1}) = \frac{f_{k+1}(Y_{k+1}|x)\pi_{k+1}(x|\mathcal{Y}_k)}{\int_{\mathbb{R}^m} f_{k+1}(Y_{k+1}|x)\pi_{k+1}(dx|\mathcal{Y}_k)}, \tag{5.1.4}$$

where $f_{k+1}(Y_{k+1}|x)$ is the likelihood at time t_{k+1} of observing Y_{k+1} given the state x. Lastly, because we assume the independence of the sequence (ξ_k), (Y_k) is a Markov process and it suffices to consider just the latest observation Y_k instead of the entire history $\mathcal{Y}_k$ for the prior and posterior distributions.

5.1.1 Sequential Importance Sampling

Ultimately, we would like to be able to sample from $\pi_{k|k}$ at each time t_k to calculate statistics as in Eq. 5.1.3. Although we cannot do this directly, we can use the principle of importance sampling to approximate this action.

In importance sampling, we consider the problem where π is a distribution that is difficult to sample

from, yet proportional to a distribution, ψ, that is easy to evaluate, $\pi \propto \psi$. We then assume that there exists a distribution q, called the *importance* or *proposal distribution*, that is easy to sample from and is absolutely continuous with respect to π, denoted as $q \ll \pi$. Being absolutely continuous with respect to another distribution implies that there is a density representation of q with respect to π. Hence, we define the *importance weights* $w \equiv \psi/q$, so that $\pi \propto wq$.

The use of sequential importance sampling is common in particle filtering approaches, which we follow in Section 5.1.2. The technique is also useful for more advanced methods that aim to approximate the optimal proposal, such as the approach presented in Section 5.5.1.

5.1.2 The Sequential Importance Sampling Particle Filter (PF)

Recall Eq. 5.1.4, but consider writing the update equation without explicit representation of the normalizer,

$$\pi_{k+1}(x|\mathcal{Y}_{k+1}) \propto f_{k+1}(Y_{k+1}|x)\pi_{k+1}(x|\mathcal{Y}_k).$$

Then applying the principle of importance sampling in this setting, we have

$$\pi_{k+1}(x|\mathcal{Y}_{k+1}) \propto w_k q_{k+1}(x),$$

where

$$w_k = \frac{f_{k+1}(Y_{k+1}|x)\pi_{k+1}(x|\mathcal{Y}_k)}{q_{k+1}(x)}.$$

Now we can approximate the posterior distribution as a weighted collection of Dirac distributions. In particular, consider an ensemble of independent particles indexed by a set $\mathcal{A} = \{1, \ldots, N\}$, $N \in \mathbb{N}$, with the particles evolving according to the signal process in Eq. 5.1.1. Each particle represents a stochastic realization of the signal process. We denote the set of values that the particles take in the signal state space at time t_k as $\mathcal{A}_k^x$ and the values by individual particles with similarly notation $\mathcal{A}_k^x(j)$ for $j \in \mathcal{A}$. The probability of each particle representing the true signal process at time t is given by the set of time-varying weights $\{w_t^j\}_{j\in\mathcal{A}}$. Then the posterior distribution is approximated at time t_k by a weighted sum of Dirac distributions,

$$\pi_k(\xi|Y_k) = \sum_{j\in\mathcal{A}} w_k^j \delta_k^j(\xi),$$

where δ_k^j has support on the singleton given by $\mathcal{A}_k^x(j)$, and $w_k^j \in [0,1]$ with $\sum_{j\in\mathcal{A}} w_k^j = 1$ for each t_k.

For convenience, we now make a common choice for the importance distribution, setting $q_{k+1}(x)$ equal to the prior distribution. Then given a posterior distribution $\pi_k(x|Y_k)$ at time t_k, the importance (prior) distribution is simply

$$q_{k+1}(x) = \pi_{k+1}(x|Y_k) = \sum_{j\in\mathcal{A}} w_k^j \delta_{k+1}^j(x).$$

And the posterior distribution at t_{k+1} is,

$$\pi_{k+1}(x|Y_{k+1}) = \sum_{j\in\mathcal{A}} w_{k+1}^j \delta_{k+1}^j(x) \propto \sum_{j\in\mathcal{A}} w_k^j f_{k+1}(Y_{k+1}|x)\delta_{k+1}^j(x).$$

Therefore, when new observation data is available, the weights are updated according to

$$w_{k+1}^j \propto w_k^j f_{k+1}(Y_{k+1}|\mathcal{A}_{k+1}^x(j)).$$

Since $\sum_{j\in\mathcal{A}} w_k^j = 1$ for each t_k, these new weights must be normalized. Note that in the case where our observation is a Gaussian process, as defined by Eq. 5.1.2, then denoting $\Delta Y_{k+1}(x) \equiv Y_{k+1} - h(x)$, the weights are updated according to,

$$w_{k+1}^j(x) \propto w_k^j \exp\left(-\frac{1}{2}\Delta Y_{k+1}(x)^T R^{-1} \Delta Y_{k+1}(x))\right). \tag{5.1.5}$$

Although we consider the discrete time observation case in this dissertation, one can easily show that re-weighting the particles in the continuous time case with a Radon-Nikodym derivative (e.g., $\widetilde{D}$ from Section 2.2) that is discretized in time (due to numerical purposes), results in the same update of the weights as Eq. 5.1.5 (see for instance [Yeo17, p.35]).

Application of particle filters to high dimensional, stiff, or chaotic systems may suffer from divergence or degeneracy conditions. The main issue of degeneracy, also going by the name of particle collapse, is characterized by a situation when one particle has nearly all the weight after a small number of assimilations. That is, for one $j \in \mathcal{A}$, $w_k^j \simeq 1$ and $w_k^i \ll 1$ for $\mathcal{A} \ni i \neq j$. The a priori selection of an optimal proposal distribution would be helpful in addressing this problem, but often not possible. A technique that can provide a remedy is *resampling*. Intuitively, this just means that particles with large weights are multiplied and those with small weights are eliminated. We refer the reader to the literature [GSS93; Dou98; DM00; Aru+02] for more details regarding resampling, importance sampling and other concepts associated with basic particle filters. In this dissertation, we will use the universal (systematic) resampling technique (see

for instance [Aru+02, p.180]). The resampling technique is used when an approximation to the *effective sampling size* $N_{\text{eff,k}} \approx 1/\sum_{j\in\mathcal{A}_k}(w_k^j)^2$, introduced by Bergman [Ber99] and Liu et al. [LC98], falls below some user specified threshold. If this occurs after updating the weights, then a resampling process occurs before normalization.

In summary, our standard particle filter (PF) algorithm, that will be used in our numerical simulations has the following recursive structure:

Particle Filter (PF) Algorithm

---

1. At time t_k, set $w_k^j = 1/N$, $\forall j \in \mathcal{A}$ and

$$\pi_k(x|Y_k) = \sum_{j\in\mathcal{A}} w_k^j \delta_k^j(x).$$

2. Generate the prior at t_{k+1} by advecting each particle under the signal dynamics given by Eq. 5.1.1,

$$\pi_{k+1}(x|Y_k) = \sum_{j\in\mathcal{A}} w_k^j \delta_{k+1}^j(x).$$

3. Update the particle weights according to

$$w_{k+1}^j \propto w_k^j f_{k+1}(Y_{k+1}|\mathcal{A}_{k+1}^x(j)).$$

4a. If $N_{\text{eff,k}}$ is below a threshold (indicating particle degeneracy), then apply universal resampling and set

$$w_{k+1}^j = 1/N, \quad \forall j \in \mathcal{A}.$$

4b. Otherwise, let $|w|_2$ be the l_2 norm of the weights and re-normalize each

$$w_{k+1}^j \leftarrow w_{k+1}^j/|w|_2.$$

5.2 Multiple Timescales

In this section, we consider how to leverage the theoretical results of Chapters 3 and 4 in a real application. Recall our multiple timescale equations for the signal process from Chapter 3 (we make comments later in

the section regarding the handling of the intermediate timescale case),

$$dX_t^\epsilon = b(X_t^\epsilon, Z_t^\epsilon)dt + \sigma(X_t^\epsilon, Z_t^\epsilon)dW_t, \tag{3.0.1}$$
$$dZ_t^\epsilon = \frac{1}{\epsilon} f(X_t^\epsilon, Z_t^\epsilon)dt + \frac{1}{\sqrt{\epsilon}} g(X_t^\epsilon, Z_t^\epsilon)dV_t,$$

where $\epsilon \ll 1$ is the timescale separation parameter (note the difference in scaling parameter compared to Chapter 3, that we will use throughout the rest of the dissertation). The main computational difficulty with numerical filtering algorithms that solve for π_t^ϵ in the multiple timescale case, is that the integration step size during the predictor step of the filtering algorithm needs to be less than the timescale separation parameter, $\epsilon \ll 1$, for numerical stability. In the context of the problems in Chapters 3 and 4, where we are only interested in resolving functions of the slow states X_t^ϵ, and when for each fixed x, $Z_t^{\epsilon,x}$ is ergodic and converges rapidly to its stationary distribution, then numerical algorithms have been developed to reduce the computational complexity of simulating the slow signal dynamics with various tradeoffs in accuracy. The heterogenous multiscale method (HMM) [EE03; E+07; FV04] outlines an algorithm for efficient multiscale integration leveraging stochastic averaging. Analysis proving weak and strong convergence theorems for the algorithm are provided by E et al. [ELV05]. In contrast, deterministic and stochastic parameterization approaches [Wil05; CV08] using autoregressive processes and Markov chain models respectively, have been used to replace the fast scales when the structure of the signal dynamics allow, resulting in a simpler model for the slow signal.

In the filtering context, the HMM has been leveraged in ensemble based filters. In particular the use of HMM in particle filtering methods is outlined and demonstrated by a number of authors [PNY11; YPN11; Lin+12] and below in Section 5.3, with the ensemble Transform Kalman filter [BEM01] by Harlim [Har11], as well as Kang and Harlim [KH12] for the ensemble Kalman filter. The problem of how to improve the updated representation of the fast scales in the HMM when the fast scales are not mixing or the scale separation is not large have been handled by Harlim [Har11] and Kang and Harlim [KH12] with a pseudo-observation and solution of an inverse problem.

In this section, we assume sufficient timescale separation and that $Z_t^{\epsilon,x}$ is ergodic and converges exponentially fast to its stationary distribution. Based on these assumptions, we make use of the results in Chapters 3 and 4 that provide the theoretical justification for the HHPF algorithm presented in Section 5.3. In Section 5.3.1 we explain how specific structure in multiple scale problems can be potentially exploited to reduce online computational complexity while maintaining a fixed accuracy of filtering on the slow states.

5.2.1 The Heterogenous Multiscale Method

We define the necessary notation and briefly explain HMM in this section. The reader is referred to the work by E et al. [ELV05] for additional details. The numerical motivation for HMM, is that the stability of simulating the signal process $(X_t^\epsilon, Z_t^\epsilon)$ of Eq. 3.0.1 requires an integration step size, δ_m, which must be smaller than ϵ. The key idea of HMM is to integrate (x, Z_t^ϵ), that is the fast process with fixed $X_t^\epsilon = x$, with an integration step size $\delta_m < \epsilon$ for a small period of time $\Delta_m > \delta_m$ and with a finite number of realizations $\mathcal{R} \in \mathbb{N}$. We call Δ_m the fast-macro step size. From this simulation, a transition density $\mu_{\Delta_m}(z; x, z_0)$ is constructed and should be close to $\mu_\infty(z; x)$. Then the averaged coefficients of Section 3.2 can be approximated, so that filtering can be applied to the evolution equation governing the filtering process–the Kushner-Stratonovich or Zakai equation. Since $\mu_\infty(z; x)$ is dependent on x, the averaged coefficients must be recalculated, but on larger time-scales then Δ_m. We denote $\Delta_M \geq \Delta_m$, the slow-macro step size, which is the interval of time upon which the transition density $\mu_{\Delta_m}(z; x, z_0)$ and hence coefficients $\bar{b}, \bar{a}, \bar{\sigma}, \bar{h}$ are assumed to hold accurately. During this time-interval a slow-integration step size $\delta_M > \delta_m$ is used to integrate the averaged SDE with generator $\overline{\mathcal{G}_S}$.

In the case that HMM is to be applied to the signal model with intermediate timescale forcing (e.g., Eq. 4.0.1), then the averaged SDE has generator $\mathcal{G}^\dagger = \overline{\mathcal{G}_S} + \widetilde{\mathcal{G}}$. To get the drift $\widetilde{b}$, and diffusion $\widetilde{a}$ coefficients of $\widetilde{\mathcal{G}}$, we need the solution of the Poisson equation $\mathcal{G}_F^{-1}(b_{\mathrm{I}})(x, z)$ integrated against the stationary distribution $\mu_\infty(dz; x)$. Solving the Poisson equation with standard numerical methods for PDEs on even a subset of $\mathbb{R}^m \times \mathbb{R}^n$ is not tenable if $m+n$ is greater than even dimension three. Therefore a probabilistic representation is useful. The solution of the Poisson equation on $\mathbb{R}^m \times \mathbb{R}^n$ has the representation

$$\mathcal{G}_F^{-1}(b_{\mathrm{I}})(x, z) = \int_0^\infty \int_{\mathbb{R}^n} b_{\mathrm{I}}(x, z') p_t(dz'; x, z) dt.$$

From the exponential convergence of the transition density $p_t(z'; x, z)$ to the stationary distribution $\mu_\infty(x)$ (or density $p_\infty(z, x)$) and the property that b_{I} is centered with respect to $\mu_\infty(x)$, it is suggestive that the Poisson equation solution could be approximated by integrating b_{I} against the transition density from the initial time up to the final time Δ_m.

5.2.2 The Lorenz 1996 Model

The Lorenz '96 model was originally introduced by Lorenz [Lor95] to mimic multiscale mid-latitude atmospheric dynamics for an unspecified scalar meteorological quantity. A latitude circle is divided into K = 6 sectors,

and each sector is subdivided into J = 9 subsectors, with the following dynamics in each sector:

$$\begin{aligned} dX_t^k &= (X_t^{k-1}(X_t^{k+1} - X_t^{k-2}) - X_t^k + F + \frac{h_x}{J}\sum_{j=1}^{J} Z_t^{k,j})dt \\ dZ_t^{k,j} &= \frac{1}{\epsilon}\left(Z_t^{k,j+1}(Z_t^{k,j-1} - Z_t^{k,j+2}) - Z_t^{k,j} + h_z X_t^k\right)dt \end{aligned} \tag{5.2.1}$$

where $k = 1, \ldots, K$ and $j = 1, \ldots, J$. A visual representation of this model is provided in Figure 5.1. X_t^k represents a slow-scale atmospheric variable at time t in the k-th sector. In this chapter, we use the version of the model by Fatkullin and Vanden-Eijnden [FV04], but with different values for K and J. This version of the model was also used by Kang and Harlim [KH12]. In Eq. 5.2.1, the nonlinear, linear and slow scale effects in the fast dynamics are all of order one. In this setting, Fatkullin and Vanden-Eijnden [FV04] showed that the fast scale dynamics display ergodic properties such that the averaging technique can be used to average out the fast dynamics when we are only interested in the slow dynamics (coarse-grained dynamics). In Eq. 5.2.1, F is a slow-scale forcing, and h_x, h_z are coupling terms.

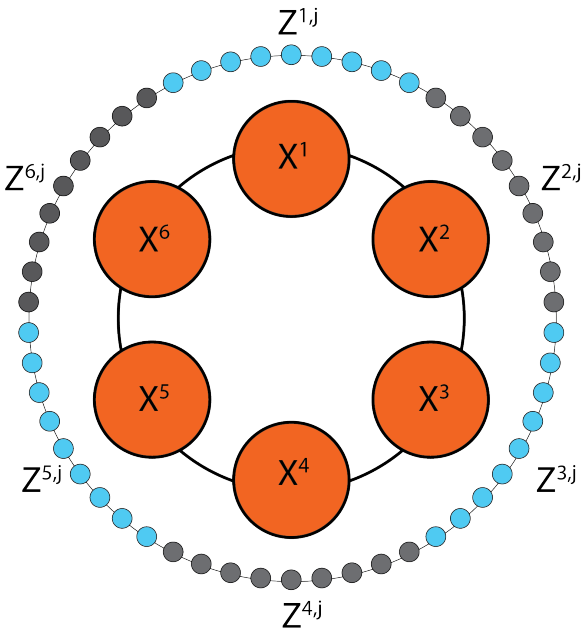

Figure 5.1: A recreation of a similar image by Wilks [Wil05], that provides a visualization of the two timescale Lorenz '96 model.

The dynamics of unresolved modes can be represented by adding forcing in the form of stochastic terms (see for example [MTV01; MTV03]). The use of stochastic terms to represent nonlinear self-interaction effects at short timescales in the unresolved modes is appropriate if we are only interested in the coarse-grained dynamics occurring in the long, slow timescale. This is called stochastic consistency by Majda et al. [MTV03].

Considering Eq. 5.2.1, where only quadratic nonlinearity is present in the fast process, the motivation behind adding stochastic forcing is to model higher-order self-interaction effects.

Particle filtering is improved if there is some noise in the dynamics, and a stochastic signal will be required for the nudged particle method mention in Section 5.5.1. For these reasons, as well as for the reason of stochastic consistency, let us write Eq. 5.2.1 in a standard form with additive stochastic forcing,

$$\begin{aligned} dX_t^\epsilon &= b(X_t^\epsilon, Z_t^\epsilon)dt + \sigma_x dW_t, & X_t^\epsilon &\in \mathbb{R}^6, \\ dZ_t^\epsilon &= \frac{1}{\epsilon} f(X_t^\epsilon, Z_t^\epsilon)dt + \frac{1}{\sqrt{\epsilon}}\sigma_z dV_t, & Z_t^\epsilon &\in \mathbb{R}^{54}, \end{aligned} \tag{5.2.2}$$

and consider discrete time, sparse observations,

$$Y_{t_k}^\epsilon = X_{t_k}^\epsilon + U_{t_k}, \quad \text{and} \quad U_{t_k} \sim \mathcal{N}(0_{6\times 1}, \Delta t\, \mathrm{Id}._{6\times 6}).$$

Following the work of Beeson and Namachchivaya [BN19b], we now fix our model parameters, for the purpose of understanding the behavior of Eq. 5.2.1 and making comparisons with the numerical solution of the averaged dynamics. Let the simulation parameters be: $\epsilon =$ 1E-2, $F = 10$, $(h_x, h_z) = (-1, 1)$, σ_x, σ_z sparse square matrices with 1 along the diagonal and 0.05 on the first two sub and super-diagonals, $K = 6$ and $J = 9$. Hence $(X_t, Z_t) \in \mathbb{R}^6 \times \mathbb{R}^{54}$ and the averaged dynamics have $X_t^0 \in \mathbb{R}^6$, so a state space dimension a 10th of the original. Figure 5.2 illustrates the behavior of a generic slow state X_t^1 (shown in orange), the fast states in the 1st sector, that is $Z_t^{1,1}, \ldots, Z_t^{1,9}$ (shown in gray), and the fast scale forcing that enters Eq. 5.2.1 for the X_t^1 component (shown in light blue); the fast scale forcing is $(h_x/J)\sum_{j=1}^J Z_t^{1,j}$.

Due to the symmetry of the model, it is sufficient to look at one sector to get a glimpse of the qualitative behavior of the dynamics. According to Lorenz [Lor95], the time scale used here, $T = 20$, is approximately equivalent to mimicking 100 days in 'real' time. The solution shown in Figure 5.2 was produced by integrating the initial conditions with an Euler-Maruyama integration scheme with a step size of $\delta =$ 1E-4.

The parameters we use in this chapter are slightly different from those Fatkullin and Vanden-Eijnden [FV04]. Therefore we should confirm the applicability of HMM to our problem. We do this numerically, setting the relevant simulation parameters to $\mathcal{R} = 1$, $\delta_m =$ 1E-4, $\delta_M =$ 1E-2, $\Delta_m = 5\delta_m$, and $\Delta_M = 10\delta_M$. With these parameters, and the same initial conditions as used in Figure 5.2, we get the result shown in Figure 5.3 when integrating with HMM using the Euler-Maruyama integration schemes for both the fast and slow-scale processes. After some time, the qualitative behavior seen in Figure 5.2 and Figure 5.3 are quite different, but Figure 5.4 and Figure 5.5 show us that on shorter time scales (the first 0.8 time units of the simulations), the dynamics of the numerically averaged X_t^0 are indeed near the original X_t.

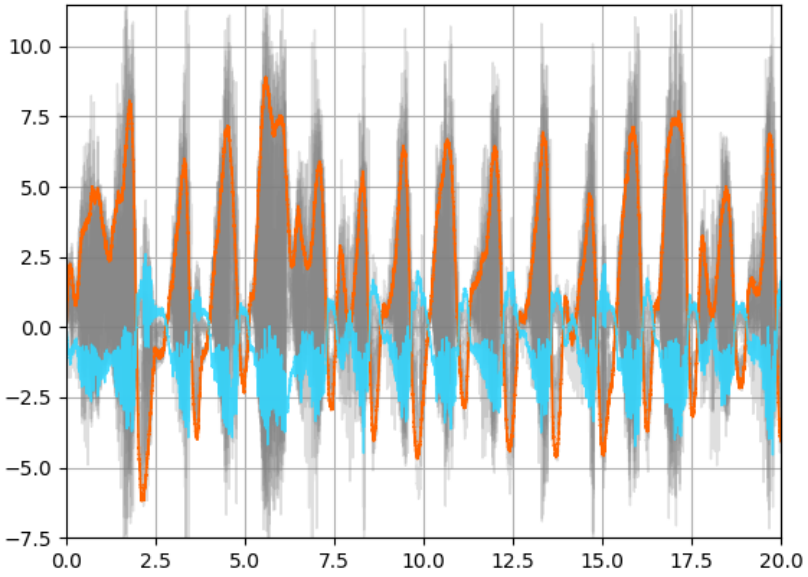

Figure 5.2: Direct numerical solution of the Lorenz '96 model: X_t^1 in orange, $Z_t^{1,1} \ldots, Z_t^{1,9}$ in gray, and the fast scale forcing $(h_x/J)\sum_{j=1}^{J} Z_t^{1,j}$ on X_t^1 in light blue.

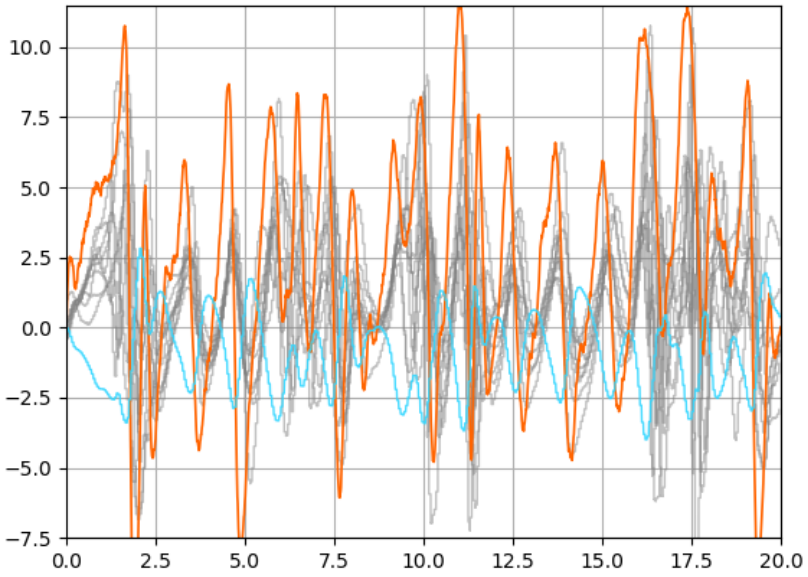

Figure 5.3: An HMM solution of the Lorenz '96 model: $X_t^{0,1}$ in orange, $\mathcal{R} = 1$ realizations of $Z_t^{1,1} \ldots, Z_t^{1,9}$ with fixed X_t^0 in gray, and the averaged fast scale forcing on $X_t^{0,1}$ in light blue.

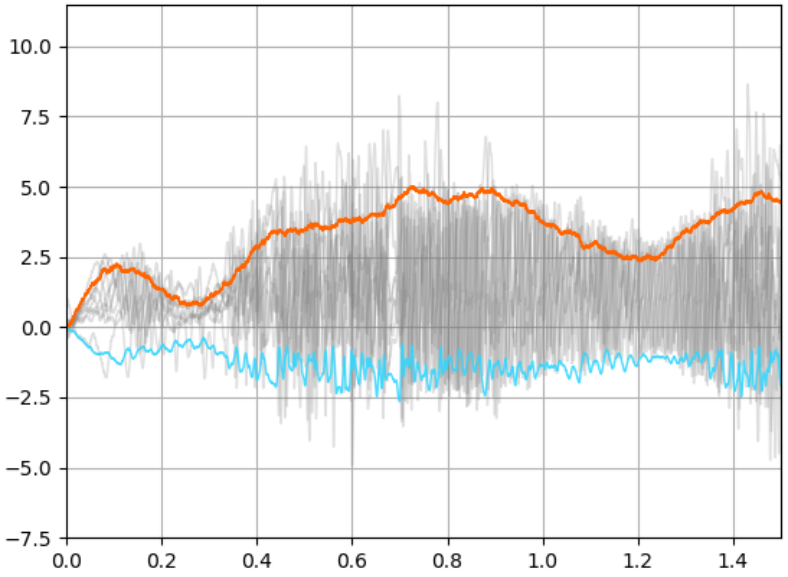

Figure 5.4: Direct numerical solution of the Lorenz '96 model: X_t^1 in orange, $Z_t^{1,1} \ldots, Z_t^{1,9}$ in gray, and the fast scale forcing $(h_x/J)\sum_{j=1}^{J} Z_t^{1,j}$ on X_t^1 in light blue.

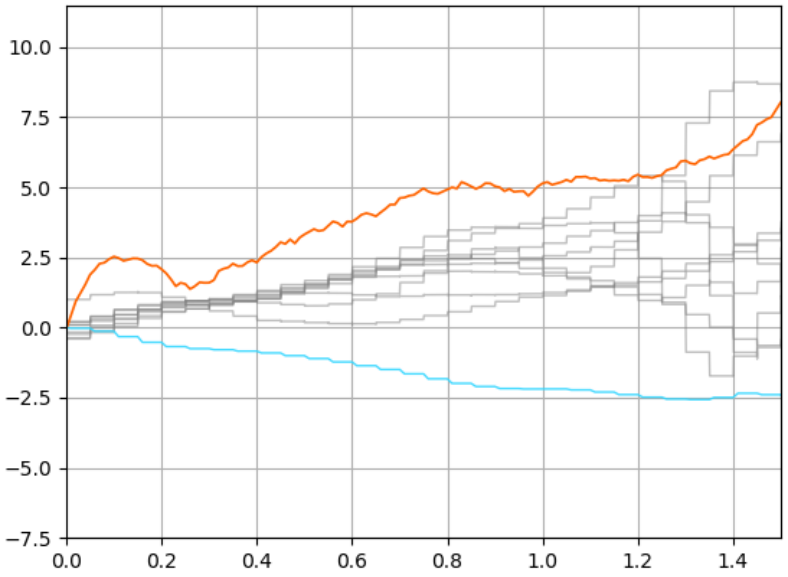

Figure 5.5: An HMM solution for the Lorenz '96 model: $X_t^{0,1}$ in orange, $\mathcal{R} = 1$ realizations of $Z_t^{1,1} \ldots, Z_t^{1,9}$ with fixed X_t^0 in gray, and the averaged fast scale forcing on $X_t^{0,1}$ in light blue.

The fact that the numerically averaged solution is close on shorter time scales is sufficient in the filtering context of sparse in-time observations if the observations occur before the X_t and X_t^0 solutions separate too much. For instance, in Sections 5.3.2 and 5.4 we will assume that the observations come every $\Delta t = 10\delta_M$, which is $\Delta t = 0.1$ for our parameters. The solutions X_t and X_t^0 are certainly visually close in Figure 5.4 and Figure 5.5 over the time interval $[0, 0.1]$. The update step at $t = 0.1$ in filtering will then improve the estimate of X_t at time $t = 0.1$ and therefore limit the separation that may have occurred over the interval $[0, 0.1]$.

A more rigorous numerical verification that HMM is appropriate for our model comes from two investigations: 1. comparing the effective (stationary) density associated with X_t^0 with the x-marginal of the transition density of X_t^ϵ with our time scale separation parameter $\epsilon =$ 1E-2, and 2. showing that the (x, Z_t^ϵ) process converges exponentially to it's invariant distribution, regardless of initial condition on $Z_t^\epsilon = z \in \mathbb{R}^n$. Technically, we should see this last result occur within a time interval of length Δ_m, which implies that the application of HMM is well founded for our choice of parameter. Again, in the context of filtering, we are able to relax this last requirement and still effectively filter.

For the first investigation, Figure 5.6 provides a numerical confirmation that Eq. 5.2.1 with $\epsilon =$ 1E-2 produces X_t^ϵ with a marginal density close to the effective density for X_t^0. Specifically, Figure 5.6 compares the marginal density of the first slow component X_t^1 for $\epsilon =$ 1E-2 and 1E-3, which are nearly the same, implying that the statistics for the dynamics of X_t^ϵ with $\epsilon =$ 1E-2 is close to X_t^0. Because of the symmetry of the signal model of Eq. 5.2.1, all slow components X_t^k have the same marginal density, hence comparing against only the X_t^1 marginal density is appropriate.

In Figure 5.7 we show the marginal density of the first component of the fast process for four different simulations. For this analysis, we simulate the full model from a randomly generated initial condition to eliminate transient effects. Then we fix the slow process $X_t^\epsilon = x$ and simulate the fast process for randomly generated Z_0^ϵ, where each component of Z_0^ϵ is chosen according to $\mathcal{N}(0, 1)$; normal distribution with mean zero and variance one. Figure 5.7 shows the convergence of the transition densities $\mu_{15\cdot\Delta_m}(z; X_0^\epsilon = x, Z_0^\epsilon)$ for the first component of Z_t^ϵ; showing that on a macro step of $15\Delta_m$ we have sufficient convergence from most initial states of Z_0^ϵ. When using HMM in our estimation implementation of HHPF, we can in fact relax the condition for convergence of the transition densities and still effectively filter. Hence why we will use a macro step of only Δ_m in Sections 5.3.2 and 5.4.

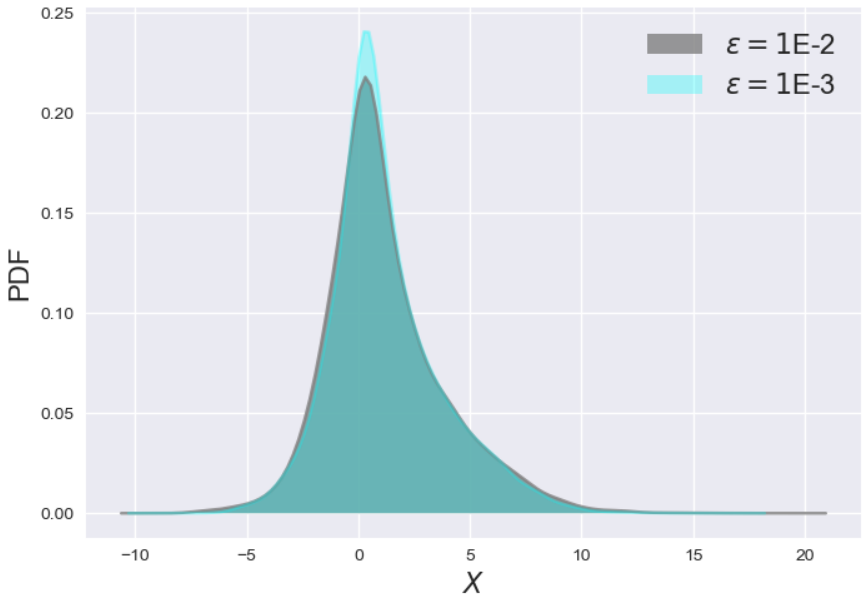

Figure 5.6: Simulation of Eq. 5.2.2. Shown in gray is the X_t^1 (i.e., first component) marginal density when $\epsilon =$ 1E-2 and similarly in light blue the X_t^1 marginal density when $\epsilon =$ 1E-3.

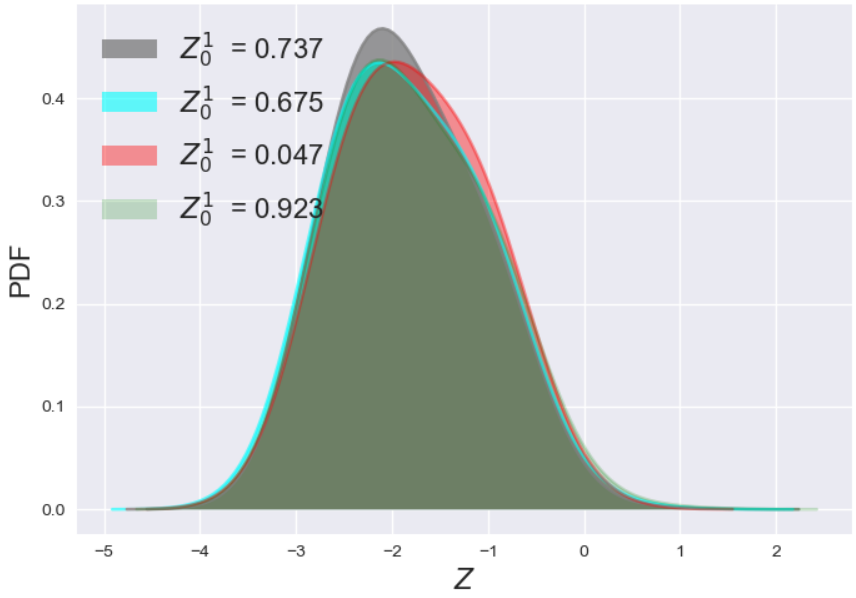

Figure 5.7: Transition densities of the first component of Z_t^ϵ: $\mu_{15\cdot\Delta_m}(z; X_0^\epsilon = x, Z_0^\epsilon)$, for randomly generated Z_0^ϵ; the first component of Z_0^ϵ is shown as Z_0^1 in the legend for four different simulations. $X_0^\epsilon = x$ is a fixed slow state.

5.3 Homogenized Hybrid Particle Filter (HHPF)

HHPF differs from regular particle filtering in the sense that particles are used to represent X^0 instead of (X^ϵ, Z^ϵ). Hence the particles and their weights approximate the reduced order filter π_t^0. The numerical integration of the particles $\mathcal{A}_t^x(j)$ under the SDE with generator $\overline{\mathcal{G}_S}$ requires multiscale integration techniques to approximate the averaged drift and diffusion coefficients. Similarly, multiscale techniques are needed for the averaged observation coefficient,

$$\bar{h}(x) \equiv \int h(x,z)\mu_\infty(dz;x), \tag{5.3.1}$$

for observation and updating of the particle weights $\{w_t^j\}_{j\in\mathcal{A}}$. Additional details on HHPF are given in several papers [PNY11; YPN11; Lin+12]; here we simply summarize the algorithm steps:

Homogenized Hybrid Particle Filter (HHPF) Algorithm

1. Same as (PF) step 1)
2. Apply the HMM multiscale integration technique and compute the averaged coefficients $\bar{b}, \bar{a}^{1/2}, \bar{h}$.
3. Generate the prior at t_{k+1} by advecting each particle under the homogenized signal dynamics given by the generator $\overline{\mathcal{G}_S}$.
4. Same as (PF) step 3) but using $\bar{h}$ in the likelihood distribution.
5. Same as (PF) steps 4a) and 4b)

5.3.1 Exploiting Model Symmetry and Parameterizations

In addition to assuming scale separation and ergodicity of $Z_t^{\epsilon,x}$, if our signal dynamics has certain structural properties, then it may be advantageous to move some of the online computations related to resolving the transition density $\mu_{\Delta_m}(z;x,z_0)$ or averaged coefficients offline. As a first step, if $\mu_{\Delta_m}(z;x,z_0) \to \mu_\infty(z;x)$ fast enough, then one could consider precomputing an approximation to the map

$$\begin{aligned} \psi(x) : \mathbb{R}^m &\longrightarrow \mathcal{M}(\mathbb{R}^n) \\ (x) &\longmapsto \mu_\infty(z;x). \end{aligned}$$

Here $\mathcal{M}(\mathbb{R}^n)$ is the space of measures on $\mathbb{R}^n$. A naive approach here would most likely be computationally intractable unless $x \in \mathbb{R}^m$ is of small dimension or the dynamics are simple - the reason being that one may

need an immense amount of storage and pre-processing to well approximate $\psi(x)$. And in this case, one would still have to calculate $\bar{b}, \bar{a}, \bar{h}$ online.

If we further consider that the coefficients of the slow signal and observation can be written in the following form,

$$\begin{aligned} b(X_t^\epsilon, Z_t^\epsilon) &= b_1(X_t^\epsilon) + b_2(X_t^\epsilon) b_3(Z_t^\epsilon), \\ \sigma(X_t^\epsilon, Z_t^\epsilon) &= \sigma_1(X_t^\epsilon) + \sigma_2(X_t^\epsilon) \sigma_3(Z_t^\epsilon), \\ h(X_t^\epsilon, Z_t^\epsilon) &= h_1(X_t^\epsilon) + h_2(X_t^\epsilon) h_3(Z_t^\epsilon), \end{aligned} \tag{5.3.2}$$

then all computations of the averaged coefficients can also be moved offline to a pre-processing mode - removing a potentially costly numerical integration online. Still the fact that $\mathbb{R}^m$ may be of high dimension could be problematic. The next property is therefore quite useful.

Multiscale problems often have a natural subgrid structure, where a subset of the fast states only couple to a single slow state, and this same slow state is the only slow state coupled to the subset of fast states. For instance, the first slow state X_t^1 may be solely coupled to J fast states $Z_t^{1,1}, \ldots, Z_t^{1,J}$ and the other slow states $\{X_t^k\}$. And similarly X_t^2 solely coupled to $Z^{2,1}, \ldots, Z_t^{2,J}$ and $\{X_t^k\}$. In contrast, $Z_t^{k,j}$ is only dependent on X_t^k and any other $Z_t^{k,j'}$ in its sector. This is the form of the Lorenz '96 model, which will be tested in Section 5.3.2. This form is important because building on the previous observations and assumptions, implies that ψ can simplify to a one-dimensional map,

$$\begin{aligned} \psi_f(x) : \mathbb{R} &\longrightarrow \mathbb{R} \\ (x) &\longmapsto \int f(z) \mu_\infty(dz; x), \end{aligned}$$

yielding an averaged coefficient or forcing for the averaged dynamics. For example, take $b_3(Z_t^\epsilon)$ in Eq. 5.3.2. Our mapping would then yield $\psi_{b_3}(x) = \int b_3(z) \mu_\infty(dz; x)$.

The approximation of $\psi_f(x)$ may be accomplished by a number of ways, for example: polynomial regression, learning methods (e.g., neural networks), or a simple table lookup approach (i.e., regression with simple functions). Although slightly less numerically efficient than a polynomial regression, we use a table lookup in Section 5.3.2 for simplicity and because the timing difference for our test problem would not have been significant. Using this approach, we modify the HHPF algorithm and designate it as eHHPF.

Efficient Homogenized Hybrid Particle Filter (eHHPF) Algorithm

1. Offline pre-computation of data to approximate

$$\psi_{b_3}(x), \psi_{\sigma_3\sigma_3^*}(x), \psi_{\sigma_3}(x), \psi_{h_3}(x).$$

2. Possible offline data compression of

$$\psi_{b_3}(x), \psi_{\sigma_3\sigma_3^*}(x), \psi_{\sigma_3}(x), \psi_{h_3}(x).$$

3. Same as (PF) step 1)

4. Generate the prior at t_{k+1} by advecting each particle under the homogenized signal dynamics given by the generator $\overline{\mathcal{G}_S}$, evaluating

$$\psi_{b_3}(x), \psi_{\sigma_3\sigma_3^*}(x), \psi_{\sigma_3}(x),$$

as necessary.

5. Same as (PF) step 3) with evaluation of $\psi_{h_3}(x)$ for the likelihood distribution.

6. Same as (PF) steps 4a) and 4b)

7. Return to Step 3)

Before we demonstrate some numerical filtering results, we return to comparing the dynamics of the Lorenz '96 model when direct numerical integration, HMM, and the averaging method of this section are used. In Figures 5.8, 5.9, and 5.10 we illustrate the behavior of a generic slow state X_t^1 (shown in orange), the fast states (if applicable) in the 1st sector, that is $Z_t^{1,1}, \ldots, Z_t^{1,9}$ (shown in gray), and the fast scale forcing that enters Eq. 5.2.1 for the X_t^1 component (shown in light blue). Again, due to the symmetry of the model, it is sufficient to look at one sector to get a glimpse of the qualitative behavior of the dynamics. For all analysis in this chapter, we use an Euler-Maruyama integration scheme. Figure 5.8 shows the behavior of the direct numerical simulation with an integration step size of 1E-4. Figure 5.9 is the HMM method with parameters $\mathcal{R} = 1$, $\delta_m =$ 1E-4, $\delta_M =$ 1E-2, $\Delta_m = 5\delta_m$, and $\Delta_M = 10\delta_M$. And lastly, Figure 5.10 depicts integration of X_t^0 using an integration step size of 1E-2 and calling ψ_{η^1} to produce the fast forcing on X_t^1. According to Lorenz [Lor95], the time scale used here, $T = 10$, is approximately equivalent to mimicking 50 days in 'real' time.

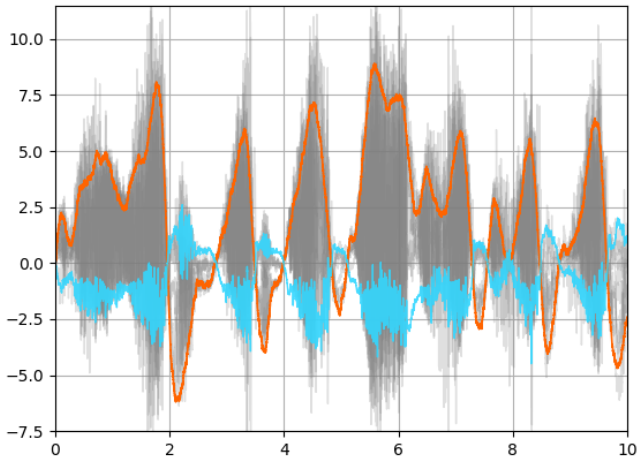

Figure 5.8: Direct numerical simulation of the Lorenz '96 model: X_t^1 in orange, $Z_t^{1,1} \ldots, Z_t^{1,9}$ in gray, and the fast scale forcing η_t^1 on X_t^1 in light blue.

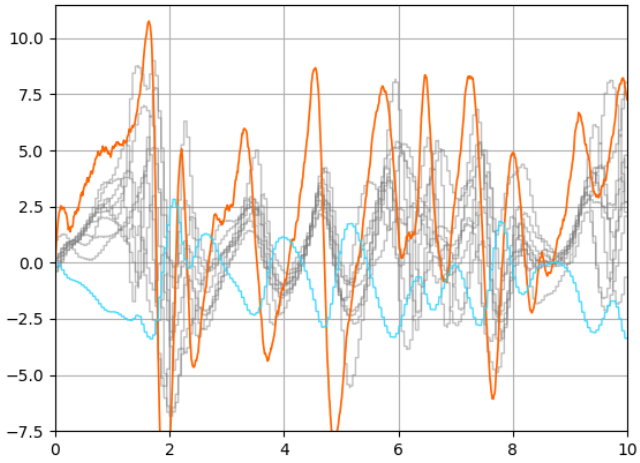

Figure 5.9: An HMM simulation of the Lorenz '96 model: X_t^1 in orange, $Z_t^{1,1} \ldots, Z_t^{1,9}$ in gray, and the fast scale forcing η_t^1 on X_t^1 in light blue.

5.3.2 Application to the Lorenz 1996 Model

We now provide some simulation comparisons between the various particle filtering algorithms thus far discussed. In the simulations that follow, we run each for $T = 20$. Recall that we will take observations every $\Delta t = 10\delta_M$, which is $\Delta t = 0.1$ for our parameters. In total we consider 12 experiments each with 24 simulations, the results and pertinent parameters are given in Tables 5.1, 5.2, and 5.3. In each of those tables,

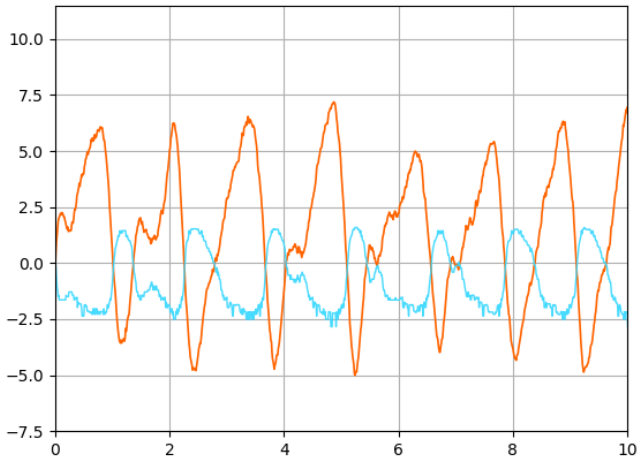

Figure 5.10: A solution of the Lorenz '96 model using pre-computed $\psi_\eta(x)$: X_t^1 in orange and the sampled fast scale forcing ψ_{η^1} on X_t^1 in light blue.

the average root-mean squared error (RMSE) is calculated as,

$$\text{RMSE} = \sqrt{\sum_{k=1}^{T/\Delta t} \left| X_{t_k}^\epsilon - \mathbb{E}\left[X_{t_k}^\epsilon\right] \right|_2^2}, \tag{5.3.3}$$

and used to quantify the accuracy of the filtering algorithm. The average simulation run-time and number of particles is also given.

Starting with the results in Table 5.1, one can see that the HHPF algorithm yields a greater than ten time speed up over PF, but with degraded accuracy when the number of particles is held constant. Doubling the number of particles gives the HHPF almost a ten time speed up and accuracy on par with PF. Following the same procedure with our eHHPF algorithm, we attain better performance than the HHPF algorithm in terms of both accuracy and computational efficiency. In particular the 32 particle case only requires two-thirds the run-time of HHPF and still yields an average RMSE that is lower.

Table 5.1: Filtering application of PF, HHPF, and eHHPF to the Lorenz '96 model.

Filter	PF	HHPF	HHPF	eHHPF	eHHPF
# Particles	16	16	32	16	32
RMSE	1.84	2.90	1.80	2.34	1.67
Run-Time	859 s	73.6 s	90.0 s	59.3 s	63.5 s

The algorithm, eHHnPF, used in Table 5.2 has not yet been given. To be clear, it is a combination of the nPF algorithm given in Section 5.5.1 and the eHHPF stated in this section. The main idea in Section 5.5.1 is

that the particles can be controlled (nudged), hence the subscript n in the naming convention. The prefix of 'e' is then the equivalent method of eHHPF, but with this particle control feature. One key drawback of this method is that it can be numerically expensive, yet this is offset by the fact that a smaller ensemble of particles is required to have low RMSE.

Of interest was whether the eHHnPF algorithm could further decrease run-time with comparable accuracy to the eHHPF 32 particle case. The nudged algorithm does require the solution of the tangent map and hence has a larger computational overhead per particle, yet requires less total particles to achieve a similar average RMSE. Comparing Tables 5.1 and 5.2, shows that the eHHnPF algorithm with eight particles is comparable in accuracy to eHHPF with 32 particles. It may be that on problems that are inherently more chaotic than the test problem considered in this work, that the nudged method would ultimately prove superior. The Lorenz '96 problem gains additional positive Lyapunov exponents, that grow in magnitude, as the forcing F becomes larger; resulting in a more chaotic system. Hence more extensive testing could be carried out on the Lorenz '96 model to provide a greater comparison.

Table 5.2: Filtering application of eHHnPF to the Lorenz '96 model.

Filter	eHHnPF	eHHnPF
# Particles	8	16
RMSE	1.80	1.49
Run-Time	64.6 s	70.0 s

An interesting question is whether the problem at hand really requires filtering methods that account for the fast scales. That is, given a sufficient number of particles, could the PF algorithm be applied directly to the slow scale dynamics, but ignoring the fast scale, and hence fast scale forcing. We designate this algorithm as PF_{X} and show the results in Table 5.3. The results indicate that indeed attempting to filter with the standard PF algorithm, and without accounting for the effects of the fast states on the slow states, one can not adequately reduce the RMSE. We only carry out the simulations up to 192 particles, since already at that point the eHHPF and eHHnPF algorithms are superior in both run-time and average RMSE.

Table 5.3: Filtering application of PF to the Lorenz '96 model with fast forcing neglected.

Filter	PF_{X}	PF_{X}	PF_{X}	PF_{X}	PF_{X}
# Particles	16	32	64	128	192
RMSE	5.88	4.55	3.46	2.37	2.56
Run-Time	57.6 s	58.5 s	61.7 s	67.56 s	73.7 s

The last observation we make of our results is that the process of approximating the normalized fast forcing on the slow states by ψ_η results in a particle ensemble with potentially worse overall statistics. In

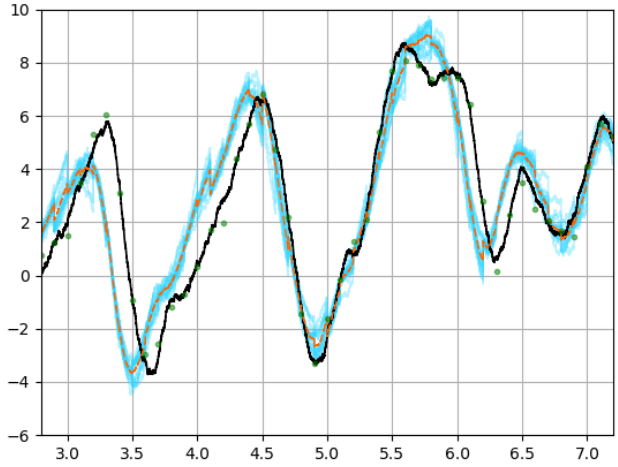

Figure 5.11: PF showing the signal $X_t^{\epsilon,1}$ (first component) in black, the estimate $\mathbb{E}\, X_t^{\epsilon,1}$ in orange, observations in green, particles in light blue.

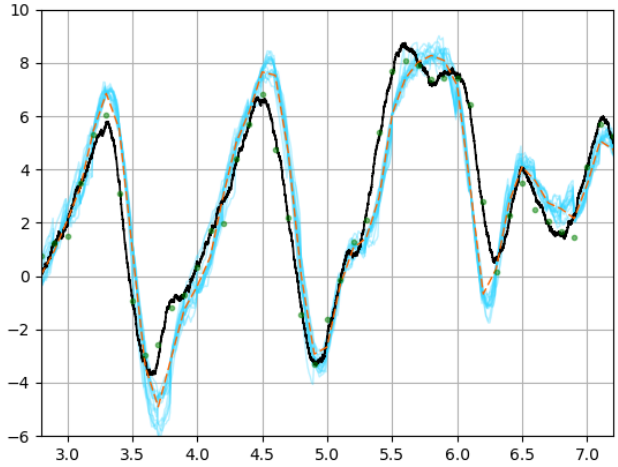

Figure 5.12: eHHPF showing the signal $X_t^{\epsilon,1}$ (first component) in black, the estimate $\mathbb{E}\, X_t^{\epsilon,1}$ in orange, observations in green, 16 particles in light blue.

particular the particles are not as diffusive. This can be seen by comparing a snapshot of a representative solution of the PF in Figure 5.11 to the eHHPF in Figure 5.12, both with the same number of particles. A similar trend is seen in the HHnPF algorithm and becomes slightly more pronounced in the eHHnPF. This potential deficiency could be mitigated by constructing ψ_η to also approximate higher order moments besides just the mean of η.

5.4 Correlated Noise

Neither the PF nor HHPF algorithms already described provide details of how we should account for correlation between the sensor and signal noise in the discrete time observation process; that is an observation process of the form,

$$Y_{t_k} = h(X_{t_k}) + \int_{t_{k-1}}^{t_k} \alpha dW_s + \gamma U_{t_k}, \tag{5.4.1}$$

with $\alpha \neq 0$ and $\gamma \succ 0$. Following the PF algorithm, when we select the proposal distribution as the prior distribution, then we must derive the likelihood distribution for updating the particle weights. In this section, we derive the likelihood for this case and demonstrate a numerical implementation of it on the Lorenz '96 model.

5.4.1 Likelihood for Correlated Sparse Observation

To derive the likelihood distribution, consider discrete time signal and observation processes of the form,

$$\begin{aligned}
x_j &= f_j(x_{j-1}) + G_j v_{j-1}, \\
&\vdots \\
x_{k-1} &= f_{k-1}(x_{k-2}) + G_{k-1} v_{k-2}, \\
x_k &= f_k(x_{k-1}) + G_k v_{k-1}, \\
y_k &= h_k(x_k) + e_k.
\end{aligned} \tag{5.4.2}$$

As before, subscript indices indicate times, x_k is the signal process, y_k the observation process, and $\{v_j\}$ is a sequence of independent Gaussian random variables. The sequence $\{e_j\}$ are also Gaussian, but correlated with $\{v_j\}$; specifically, the random variable e_k is correlated with $v_{j-1}, \ldots, v_{k-1}$. Figure 5.13 provides a pictorial representation of Eq. 5.4.2.

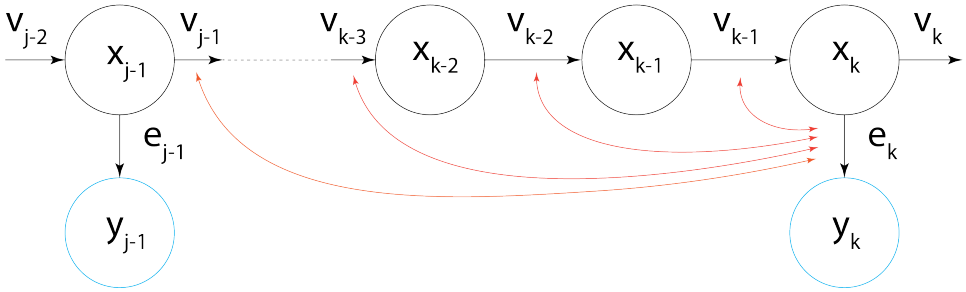

Figure 5.13: A pictorial representation of Eq. 5.4.2 with arrows between v_j and e_k indicating sensor-signal correlation.

The noises $v_{j-1}, \ldots, v_{k-2}, v_{k-1}, e_k$ are jointly Gaussian,

$$\begin{pmatrix} v_{j-1} \\ \vdots \\ v_{k-2} \\ v_{k-1} \\ e_k \end{pmatrix} \in \mathcal{N}\left(0, \begin{bmatrix} Q_{j-1} & \ldots & 0 & 0 & S_{j,k} \\ 0 & \ddots & 0 & 0 & \vdots \\ 0 & 0 & Q_{k-2} & 0 & S_{k-1,k} \\ 0 & 0 & 0 & Q_{k-1} & S_{k,k} \\ S_{j,k}^T & \ldots & S_{k-1,k}^T & S_{k,k}^T & R_k \end{bmatrix}\right),$$

with Q_j the covariance matrix associated with v_j, R_k with e_k and $S_{j,k}$ the covariance of v_{j-1} and e_k for instance.

For simplicity of discussion, let us assume $f = f_j$ and $h = h_j$, $\forall j$. Also, define $\widehat{G}_j \equiv G_j Q_{j-1} G_j^T$, $\widehat{S}_{j,k} \equiv G_j S_{j,k}$, and

$$\mathfrak{R} \equiv \begin{bmatrix} \widehat{G}_j & \ldots & 0 & 0 & \widehat{S}_{j,k} \\ 0 & \ddots & 0 & 0 & \vdots \\ 0 & 0 & \widehat{G}_{k-1} & 0 & \widehat{S}_{k-1,k} \\ 0 & 0 & 0 & \widehat{G}_k & \widehat{S}_{k,k} \\ \widehat{S}_{j,k}^T & \ldots & \widehat{S}_{k-1,k}^T & \widehat{S}_{k,k}^T & R_k \end{bmatrix} = \begin{bmatrix} \widetilde{Q} & \widetilde{S} \\ \widetilde{S}^T & R_k \end{bmatrix}.$$

The probabilistic description of the state space model is then given by,

$$p\left(\left.\begin{pmatrix} x_j \\ x_{j+1} \\ \vdots \\ x_k \\ y_k \end{pmatrix}\right| x_{j-1}\right) = \mathcal{N}\left(\begin{pmatrix} f(x_{j-1}) \\ \mathbb{E}\left[f(x_j)\right] \\ \vdots \\ \mathbb{E}\left[f(x_{k-1})\right] \\ \mathbb{E}\left[h(x_k)\right] \end{pmatrix}, \mathfrak{R}\right)$$

$$= \mathcal{N}\left(\begin{pmatrix} \mathbb{E}\left[f(X_{j-1:k})\right] \\ \mathbb{E}\left[h(x_k)\right] \end{pmatrix}, \begin{bmatrix} \widetilde{Q} & \widetilde{S} \\ \widetilde{S}^T & R_k \end{bmatrix}\right),$$

where we used the notation $X_{j-1:k}$ to be the vector $(x_k, \ldots, x_{j-1})$. We will need the following lemma on conditional Gaussian distributions.

Lemma 5.4.1

Let X, Y be two vectors with jointly Gaussian distribution:

$$\begin{pmatrix} X \\ Y \end{pmatrix} \sim \mathcal{N}\left(\begin{pmatrix} \mu_x \\ \mu_y \end{pmatrix}, \begin{bmatrix} P_{xx} & P_{xy} \\ P_{yx} & P_{yy} \end{bmatrix}\right)$$

Then the conditional Gaussian distribution for Y given $X = x$ is Gaussian distributed,

$$(Y|X = x) \sim \mathcal{N}\left(\mu_y + P_{yx}P_{xx}^{-1}(x - \mu_x), P_{yy} - P_{yx}P_{xx}^{-1}P_{xy}\right).$$

Using Lemma 5.4.1, the likelihood $p(y_k|x_k, x_{k-1}, \ldots, x_{j-1})$ is,

$$p(y_k|x_k, x_{k-1}, \ldots, x_{j-1}) \propto \mathcal{N}\left(h(x_k) + \widetilde{S}^T\widetilde{Q}^{-1}(X_{j-1:k} - f(X_{j-1:k})), R_k - \widetilde{S}^T\widetilde{Q}^{-1}\widetilde{S}\right).$$

As we have already seen in this chapter, a continuous time signal does become discrete once we apply a numerical filtering algorithm to the problem (i.e., we are forced to numerically integrate and therefore the continuous time signal becomes a discrete time process). For instance, our application of an Euler-Maruyama integration scheme means that each Euler step can be thought of as one line from Eq. 5.4.2. It is in this sense that we will apply the results of this subsection with PF and HHPF to solve the correlated filtering problem. For a simple two-dimensional example demonstrating correlated filtering with the aforementioned methods, see the work of Beeson et al. [Bee+18]. For the reader interested in algorithms for the continuous time signal

and observation case with correlated sensor noise, see the work of Crisan [Cri06], where a branching particle filter is presented for solution of the Zakai equation.

5.4.2 Application to the Lorenz 1996 Model

In this section we apply the PF, HHPF, and HHnPF algorithms to a correlated sensor-signal noise filtering problem of the Lorenz '96 model with continuous time signal and discrete time observation. We use the same Lorenz '96 model and HMM parameters as given in Section 5.2.2, and Eq. 5.2.1, in the form of Eq. 5.2.2. For the observation process, we use Eq. 5.4.1 with (t_k) the observation times and in the non-correlated case,

$$\alpha \equiv 0_{m\times m}, \quad \gamma \equiv \sigma_x,$$

and in the correlated case,

$$\alpha \equiv \frac{1}{\sqrt{2}}\sigma_x, \quad \gamma \equiv \frac{1}{\sqrt{2}}\sigma_x.$$

The choice of α, γ in Eq. 5.4.1 means that in both the non-correlated or correlated case, the observation has the same statistics. Here we define $h \equiv \mathrm{Id}_{m\times m}$, an $m \times m$ identity matrix that acts on $x \in \mathbb{R}^m$ by matrix-vector multiplication. In the case of the homogenized hybrid particle filters, the sensor function $\bar{h}(\cdot)$, is a function of $X^0_{t_k}$.

As before, in the simulations that follow, we use an observation step size $\Delta t = 10\delta_M = 0.1$ and total simulation time of $T = 20$, which approximately corresponds to 0.5 and 100 'real' days according to Lorenz [Lor95]. The deterministic Lorenz '96 model investigated by Lorenz [Lor95] has an error doubling time of approximately 1.6 'real' days. In all simulations, the true signal is correlated, but we will conduct one experiment with the HHPF filter assuming a sensor-signal model of the non-correlated type (i.e., $\alpha = 0_{m\times m}$ and $\gamma = \sigma_x$). In all but one simulation, we use N = 16 particles, with an effective number of $N_{\text{eff}} = 8$. For one HHnPF experiment we will use $N = 8$ and $N_{\text{eff}} = 4$. In total, we consider 5 experiments with their defining parameters given in Table 5.4. Each experiment consisting of 24 simulations. The average RMSE is calculated according to Eq. 5.3.3, and is shown for each experiment in Table 5.4 alongside the average simulation run-time.

Figure 5.14 shows the result of the PF applied to the Lorenz '96 problem over the time interval $[0, 20]$. The average RMSE was 1.52 and average simulation time 1,019 seconds. With the exception of the interval $[1, 2.5]$, the PF with 16 particles is able to track well $X^{\epsilon,1}_t$; the first component of X^ϵ_t, but at the expense of long simulation times. In Figures 5.15 and 5.16 we show the corresponding result for the HHPF experiments,

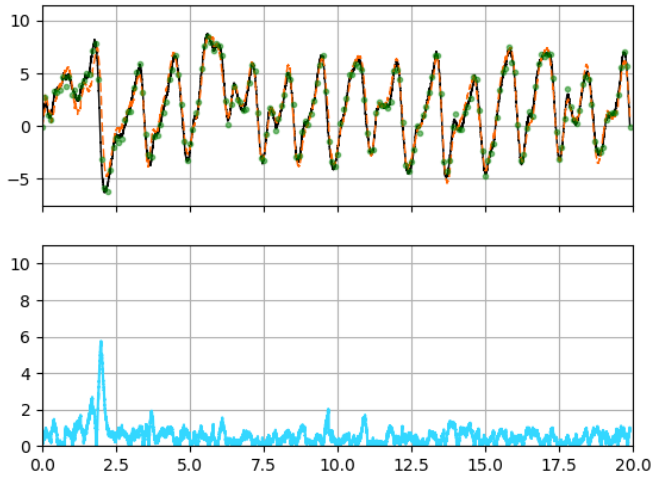

Figure 5.14: PF, $\alpha = \gamma = \sigma_x/\sqrt{2}, N = 16, N_{\text{eff}} = 8$. Top graph: the signal $X_t^{\epsilon,1}$ (first component) in black, the estimate $\mathbb{E}\, X_t^{\epsilon,1}$ in orange, observations in green. Bottom graph: RMSE in light blue.

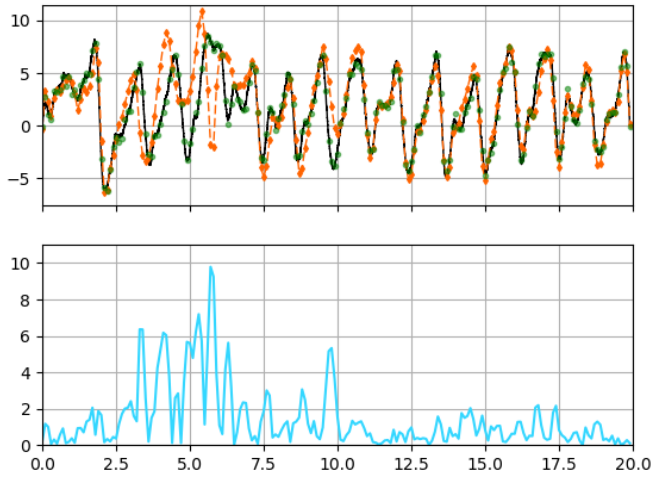

Figure 5.15: HHPF, $\alpha = 0, \gamma = \sigma_x, N = 16, N_{\text{eff}} = 8$. Top graph: the signal $X_t^{\epsilon,1}$ (first component) in black, the estimate $\mathbb{E}\, X_t^{\epsilon,1}$ in orange, observations in green. Bottom graph: RMSE in light blue.

and in Figures 5.18 and 5.17 the results when nudging is used.

As one might expect, the use of HHPF results in a slight degradation in the accuracy of the estimate of the signal in comparison to the PF for a fixed number of particles, but with a significant reduction in simulation run-time. For instance, Table 5.4 shows that the HHPF simulations result in more than a ten time speed-up over the PF. The result shown in Figure 5.15 has the least accurate tracking of the signal out

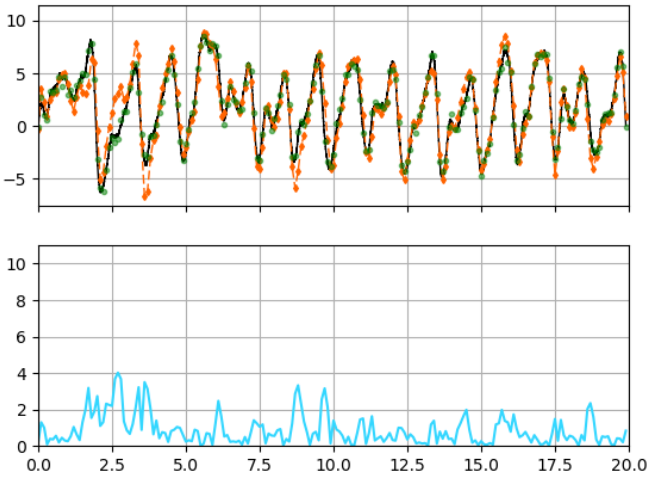

Figure 5.16: HHPF with $\alpha = \gamma = \sigma_x/\sqrt{2}, N = 16, N_{\text{eff}} = 8$. Top graph: the signal $X_t^{\epsilon,1}$ (first component) in black, the estimate $\mathbb{E}\, X_t^{\epsilon,1}$ in orange, observations in green. Bottom graph: RMSE in light blue.

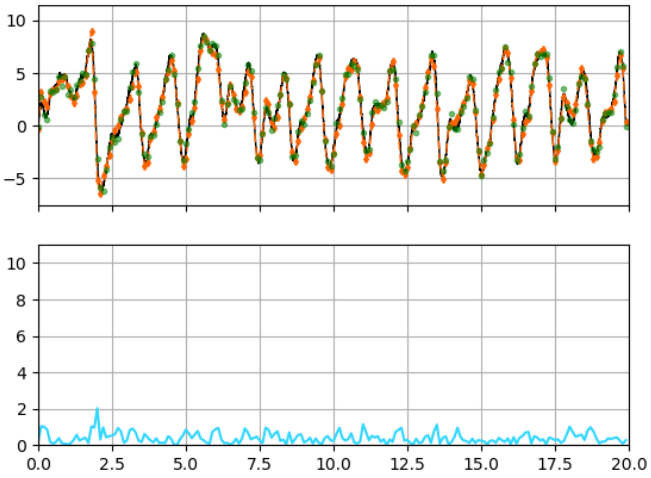

Figure 5.17: HHnPF with $\alpha = \gamma = \sigma_x/\sqrt{2}, N = 16, N_{\text{eff}} = 8$. Top graph: the signal $X_t^{\epsilon,1}$ (first component) in black, the estimate $\mathbb{E}\, X_t^{\epsilon,1}$ in orange, observations in green. Bottom graph: RMSE in light blue.

of all experiments. This is expected, since this experiment does not model the correlated sensor-signal noise and filters on the homogenized dynamics. Figure 5.16 shows that an improvement in accuracy for the same run-time can be made by using the correlated algorithm in Section 5.4.1.

Figure 5.17 depicts the type of improvement in tracking that using nudging provides over HHPF. The HHnPF solution in Figure 5.17 uses the same number of particles as the HHPF simulations, $N = 16$, and

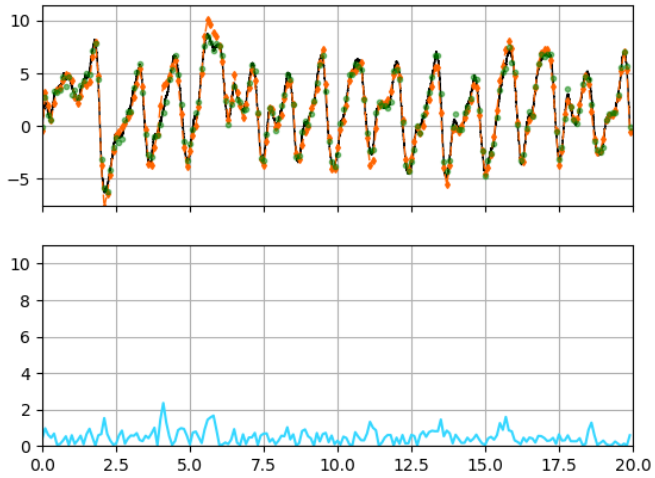

Figure 5.18: HHnPF with $\alpha = \gamma = \sigma_x/\sqrt{2}, N = 8, N_{\text{eff}} = 4$. Top graph: the signal $X_t^{\epsilon,1}$ (first component) in black, the estimate $\mathbb{E}\, X_t^{\epsilon,1}$ in orange, observations in green. Bottom graph: RMSE in light blue.

uses four realizations for calculation of the Feynman-Kac formulas in Eqs. 5.5.5 and 5.5.6. The calculation of the control, which is calculated once over each observation interval–and held fixed, results in a slower average run-time of 159 seconds per simulation, but with a much improved RMSE of the coarse-grain states. Figure 5.18 is also an HHnPF simulation, but with the number of particles reduced to $N = 8$, which still results in good tracking due to the nudging of the particles, and a reasonable run-time of 110 seconds per simulation on average; the RMSE average of 1.30 is still lower than that of the PF average RMSE.

Table 5.4: Filtering results for various filter algorithms applied to the Lorenz '96 model. RMSE integrated over time, and filter run-time (per simulation) averaged over 24 experiments.

Experiment	1st	2nd	3rd	4th	5th
Filter	PF	HHPF	HHPF	HHnPF	HHnPF
N_{eff}	8	8	8	8	4
N	16	16	16	16	8
α	$\sigma_x/\sqrt{2}$	0	$\sigma_x/\sqrt{2}$	$\sigma_x/\sqrt{2}$	$\sigma_x/\sqrt{2}$
γ	$\sigma_x/\sqrt{2}$	σ_x	$\sigma_x/\sqrt{2}$	$\sigma_x/\sqrt{2}$	$\sigma_x/\sqrt{2}$
RMSE	1.52	2.47	2.10	1.11	1.30
Run-Time	1019 s	85 s	85 s	159 s	110 s

In Figures 5.19 - 5.23, we provide a magnified view of the interval $[2.5, 7.5]$ for the estimate of the signal in Figures 5.14 - 5.18. Besides showing the signal, estimate of the signal, and observations in these figures, we also show the history of the particles (shown in light blue). The error in the observation of the signal is more apparent in these figures. One can also see when re-sampling occurs; a rapid collapse of particles far from

the observations to locations closer to the observation at observation times. The diffusion of the particles between observation times, partly exacerbated by the chaotic property of the model, is also apparent. In Figures 5.22 and 5.23, the particle traces in light blue show that although we apply control to the particles to nudge them towards observations, the running cost associated with applying control in Eq. 5.5.1 means that the control is not allowed to dominate the true dynamics by too much.

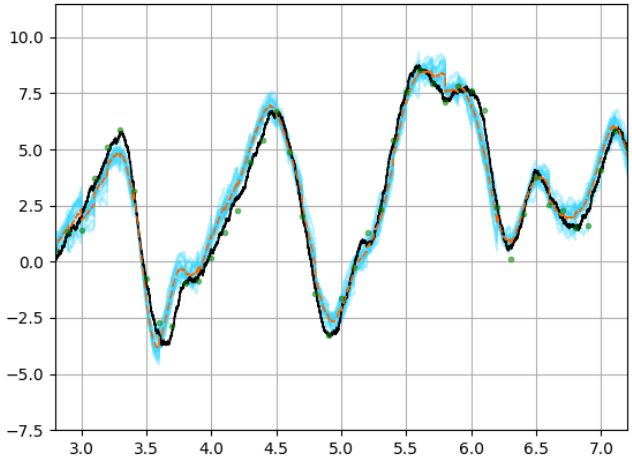

Figure 5.19: PF with $\alpha = \gamma = \sigma_x/\sqrt{2}, N = 16, N_{\text{eff}} = 8$. The signal $X_t^{\epsilon,1}$ (first component) in black, the estimate $\mathbb{E}\, X_t^{\epsilon,1}$ in orange, observations in green, particles in light blue.

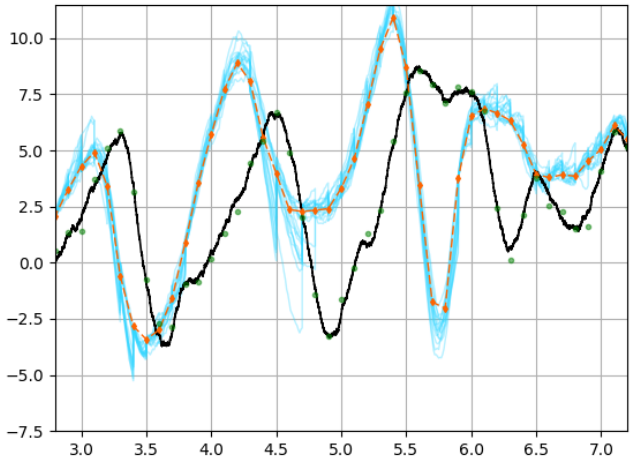

Figure 5.20: HHPF with $\alpha = 0, \gamma = \sigma_x, N = 16, N_{\text{eff}} = 8$. The signal $X_t^{\epsilon,1}$ (first component) in black, the estimate $\mathbb{E}\, X_t^{\epsilon,1}$ in orange, observations in green, particles in light blue.

The last figure that we include is of the effective number N_{eff}, of the solutions shown in Figures 5.14,

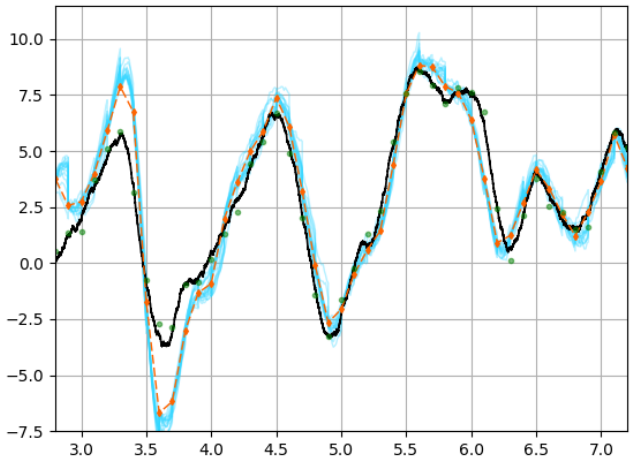

Figure 5.21: HHPF with $\alpha = \gamma = \sigma_x/\sqrt{2}, N = 16, N_{\text{eff}} = 8$. The signal $X_t^{\epsilon,1}$ (first component) in black, the estimate $\mathbb{E}\, X_t^{\epsilon,1}$ in orange, observations in green, particles in light blue.

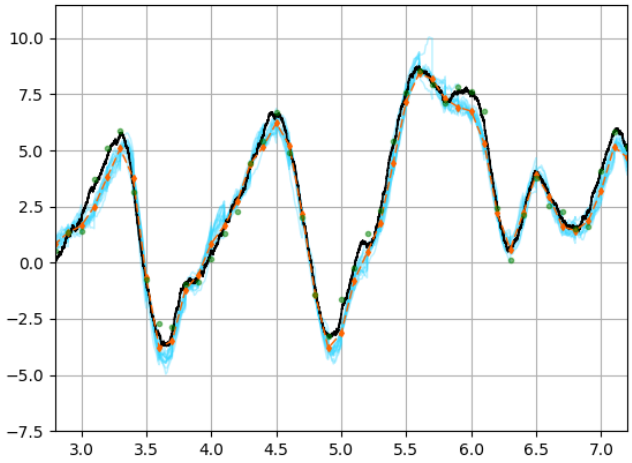

Figure 5.22: HHnPF with $\alpha = \gamma = \sigma_x/\sqrt{2}, N = 16, N_{\text{eff}} = 8$. The signal $X_t^{\epsilon,1}$ (first component) in black, the estimate $\mathbb{E}\, X_t^{\epsilon,1}$ in orange, observations in green, particles in light blue.

5.16, 5.17; having simulation parameters corresponding to the 1st, 3rd, and 4th experiments in Table 5.4 respectively. Figure 5.24 shows the effective number at observation times for these simulations. Since we set the threshold of N_{eff} equal to eight, this implies that for all three of these simulations, re-sampling occurred after every observation. The other simulations, corresponding to the results in Figures 5.15 and 5.18, re-sampled on most, but not every observation. It is interesting that even with nudging, Figure 5.24 shows that the HHnPF approach on the Lorenz '96 model still results in significant resampling.

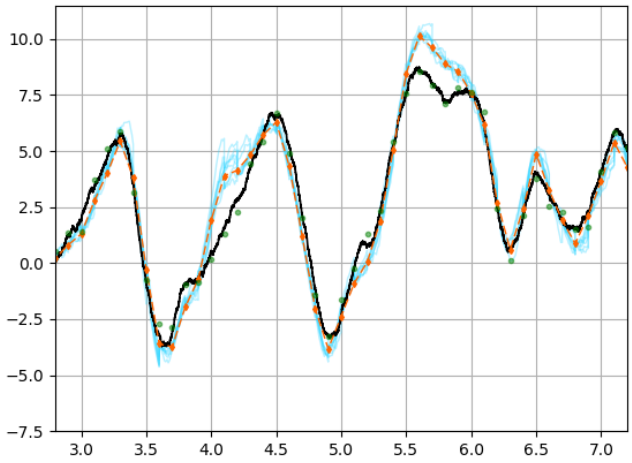

Figure 5.23: HHnPF with $\alpha = \gamma = \sigma_x/\sqrt{2}, N = 8, N_{\text{eff}} = 4$. The signal $X_t^{\epsilon,1}$ (first component) in black, the estimate $\mathbb{E}\, X_t^{\epsilon,1}$ in orange, observations in green, particles in light blue.

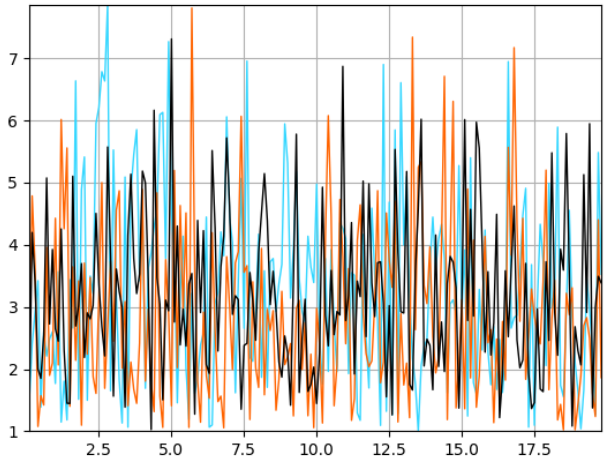

Figure 5.24: The effective number N_{eff} at observation times versus time. PF shown in black, HHnPF in orange, and HHPF in light blue. Values below 8 indicate re-sampling occurs.

5.5 Optimal Proposal Particle Filtering and Tempering

The choice of the prior as the proposal distribution in the particle filter described in Section 5.1.2, is convenient, but suboptimal. If one can more closely approximate the optimal proposal (the proposal density that gives a minimal variance of the weights [DdG01]), then using this distribution will yield a better approximation of the posterior distribution. In this section, we describe a method to construct an approximation of the optimal proposal by solving an optimal control problem for the steering of the particles toward the observations,

but staying mostly true to the natural dynamics. This method was developed in a series of papers [Lin+12; Lin+14; Yeo+20], and is similar in concept, but quite different from a number of other efforts to exploit the optimal proposal technique [Lee10; CMT10].

Additionally, we improve the diversity of the particle samples by combining the controlled particle technique with tempering of the likelihood [Nea96; MDJ06; BCJ14]. This combined method is then compared against another optimal proposal technique that introduces a control on the particle–the relaxation method by van Leeuwen [Lee10]. The strengths of the optimal control technique described in this chapter is further illustrated on the chaotic and nonlinear Lorenz '63 model.

5.5.1 The Nudged Particle Filter (nPF)

The construction of what will be called the *nudged particle filter* (nPF), begins by modifying the dynamics of the particles by introducing a time-varying control term u_t. Each particle will then be advected under the following dynamics,

$$d\widehat{X}_t = b(\widehat{X}_t)dt + u_t dt + \sigma(\widehat{X}_t)dW_t, \tag{5.5.1}$$

where we use the $\widehat{\cdot}$ symbol to distinguish a solution obeying the controlled dynamics as opposed to the natural dynamics given in Eq. 5.1.1. For $t \in [t_k, t_{k+1}]$, the control is chosen to minimize the cost functional:

$$J(t_k, x, u) \equiv \mathbb{E}_{\widehat{X}^x_{t_k}}\left[\frac{1}{2}\int_{t_k}^{t_{k+1}} u(s)^T Q(\widehat{X}_s)^{-1} u(s) ds + g\left(Y_{t_{k+1}}, \widehat{X}_{t_{k+1}}\right)\right],$$

where $\mathbb{E}_{\widehat{X}^x_{t_k}}$ is the expectation with respect to the probability measure of the process that starts at $\widehat{X}^x_{t_k} = x$ at time t_k, $Q(x) = \sigma\sigma^T(x)$ and

$$g(y, x) \equiv \frac{1}{2}(y - h(x))^T R^{-1}(y - h(x)), \tag{5.5.2}$$

with R the variance of the observation noise. For brevity in what follows, we suppress the argument of Q.

The solution of this optimal control problem is given by the Hamilton-Jacobi-Bellman equation [FS06, Chapter 4.3, p.155],

$$-\frac{\partial V}{\partial t} + H(t, x, D_x V, D_x^2 V) = 0,$$
$$V(t_{k+1}, x) = g(Y_{k+1}, x),$$

where $V(t,x) \equiv \inf_u J(t,x,u)$ for $t \in [t_k, t_{k+1}]$ is the value function and

$$H(t,x,p,P) \equiv \sup_u \left[-(b(x)+u)^T p - \frac{1}{2} u^T Q^{-1} u - \frac{1}{2} \operatorname{tr}(QP) \right],$$

is the Hamiltonian of the control problem. The optimal control is

$$u(t, \widehat{X}_t) = -Q \nabla_x V(t, \widehat{X}_t). \tag{5.5.3}$$

Solving for $u(t, \widehat{X}_t)$ in Eq. 5.5.3 requires the solution of the gradient of the value function, which in turn requires the solution of a second order nonlinear partial differential equation (PDE). Yet, as shown by Yeong et al. [Yeo+20], one can perform a log transformation, $V(t,x) = -\log \Phi(t,x)$, to transform the nonlinear PDE to a linear PDE, which may then be solved by the Feynman-Kac formula. The optimal control is then expressed by

$$u(t, \widehat{X}_t) = \frac{1}{\Phi(t, \widehat{X}_t)} Q \nabla_x \Phi(t, \widehat{X}_t). \tag{5.5.4}$$

This first linear PDE only yields $\Phi(t,x)$ and hence the value function, and one still needs to solve for the gradient, which in general can be found with the Clark-Ocone formula from Malliavin calculus. A simplifying case is when the signal variance, Q, is constant (i.e., additive forcing). Yeong et al. [Yeo+20] showed that a second Feynman-Kac formula can then be leveraged to yield the gradient information.

Let $g_{k+1}(x) \equiv g(Y_{k+1}, \eta_{k+1}^{t,x})$, then the first Feynman-Kac formula gives the solution,

$$\Phi(t,x) = \mathbb{E}_{t,x} \left[e^{-g_{k+1}(x)} \right]. \tag{5.5.5}$$

Whereas the second application of Feynman-Kac gives,

$$\nabla_x \Phi(t,x) = -\mathbb{E}_{t,x} \left[e^{-g_{k+1}(x)} e^{\int_t^{t_{k+1}} (\nabla_x b(\eta_s^{t,x}))^T ds} \nabla_x g_{k+1}(x) \right]. \tag{5.5.6}$$

In both cases, $\mathbb{E}_{t,x}$ is the expectation with respect to the sample paths η generated by

$$d\eta_s^{t,x} = b(\eta_s^{t,x}) ds + \sigma dU_s, \quad \eta_t^{t,x} = x, \tag{5.5.7}$$

where U is a standard Brownian motion independent of the previously mentioned random processes.

Because the particles of the nPF algorithm will follow the controlled dynamics given by Eq. 5.5.1, instead

of the natural dynamics of Eq. 5.1.1, the weights of the particles must be adjusted to account for the control. In continuous time dynamics, the change of weight is given by a Radon-Nikodym derivative $d\mu^j/d\widehat{\mu}^j$ for particle j, where μ^j is the measure on path space generated by a process following the dynamics given by Eq. 5.1.1 and $\widehat{\mu}^j$ is the measure on the path space generated by a process following the dynamics prescribed by Eq. 5.5.1. The change in weights for the j-th particle at time t_{k+1} is then given by

$$w_{k+1}^j \propto w_k^j f_{k+1}(Y_{k+1}|\mathcal{A}_{k+1}^x(j))\frac{d\mu^j}{d\widehat{\mu}^j}(t_{k+1}, \widehat{X}_{t_k,t_{k+1}}^j),$$

where

$$\frac{d\mu^j}{d\widehat{\mu}^j}(t_{k+1}, \widehat{X}_{t_k,t_{k+1}}^j) = \exp\left(-\int_{t_k}^{t_{k+1}} v(s, \widehat{X}_s^j)^T dB_s - \frac{1}{2}\int_{t_k}^{t_{k+1}} v(s, \widehat{X}_s^j)^T v(s, \widehat{X}_s^j) ds\right), \tag{5.5.8}$$

and

$$v(s, \widehat{X}_s^j) \equiv -\sigma\nabla_x V(s, \widehat{X}_s^j).$$

Some final remarks are that the nPF algorithm requires noise in the signal process to facilitate the change of measure defined by Eq. 5.5.8, whereas the PF algorithm can be applied to deterministic systems. For further insight and remarks into the nPF algorithm, we direct the interested reader to the work of Yeong et al. [Yeo+20].

Nudged Particle Filter (nPF) Algorithm

1. At time t_k, set $w_k^j = 1/N$, $\forall j \in \mathcal{A}$ and

$$\pi_k(x|Y_k) = \sum_{j\in\mathcal{A}} w_k^j \delta_k^j(x).$$

2. Collect the observation Y_{k+1}.

3. For each particle, advect to t_{k+1} under the controlled dynamics–solving for the control given by Eq. 5.5.4 using Eqs. 5.5.5 and 5.5.6 with realizations following the dynamics of Eq. 5.5.7.

4. While advecting the particles, update the particle weights using Eq. 5.5.8. Let $\widehat{w}_{k+1}^j$ be the prior weight updated due to the Radon-Nikodym derivative from time t_k to t_{k+1}.

5. Denote the (optimal proposal) prior at t_{k+1} by

$$\pi_{k+1}(x|Y_k) = \sum_{j\in\mathcal{A}} \widehat{w}^j_{k+1}\delta^j_{k+1}(x).$$

6. Update the particle weights according to

$$w^j_{k+1} \propto \widehat{w}^j_{k+1} f_{k+1}(Y_{k+1}|\mathcal{A}^x_{k+1}(j)).$$

7. See the PF algorithm 4a. and 4b. regarding resampling and normalization.

5.5.2 Insight on the Nudged Particle Filter

Some useful comments regarding step 3. of the implementation of the nPF algorithm is that the control can be calculated for each integration step of the advection, but this often proves too costly and unnecessary for sparse in-time observations. One can specify a coarser partition of the time interval $[t_k, t_{k+1}]$, calculate a control based on the initial time of each part of the partition and hold this control constant across that part. The nPF algorithm is numerical more complex in comparison to the standard PF algorithm because of step 3., where the control must be calculated for each of these part of the time partition and for a user specified number of realizations for each of these controls. The improvement in filtering capability means that the nPF can drastically reduce the number of particles necessary to avoid degeneracy and therefore quickly becomes advantageous in comparison to the standard particle filter.

Besides the tradeoff of the increased complexity per particle versus a smaller ensemble size for the nudged particle filter, there are other issues that arise when using the controlled particle framework. If handled correctly, the nPF can be a superior method to the standard PF. To illustrate some of these remarks, we show in Figure 5.25 a simulation of the PF method on the Lorenz '63 model (to be introduced in Section 5.5.4).

Figure 5.25 shows the discrete time observations in green and the paths of the particle ensemble. Each path being an individual particle. The paths are colored according to the weight that each particle has relative to the ensemble average. Therefore in Figure 5.25, we see that times between observations where a path is colored white indicates that its weight is neutral. If all paths are white, then the ensemble has particles all of the same weight. This is the ideal situation for a well balanced ensemble (it has perfect diversity of the particles). Characteristic of the PF method is that the particle weights are constant between observations and only change after the application of the likelihood function and resampling.

In Figure 5.26, we show the same simulation, but this time using the nPF algorithm. The first striking

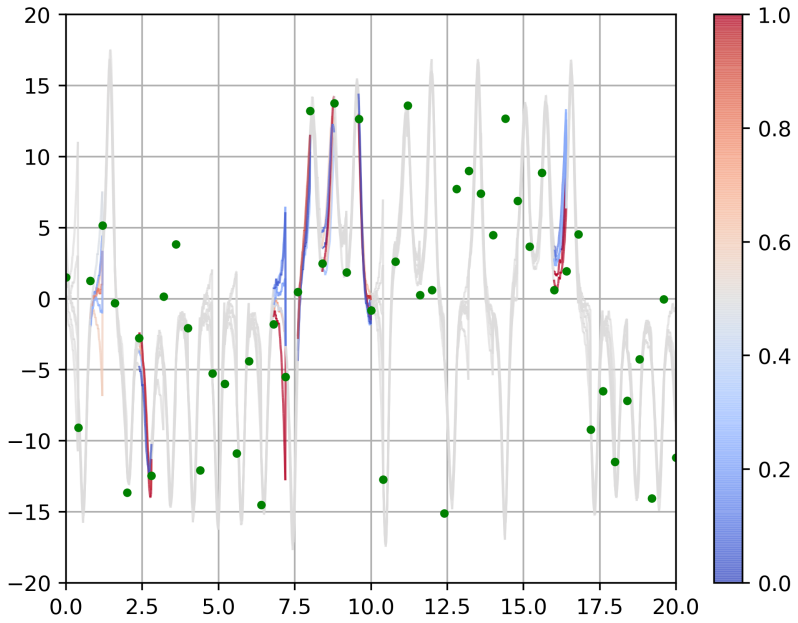

Figure 5.25: Time history of relative particle weights for a simulation of PF on the Lorenz '63 model (see Section 5.5.4). Observations are shown in green. Particles that are blue have essentially zero weight relative to the rest of the ensemble. A color of white indicates an average weight relative to the ensemble, and coloring of red indicates the particle is overweighted relative to the rest of the ensemble.

difference is that for the majority of the time, the ensemble weights are quite imbalanced, with some particles heavily weighted and otherwise essentially meaningless. The particles also have weights that change between observations, and therefore an evenly balanced ensemble can quickly become unevenly weighted shortly after an observation time. The weights of the particles are lowered due to any nudging that they perform to correct their trajectories so that the expected final location at the next observation time is appropriately closer to the actual observation. This will result in a better weight update at observation time and this action is not visually apparent from this figure (but see comment below regarding Figure 5.27, which does illustrate the effect of the observation time weight update).

An important remark to make when comparing Figure 5.25 and Figure 5.26 is that the nPF particles are able to strongly correct their trajectories when needed (and as expected by the method). But this can result in the particles having a very low weight. Because we are working with a discrete and finite number system (floating point system) when performing numerical simulations, and because of the presence of taking exponential and logarithms at various times in the algorithms of PF and nPF, there is the real danger of having a particle that gets assigned a NaN (not a number) weight (i.e., the particle should have a nearly

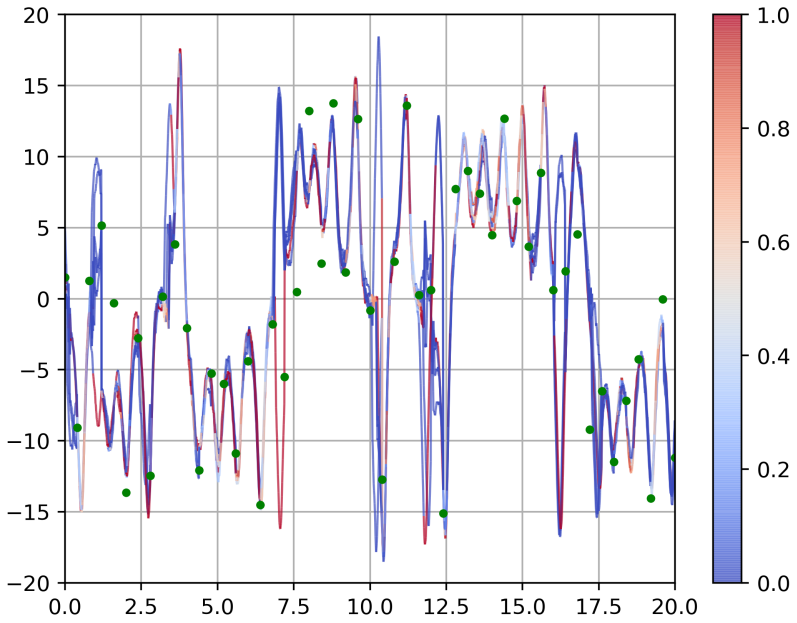

Figure 5.26: Time history of relative particle weights for a simulation of nPF on the Lorenz '63 model (see Section 5.5.4). Observations are shown in green. Particles that are blue have essentially zero weight relative to the rest of the ensemble. A color of white indicates an average weight relative to the ensemble, and coloring of red indicates the particle is overweighted relative to the rest of the ensemble.

zero weight, but underflow occurs and then an undefined operation). This issue is not of great concern for the PF method, unless a very small ensemble is being used. But due to the nudging (Radon-Nikodym derivative), it is much more pronounced for the nPF method. And therefore any implementation of nPF needs to appropriately account for the fact that particles may "die" or "vanish" between observations if the nudging control is allowed to be too large. This issue is especially pronounced when applied to chaotic systems (e.g., the Lorenz '63 model). Hence, it has been found that some saturation on the ability for a particle to nudge may be needed (i.e., once a particles weight crosses a threshold, additional nudging control is not allowed). In the same sense, another approach that has been tried is to only allow control during certain subintervals of the time between observations (e.g., the first or second half of the time between observations). The explicit accounting of the weights and avoidance of this issue in the optimal control problem would be an interesting and useful future endeavor.

We include in Figure 5.27 the comparison of the effective sample size for the simulations shown in Figures 5.25 and 5.26. The simulations had an ensemble sample size of 6 particles and we used an effective sample size threshold of 3 (i.e., resampling occurs if N_{eff} drops below 3). Figure 5.27 shows that both filters require

re-sampling after most observations. The average N_{eff} in both cases indicates that about 1 or 2 particles at any given time have almost all the weight.

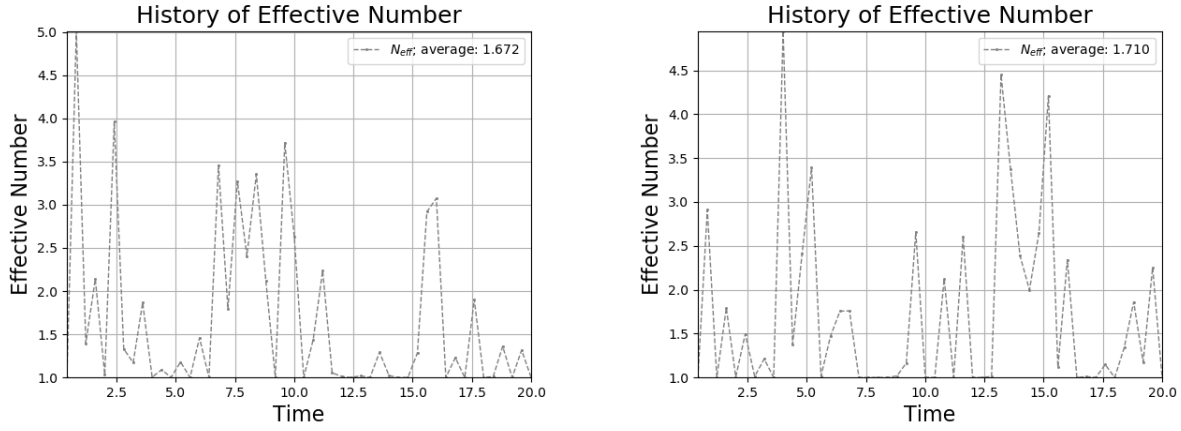

(a) PF (b) nPF

Figure 5.27: Time history (at observation time) of effective sample size (number) for a simulation of PF and nPF on the Lorenz '63 model (see Section 5.5.4).

5.5.3 Relaxed Particle Filter (rPF)

Another particle filtering method using a nudging term to steer particles towards observations has been considered by van Leeuwen [Lee10]. In the interval between available observations $[t_k, t_{k+1}]$, particles are steered by an exponential function dependent on the time within the interval, such that the steering magnitude is proportional to the signal noise covariance and the distance of the particle locations from the next observation. The method by van Leeuwen [Lee10] also includes a procedure to make particle weights almost equal immediately before the time step of the next available observation, which minimizes the weights variance for the entire sample. We apply this particle filtering method in Section 5.5.5 alongside the PF and nPF methods.

Chorin et al. [CMT10] take a different, more general approach to constructing an optimal importance sampling density, in which particles with high posterior probabilities are selected using the standard Gaussian distribution. For the i-th particle, let G_i be a specified function on the state space, related to the posterior as

$$e^{-G_i(\mathcal{A}_i^x(k))} = f_k(Y_k|\mathcal{A}_i^x(k))\rho_{k|k-1}(\mathcal{A}_i^x(k)|\mathcal{A}_i^x(k-1)).$$

Let ξ be a standard Gaussian random variable. The objective is to determine a map $\xi \to x$, such that $G_i(x) - \min G_i(x) = \frac{1}{2}\xi^T\xi$. The corresponding x that satisfies this map (specified by the relation between

G_i and ξ) is chosen as the new location of the i-th particle. Since ξ is Gaussian, the highly likely values of ξ are in the neighborhood of 0, and these values of ξ will map to states near the minimum of G_i, which is where high posterior probability of the i-th particle occurs.

5.5.4 The Lorenz 1963 Model

We will apply the rPF method as well as tempering in Section 5.5.5 to the well known Lorenz '63 model. We introduce a stochastic variant of that model in this section and provide the parameters that will be used later in the simulations. A stochastic Lorenz '63 system [Lor63] is given by

$$d\begin{bmatrix} x_t \\ y_t \\ z_t \end{bmatrix} = \begin{bmatrix} -\sigma & \sigma & 0 \\ \rho & -1 & 0 \\ 0 & 0 & -\beta \end{bmatrix} \begin{bmatrix} x_t \\ y_t \\ z_t \end{bmatrix} dt + \begin{bmatrix} 0 \\ -x_t z_t \\ x_t y_t \end{bmatrix} dt + \sigma_x dW_t, \tag{5.5.9}$$

where $\sigma = 10$, $\rho = 28$ and $\beta = \frac{8}{3}$. We have added standard Brownian motion noise W to the system in Eq. 5.5.9, with variance $\sigma_x \sigma_x^*$. The choice of σ_x, the observation sequence Y_{t_k}, and sensor matrix H are defined as,

$$\sigma_x = \begin{bmatrix} 2 & 1 & 0.5 \\ 1 & 2 & 1 \\ 0.5 & 1 & 2 \end{bmatrix}, \qquad Y_{t_k} = H \begin{bmatrix} x_{t_k} \\ y_{t_k} \\ z_{t_k} \end{bmatrix} + B_{t_k}, \qquad \text{and} \qquad H = \begin{bmatrix} 1 & 0 & 0 \end{bmatrix}.$$

We set the observation covariance to be $B_{t_k} \sim \mathcal{N}(0, 2I_{3\times 3})$ for all $k = 1, 2, \ldots$ Simulation of Eq. 5.5.9 is taken as the truth, with observations recorded every 0.4 time units.

The deterministic system is chaotic, with one positive Lyapunov exponent $\lambda = 0.9065$. This means that a small initial perturbation ϵ_0 grows as $\epsilon_t = \epsilon_0 e^{\lambda t}$. Let us denote the error doubling time as τ_d (i.e. the amount of time that is required for a small error to double in size). Then solving $\epsilon_{\tau_d} = 2\epsilon_0$, gives the error doubling time of $\tau_d = 0.76$ time units. Therefore, in the experiments shown in this section, the time between observations is slightly more than half the error doubling time.

5.5.5 Tempering

In previous sections, we have seen that an accurate estimate can be obtained based on sample mean from a concentrated family of particles (e.g., the nPF algorithm performance), but we often desire a diverse sample to properly capture the distribution of the true signal. The approximation of the effective sample size serves

as a metric to indicate the level of diversity in the sample. In this section, we leverage the work on tempering of the likelihood [Nea96; MDJ06; BCJ14], combining tempering with the optimal particle filter algorithm and testing on the Lorenz '63 model, to show that the sample of the optimal particle filter algorithm can be improved while maintaining an accurate estimate of the hidden signal process. We also further clarify the strengths of the optimal particle filter algorithm in comparison to a similar optimal proposal method, the relaxation method by van Leeuwen [Lee10; Lee11], which was briefly mentioned near the end of Section 5.5.3.

Figure 5.24 demonstrates that the optimal particle filter algorithm does not maintain a diverse sample of particles, and hence often requires resampling after the particle weights are weighted by the likelihood in the Bayesian update. The concept of tempering of the likelihood is succinctly described in the recent review by van Leeuwen et al. [Lee+19]. Tempering of the likelihood falls under the category of transportation particle filters, where one considers a transformation of the particles from the prior to the posterior that does not necessarily take place in one step. In this approach, one considers a factorization of the likelihood as

$$f(y|x) = f(y|x)^{\gamma_1} \dots f(y|x)^{\gamma_m}, \quad \gamma_j > 0, \ \forall j \in \{1, \dots m\}, \quad \text{and} \quad \sum_{j=1}^{m} \gamma_j = 1.$$

Algorithmically, one modifies the prior weights based on the likelihood $f(y|x)^{\gamma_1}$, performs a re-sampling, and then repeats until the last factor $f(y|x)^{\gamma_m}$ is applied. The intuition behind such a method is that the re-weighting by the likelihood is gradual and particles that may not be very near to the observation are not immediately killed off, leading to a low effective sample size. As van Leeuwen et al. [Lee+19] mentions in their work, the resampled particles between re-weightings with the likelihood factors require some "jittering" or noise to be added, otherwise particles will be supported on the same state. Rigorously, one should make sure the perturbations of the re-sampled particle preserve the approximation of the posterior distribution. In the testing demonstrated in this section, we perturb the re-sampled particles by adding a random variable sampled from a standard normal distribution to the particle state. Although not rigorous, the approximation used here seems reasonable, since the noise is not too large in relation to the scaling of the problem and the observation noise is normally distributed.

To demonstrate the improvements gained by combining the optimal particle filtering algorithm with tempering of the likelihood, we test on the Lorenz '63 model. Since we will also compare against the relaxation method used by van Leeuwen [Lee10], we have selected the problem parameters to be the same as those tested in that work. We use 20 particles and re-sampling will occur if the effective sample size drops below 10. The initial condition is the same as that by van Leeuwen [Lee10]. Lastly, an RK4 integrator is used for the drift integration and the direction of control for nudging of the particles is constant for every 0.04 time-units.

The relaxation method similarly nudges the particles toward the observation by introducing control to the particle signal dynamics. For this method, the control in the signal dynamics takes the form,

$$X_{t_j} = f(X_{t_j}) + \hat{\beta}_{t_j} + K\left[Y_{t_k} - H(X_{t_j})\right],$$

where $t_{k-1} < t^* < t_j < t_k$ and $t^* = t_{k-1} + (t_k - t_{k-1})/2$. Therefore t_j is some integration step in the second half of the interval between the observations occurring at t_{k-1} and t_k. The term $\hat{\beta}_{t_j}$, is a noise that does not have to be the same as the original noise in the signal process. The matrix K is a gain matrix that is selected to provide sufficient nudging of the particle at X_{t_j} towards the observation Y_{t_k}. A central difference between this scheme and the optimal particle filter algorithm is that the nudging in the relaxation method does not consider where the particle is expected to arrive at time t_k, when the observation will occur, instead nudging based on its current state toward the observation. The optimal particle filtering algorithm is better suited for chaotic nonlinear problems in this sense, because it does account for the nonlinear flow and expected divergence due to any intrinsic chaotic stretching.

Figure 5.28 shows a typical result of the relaxation method with two different values of the gain matrix K, and where $Q = 2\sigma_x$. In particular, the solution in Figure 5.28(b) shows that if the gain matrix is too large, the method results in an estimated path of the signal that clearly disobeys the nonlinear dynamics of the problem; it over-nudges the particles towards the observation. Some of this behavior is seen in Figure 5.28(a), but it is less nuanced.

Figure 5.29 shows the results of a typical optimal particle filter algorithm on the same problem as in Figure 5.28, with Figure 5.29(b) not using tempering of the likelihood and Figure 5.29(a) using tempering of the likelihood applied in eight steps, each step with an exponent of 1/8. From this example, the mean of the particles may accumulate a larger error with the tempering of likelihood approach, but the spread of the particles is also increased, improving diversity, and the nudging of the optimal particle filter is able to successful bring the family of particles back towards the true signal path.

Table 5.5 summarizes the result of 32 trials of the standard particle filter (PF), the relaxation particle filter (rPF_K)–where K denotes the value of the gain matrix, the relaxation particle filter with tempering ($\text{rPF}_{\text{K,t}}$), the nudged particle filter using only one particle realization for calculation of the control nPF, and the tempered nudged particle filter nPF_t (again with only one particle realization for calculation of the control). All tempering refers to eight steps, each with an exponent of 1/8. The average RMSE in the table is the average expected at each integration step. The main conclusion is that increasing the gain of the relaxation method does not result in a lower average RMSE in comparison to nPF, nor the tempered

version nPF_t, and results in an estimated signal path that can strongly violate the natural dynamics of the problem. The table also shows that the tempering of the likelihood results in a significant increase in the effective sample size of the optimal particle filter algorithm, while forfeiting a modest amount of accuracy for estimation of the mean.

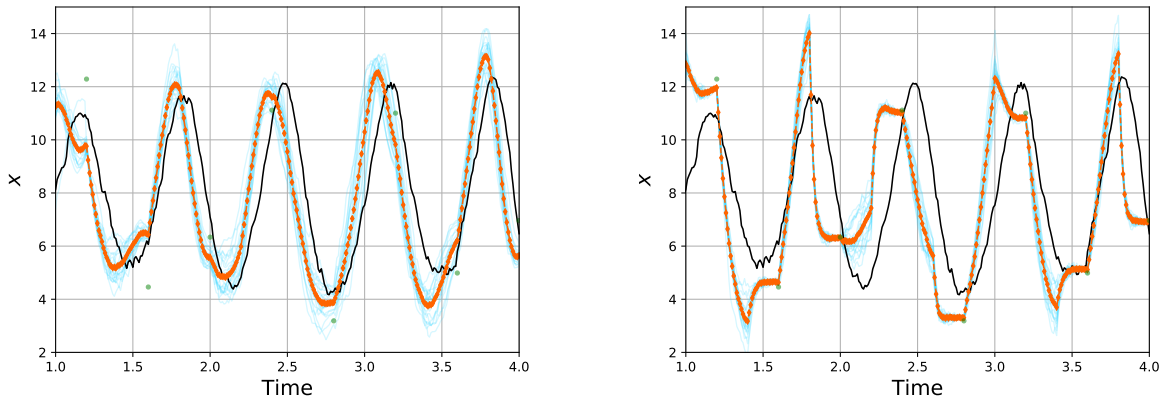

(a) Relaxation with K = 25 Q

(b) Relaxation with K = 300 Q

Figure 5.28: Relaxation method applied to the Lorenz '63 model. True signal shown in black, particles in light blue, mean of the particles in orange, and observation in green.

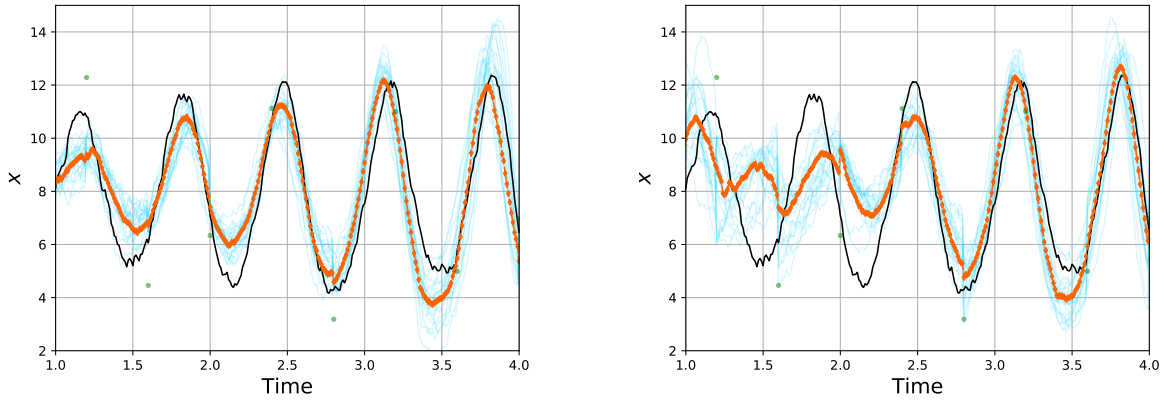

(a) nPF

(b) nPF_t, with eight equal tempering steps

Figure 5.29: Optimal particle filter method without and with tempering of the likelihood applied to the Lorenz '63 model. True signal shown in black, particles in light blue, mean of the particles in orange, and observation in green.

Table 5.5: Average RMSE at each integration step, averaged over 32 experiments.

Filter	PF	rPF_{25Q}	$\text{rPF}_{25Q,t}$	rPF_{300Q}	nPF	nPF_t
RMSE	12.28	7.66	7.58	6.71	5.79	6.51
Neff	10.88	14.98	16.95	17.07	7.49	11.90

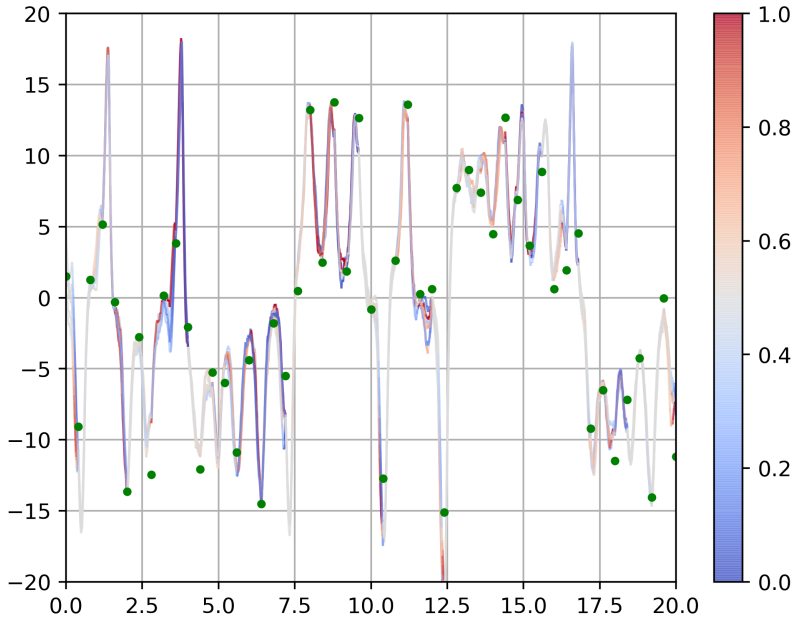

Figure 5.30: Time history of relative particle weights for a simulation of rPF on the Lorenz '63 model (see Section 5.5.4). Observations are shown in green. Particles that are blue have essentially zero weight relative to the rest of the ensemble. A color of white indicates an average weight relative to the ensemble, and coloring of red indicates the particle is overweighted relative to the rest of the ensemble.

Before moving onto the next chapter, we return to our comparison of the PF and nPF method on the Lorenz '63 model, which compared their typical particle weight history and N_{eff} values. Specifically, we look at the particle weight history of the rPF method on the same problem and show the result in Figure 5.30. In comparison to the PF and nPF weight histories, we see that the rPF is able to achieve a result somewhere between the two. That is, the ensemble is often balanced or only slightly imbalanced, and yet when particles truly are on the wrong course, they can correct by applying control. Of course a downside of rPF versus nPF was just highlighted in the previous example, which shows that rPF does require some tuning upfront (selection of the gain matrix), whereas nPF is essentially hands-off (i.e., nPF is more aware of the dynamical systems properties and therefore the algorithm shouldn't need tuning if the objective function was appropriate). In Figure 5.31, we make a comparison of the effective sample size of the rPF and nPF simulations. Showing that indeed the better balanced ensemble of Figure 5.30 translated to a higher N_{eff}

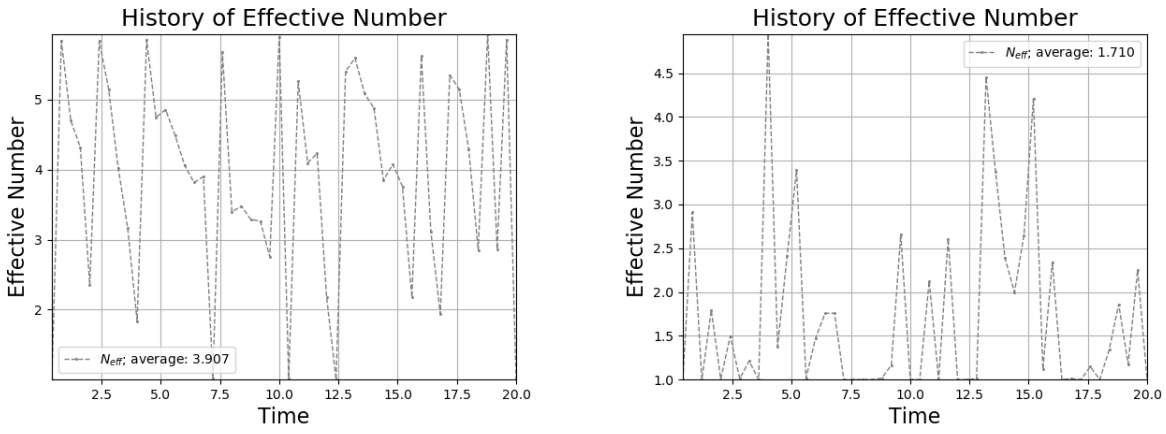

(a) rPF with K = 25 Q

(b) nPF

Figure 5.31: Time history (at observation time) of effective sample size (number) for a simulation of rPF and nPF on the Lorenz '63 model (see Section 5.5.4).

that required less re-sampling after observations.

Chapter 6

Particle Filtering and High Dimensional Chaotic Systems

In this chapter, we combine tools from the study of chaotic dynamical systems with nonlinear non-Gaussian data assimilation algorithms to produce novel particle filtering algorithms, where the use of dynamical information improves both the accuracy of estimation of the unknown state as well as improves the diversity of the particles that collectively represent the posterior distribution. Unlike past efforts of assimilation in the unstable subspace, we focus not on the deterministic signal and low observation noise case, but instead on the case of moderate signal and observation noise. Filtering algorithms using finite-time Lyapunov vectors, left-singular vectors, and a novel concept of future right-singular vectors, to project observations onto reduced subspaces are developed and tested against two regimes of the single scale Lorenz '96 model–a weakly chaotic, non-Gaussian regime and a strongly chaotic, near-Gaussian regime. As modeling in the geosciences continue to improve resolution and fidelity of finer physical processes, the models are requiring data assimilation techniques that can handle the fully nonlinear, non-Gaussian case and represent multimodal distributions in high dimensional spaces. This chapter contributes to pushing the boundary of nonlinear data assimilation by aiming to improve particle filtering algorithms for high dimensional chaotic systems. The results of this chapter have appeared in [BS20].

6.1 Introduction

The approach taken in this chapter follows a thread of logic started by Trevisan et al. [TDT10; PCT13] for deterministic signal processes with low observation noise and for the linear Gaussian assimilation case. Through these and several other works, the terminology of assimilation in the unstable subspace (AUS) took hold. The idea is to perform the assimilation step in a subspace so as to improve the filtering method in some way. In the case of Trevisan's efforts, this meant decreased run-time and simpler algorithm setup. They showed that modifying an extended Kalman filter (EKF) with AUS resulted in filtering nearly as well as the standard EKF, and that 4D-var with AUS was a slight improvement in estimation capability as well as numerical efficiency. Bocquet and Carrassi [BC17] have extended these ideas to an iterative ensemble Kalman

smoother (IEnKS) and have tested on cases with moderate observation noise. Most recently, efforts to bring these ideas across to particle filtering have begun [Lee+18; MV19], still in the case of deterministic signal, low observation noise, and like the other works, only using finite-time Lyapunov vectors–to be explained in Section 6.2. In the linear Gaussian case, it has been shown that the AUS has theoretical convergence results [TP11; Boc+17]

In this chapter, we take a step to remedy the divergence and degeneracy issues of particle filters by using the local geometry defined from unstable, neutral, and stable subspaces of the chaotic system that we are performing filtering on. In Section 6.2 we will review the background on Lyapunov exponents and vectors and Oseledets' subspaces that provide this geometric splitting of the tangent bundle. We then proceed to discuss related finite-time variants of Lyapunov exponents and vectors that also approximate local subspaces where error growth occurs fastest. Section 6.3 will introduce a parameterized chaotic model that is often used in testing of new assimilation methods, and will be our testbed model for numerical investigation in Section 6.4. In Section 5.1.2 we provided the theory and algorithms behind standard sequential importance sampling particle filtering, and in Section 5.5.1, the nudged particle filter method that performs well for chaotic systems was introduced. Variants of these two approaches will be constructed in Section 6.3.3, such that they use assimilation in the unstable subspace. We finish this chapter by analyzing the performance of the various filtering methods in Section 6.4 and provide many useful statements regarding potential improvements in Section 6.5.

6.2 Lyapunov Exponents, Vectors, and Variants

Lyapunov exponents and their associated vectors provide a powerful tool to characterize dynamical systems, in particular ergodic systems. We briefly recall the main ideas of the theory to set notation and stage for the ideas to be used in this chapter.

Consider a dynamical system defined by a flow $\varphi : M \times \mathbb{R} \to M$ on a smooth Riemannian manifold M. For concreteness, one can consider a deterministic process given by,

$$dX_t = b(X_t)dt, \qquad X_0 = p \in M, \tag{6.2.1}$$

then the orbit $(X_t)_{t\in I}$, for some $I \subset \mathbb{R}$ interval, is equivalent to the flow evaluated at p for $t \in I$; that is, $(\varphi_t(p))_{t\in I}$.

Denote the tangent bundle as $TM \equiv \coprod_{p\in M} T_pM$, where $p \in M$ and hence TM is the disjoint union of the tangent spaces T_pM at each point $p \in M$. The elements $v \in T_pM$ are tangent vectors. Let $D\varphi_t$ denote

the differential of the flow map from time zero to time t. $D\varphi_t(p)$ has the action of moving tangent vectors from T_pM to tangent vectors at $T_{\varphi_t(p)}M$. Define the *Lyapunov exponent* at $(p, v) \in TM$ as follows:

$$\begin{aligned} \lambda : TM &\longrightarrow \mathbb{R} \\ (p, v) &\longmapsto \lambda(p, v) \equiv \lim_{t\to\infty} \frac{1}{|t|} \ln \|D\varphi_t(p)v\|, \end{aligned} \tag{6.2.2}$$

with the condition that the limit exists.

Oseledets' multiplicative ergodic theorem [Ose68] states that if (φ, M, μ) is an ergodic dynamical system with μ an ergodic measure on M for which φ, a diffeomorphism, is a measure preserving map, then there are constant numbers,

$$\lambda_1(p) > \cdots > \lambda_r(p),$$

with multiplicities $m_r(p), \ldots, m_1(p)$, and a splitting of the tangent space,

$$T_pM = E_p^1 \otimes \cdots \otimes E_p^r$$

such that

$$\begin{aligned} E^i_{\varphi_t(p)} &= D\varphi_t(p)E^i_p \\ \lambda_i &= \lim_{t\to\pm\infty} \frac{1}{|t|} \ln \|D\varphi_t(p)v_i\|, \end{aligned}$$

for all $1 \leq i \leq r$, $v_i \in E^i_p$ and the result holds for μ-a.e. $p \in M$. Further, the sum of the multiplicities m_i equal $\dim(M)$. Hence, on a finite dimensional space, we can characterize the asymptotic behavior of infinitesimal perturbations for almost every point using a finite number of constant values and a subspace filtration of the tangent space. The *Lyapunov vectors*[1] are then defined as a basis of the subspaces that are covariant under $D\varphi_t$ in the sense that the Lyapunov vector v_i associated with λ_i will map forward or backward in time to the subspace $E^i_{\varphi_t}$. The above result can also be extended to random dynamical systems (see for instance [Arn03]).

The number of positive Lyapunov exponents sets a lower bound on the dimension of the subspace of the tangent space that any predictive or assimilation method should account for. The numerical generation of the Lyapunov exponents and vectors is well described in several papers [Ben+80; WS07; KP12; Gin+13].

[1] Also referred to as covariant Lyapunov vectors by some authors, for the purpose of distinguishing from finite-time Lyapunov vectors.

6.2.1 Dimension of the Attractor and Entropy

When the chaotic system is dissipative, solutions will eventually reside on an attractor. The dimension of the attractor, and hence the minimum number of degrees of freedom needed to describe a point on it, can be well approximated by the Kaplan-Yorke[2] dimension [Fre+83]. Let $j \in (1, \ldots, r)$ correspond to the largest index such that $\sum_{i=1}^{j} \lambda_j m_j > 0$. Then the Kaplan-Yorke dimension is given by

$$\begin{cases} \dim(M), & \text{if } \sum_{i=1}^{j} m_i = \dim(M), \\ \sum_{i=1}^{j} m_i - \frac{1}{\lambda_{j+1}} \sum_{i=1}^{j} \lambda_i m_i, & \text{otherwise.} \end{cases}$$

A similarly important characterization of a chaotic dynamical system is given by the definition of the metric entropy, or Kolmogorov-Sinai entropy, which measures the rate of increase in dynamical complexity as the system evolves with time. Pesin [Pes77] and Ruelle [Rue78] proved relations linking metric entropy and the positive Lyapunov exponents. The general case given by Ruelle is,

$$h_\mu(\varphi) \leq \int_M \sum_{i \in J} \lambda_i(p) \dim(E_p^i) \mu(dp), \tag{6.2.3}$$

where $h_\mu(\varphi)$ is the metric entropy of (φ, M, μ) (see [BP02, p.130] for a definition), and J is the index set corresponding to positive Lyapunov exponents. Pesin [Pes77] showed that there is no wasted expansion in conservative systems–all expansion goes into the creation of entropy, that is, if μ is equivalent to Lebesgue measure (i.e., $\mu \ll \mu_L$), then we have an equality in Eq. 6.2.3. In the case of dissipative systems, as considered in this chapter, the invariant measure of interest is called a Sinai-Ruelle-Bowen (SRB) measure. Ledrappier and Young [LY84] showed that when $\lambda_1 > 0$, equality in Eq. 6.2.3 holds if and only if μ is an SRB measure. In a subsequent paper, they showed that in the case of random diffeomorphisms of a compact manifold, that if $\mu \ll \mu_L$ and $\lambda_1 > 0$ then again equality of Eq. 6.2.3 holds [LY88]; which reinforces the idea that evolution in the unstable Lyapunov subspace explains the uncertainty in prediction, and motion in the stable directions is inconsequential. We will use this last result in Section 6.3 alongside the characterization of SRB measures as the zero-noise limit [You13] to rationalize the calculation of the Kolmogorov-Sinai entropy.

6.2.2 Finite-Time Lyapunov Exponents and Vectors

As readily seen from Eq. 6.2.2, the definition of Lyapunov exponents and vectors is in the limit as time tends to infinity, but more often in applications one is interested in a finite-time interval. In that case, a similar

[2] Also referred to as the Lyapunov dimension

definition can be given,

$$\lambda_t(p, v) \equiv \frac{1}{|t|} \ln \|D\varphi_t(p)v\|,$$

for any $t \in [0, \infty)$. In this case, we do not have Oseledets' result and must consider the base point when calculating the *finite-time Lyapunov exponent*.

The numerical calculation of the finite-time Lyapunov exponents and vectors can be achieved following a QR based algorithm by Benettin et al. [Ben+80]. To do so, one calculates the fundamental matrix $D\varphi_{\delta t} \in \mathbb{R}^{m\times m}$ by integrating an orthogonal set of basis vectors Q_0 under the tangent linear dynamics for a small time interval δt and then applying a QR decomposition of $D\varphi_{\delta t}$, which yields an orthogonal matrix Q_1 of basis vectors and an upper triangular matrix R_1. The new orthogonal matrix Q_1 is in turn integrated forward and another QR decomposition is performed. This is continued until the desired final finite-time is reached. The final orthogonal matrix Q^* provides a basis for the final tangent space and the finite-time Lyapunov exponents can be calculated based on the history of matrices (R_i). Because of the use of a modified Gram-Schmidt procedure to produce Q_i during each QR decomposition, the finite-time Lyapunov vectors are sometimes referred to as Gram-Schmidt vectors.

Of importance is the fact that the first finite-time Lyapunov vector will tend toward the maximal covariant Lyapunov vector. Further, the finite-time Lyapunov vectors provide a splitting of the tangent space at the final time into an associated unstable, neutral, and stable subspace with respect to their associated finite-time Lyapunov exponents. For these reasons, finite-time Lyapunov exponents and vectors have been the choice for defining the unstable and neutral subspaces used in assimilation in the unstable subspace methods [TDT10; PCT13; BC17; MV19].

6.2.3 Singular Vectors of the Fundamental Matrix

In this chapter, we look instead to a different set of vectors that similarly define subspaces corresponding to local dynamics that expand or contract. These vectors are called *singular vectors* due to the numerical operation by which they are retrieved from the decomposition of a matrix. Although any matrix will do, let us consider the fundamental matrix $D\varphi_t(p) \in \mathbb{R}^{m\times m}$ along an orbit $\varphi_t(p)$ from time zero to time t. This matrix can always be decomposed into the following,

$$D\varphi_t(p) = U\Sigma V^T,$$

where U is a unitary matrix of *left-singular vectors* of $D\varphi_t(p)$ and V a unitary matrix of *right-singular vectors*. Σ is a diagonal matrix with non-negative elements along the diagonal called *singular values* and denoted by $(\sigma_i)_{i\in\{1,\dots,m\}}$. The singular values are ordered: $\sigma_1 \geq \sigma_2 \geq \cdots \geq \sigma_n \geq 0$.

Having decomposed a matrix A into its singular valued decomposition (SVD), $A = U\Sigma V^T$, one can interpret the mapping of a vector ξ under $A\xi$ as performing three operations: 1. V^T rotates ξ into a new coordinate frame, 2. Σ expands or contracts $V^T\xi$ along the canonical directions of this new frame, 3. U rotates the expanded or stretched vector back to the original coordinate frame. A second convenient notation for the SVD is $A = \sum_i \sigma_i \cdot u_i \otimes v_i$, which emphasis that fact that the SVD will map the vectors v_i to u_i and stretch by the factor σ_i. If $\sigma_i > 1$, then expansion occurs, and similarly $\sigma_i < 1$ corresponds to contraction. Because of the ordering of (σ_i), this implies an ordering of the vectors from the domain which are stretched the most–with v_1 being the direction that is extended the most.

In this chapter, we use the singular vectors to perform our assimilation in a subspace corresponding to instability. In particular, we will use the right-singular vectors of the future observation interval. Both choices are novel and prove effective on a model with moderate signal and observation noise, despite the fact that all stability indices, including singular vectors, are only true for describing infinitesimal growth. One study from the literature that provides motivation for the use of singular vectors instead of Lyapunov vectors comes from a paper by Norwood et al. [Nor+13], where they compared the behavior and predictive quality of Lyapunov vectors, singular vectors and bred vectors on the Lorenz '63 model as well as a coupled Lorenz '63 model. One of the central results is that singular vectors grew much faster and were the most accurate predictors of regime change.

6.3 The Single Timescale Lorenz 1996 Model

The chaotic model that will be used in this chapter to explore ideas of nonlinear non-Gaussian data assimilation with projection operators onto unstable and neutral subspaces is the single timescale Lorenz '96 model, which was first introduced by Lorenz [Lor95] to study predictability of atmospheric dynamics. One will recognize this is the same model as given in Section 5.2.2, but without the fast scale. The model is not derived from physical laws, but simply mimics properties of geophysical models such as energy-preserving advection, damping and forcing. The model is given by

$$dX_t^j = (X_t^{j-1}(X_t^{j+1} - X_t^{j-2}) - X_t^j + F)dt, \tag{6.3.1}$$

where $j \in \{0, \ldots, J\}$ and the model has a periodic boundary condition $X_t^0 = X_t^J$ for all t. With $J = 40$, one can think of X as representing an unspecified scalar meteorological quantity equally spaced along a midlatitude belt of approximately 30,000 km, thereby giving the model the correct synodic scale to mimic Rossby waves. Because the model mimics this atmospheric feature, Lorenz suggests that one consider 0.05 time units to equate to a 6 hour interval, which is common to assume when choosing parameters for data assimilation trials. We will do the same in this chapter.

As shown by Majda et al. [AG05], the model can vary from weak to strongly chaotic and turbulent based on the strength of the forcing F. Decorrelation times also suggest the model to be ergodic. Because the model mimics geophysical process and can be varied in resolution as well as dynamical characteristics, the model has become a regular testbed for demonstrating new data assimilation methods–as we do in this chapter.

The data assimilation algorithm described in Section 5.5.1 requires that the dynamical process to be estimated is a stochastic process. For this reason and because modelers are increasingly using stochastic models in practice, we will consider a variant of the Lorenz '96 model with an additive noise term. First consider Eq. 6.3.1 in the abstract form of Eq. 6.2.1, then we will consider the stochastic Lorenz '96 model, which we will refer to as Lorenz '96 from here forward, as

$$dX_t = b(X_t)dt + \sigma dW_t, \tag{6.3.2}$$

where W is a standard Brownian motion taking values in $\mathbb{R}^{40}$ and $Q \equiv \sigma\sigma^T = I$ is simply the identity matrix. We write Eq. 6.3.2 with σ to improve the generality of the theory in Section 5.1. Modeling physical processes with stochastic terms is becoming more relevant as a technique to capture unmodeled smaller scale processes that have been removed or truncated from the original process. Therefore, one can rationalize the term, σdW_t, as capturing these unmodeled processes.

Our earlier reference to the result by Ledrappier and Young [LY88] regarding a relation between Kolmogorov-Sinai entropy and Lyapunov exponents required the random diffeomorphisms of a compact manifold. We do not have a compact manifold, but a recurrent condition is sufficient to replace this condition, and Eq. 6.3.1 will satisfy this–one needs that for some $r > 0$ any state x outside of a sufficiently large ball, we have $\langle b(x), x/|x| \rangle < -r|x|$. This condition provides the existence of a stationary distribution and the strict positive definiteness of Q provides uniqueness.

6.3.1 Weakly Chaotic, Non-Gaussian Regime

In Section 6.4, we will be interested in exploring the efficacy of the data assimilation algorithms developed in Sections 5.1.2, 5.5.1, and 6.3.3. First, we will consider the capability of the algorithms when applied to a weakly chaotic system that mimics synodic scale dynamics and for which one can show to be strongly non-Gaussian in its modes. Setting the Lorenz '96 model with $F = 5$ achieves exactly this case [AG05].

A solution of the deterministic equations, Eq. 6.3.1, for $F = 5$ is shown in Figure 6.1 and contrasts with a single realization of Eq. 6.3.2 with $F = 5$ and the same initial conditions. We use an RK4 integrator for the deterministic case and RK4-Maruyama for stochastic integration, both with a step size of 1E-2. A Lanczos interpolation scheme has been used to enhance visualization. The ability of the signal noise to disrupt the more coherent patterns of the deterministic case is clear. The bottom axis provides a time change to what we call Lyapunov time $\lambda_1 t$, with λ_1 being the top (maximal) Lyapunov exponent.

Dynamical Characterization

Using the ideas and results of Section 6.2, we can provide a characterization of the dynamical system based on the Lyapunov exponents. In particular, a simulation of 100 time units, with modified Gram-Schmidt regularization every 0.1 time units, and $F = 5$ yields the following:

- Largest Lyapunov exponent: $\lambda_1 = 0.397$
- Error doubling time: 1.745
- Number of strictly positive Lyapunov exponents: 9
- Number of neutral, $\lambda \in$ [-1E-2, 1E-2], exponents: 2
- Number of strictly negative Lyapunov exponents: 31
- Kaplan-Yorke dimension: 15.429
- Kolmogorov-Sinai entropy: 1.297.

The dynamical characterization of the model just given indicates that: 1. it is a chaotic model, 2. the average amount of time for error to double due to stretching is 1.745 time units, 3. ensemble methods (i.e., particle based filtering methods) should require on average 9 to 11 particles to span the unstable and neutral subspaces, 4. but the attractor dimension is approximated by Kaplan-Yorke and suggests a higher number of 15 to 16.

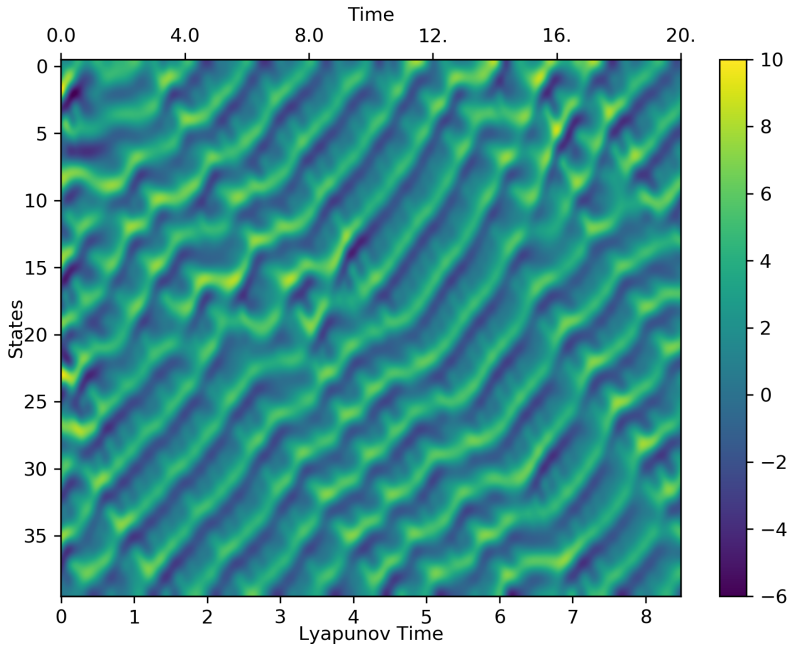

Figure 6.1: Depiction of the dynamics of the Lorenz '96 model with $F = 5$ and $J = 40$. The top x-axis provides time in the natural units of the Lorenz '96 model, while the bottom x-axis provides the Lyapunov time $\lambda_1 t$.

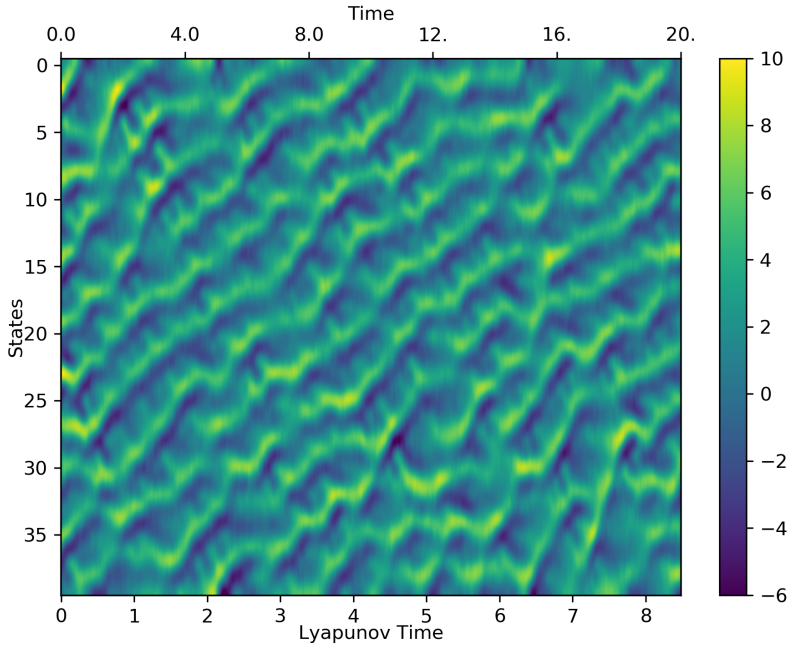

Figure 6.2: Depiction of a stochastic realization of the Lorenz '96 model with $F = 5, J = 40$ and $Q = I$. The top x-axis provides time in the natural units of the Lorenz '96 model, while the bottom x-axis provides the Lyapunov time $\lambda_1 t$, with λ_1 calculated from the deterministic model.

6.3.2 Strongly Chaotic, Near-Gaussian Regime

A perhaps more widely benchmarked parameterization of the Lorenz '96 model is with $F = 8$. In this case, the model is nearly-Gaussian, but strongly chaotic. As F approaches 16, the model becomes fully turbulent. Our motivation to also test in the strongly chaotic regime is due to the increasing resolution in numerical weather prediction and hence need to model convective scale processes (see for instance [Yan+18; Car+18]). This is part of the motivation for greater capability with particle filters–alongside the non-Gaussian multimodal case.

We again contrast a deterministic simulation of Lorenz '96 with a stochastic realization in Figures 6.3 and 6.4. Because the model is strongly chaotic, it is slightly harder to discern the change in patterns of the flow between the two simulations. The legend in Figures 6.3 and 6.4 are capped to the minimal and maximal same values based on Figure 6.3 results, but it is clear that the stochastic realization seems to saturate more at the minimal and maximal values due to the random fluctuations.

Dynamical Characterization

Again, using the ideas and results of Section 6.2, we can provide a characterization of the dynamical system based on the Lyapunov exponents and compare against those for the $F = 5$ case. A simulation of 100 time units, with modified Gram-Schmidt regularization every 0.1 time units, yields the following when $F = 8$:

- Largest Lyapunov exponent: $\lambda_1 = 1.753$
- Error doubling time: 0.395
- Number of strictly positive Lyapunov exponents: 14
- Number of neutral, $\lambda \in$ [-1E-2, 1E-2], exponents: 0
- Number of strictly negative Lyapunov exponents: 26
- Kaplan-Yorke dimension: 27.218
- Kolmogorov-Sinai entropy: 10.805.

The $F = 8$ has a much larger maximal Lyapunov exponent, resulting in an error doubling time that would equate to approximately 2 days using the typical 0.05 time-units to 6 hour conversion. In the strongly chaotic regime, the unstable subspace and dimension of the attractor are much greater, implying the need for a larger ensemble to adequately capture the posterior distribution.

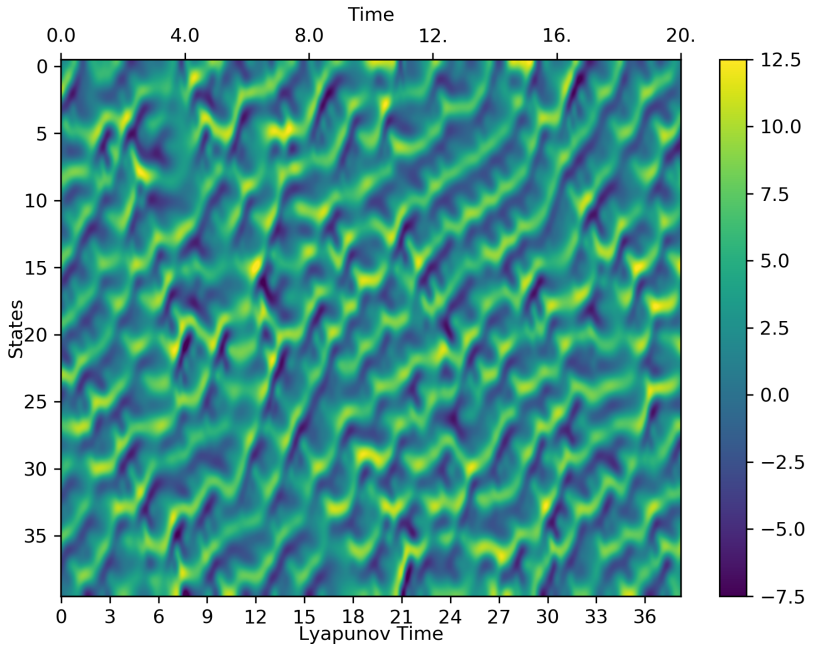

Figure 6.3: Depiction of the dynamics of the Lorenz '96 model with $F = 8$ and $J = 40$. The top x-axis provides time in the natural units of the Lorenz '96 model, while the bottom x-axis provides the Lyapunov time $\lambda_1 t$.

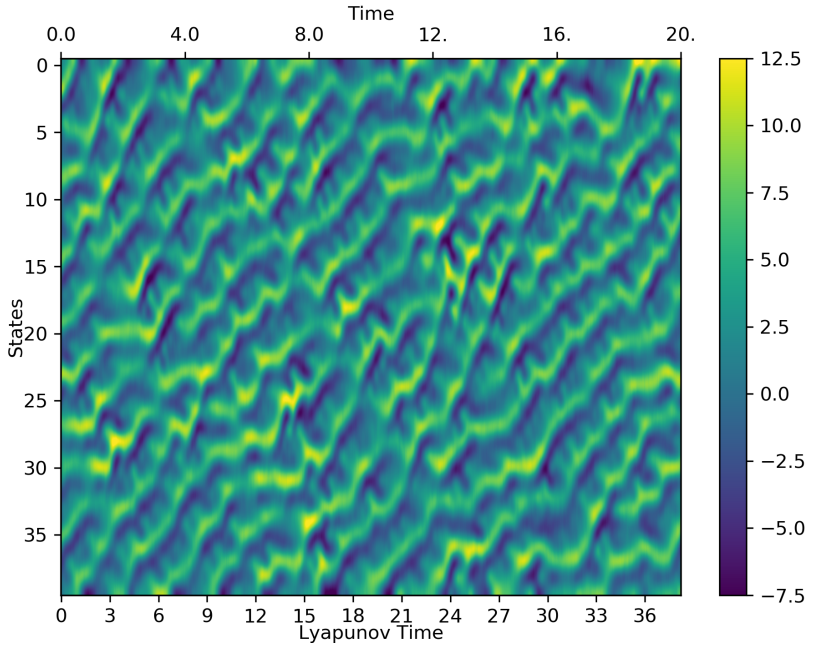

Figure 6.4: Depiction of a stochastic realization of the Lorenz '96 model with $F = 8, J = 40$ and $Q = I$. The top x-axis provides time in the natural units of the Lorenz '96 model, while the bottom x-axis provides the Lyapunov time $\lambda_1 t$, with λ_1 calculated from the deterministic model.

6.3.3 Projected Particle Filtering

In this section, both the PF and nPF algorithms given in Sections 5.1.1 and 5.1.2 are expanded into new filtering algorithms using various projections onto associated unstable subspaces. All of the aforementioned algorithms are then tested and compared on the Lorenz '96 model in Section 6.4.

As previously remarked, particle filters suffer from filter divergence and degeneracy. The nPF algorithm remedies the divergence issue by adding a nudging term to the particles that ensure their ability to move to a more appropriate neighborhood of the observation and therefore avoid receiving an extremely low weight during the likelihood update (see step 3. of the PF algorithm, step 6. of the nPF algorithm). In the case where observation noise is quite low, for example R is a diagonal matrix with small values, then particles are heavily penalized for being moderately far from the observations in the likelihood update. Numerically, the low observation noise case is often quite worse, because underflow can occur, due to the finite floating point precision, and therefore, particles can attain a weight of zero–what we refer to as a *dead* particle. More often, after the re-weighting of the particles (see step 4. of the PF algorithm, step 7. of the nPF algorithm), one particle has most of the weight, whereas the others are nearly zero. This is the case of particle degeneracy or particle collapse.

As shown by Snyder et al. [Sny+08; SBM15] through simplifying asymptotic analysis, one needs an exponentially increasing number of particles, dependent on the dimension of the observation space, to avoid such collapse. Experience with simulations in the finite-time case, mean that such a scaling is not quite as bad. It does lend credence to the idea of minimizing the observation space dimension and therefore reducing the chance of degeneracy, as well as promoting a more diverse, evenly weighted population of particles. It is with this motivation, as well as the theoretical result of the asymptotic convergence of the support of the covariance matrix in the case of linear Gaussian data assimilation to the unstable subspace [TP11; Boc+17], that we consider the projection of our observations into a reduced subspace and applying assimilation–the likelihood update–in this reduced space. A further remark is that with projecting the observation to a subspace, one expects to lose information that may be valuable, but if the subspace is chosen appropriately, the amount of information may be insignificant and the ability to assimilate in a lower dimensional space will out-weight the loss of said information.

Projection Operators

We now describe the projection of the observation error and finish with describing how we modify the PF and nPF algorithms to use such projections. We follow a similar thread of ideas as outlined in the projection framework by Maclean and Van Vleck [MV19]. Because we will only construct dynamical vectors that are

orthogonal, for instance, the finite-time Lyapunov vectors or left, right-singular vectors in Section 6.2, we will only be concerned with orthogonal projection operators using the dynamical information.

First, let $S \in \mathbb{R}^{m \times n}$ be a matrix with orthogonal columns and $m > n$. Then an orthogonal projection operator from $\mathbb{R}^m$ to the subspace of dimension n spanned by the columns of S is given by $P = SS^T$. Based on the dynamical vectors discussed in Section 6.2, S could be the vectors of the finite-time Lyapunov vectors associated with positive and neutral exponents, or similarly the left or right-singular vectors associated with singular values indicating directions of expansion. An oblique projection operator is needed if one is to use the covariant Lyapunov vectors, since these are in general non-orthogonal.

Consider H to be a linear sensor function and $\epsilon = y - Hx$ to be the observation error. Because our projection operator P just defined is a mapping in the dynamical state space, we must map the observation error to this space. This is easily accomplished by defining a normalized projection factor $\widehat{H} = H^T(HH^T)^{-1}$. In the case that $H = I$, the identity matrix, as considered in Section 6.4, then $\widehat{H} = I$ trivially. The projected observation error is then $\widehat{\epsilon} = \widehat{H}\epsilon$.

Combining the mapping from observation space with the projection into a reduced subspace of the state space, we define the following projection factor, $\widehat{S} \equiv S^T\widehat{H}$, which can be used to define a projected observation covariance $\widehat{R} \equiv \widehat{S}R\widehat{S}^T$, that will be used in the following algorithms.

Particle Filters with Finite-Time Lyapunov Vectors

Using the projection operators described in Section 6.3.3, we now construct a particle filter algorithm that uses the finite-time Lyapunov exponents and vectors generated between observations to reduce the effective observation dimension. Given the posterior distribution at time t_k, let $\overline{p}$ be the expected state. The QR algorithm described in Section 6.2 is then used to continually orthogonalize the fundamental matrix $D\varphi_{t_{k+1}}(t_k, \overline{p})$, providing a final orthogonal matrix $\widetilde{S} \in \mathbb{R}^{m \times m}$ and m finite-time Lyapunov exponents. We now define S to be the subset of $\widetilde{S}$ of columns corresponding to the positive finite-time Lyapunov exponents. If no positive finite-time Lyapunov exponents exists during an observation interval–unlikely in the high dimensional and strongly chaotic case–then we choose the first column of $\widetilde{S}$ for defining S. Following the projection operator construction given in Section 6.3.3, we redefine the likelihood update in the PF and nPF algorithms (steps 3. and 6. respectively) to be,

$$w_{k+1}^j \propto w_k^j \exp\left(-\frac{1}{2}\widehat{\epsilon}^T\widehat{R}^{-1}\widehat{\epsilon}\right). \tag{6.3.3}$$

Particle Filters with Future Right-Singular Vectors

The novelty of the algorithm described in this section is twofold: 1. we build our projection operators based on singular vectors, and more importantly, 2. we use a future set of right-singular vectors to do so. What is meant by future right-singular vectors is that if the current posterior is for time t_k, the next observation is at time t_{k+1}, then we generate the fundamental matrix from time t_{k+1} to t_{k+2} driven by an orbit with initial condition being the observation received at time t_{k+1}, and then extract the right-singular vectors from this fundamental matrix. Similar to the idea of the nPF algorithm, we are using the observation at the next time to produce some control over the particle filtering algorithm, in this instance the projection of the observation to a reduced subspace. The reasoning for using the future right-singular vectors, is that the subspace spanned by the subset of these vectors corresponding to positive growth, will be the directions where error will grow most over the future observation interval. Therefore emphasizing the importance of particles that perform well in that reduced subspace should promote a healthier collection of particles at the t_{k+2} observation.

Just as in the algorithm using the finite-time Lyapunov vectors, we set S to be the columns of V–the right-singular vectors of $D\varphi_{t_{k+2}}(t_{k+1}, y_{k+1})$–corresponding to the singular values taking values greater than one. And in the rare case that no singular values correspond to growth, we again select just the leading right-singular vector. Following the general procedure, the new likelihood update is the same as that in Eq. 6.3.3.

Particle Filters with Left-Singular Vectors

For a final comparison of projection operators, we also consider the use of the left-singular vectors, but generated from the current time t_k to the observation time t_{k+1}. Like the finite-time Lyapunov vectors, the left-singular vectors corresponding to singular values of growth will span a subspace at the observation time to which the largest growth in error will be mapped. Hence, the desire to use left-singular vectors is to emphasis weighting of particles at observation time based on directions where error would have had the most relative growth.

6.4 Application to the Single Timescale Lorenz 1996 Model

In this section, we perform numerical experiments of the various particle filtering approaches. We do this on both the weakly chaotic, non-Gaussian form of the Lorenz '96 model, as well as the strongly chaotic, near-Gaussian regime. In both cases, we use moderate signal and observation noise, $Q = R = I$. And use a sensor matrix $H = I$, implying that all states are observed. Observations occur every $\Delta t = 0.05$ time

units, corresponding to 6 hours, and we simulate for $t_f = 20$ time units, or 100 days. The threshold for resampling occurs when N_{eff} falls below $N/2$, half the number of particles. We trial each particle filtering algorithm on 96 simulations and compute averages based on these results. An RK4 integrator is used for deterministic integration (e.g., to compute the finite-time Lyapunov vectors or singular vectors) and an RK4-Maruyama scheme is applied for stochastic integration, both with a step size of 1E-2. In the case of the nPF algorithms, we use four control steps between observations with two realizations per particle to calculate control. We denote algorithms using the finite-time Lyapunov vectors for projection with the superscript $\cdot^\star$, the left-singular vectors with $\cdot^\dagger$, and the future right-singular vectors with $\cdot^\ddagger$. Lastly, the root-mean-square error (RMSE) at time t is given by,

$$\text{RMSE}(t) = \sqrt{\langle X_t - \mathbb{E}X_t \rangle},$$

where X_t is the true solution. The average RMSE over time is then $\frac{1}{M}\sum_{i=1}^{M} \text{RMSE}(t_i)$, where M is the total number of integration steps.

6.4.1 Results of the Weakly Chaotic, Non-Gaussian Regime

We first consider the case where $F = 5$ for the Lorenz '96 model. We set the number of particles to $N = 8$, slightly less than the number of positive Lyapunov exponents.

Figures 6.5 and 6.6 show the absolute mean error of a typical single simulation using the PF and nPF algorithms for this case. Any absolute error above three is saturated for the figures. Vertical streaks, that appear as "artifacts", are an indication of resampling occurring at those times. As expected, Figure 6.6 shows that the nPF performance is a clear improvement over the PF algorithm shown in Figure 6.5.

Table 6.1 provides a comparison of the average RMSE, average effective sample size and total run-time of the PF, PF‡, nPF, and nPF‡ algorithms. What is clear from the results in this table is that the nPF algorithm is able to provide a much improved tracking of the mean over the PF algorithm, but with only slightly improved effective sample size. In both cases of the PF and the nPF algorithms, the addition of using the future right-singular vectors (i.e., the PF‡ and nPF‡ algorithms) provided a noticeable improvement in the average RMSE and effective sample size. Although this required additional run-time due to the computation of the fundamental matrix, SVD decomposition and associated linear algebra for the projection operations, the offset is likely worth it–as opposed to increasing the number of particles in the non-projection based algorithms. It should be further noted that the extra run-time required in these simulations was not optimized, with every particle performing the SVD decomposition, and all associated linear algebra for the

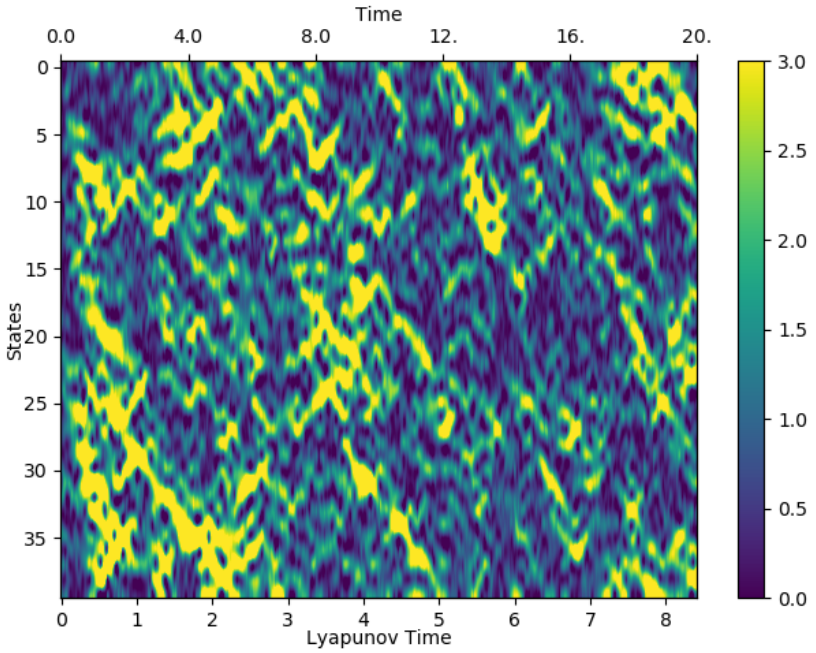

Figure 6.5: The absolute error between the true state and the mean state for a single simulation of the Lorenz '96 model with $F = 5$ using the PF algorithm. The average RMSE for this simulation was 10.85. The top x-axis provides time in the natural units of the Lorenz '96 model, while the bottom x-axis provides the Lyapunov time $\lambda_1 t$.

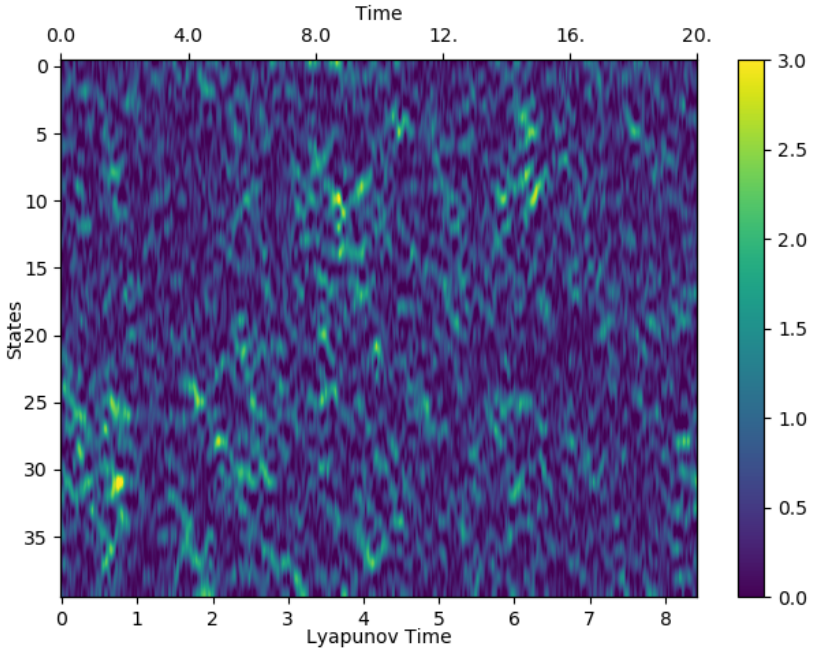

Figure 6.6: The absolute error between the true state and the mean state for a single simulation of the Lorenz '96 model with $F = 5$ using the nPF algorithm. The average RMSE for this simulation was 4.31. The top x-axis provides time in the natural units of the Lorenz '96 model, while the bottom x-axis provides the Lyapunov time $\lambda_1 t$.

projection operations, and hence, this extra run-time could be substantially decreased.

Table 6.1: Results for 96 simulations of filtering on the Lorenz '96 model with $F = 5$, using 8 particles and $\Delta t = 0.05$. The average rank of the right-singular value projection operators was 14.6, in comparison to the dimension Lorenz '96 at $N = 40$. The average RMSE for the observation error was 1.41.

Filter	PF	PF‡	nPF	nPF‡
Avg. RMSE	14.3	13.8	4.66	4.56
Avg. N_{eff}	2.00	2.51	2.48	2.86
Total Run-Time	170 s	429 s	2140 s	2404 s

Table 6.2 provides some further comparisons for just the PF algorithm with the various projection operators, the nPF case yielding similar trends. The result shows that only the future right-singular vectors (PF‡) were able to both reduce RMSE and improve N_{eff}. It is important that both occur, since it is possible to have the ensemble diverge slightly from the truth, resulting in a worse RMSE and yet improved N_{eff}–this would appear to be the case of the finite-time Lyapunov vector (PF*) algorithm. The left-singular vector algorithm (PF†) also follows this trend, but to a lesser extent. The fact that the average rank of the projection (Avg. Proj. Rank) created from finite-time Lyapunov vectors is so much smaller than the singular vectors is surprising, yet in-line with the observation by Norwood et al. [Nor+13] that the singular vectors react much quicker to growth and contraction.

Table 6.2: Results for 96 simulations of filtering on the Lorenz '96 model with $F = 5$, using 8 particles and $\Delta t = 0.05$. The average RMSE for the observation error was 1.41.

Filter	PF	PF*	PF†	PF‡
Avg. RMSE	14.3	20.7	15.3	13.8
Avg. N_{eff}	2.00	4.62	2.26	2.51
Avg. Proj. Rank	—	1.8	14.8	14.6
Total Run-Time	170 s	272 s	461 s	429 s

The slightly longer run-time of the left-singular vector case versus the right-singular vector is due to the fact that the average projection rank is slightly higher for the left-singular vector case and therefore the linear algebra is on average slightly more expensive. Because an SVD routine is not required for the finite-time Lyapunov vector algorithm (PF*), it is substantially faster than either the PF† or PF‡ algorithms. In the case of the nPF* or nPF† algorithms, it may be possible to improve run-time a bit further than nPF‡, since the fundamental matrix must be generated for each realization of the nudging control in Eq. 5.5.6 and hence, it may be possible to use this matrix or an expectation of this matrix instead of generating an additional approximation for each observation interval.

6.4.2 Results of the Strongly Chaotic, Near-Gaussian Regime

For the case where $F = 8$, we set the number of particles to $N = 16$. This is slightly more than the number of positive Lyapunov exponents, but far less than the Kaplan-Yorke dimension.

The results of the PF, nPF and algorithm variants using the future right-singular vectors is shown in Table 6.3. The difficulty of filtering this strongly chaotic system with so few particles is apparent by the extra entry in the table labeled *Dead Simulations*. In the case of the PF algorithm, 17 of the 96 simulations did not finish because at some observation, all the particles had weights zero or essentially zero, such that nothing significant could be said about the statistics at that time nor could a meaningful resampling occur. The ability for the PF‡ simulation to solve all 96 cases is a reflection that the assimilation occurring in the reduced subspace spanned by the future right-singular vectors was indeed beneficial to improving the effective sample size of the ensemble. Though the quality of filtering with the PF variants is insufficient with 16 particles, we include Table 6.4 to show that both finite-time Lyapunov vectors (PF*) and left-singular vectors (PF†) similarly improve overall filtering performance by also avoiding dead simulations, though neither have an RMSE as low as the right-singular vector case. Both finite-time Lyapunov vectors and left-singular vectors improve the effective sample size. The PF* algorithm has a much higher effective sampling size than the other variants, but unless RMSE is also lowered, the value of N_{eff} is not as meaningful.

Table 6.3: Results for 96 simulations of filtering on the Lorenz '96 model with $F = 8$, using 16 particles and $\Delta t = 0.05$. For the projected filters, indicated by $\cdot^{\ddagger}$, the average rank of the projection operator was 15.6, in comparison with the dimension Lorenz '96 at $N = 40$. The average RMSE for the observation error was 1.41. An asterisk in the results identifies that the average (or total run-time) was only taken for those simulations that completed.

Filter	PF	PF‡	nPF	nPF‡
# Dead Simulations	17	0	0	0
Avg. RMSE	26.5*	26.2	7.25	6.38
Avg. N_{eff}	1.71*	2.15	2.56	3.29
Total Run-Time	290* s	941 s	4322 s	4969 s

Table 6.4: Results for 96 simulations of filtering on the Lorenz '96 model with $F = 8$, using 16 particles and $\Delta t = 0.05$. The average RMSE for the observation error was 1.41. An asterisk in the results identifies that the average (or total run-time) was only taken for those simulations that completed.

Filter	PF	PF*	PF†	PF‡
# Dead Simulations	17	0	0	0
Avg. RMSE	26.5*	29.7	27.9	26.2
Avg. N_{eff}	1.71*	4.22	1.97	2.15
Avg. Proj. Rank	—	5.8	15.7	15.6
Total Run-Time	290* s	463 s	955 s	941 s

Returning to the results of Table 6.3, the trend for the nPF and nPF‡ is similar to that for the case of $F = 5$ shown in Table 6.1. In particular, the use of the future right-singular vectors is able to improve RMSE and N_{eff} in a significant manner with modest additional computation time–that again could be further improved.

6.5 Remarks

The aim of this chapter was to improve data assimilation methods for high dimensional chaotic problems, which increasingly is the reality of analysts performing assimilation in the geosciences. For instance, as the resolution of atmospheric models improves, convective processes must be included in numerical weather predictions. In turn, the need for fully nonlinear non-Gaussian assimilation methods is increasing. Particle filtering is a flexible and general assimilation approach that can handle the fully nonlinear non-Gaussian regime, but suffers in high dimensional systems due to particle collapse. When the system is chaotic and dissipative, the true process will tend toward an attractor, which often is of much smaller dimension. In this case, which is believed to be very common in the geosciences, we aim to use the properties and geometry of the chaotic system to remedy the issue of particle collapse and improve the filtering accuracy.

This chapter has presented for the first time the application of assimilation in the unstable space for particle filters on models with moderate signal and observation noise. The case of deterministic signal and mostly low observation noise has been previously worked on by others [TDT10; PCT13; BC17; Lee+18; MV19], all of which have focused on the finite-time Lyapunov vectors. In this chapter, we also demonstrated the ability of singular vectors for the first time in the context of assimilation in the unstable subspace, and show a very interesting result when we use the novel idea of future right-singular vectors. The result is surprising since for 1. neither the finite-time Lyapunov vectors nor left-singular vectors show the same improvement, 2. all the vectors are technically related to infinitesimal growth behavior, but our model was noisy and in one case strongly chaotic. At the same time, results by Norwood et al. [Nor+13] have shown that singular vectors react very quickly to dynamical regime change, and therefore, it should not be overly surprising that the right-singular vectors performed well. In the end, what set apart the finite-time Lyapunov vectors and left-singular vectors from the right-singular vectors was the interval of time over which they were generated. Hence, the emphasis on the future vectors is a key conclusion from the chapter as well.

The chapter additionally combined the dynamical systems techniques with the controlled particle filtering method (nPF). The nudged particle filter is implicitly aware of the chaotic dynamics since an optimal control problem is formulated and solved to choose the amount and direction of nudging; this requires realizations of

the signal process, and therefore, the chaotic dynamics affect the choice of control. Furthermore, the need to calculate the fundamental matrix in Eq. 5.5.6 implies that information regarding the unstable subspace is also explicitly present in the calculation and further investigation of this matter as well as nudging in the unstable subspace may provide additional avenues to improve the effective sampling size of the nudged particle filter and the numerical efficiency of the algorithm when combined with projections onto the finite-time Lyapunov vectors or left-singular vectors. Numerical trials of a reduced terminal cost function, g in Eq. 5.5.2, by way of the projection operators presented in this chapter, was conducted but showed no improvement for the future right-singular vectors and a slight deterioration in results for the finite-time Lyapunov vectors and left-singular vectors.

Chapter 7

Conclusions

This dissertation has taken both a theoretical and numerical approach to answering questions that will be useful for improving data assimilation methods for high dimensional, multiple timescale, chaotic systems that may have correlation between the signal and observation processes. The first half concentrated on the theoretical question of filter convergence in the limit of large timescale separation. The second half of the dissertation developed filtering algorithms to realize the theoretical results, as well as address issues for particle filtering in high dimensional chaotic systems.

Chapters 3 and 4 addressed the question of filter convergence in the context of multiple timescale nonlinear systems that may have correlation between the slow signal and observation processes. The specific question was whether the marginal normalized conditional distribution converges to a lower dimensional version in the limit of large timescale separation.

The system considered in Chapter 3 consisted of a slow and fast signal process, with correlation between the slow signal process and observation process. The main result from that chapter, is that indeed we can show convergence and even a rate of convergence. We show that for fixed test functions, the difference of the filters acting on the test functions converge in L^p with a rate of ϵ^p (the fast process is of order two relative to the order one slow process). From this we constructed a metric that generates the topology of weak convergence on the space of probability measures on $\mathbb{R}^m$ and got a rate for weak convergence of ϵ. It is straightforward from this rate to then get convergence in this metric almost surely. We showed at the end of this chapter that it does not seem possible to get the same result using our approach of BSPDEs and BDSDEs for the case of a multiple timescale problem possessing an intermediate timescale forcing in the slow process or when correlation between the fast signal and observation processes exist.

The same questions as raised by Imkeller et al. [Imk+13] and Yeong et al. [Yeo17], regarding the restrictive conditions on the coefficients of the signal and observation processes, are still true in our work. In particular, the assumptions of the main theorem in Chapter 3 rules out the case of linear models. The limiting step in weakening the conditions in this approach is the use of the classical results for SPDEs. Echoing the remarks by Imkeller et al. [Imk+13]: weak solutions may not help improve the conditions much, using viscosity

solutions or relying entirely on probabilistic arguments may help, but it does not seem possible to then get a rate of convergence. The constant C that appears in the main theorem is dependent on the time interval considered, the bounds on the coefficients, and the exponent p. Future efforts may want to consider whether methods from stability of nonlinear filters can be of use in this regard (see for instance [CR11, Chapter 4]).

In Chapter 4 we again addressed the question of filter convergence for the multiple timescale correlated problem, but this time with consideration for an intermediate timescale forcing on the slow process. This required a new approach, and our technique paralleled that by Kushner [Kus90, Chapter 6]. We considered the difference of the marginal filter and the averaged filter as a random variable in the space of continuous time paths from $[0,T]$ to the space of signed measures on $\mathbb{R}^m$, $C([0,T];S(\mathbb{R}^m))$. We showed that the ϵ-parameterized family of induced measures is tight, and therefore that weak limit points exist. This made use of the work by Jakubowski [Jak86]. We characterized the limiting equation of the signed measure-valued process and showed that it possesses a unique solution using the work of Rozovskii [Roz91]. The aforementioned steps made use of the method of perturbed test function (also known as method of corrector), where the corrector is a solution to a Poisson equation, to handle the intermediate timescale forcing term. The end result shows that in probability, the filter weakly converges to an averaged filter.

Although the necessary conditions for the main theorem in Chapter 4 are weaker than those in Chapter 3, we still have the issue that they are too strong, such that linear models could not be considered with the result. This time the restriction comes from the results on the transition densities, semigroups and Poisson solutions developed by Pardoux and Veretennikov [PV03] (see Section 4.6, which provides some remarks regarding a correction for the stated results by Pardoux and Veretennikov [PV03] on semigroup and Poisson solutions, and therefore also the diffusion approximation result there). Some of the conditions required by Rozovskii [Roz91] on uniqueness of the Zakai equation also provide barriers to weakening conditions on our main theorem. Because the results in Pardoux and Veretennikov [PV03] rely on PDE arguments instead of probabilistic ones, there may be an opportunity to relax the conditions in Chapter 4 if the same results by Pardoux and Veretennikov [PV03] can be attained in a different manner. If one is willing to consider the case of the fast process not driven by the slow process, then the probabilistic arguments from an earlier paper by Pardoux and Veretennikov [PV01] could possibly be extended to achieve this result.

With Chapters 5 and 6, we turned to the development of numerical algorithms for filtering equations applied to high dimensional, chaotic, multiple timescale and correlated problems. In particular, we focused on the development of particle filtering methods (otherwise known as sequential Monte Carlo methods). The new contributions of Chapter 5 included: 1. an outline of how to extend the HMM and HHPF algorithms to the multiple timescale case with intermediate scale forcing; 2. algorithms to address the question of alternative

ways to model the fast scale effects on the slow process, and demonstrating one way that is advantageous for models having a symmetric graph structure for their system of equations (common for many geoscience problems); 3. results on how to incorporate the effect of the correlated noise case for continuous time signal, discrete time observation on particle filtering algorithms; 4. insights into the behavior of the nudged particle filter and a best practices guideline for implementation; 5. a comparison of the nudged particle filter and the relaxed particle filter by van Leeuwen [Lee10]; 6. demonstration of tempering of the likelihood for optimal proposal particle filtering.

The results of Tables 5.1, 5.2, and 5.3 demonstrated that on the Lorenz '96 model, the fast scale effect on the slow process cannot be neglected and that our multiple timescale algorithms were 10 to 12-times faster while achieving the same accuracy of estimation in comparison to traditional standard particle filtering. Test results on a correlated signal-sensor variant of the Lorenz '96 problem were shown in Table 5.4, and demonstrates that our derivation on how to account for the correlated noise ensures that accurate filtering can be achieved. In the final sections of the chapter, we compared our nudged particle filtering algorithm, with and without tempering of the likelihood, against the relaxed particle filter by van Leeuwen [Lee10] on the Lorenz '63 model. We show in Table 5.5 that our nudging approach yields a lower RMSE for the same number of particles and that tempering of the likelihood benefits both algorithms, but more so for the relaxed particle filter.

Future directions from Chapter 5 should include looking at the full development of the HHPF algorithm to the multiple timescale problem with intermediate scale forcing. The work in Section 5.3.1 raises the question of how stochastic parameterizations for high dimension multiple timescale models can be improved. Importantly, we showed in that section that ignoring the fast scale contribution in the Lorenz '96 model is not a tractable approach when filtering with temporally sparse observations. Hence the effects of the fast scale need to be accounted for to attain useful estimates. Current efforts by the greater academic community on topics regarding compressive sensing and machine learning may play a useful role here. Regarding the optimal proposal particle filters, an interesting proposition would be to consider the inclusion of a constraint on the relative particle weights in the optimal control problem for the nudged particle filter.

In Chapter 6 we addressed the issue of particle collapse in high dimensional chaotic systems by leveraging the properties of the chaotic system to find a subspace to perform the likelihood update of the particles (i.e., effectively reducing the dimension of the problem from the point of view of the particle collapse issue). Taking a cue from previous work on assimilation in the unstable subspace for Kalman filter based approaches, we developed several novel approaches for assimilation in the unstable subspace for particle filters. We demonstrate this approach on the moderate signal and observation noise case, which does not seem to have

been reported in the literature. We demonstrated the ability of using singular vectors for the first time in the context of assimilation in the unstable subspace, and show a very interesting result when we use the novel idea of future right-singular vectors.

On the weakly chaotic, non-Gaussian regime of the single scale Lorenz '96 model, we demonstrated the capabilities of our assimilation in the unstable subspace methods. In particular, the methods using the future right-singular vectors were capable of reducing the RMSE and increasing the effective sample size versus the standard particle filtering approaches (see Tables 6.1 and 6.2). Testing on a strongly chaotic, near-Gaussian regime variant of the Lorenz '96 model showed that the aforementioned approaches were even more valuable, since our projected particle methods prevented complete collapse of the filtering distribution (see Tables 6.3 and 6.4), which was common in the standard particle filtering approach.

In Chapter 6 we additionally combined the dynamical systems techniques with the controlled particle filtering method (nPF). The need to calculate the fundamental matrix in the nPF algorithm implies that information regarding the unstable subspace is shared across the nPF algorithm and projected particle methods, and therefore there is future potential to produce a method that better leverages the shared information of both.

A comparison with the inherently nonlinear bred vectors by Toth and Kalnay [TK93] would also be an interesting extension to the work presented in Chapter 6. A last remark on interesting future developments would be an effort to combine the novel ideas of Chapter 6 with local particle filtering approaches. Local particle filters are the analogy of local ensemble Kalman filter methods developed by Ott et al. [Ott+04] and are an extremely active topic in both research and applications at the current time [Pot16; PWR19].

Appendix

A.1 Inverses and Factorizations of Symmetric Positive Definite Matrices

Proposition A.1.1

If $K \succ 0$ and $K = K^*$, then $\exists! K^{-1}$.

Proof. The existence proof is quite basic, we just use the fact that there is always an SVD factorization. Hence $K = U\Sigma V^*$ and then $K^{-1} = V\Sigma^{-1}U^*$, which is well posed since Σ is a diagonal matrix with positive values (we only used the fact that K was positive definite).

For uniqueness, we first note that $\exists! L$ such that $K = LL^*$ and L is positive definite, therefore $\exists L^{-1}$. Again we make use of the SVD factorization, but this time of $L = U\Sigma V^*$. Then

$$L^{-1} = V\Sigma^{-1}U^*.$$

Now $\exists K^{-1}$, since it is positive definite, and therefore properties of matrix multiplication give

$$K^{-1} = (L^*)^{-1}L^{-1}.$$

Note that K^{-1} must be symmetric and whats more, positive definite. Now assume that G is also an inverse of K. Then $GK = I$, where I is the unit matrix. But then we have the following,

$$\begin{aligned} GK &= I \\ GLL^* &= I \\ G &= (L^*)^{-1}L^{-1} \\ &= K^{-1} \end{aligned}$$

□

Proposition A.1.2

Let $A = A^*, A \succ 0$, then $\exists! L$ such that $A = LL^*$ and the following is true,

$$\left(L^{-1}\right)^* = (L^*)^{-1},$$

that is the operations of $\cdot^{-1}$ and $\cdot^*$ commute on lower triangular positive definite matrices.

Proof. From the properties of A, we have by Proposition A.1.1, that $\exists! A^{-1}$ which is symmetric and positive definite. Hence, $\exists! J$ such that $A^{-1} = JJ^*$. At the same time, $A^{-1} = (L^*)^{-1}L^{-1}$. From uniqueness of $J = (L^*)^{-1}$ and $J^* = L^{-1}$. Taking the transpose of the last relation $J = (L^{-1})^*$, which gives the desired result:

$$J = (L^*)^{-1} = (L^{-1})^*.$$

□

Proposition A.1.3

If $L \succ 0$ is a lower triangular matrix, then $\exists! L^{-1} \succ 0$, and L^{-1} is lower triangular.

Proof. A direct way to prove the result is to construct the first two rows of L^{-1} by hand and then follow the procedure by induction to see that the structure is lower triangular (i.e., the same basic technique that could be used to show that the inverse exists). For instance let L_{ij} be the i-th row and j-th column entry of L. Then the first entry of $(L^{-1})_{11} = 1/L_{11}$ exists and is unique. At the second step of construction, one has

$$\begin{bmatrix} L_{11} & L_{21} \\ 0 & L_{22} \end{bmatrix} \begin{bmatrix} L_{21}^{-1} \\ L_{22}^{-1} \end{bmatrix} = \begin{bmatrix} 0 \\ 1 \end{bmatrix}.$$

The solution exists since the matrix on the left side of the equation is invertible from $L \succ 0$. And this solution is unique, since the matrix is full rank. This procedure can be continued until completion. □

A.2 Extension of Itô's Formula

The following Lemma A.2.1 and subsequent Corollary A.2.1, are extensions of the Itô formula for the case of backward doubly stochastic differential equations (cf. [PP94, Lemma 1.3, p.213]).

Lemma A.2.1

Let θ to be the first component of the pair solution (θ, η) to the backward doubly stochastic differential equation

$$\theta_t = \theta_T + \int_t^T \mathcal{F} ds + \int_t^T \mathcal{G} dB_s - \int_t^T \eta dW_s.$$

Assume the general case of θ_t taking values in $\mathbb{R}^k$. Here B is a $\mathbb{R}^b$ backward Brownian motion, which is independent of the $\mathbb{R}^w$ forward Brownian motion W. The dispersion coefficients G, η are matrices with values in $\mathbb{R}^{k\times b}$ and $\mathbb{R}^{k\times w}$ respectively. Let $(\cdot,\cdot)$ be the standard Euclidean inner product on $\mathbb{R}^k$, $|\cdot|$ the induced norm, and $\langle\cdot,\cdot\rangle$ the quadratic variation. Then we have the following for $|\theta|^p$ for $p > 2$

$$\begin{aligned}
|\theta_t|^p = |\theta_T|^p &+ \int_t^T \left(p|\theta_s|^{p-2}\theta_s, \mathcal{F} ds\right) + \int_t^T \left(p|\theta_s|^{p-2}\theta_s, \mathcal{G} dB_s\right) - \int_t^T \left(p|\theta_s|^{p-2}\theta_s, \eta dW_s\right) \\
&+ \frac{p}{2}\int_t^T |\theta_s|^{p-2} \operatorname{Tr}(\mathcal{G}\mathcal{G}^*) ds + \frac{p(p-2)}{2}\int_t^T |\theta_s|^{p-4} \left(\mathcal{G}\mathcal{G}^*\theta_s, \theta_s\right) ds \\
&- \frac{p}{2}\int_t^T |\theta_s|^{p-2} \operatorname{Tr}(\eta\eta^*) ds - \frac{p(p-2)}{2}\int_t^T |\theta_s|^{p-4} \left(\eta\eta^*\theta_s, \theta_s\right) ds.
\end{aligned}$$

Further, if the stochastic integrals are martingales and if $\theta_T = 0$ a.s., the p-th moment of θ is

$$\begin{aligned}
\mathbb{E}\left[|\theta_t|^p\right] = &\int_t^T \mathbb{E}\left[\left(p|\theta_s|^{p-2}\theta_s, \mathcal{F}\right)\right] ds \\
&+ \frac{p}{2}\int_t^T \mathbb{E}\left[|\theta_s|^{p-2} \operatorname{Tr}(\mathcal{G}\mathcal{G}^*)\right] ds + \frac{p(p-2)}{2}\int_t^T \mathbb{E}\left[|\theta_s|^{p-4} \left(\mathcal{G}\mathcal{G}^*\theta_s, \theta_s\right)\right] ds \\
&- \frac{p}{2}\int_t^T \mathbb{E}\left[|\theta_s|^{p-2} \operatorname{Tr}(\eta\eta^*)\right] ds - \frac{p(p-2)}{2}\int_t^T \mathbb{E}\left[|\theta_s|^{p-4} \left(\eta\eta^*\theta_s, \theta_s\right)\right] ds.
\end{aligned}$$

(cf. [PP94, Lemma 1.3, p.213])

Proof. We first rearrange the evolution equation for θ to get,

$$\theta_T = \theta_t - \int_t^T \mathcal{F} ds - \int_t^T \mathcal{G} dB_s + \int_t^T \eta dW_s.$$

Then note that

$$\begin{aligned}
\nabla_\theta |\theta|^p &= \partial_\theta (\theta,\theta)^{p/2} = p\theta(\theta,\theta)^{(p/2)-1} = p|\theta|^{p-2}\theta \\
\nabla_\theta^{\otimes 2} |\theta|^p &= p|\theta|^{p-2} \operatorname{Id} + p(p-2)|\theta|^{p-4}\theta\theta^*, \\
&= p|\theta|^{p-4}\left(|\theta|^2 \operatorname{Id} + (p-2)\theta\theta^*\right).
\end{aligned}$$

Then for $p > 2$, we can apply Itô's formula to yield

$$\begin{aligned}
|\theta_T|^p &= |\theta_t|^p + \int_t^T \left(p|\theta_s|^{p-2}\theta_s, d\theta_s\right) + \frac{1}{2}\int_t^T \sum_{i,j}^k p|\theta_s|^{p-4}\left(|\theta_s|^2 \operatorname{Id} + (p-2)\theta_s\theta_s^*\right)_{i,j} \langle d\theta_s^i, d\theta_s^j\rangle \\
&= |\theta_t|^p - \int_t^T \left(p|\theta_s|^{p-2}\theta_s, \mathcal{F}ds\right) - \int_t^T \left(p|\theta_s|^{p-2}\theta_s, \mathcal{G}dB_s\right) + \int_t^T \left(p|\theta_s|^{p-2}\theta_s, \eta dW_s\right) \\
&- \frac{1}{2}\int_t^T \sum_{i,j}^k p|\theta_s|^{p-4}\left(|\theta_s|^2 \operatorname{Id} + (p-2)\theta_s\theta_s^*\right)_{i,j} (\mathcal{G}\mathcal{G}^*)_{i,j}\, ds \\
&+ \frac{1}{2}\int_t^T \sum_{i,j}^k p|\theta_s|^{p-4}\left(|\theta_s|^2 \operatorname{Id} + (p-2)\theta_s\theta_s^*\right)_{i,j} (\eta\eta^*)_{i,j}\, ds.
\end{aligned}$$

Using the fact that

$$\sum_{i,j}^k \operatorname{Id}_{i,j}(\mathcal{G}\mathcal{G}^*)_{i,j} = \operatorname{Tr}(\mathcal{G}\mathcal{G}^*),$$

and

$$\sum_{i,j}^k (\theta\theta^*)_{i,j}(\mathcal{G}\mathcal{G}^*)_{i,j} = (\mathcal{G}\mathcal{G}^*\theta, \theta),$$

we can simplify the terms coming from the quadratic variation to get

$$\begin{aligned}
|\theta_T|^p &= |\theta_t|^p - \int_t^T \left(p|\theta_s|^{p-2}\theta_s, \mathcal{F}ds\right) - \int_t^T \left(p|\theta_s|^{p-2}\theta_s, \mathcal{G}dB_s\right) + \int_t^T \left(p|\theta_s|^{p-2}\theta_s, \eta dW_s\right) \\
&- \frac{p}{2}\int_t^T |\theta_s|^{p-2} \operatorname{Tr}(\mathcal{G}\mathcal{G}^*)ds - \frac{p(p-2)}{2}\int_t^T |\theta_s|^{p-4} (\mathcal{G}\mathcal{G}^*\theta_s, \theta_s)\, ds \\
&+ \frac{p}{2}\int_t^T |\theta_s|^{p-2} \operatorname{Tr}(\eta\eta^*)ds + \frac{p(p-2)}{2}\int_t^T |\theta_s|^{p-4} (\eta\eta^*\theta_s, \theta_s)\, ds.
\end{aligned}$$

Rearranging, we get the useful expression

$$\begin{aligned}
|\theta_t|^p &= |\theta_T|^p + \int_t^T \left(p|\theta_s|^{p-2}\theta_s, \mathcal{F}ds\right) + \int_t^T \left(p|\theta_s|^{p-2}\theta_s, \mathcal{G}dB_s\right) - \int_t^T \left(p|\theta_s|^{p-2}\theta_s, \eta dW_s\right) \\
&+ \frac{p}{2}\int_t^T |\theta_s|^{p-2} \operatorname{Tr}(\mathcal{G}\mathcal{G}^*)ds + \frac{p(p-2)}{2}\int_t^T |\theta_s|^{p-4} (\mathcal{G}\mathcal{G}^*\theta_s, \theta_s)\, ds \\
&- \frac{p}{2}\int_t^T |\theta_s|^{p-2} \operatorname{Tr}(\eta\eta^*)ds - \frac{p(p-2)}{2}\int_t^T |\theta_s|^{p-4} (\eta\eta^*\theta_s, \theta_s)\, ds.
\end{aligned}$$

If the stochastic integrals in this expression are martingales (e.g., using the Burkholder-Davis-Gundy

inequality), then we get the following for the expectation of $|\theta_t|^p$,

$$\begin{aligned}\mathbb{E}\left[|\theta_t|^p\right] = \mathbb{E}\left[|\theta_T|^p\right] &+ \int_t^T \mathbb{E}\left[\left(p|\theta_s|^{p-2}\theta_s, \mathcal{F}\right)\right] ds \\ &+ \frac{p}{2}\int_t^T \mathbb{E}\left[|\theta_s|^{p-2}\operatorname{Tr}(\mathcal{G}\mathcal{G}^*)\right] ds + \frac{p(p-2)}{2}\int_t^T \mathbb{E}\left[|\theta_s|^{p-4}\left(\mathcal{G}\mathcal{G}^*\theta_s, \theta_s\right)\right] ds \\ &- \frac{p}{2}\int_t^T \mathbb{E}\left[|\theta_s|^{p-2}\operatorname{Tr}(\eta\eta^*)\right] ds - \frac{p(p-2)}{2}\int_t^T \mathbb{E}\left[|\theta_s|^{p-4}\left(\eta\eta^*\theta_s, \theta_s\right)\right] ds.\end{aligned}$$

Further, in the case where $\theta_T = 0$ a.s., then this equation simplifies further to

$$\begin{aligned}\mathbb{E}\left[|\theta_t|^p\right] = &\int_t^T \mathbb{E}\left[\left(p|\theta_s|^{p-2}\theta_s, \mathcal{F}\right)\right] ds \\ &+ \frac{p}{2}\int_t^T \mathbb{E}\left[|\theta_s|^{p-2}\operatorname{Tr}(\mathcal{G}\mathcal{G}^*)\right] ds + \frac{p(p-2)}{2}\int_t^T \mathbb{E}\left[|\theta_s|^{p-4}\left(\mathcal{G}\mathcal{G}^*\theta_s, \theta_s\right)\right] ds \\ &- \frac{p}{2}\int_t^T \mathbb{E}\left[|\theta_s|^{p-2}\operatorname{Tr}(\eta\eta^*)\right] ds - \frac{p(p-2)}{2}\int_t^T \mathbb{E}\left[|\theta_s|^{p-4}\left(\eta\eta^*\theta_s, \theta_s\right)\right] ds,\end{aligned}$$

which proves the desired results. □

Corollary A.2.1

Assume the same setup as Lemma A.2.1, but for the case $\theta_t \in \mathbb{R}$. B and W may still be multidimensional Brownian motions. Then the same result there becomes,

$$\begin{aligned}|\theta_t|^p = |\theta_T|^p &+ \int_t^T p|\theta_s|^{p-2}\theta_s\mathcal{F}ds + \int_t^T \left(p|\theta_s|^{p-2}\theta_s\mathcal{G}, dB_s\right) - \int_t^T \left(p|\theta_s|^{p-2}\theta_s\eta, dW_s\right) \\ &+ \frac{p(p-1)}{2}\int_t^T |\theta_s|^{p-2}|\mathcal{G}|^2 ds - \frac{p(p-1)}{2}\int_t^T |\theta_s|^{p-2}|\eta|^2 ds.\end{aligned}$$

Further, if the stochastic integrals are martingales and if $\theta_T = 0$ a.s., the p-th moment of θ is

$$\mathbb{E}\left[|\theta_t|^p\right] = \int_t^T \mathbb{E}\left[p|\theta_s|^{p-2}\theta_s\mathcal{F}\right] ds + \frac{p(p-1)}{2}\int_t^T \mathbb{E}\left[|\theta_s|^{p-2}|\mathcal{G}|^2\right] ds - \frac{p(p-1)}{2}\int_t^T \mathbb{E}\left[|\theta_s|^{p-2}|\eta|^2\right] ds.$$

A.3 An Inequality and Limits

Lemma A.3.1

Let $A \in \mathbb{R}^{d\times m}$ and $\theta \in \mathbb{R}^m$, then

$$|A\theta|^2 = \langle A\theta, A\theta\rangle = \langle A^*A\theta, \theta\rangle \lesssim |\theta|^2 \operatorname{Tr}(A^*A). \tag{A.3.1}$$

Proof. Expanding the left side of Eq. A.3.1, we get

$$(A^*A\theta, \theta) = \sum_{i,j}^{m} \theta_i \theta_j \langle A_{:,i}, A_{:,j} \rangle.$$

If $i = j$, then each term is simply

$$\theta_i \theta_i \langle A_{:,i}, A_{:,i} \rangle.$$

If $i \neq j$, then application of Young's inequality to each term gives,

$$\theta_i \theta_j \langle A_{:,i}, A_{:,j} \rangle = \langle \theta_i A_{:,i}, \theta_j \mathcal{G}_{:,j} \rangle \leq \frac{\beta_{i,j}}{2} \theta_i^2 \langle A_{:,i}, A_{:,j} \rangle + \frac{1}{2\beta_{i,j}} \theta_j^2 \langle A_{:,j}, A_{:,i} \rangle.$$

Putting all the terms together yields the desired result. □

Lemma A.3.2

Let $p > 0$, $q \in \mathbb{R}$, then

$$\lim_{\epsilon \to 0^+} \epsilon^p (-\ln \epsilon)^q = 0$$

Proof. In the case $q \leq 0$ the result is trivial since both ϵ^p and $(-\ln \epsilon)^q$ tend to zero as $\epsilon \to 0^+$. Therefore, consider the case $q > 0$. We apply L'Hopital's rule with $f = (-\ln \epsilon)^q$, $g = \epsilon^{-p}$, such that $f/g = \epsilon^p (-\ln \epsilon)^q$. Then the derivatives of f and g with respect to ϵ are,

$$\frac{\partial f}{\partial \epsilon} = f' = -q\epsilon^{-1}(-\ln \epsilon)^{q-1}, \quad \text{and} \quad \frac{\partial g}{\partial \epsilon} = g' = -p\epsilon^{-p-1}.$$

Therefore

$$\frac{f'}{g'} = \frac{q}{p} \epsilon^p (-\ln \epsilon)^{q-1}.$$

If $q - 1 \leq 0$, then the result follows. Otherwise repeated application will eventually give $(-\ln \epsilon)^{q-k}$ for some $k \in \mathbb{N}$ such that $q - k \leq 0$ and then the result follows. □

Lemma A.3.3

Let $p \in (0, 1/8)$, $\delta(\epsilon) = \epsilon^2 (-\ln \epsilon)^p$, then

$$\lim_{\epsilon \to 0^+} \left(\frac{\delta^8}{\epsilon^{16}} + \frac{\delta^4}{\epsilon^8} \right) (\epsilon^8 + \delta^4 (1 + \epsilon^8)) \exp \left(\frac{\delta^8}{\epsilon^{16}} + \frac{\delta^4}{\epsilon^8} \right) = 0.$$

Proof. We first expand the expression with the choice of $\delta(\epsilon)$ to get,

$$\left((-\ln\epsilon)^{8p}+(-\ln\epsilon)^{4p}\right)\left(\epsilon^{8}+\epsilon^{8}(-\ln\epsilon)^{4p}+\epsilon^{16}(-\ln\epsilon)^{4p}\right)\exp\left((-\ln\epsilon)^{8p}+(-\ln\epsilon)^{4p}\right).$$

Expanding and distributing the terms, we identify the term that would be most limiting for convergence to zero,

$$(-\ln\epsilon)^{12p}\epsilon^{8}\exp\left((-\ln\epsilon)^{8p}+(-\ln\epsilon)^{4p}\right)\lesssim\epsilon^{7}\exp\left(2(-\ln\epsilon)^{8p}\right).$$

Since $8p<1$, for all sufficiently small $\epsilon>0$ we have,

$$\exp\left(2(-\ln\epsilon)^{8p}\right)\leq\exp\left(-2\ln\epsilon\right)=\epsilon^{-2},$$

and therefore

$$\lim_{\epsilon\to0^{+}}\epsilon^{7}\exp\left(2(-\ln\epsilon)^{8p}\right)\leq\lim_{\epsilon\to0^{+}}\epsilon^{5}=0.$$

□

References

[AG05] Rafail V. Abramov Andrew J. Majda and Marcus J. Grote. *Information Theory and Stochastics for Multiscale Nonlinear Systems*. American Mathematical Society, 2005 (cit. on pp. 148, 149).

[Arn03] Ludwig Arnold. *Random Dynamical Systems*. Springer-Verlag Berlin Heidelberg, 2003. ISBN: 978-3-642-08355-6. DOI: 10.1007/978-3-662-12878-7 (cit. on p. 144).

[Aru+02] M. S. Arulampalam et al. "A tutorial on particle filters for online nonlinear/non-Gaussian Bayesian tracking". In: *IEEE Transactions on Signal Processing* 50.2 (Feb. 2002), pp. 174–188. ISSN: 1053-587X. DOI: 10.1109/78.978374 (cit. on pp. 102, 103).

[BB86] A. Bensoussan and G. L. Blankenship. "Nonlinear filtering with homogenization". In: *Stochastics* 17 (1986), pp. 67–90. DOI: 10.1080/17442508608833383 (cit. on p. 19).

[BC09] Alan Bain and Dan Crisan. *Fundamentals of Stochastic Filtering*. Springer, 2009. ISBN: 978-0-387-76896-0. DOI: 10.1007/978-0-387-76896-0 (cit. on pp. 8, 11, 13, 14, 17, 28).

[BC17] Marc Bocquet and Alberto Carrassi. "Four-dimensional ensemble variational data assimilation and the unstable subspace". In: *Tellus A: Dynamic Meteorology and Oceanography* 69.1 (2017), p. 1304504. DOI: 10.1080/16000870.2017.1304504 (cit. on pp. 142, 146, 160).

[BCJ14] A. Beskos, D. Crisan, and A. Jasra. "On the stability of sequential Monte Carlo methods in high dimensions". In: *Annals of Applied Probability* 24 (2014), pp. 1396–1445. DOI: 10.1214/13-AAP951 (cit. on pp. 129, 137).

[Bee+18] R. Beeson et al. "Reduced Order Nonlinear Filters for Multi-Scale Systems with Correlated Sensor Noise". In: *2018 21st International Conference on Information Fusion (FUSION)*. July 2018, pp. 131–141. DOI: 10.23919/ICIF.2018.8455704 (cit. on pp. 99, 121).

[BEM01] Craig H. Bishop, Brian J. Etherton, and Sharanya J. Majumdar. "Adaptive Sampling with the Ensemble Transform Kalman Filter. Part I: Theoretical Aspects". In: *Monthly Weather Review* 129.3 (Mar. 2001), pp. 420–436. DOI: 10.1175/1520-0493(2001)129<0420:ASWTET>2.0.CO;2 (cit. on p. 104).

[Ben+80] Giancarlo Benettin et al. “Lyapunov Characteristic Exponents for smooth dynamical systems and for hamiltonian systems; a method for computing all of them. Part 1: Theory”. In: *Meccanica* 15.1 (Mar. 1980), pp. 9–20. ISSN: 1572-9648. DOI: 10.1007/BF02128236 (cit. on pp. 144, 146).

[Ben04] A. Bensoussan. *Stochastic Control of Partially Observable Systems*. Cambridge University Press, 2004. ISBN: 9780521611978. URL: https://books.google.com/books?id=LbxTJHEO4agC (cit. on pp. 14, 17).

[Ber99] N. Bergman. “Recursive Bayesian estimation: Navigation and tracking applications”. PhD thesis. Linköping, Sweden: Linköping University, 1999 (cit. on p. 103).

[BH14] Tyrus Berry and John Harlim. “Linear Theory for Filtering Nonlinear Multiscale Systems with Model Error”. In: *Proceedings of the Royal Society A* 470 (July 2014). DOI: 10.1098/rspa.2014.0168 (cit. on pp. 3, 19).

[BN19a] Ryne Beeson and N Sri Namachchivaya. “Efficient Nonlinear Filtering of Multiscale Systems with Specific Structure”. In: July 2019. URL: https://ieeexplore.ieee.org/document/9011425 (cit. on p. 99).

[BN19b] Ryne Beeson and N. Sri Namachchivaya. “The IMA Volumes in Mathematics and its Applications”. In: *Modeling, Stochastic Control, Optimization, and Applications*. Ed. by George Yin and Qing Zhang. Springer Nature Switzerland AG, 2019. Chap. Nudged Particle Filters in Multiscale Chaotic Systems with Correlated Sensor Noise. ISBN: 978-3-030-25497-1. DOI: 10.1007/978-3-030-25498-8 (cit. on pp. 99, 107).

[BNP20a] Ryne Beeson, N. Sri Namachchivaya, and Nicolas Perkowski. *Approximation of the Filter Equation for Multiple Timescale, Correlated, Nonlinear Systems*. Oct. 2020. arXiv: 2010.16401 [math.PR] (cit. on p. 61).

[BNP20b] Ryne Beeson, N. Sri Namachchivaya, and Nicolas Perkowski. *Quantitative Convergence of the Filter Solution for Multiple Timescale Nonlinear Systems with Coarse-Grain Correlated Noise*. Nov. 2020. arXiv: 2011.12801 [math.PR] (cit. on p. 21).

[Boc+17] Marc. Bocquet et al. “Degenerate Kalman Filter Error Covariances and Their Convergence onto the Unstable Subspace”. In: *SIAM/ASA Journal on Uncertainty Quantification* 5.1 (2017), pp. 304–333. DOI: 10.1137/16M1068712 (cit. on pp. 143, 153).

[BP02] Luis Barreira and Yakov B. Pesin. *Lyapunov Exponents and Smooth Ergodic Theory*. Vol. 23. University Lecture Series. American Mathematical Society, 2002. ISBN: 978-1-4704-2170-0. URL: https://bookstore.ams.org/ulect-23/ (cit. on p. 145).

[BS20] Ryne Beeson and N. Sri Namachchivaya. "Particle filtering for chaotic dynamical systems using future right-singular vectors". In: *Nonlinear Dynamics* 102 (2020), pp. 679–696. DOI: 10.1007/s11071-020-05727-y (cit. on p. 142).

[Car+18] Alberto Carrassi et al. "Data assimilation in the geosciences: An overview of methods, issues, and perspectives". In: *WIREs Climate Change* 9.5 (2018), e535. DOI: 10.1002/wcc.535 (cit. on pp. 98, 151).

[CMT10] Alexandre Chorin, Matthias Morzfeld, and Xuemin Tu. "Implicit particle filters for data assimilation". In: *Commun. Appl. Math. Comput. Sci.* 5.2 (2010), pp. 221–240. DOI: 10.2140/camcos.2010.5.221 (cit. on pp. 129, 135).

[CR11] Dan Crisan and B. L. Rozovskii. *The Oxford Handbook of Nonlinear Filtering*. Oxford University Press, 2011. ISBN: 978-0-19-953290-2 (cit. on p. 163).

[Cri06] Dan Crisan. "Particle Approximations for a Class of Stochastic Partial Differential Equations". In: *Applied Mathematics and Optimization* 54 (2006), pp. 293–314. DOI: 10.1007/s00245-006-0872-3 (cit. on p. 122).

[CV08] Daan Crommelin and Eric Vanden-Eijnden. "Subgrid-Scale Parameterization with Conditional Markov Chains". In: *American Meteorological Society* 65 (Aug. 2008), pp. 2661–2675. DOI: 10.1175/2008JAS2566.1 (cit. on p. 104).

[DdG01] A. Doucet, N. de Freitas, and N. Gordon. *Sequential Monte Carlo Methods in Practice*. New York: Springer Verlag, 2001. ISBN: 978-1-4757-3437-9. DOI: https://doi.org/10.1007/978-1-4757-3437-9 (cit. on p. 128).

[DM00] P. Del Moral and L. Miclo. "Branching and Interacting Particle Systems Approximations of Feynman-Kac Formulae with Applications to Non-linear Filtering". In: *Séminaire de Probabilités XXXIV, Lecture Notes in Mathematics*. Vol. 1729. Springer-Verlag Berlin, 2000, pp. 1–145 (cit. on p. 102).

[Dou98] A. Doucet. *On sequential simulation-based methods for Bayesian filtering*. Tech. rep. Cambridge University, 1998 (cit. on p. 102).

[E+07] Weinan E et al. "Heterogeneous Multiscale Methods: A Review". In: *Communications in Computational Physics* 2.3 (June 2007), pp. 367–450 (cit. on p. 104).

[EE03] Weinan E and Bjorn Engquist. "The Heterogeneous Multiscale Methods". In: *Communications in Mathematical Sciences* 1.1 (2003), pp. 87–132. URL: https://projecteuclid.org/euclid.cms/1118150402 (cit. on pp. 4, 104).

[EK08] Stewart N. Ethier and Thomas G. Kurtz. *Markov Processes; Characterization and Convergence*. John Wiley & Sons, Inc., 2008. ISBN: 9780470316658. DOI: 10.1002/9780470316658 (cit. on p. 58).

[ELV05] Weinan E, D Liu, and E. Vanden-Eijnden. "Analysis of multiscale methods for stochastic differential equations". In: *Communication on Pure and Applied Mathematics* 58 (Jan. 2005), pp. 1544–1585 (cit. on pp. 104, 105).

[Fre+83] Paul Frederickson et al. "The liapunov dimension of strange attractors". In: *Journal of Differential Equations* 49.2 (1983), pp. 185–207. ISSN: 0022-0396. DOI: https://doi.org/10.1016/0022-0396(83)90011-6 (cit. on p. 145).

[FS06] Wendell H. Fleming and Halil Mete Soner. *Controlled Markov Processes and Viscosity Solutions*. 2nd ed. Vol. 25. Stochastic Modelling and Applied Probability. Springer-Verlag New York, 2006. ISBN: 978-0-387-26045-7. DOI: 10.1007/0-387-31071-1 (cit. on p. 129).

[FV04] I. Fatkullin and E. Vanden-Eijnden. "A computational strategy for multiscale systems". In: *Journal of Computational Physics* 200.2 (Nov. 2004), pp. 605–638. DOI: 10.1016/j.jcp.2004.04.013 (cit. on pp. 104, 106, 107).

[Gin+13] Francesco Ginelli et al. "Covariant Lyapunov vectors". In: *Journal of Physics A: Mathematical and Theoretical* 46.25 (June 2013), p. 254005. DOI: 10.1088/1751-8113/46/25/254005 (cit. on p. 144).

[GSS93] N. J. Gordon, D. J. Salmond, and A. F. M. Smith. "Novel approach to nonlinear/non-Gaussian Bayesian state estimation". In: *IEE Proceedings F - Radar and Signal Processing* 140.2 (1993), pp. 107–113. DOI: 10.1049/ip-f-2.1993.0015 (cit. on p. 102).

[Han07] Ramon van Handel. "Stochastic Calculus, Filtering, and Stochastic Control". May 2007 (cit. on p. 14).

[Har11] John Harlim. "Numerical Strategies for Filtering Partially Observed Stiff Stochastic Differential Equations". In: *Journal of Computational Physics* 230.3 (Feb. 2011), pp. 744–762. DOI: 10.1016/j.jcp.2010.10.016 (cit. on p. 104).

[Ich04] Naoyuki Ichihara. "Homogenization Problem for Stochastic Partial Differential Equations of Zakai Type". In: *Stochastic and Stochastics Reports* 76.3 (2004), pp. 243–266. DOI: 10.1080/10451120410001714107 (cit. on p. 19).

[Imk+13] Peter Imkeller et al. “Dimensional reduction in nonlinear filtering: A homogenization approach”. In: *Ann. Appl. Probab.* 23.6 (Dec. 2013), pp. 2290–2326. DOI: 10.1214/12-AAP901 (cit. on pp. 3, 20, 24, 162).

[Jak86] Adam Jakubowski. “On the Skorokhod topology”. en. In: *Annales de l’I.H.P. Probabilités et statistiques* 22.3 (1986), pp. 263–285. URL: http://www.numdam.org/item/AIHPB_1986__22_3_263_0 (cit. on pp. 61, 65, 79, 86, 163).

[Kal97] Olav Kallenberg. *Foundations of Modern Probability*. Springer-Verlag New York, 1997. DOI: 10.1007/978-1-4757-4015-8 (cit. on p. 8).

[Kar83] Rajeeva L. Karandikar. “Interchanging the Order of Stochastic Integration and Ordinary Differentiation”. In: *Indian Statistical Institute* 45.1 (1983), pp. 120–124. URL: http://www.jstor.org/stable/25050420 (cit. on pp. 46, 47).

[KH12] Emily L. Kang and John Harlim. “Filtering Partially Observed Multiscale Systems with Heterogeneous Multiscale Methods-Based Reduced Climate Models”. In: *Monthly Weather Review* 140 (Mar. 2012), pp. 860–873. DOI: 10.1175/MWR-D-10-05067.1 (cit. on pp. 3, 19, 104, 106).

[KLS97] M. L. Kleptsina, R. Sh. Lipster, and A. P. Serebrovski. “Nonlinear Filtering Problem with Contamination”. In: *The Annals of Applied Probability* 7.4 (1997), pp. 917–934. URL: http://www.jstor.org/stable/2245252 (cit. on p. 20).

[KP12] Pavel V. Kuptsov and Ulrich Parlitz. “Theory and Computation of Covariant Lyapunov Vectors”. In: *Journal of Nonlinear Science* 22.5 (Oct. 2012), pp. 727–762. ISSN: 1432-1467. DOI: 10.1007/s00332-012-9126-5 (cit. on p. 144).

[KR82] N. V. Krylov and B. L. Rozovskii. “Stochastic Differential Equations and Diffusion Processes”. In: *Russian Mathematical Survey* 37.6 (1982), pp. 81–105 (cit. on p. 28).

[Kus90] Harold Kushner. *Weak Convergence Methods and Singularly Perturbed Stochastic Control and Filtering Problems*. Birkhauser Basel, 1990. DOI: 10.1007/978-1-4612-4482-0 (cit. on pp. 4, 60, 89, 163).

[KX95] Gopinath Kallianpur and Jie Xiong. “Stochastic differential equations in infinite-dimensional spaces”. In: *Stochastic differential equations in infinite-dimensional spaces*. Vol. 26. Lecture Notes–Monograph Series. Hayward, CA: Institute of Mathematical Statistics, 1995, pp. 340–342. DOI: 10.1214/lnms/1215451880 (cit. on p. 86).

[KY05] R. Z. Khasminskii and G. Yin. "Limit behavior of two-time scale diffusions revisited". In: *Journal of Differential Equations* 212 (2005), pp. 85–113. DOI: https://doi.org/10.1016/j.jde.2004.08.013 (cit. on p. 19).

[LC98] J. S. Liu and R. Chen. "Sequential Monte Carlo methods for dynamical systems". In: *Journal of American Statistical Association* 93 (1998), pp. 1032–1044 (cit. on p. 103).

[Le 14] Jean-Francois Le Gall. *Brownian Motion, Martingales, and Stochastic Calculus*. Springer Verlag, 2014. ISBN: 978-3-319-31088-6. DOI: 10.1007/978-3-319-31089-3 (cit. on pp. 9, 10, 12, 13).

[Lee+18] Bart. de Leeuw et al. "Projected Shadowing-Based Data Assimilation". In: *SIAM Journal on Applied Dynamical Systems* 17.4 (2018), pp. 2446–2477. DOI: 10.1137/17M1141163 (cit. on pp. 143, 160).

[Lee+19] Peter Jan van Leeuwen et al. "Particle filters for high-dimensional geoscience applications: A review". In: *Quarterly Journal of the Royal Meteorological Society* 145.723 (2019), pp. 2335–2365. DOI: 10.1002/qj.3551 (cit. on pp. 1, 98, 137).

[Lee10] Peter Jan van Leeuwen. "Nonlinear data assimilation in geosciences: an extremely efficient particle filter". In: *Quart. J. Royal Meteor. Soc.* 136 (Dec. 2010), pp. 1991–1999. DOI: 10.1002/qj.699 (cit. on pp. 129, 135, 137, 164).

[Lee11] P. J. van Leeuwen. "Efficient nonlinear data-assimilation in geophysical fluid dynamics". In: *Computers and Fluids* 46.1 (July 2011), pp. 52–58. DOI: 10.1016/j.compfluid.2010.11.011 (cit. on p. 137).

[LH03] Vladimir M. Lucic and Andrew J. Heunis. "Convergence of Nonlinear Filters for RandomlyPerturbed Dynamical Systems". In: *Applied Mathematics and Optimization* 48.2 (2003), pp. 93–128. DOI: 10.1007/s00245-003-0772-8 (cit. on p. 19).

[Lin+12] Nishanth Lingala et al. "Particle filtering in high-dimensional chaotic systems". In: *Chaos: An Interdisciplinary Journal of Nonlinear Science* 22.4 (Dec. 2012), pp. 047509–047509-12. DOI: 10.1063/1.4766595 (cit. on pp. 104, 112, 129).

[Lin+14] N Lingala et al. "Optimal nudging in particle filters". In: *Probabilistic Engineering Mechanics* 37 (July 2014), pp. 160–169. DOI: 10.1016/j.probengmech.2013.08.007 (cit. on p. 129).

[Lor63] Edward N Lorenz. "Deterministic Nonperiodic Flow". In: *Journal of the Atmospheric Sciences* 20.2 (Mar. 1963), pp. 130–141. DOI: 10.1175/1520-0469(1963)020<0130:DNF>2.0.CO;2 (cit. on pp. 4, 136).

[Lor95] E. N. Lorenz. “Predictability: A problem partly solved.” In: *Proceedings of the ECMWF Seminar on Predictability*. Vol. 1. ECMWF. Shinfield Park, Reading: ECMWF, 1995, pp. 1–18. URL: https://www.ecmwf.int/node/10829 (cit. on pp. 4, 105, 107, 114, 122, 147).

[LY84] F Ledrappier and Lai-Sang Young. “The Metric Entropy of Diffeomorphisms”. In: *Bulletin of the American Mathematical Society* 11.2 (Oct. 1984), pp. 343–346 (cit. on p. 145).

[LY88] F. Ledrappier and L. -S. Young. “Entropy formula for random transformations”. In: *Probability Theory and Related Fields* 80.2 (Dec. 1988), pp. 217–240. ISSN: 1432-2064. DOI: 10.1007/BF00356103 (cit. on pp. 145, 148).

[MDJ06] Pierre Del Moral, Arnaud Doucet, and Ajay Jasra. “Sequential Monte Carlo Samplers”. In: *Journal of the Royal Statistical Society. Series B (Statistical Methodology)* 68.3 (2006), pp. 411–436. URL: http://www.jstor.org/stable/3879283 (cit. on pp. 129, 137).

[MTV01] A.J. Majda, I. Timofeyev, and E. Vanden-Eijnden. “A Mathematical Framework for Stochastic Climate Models”. In: *Comm. Pure Appl. Math.* 54 (2001), pp. 891–974 (cit. on p. 106).

[MTV03] Andrew J. Majda, Ilya Timofeyev, and Eric Vanden-Eijnden. “Systematic Strategies for Stochastic Mode Reduction in Climate”. In: *J. of Atmospheric Sciences* 60 (July 2003), pp. 1705–1722 (cit. on p. 106).

[MV19] John Maclean and Erik S. Van Vleck. “Projected Data Assimilation”. stat.CO. 2019. URL: arXiv:1902.04212v2 (cit. on pp. 5, 143, 146, 153, 160).

[Nea96] R. M. Neal. “Sampling from multimodal distributions using tempered transitions”. In: *Statistics and Computing* 6 (1996), pp. 353–366. DOI: 10.1007/BF00143556 (cit. on pp. 129, 137).

[Nor+13] Adrienne Norwood et al. “Lyapunov, singular and bred vectors in a multi-scale system: an empirical exploration of vectors related to instabilities”. In: *Journal of Physics A: Mathematical and Theoretical* 46.25 (June 2013), p. 254021. DOI: 10.1088/1751-8113/46/25/254021 (cit. on pp. 147, 158, 160).

[Ose68] V. I. Oseledets. “A multiplicative ergodic theorem: Lyapunov characteristic numbers for dynamical systems”. In: *Transaction of the Moscow Mathematical Society* 19 (1968), pp. 197–231 (cit. on p. 144).

[Ott+04] Edward Ott et al. “A local ensemble Kalman filter for atmospheric data assimilation”. In: *Tellus A* 56.5 (2004), pp. 415–428. DOI: 10.1111/j.1600-0870.2004.00076.x (cit. on p. 165).

[Par80] E. Pardoux. “Stochastic partial differential equations and filtering of diffusion processes”. In: *Stochastics* 3.1-4 (1980), pp. 127–167. DOI: 10.1080/17442507908833142 (cit. on pp. 3, 20, 26).

[PCT13] Luigi Palatella, Alberto Carrassi, and Anna Trevisan. “Lyapunov vectors and assimilation in the unstable subspace: theory and applications”. In: *Journal of Physics A: Mathematical and Theoretical* 46.25 (June 2013), p. 254020. DOI: 10.1088/1751-8113/46/25/254020 (cit. on pp. 142, 146, 160).

[Pes77] Ya B. Pesin. “Characteristic Lyapunov Exponents and Smooth Ergodic Theory”. In: *Russian Mathematical Survey* 32.4 (1977), pp. 55–114. DOI: 10.1070/RM1977v032n04ABEH001639 (cit. on p. 145).

[PNY11] Jun Hyun Park, N. Sri Namachchivaya, and Hoong Chieh Yeong. “Particle Filters In a Multiscale Environment: Homogenized Hybrid Particle Filter”. In: *Journal of Applied Mechanics* 78 (Nov. 2011), pp. 061001–061001-10. DOI: doi:10.1115/1.4003167 (cit. on pp. 3, 19, 104, 112).

[Pot16] Jonathan Poterjoy. “A Localized Particle Filter for High-Dimensional Nonlinear Systems”. In: *Monthly Weather Review* 144.1 (2016), pp. 59–76. DOI: 10.1175/MWR-D-15-0163.1 (cit. on pp. 99, 165).

[PP94] Etienne Pardoux and Shige Peng. “Backward doubly stochastic differential equations and systems of quasilinear SPDEs”. In: *Probability Theory and Related Fields* 98.2 (June 1994), pp. 209–227. DOI: 10.1007/BF01192514 (cit. on pp. 31, 33, 34, 167, 168).

[PS08] Grigorios A. Pavliotis and Andrew M. Stuart. *Multiscale Methods*. 1st ed. Vol. 53. Texts in Applied Mathematics. Springer-Verlag New York, 2008. ISBN: 978-0-387-73828-4. DOI: 10.1007/978-0-387-73829-1 (cit. on pp. 19, 59).

[PSN10] J H Park, R B Sowers, and N Sri Namachchivaya. “Dimensional reduction in nonlinear filtering”. In: *Nonlinearity* 23.2 (Jan. 2010), pp. 305–324. DOI: 10.1088/0951-7715/23/2/005 (cit. on p. 19).

[PSV76] George C. Papanicolaou, Danial Stroock, and S. R. S. Varadhan. “Martingale approach to some limit theorems”. In: *Papers from the Duke Turbulence Conference*. Duke University, Durham, North Carolina, 1976 (cit. on p. 19).

[Put20] William Putnam. *Global Mesoscale Modeling with GEOS-5: Global Weather at Local Scales*. Aug. 2020. URL: https://www.nas.nasa.gov/SC14/demos/demo35.html (cit. on p. 2).

[PV01] E. Pardoux and Yu. Veretennikov. “On the Poisson Equation and Diffusion Approximation. I”. In: *Ann. Probab.* 29.3 (July 2001), pp. 1061–1085. DOI: 10.1214/aop/1015345596 (cit. on pp. 35, 163).

[PV03] E. Pardoux and A. Yu. Veretennikov. “On Poisson equation and diffusion approximation 2”. In: *Ann. Probab.* 31.3 (July 2003), pp. 1166–1192. DOI: 10.1214/aop/1055425774 (cit. on pp. 3, 19, 37, 38, 61, 67–69, 75, 95–97, 163).

[PWR19] Roland Potthast, Anne Walter, and Andreas Rhodin. “A Localized Adaptive Particle Filter within an Operational NWP Framework”. In: *Monthly Weather Review* 147.1 (2019), pp. 345–362. DOI: 10.1175/MWR-D-18-0028.1 (cit. on pp. 99, 165).

[Qia19] Huijie Qiao. “Convergence of Nonlinear Filterings for Multiscale Systems with Correlated Sensor Lévy Noises”. In: *ArXiv e-prints* (2019). URL: https://arxiv.org/abs/1910.09265v1 (cit. on p. 19).

[Roz90] Boris L. Rozovskii. *Stochastic Evolution Systems: Linear Theory and Aplications to Non-linear Filtering*. Dordrecht: Kluwer Academic Publishers, 1990, p. 315. ISBN: 0-7923-0037-8 (cit. on pp. 28, 31, 34).

[Roz91] Boris L. Rozovskii. “Stochastic Analysis”. In: ed. by Eddy Mayer-Wolf, Ely Merzbach, and Adam Shwartz. Academic Press, Inc., 1991, pp. 449–458 (cit. on pp. 25, 94, 163).

[Rue78] David Ruelle. “An inequality for the entropy of differentiable maps”. In: *Boletim da Sociedade Brasileira de Matemática - Bulletin/Brazilian Mathematical Society* 9.1 (Mar. 1978), pp. 83–87. ISSN: 1678-7714. DOI: 10.1007/BF02584795 (cit. on p. 145).

[SBM15] Chris Snyder, Thomas Bengtsson, and Mathias Morzfeld. “Performance Bounds for Particle Filters Using the Optimal Proposal”. In: *Monthly Weather Review* 143.11 (2015), pp. 4750–4761. DOI: 10.1175/MWR-D-15-0144.1 (cit. on pp. 98, 153).

[Sny+08] Chris Snyder et al. “Obstacles to High-Dimensional Particle Filtering”. In: *Monthly Weather Review* 136.12 (2008), pp. 4629–4640. DOI: 10.1175/2008MWR2529.1 (cit. on pp. 98, 153).

[Str08] Daniel W. Stroock. *Partial Differential Equations for Probabilists*. Cambridge Studies in Advanced Mathematics. Cambridge University Press, 2008. DOI: 10.1017/CBO9780511755255 (cit. on pp. 25, 33, 34, 37).

[TDT10] Anna Trevisan, Massimo D’Isidoro, and Olivier Talagrand. “Four-dimensional variational assimilation in the unstable subspace and the optimal subspace dimension”. In: *Quarterly Journal of the Royal Meteorological Society* 136.647 (2010), pp. 487–496. DOI: 10.1002/qj.571 (cit. on pp. 5, 142, 146, 160).

[TK93] Zoltan Toth and Eugenia Kalnay. "Ensemble Forecasting at NMC: The Generation of Perturbations". In: *Bulletin of the American Meteorological Society* 74.12 (1993), pp. 2317–2330. DOI: 10.1175/1520-0477(1993)074<2317:EFANTG>2.0.CO;2 (cit. on p. 165).

[TP11] A. Trevisan and L. Palatella. "On the Kalman Filter error covariance collapse into the unstable subspace". In: *Nonlinear Processes in Geophysics* 18.2 (2011), pp. 243–250. DOI: 10.5194/npg-18-243-2011 (cit. on pp. 143, 153).

[Ver16] A. Veretennikov. "On SPDE and backward filtering equations for SDE systems (direct approach)". In: *ArXiv e-prints* (July 2016). arXiv: 1607.00333 [math.PR] (cit. on p. 28).

[Ver97] A Yu Veretennikov. "On polynomial mixing bounds for stochastic differential equations". In: *Stochastic Processes and their Applications* 70.1 (Oct. 1997), pp. 115–127. DOI: 10.1016/S0304-4149(97)00056-2 (cit. on p. 35).

[Wil05] Daniel S. Wilks. "Effects of stochastic parameterizations in the Lorenz '96 system". In: *Q. J. R. Meteorol. Soc.* 131.606 (Jan. 2005), pp. 389–407. DOI: 10.1256/qj.04.03 (cit. on pp. 104, 106).

[WS07] Christopher L Wolfe and Roger M Samelson. "An efficient method for recovering Lyapunov vectors from singular vectors". In: *Tellus A* 59.3 (Apr. 2007), pp. 355–366. DOI: 10.1111/j.1600-0870.2007.00234.x (cit. on p. 144).

[Yan+18] Jun-Ichi Yano et al. "Scientific Challenges of Convective-Scale Numerical Weather Prediction". In: *Bulletin of the American Meteorological Society* 99.4 (2018), pp. 699–710. DOI: 10.1175/BAMS-D-17-0125.1 (cit. on pp. 1, 98, 151).

[Yeo+20] Hoong C. Yeong et al. "Particle Filters with Nudging in Multiscale Chaotic Systems: With Application to the Lorenz '96 Atmospheric Model". In: *Journal of Nonlinear Science* 30.4 (2020), pp. 1519–1552. DOI: 10.1007/s00332-020-09616-x (cit. on pp. 3, 19, 99, 129–131).

[Yeo17] Hoong Chieh Yeong. "Dimensional Reduction in Nonlinear Estimation of Multiscale Systems". PhD thesis. University of Illinois at Urbana-Champaign, 2017. URL: http://hdl.handle.net/2142/99320 (cit. on pp. 102, 162).

[You13] Lai-Sang Young. "Mathematical theory of Lyapunov exponents". In: *Journal of Physics A: Mathematical and Theoretical* 46.25 (June 2013), p. 254001. DOI: 10.1088/1751-8113/46/25/254001 (cit. on p. 145).

[YPN11] Hoong Chieh Yeong, Jun Hyun Park, and N. Sri Namachchivaya. "Particle Filters In a Multiscale Environment: with Application to the Lorenz-96 Atmospheric Model". In: *Stochastics and Dynamics* 11.02n03 (2011), pp. 569–591. DOI: 10.1142/S0219493711003450 (cit. on pp. 104, 112).

[ZR19] Yanjie Zhang and Jian Ren. "Data Assimilation for a Multiscale Stochastic Dynamical System with Gaussian Noise". In: *Stochastics and Dynamics* 19.3 (2019). DOI: 10.1142/S0219493719500199 (cit. on p. 20).